

# Alma Mater Studiorum - Università di Bologna

## DOTTORATO DI RICERCA IN SCIENZE DELLA TERRA

Ciclo XXVII

Settore Concorsuale di afferenza: 04/A2

Settore Scientifico disciplinare: GEO/02

Quality assessment of a landslide inventory map and its application to land-use planning. A case study in the Northern Apennines (Emilia-Romagna region, Italy)

**Presentata da:** Cristina Baroni

**Coordinatore Dottorato:**

Prof. Jo H. A. De Waele

**Relatore:**

Prof. Enzo Farabegoli

**Co-relatore:**

Dott. Giuseppe Onorevoli

**Esame finale anno 2015**

To my son, Matteo

*“Civilization exists by geological consent,  
subject to change without notice.”*

W. Durant

*“One obstacle to a simple definition of “landslide”  
is the erroneous assumption that a landslide is, simply,  
a slide of land. A similar linguistic analysis would suggest  
that a cowboy is a male calf.”*

D.M. Cruden

# ABSTRACT

Each year landslides cause casualties and millions of Euros worth of damage. Despite the United Nations efforts to reduce their impacts, landslide hazard and risk are growing as a consequence of climate change and demographic pressure. Land-use planning represents a valuable and powerful tool to manage this socio-economic problem and build sustainable and landslide resilient communities. Landslide inventory maps are a cornerstone of land-use planning and, as a consequence, their quality assessment represents a burning issue.

This work aimed to define the quality parameters of a landslide inventory and to assess its spatial and temporal accuracy with regard to its possible applications to land-use planning. In order to achieve this goal, I proceeded according to a two-steps approach. An overall assessment of the accuracy of data geographic positioning and of the geological, geomorphological, and land-use setting was performed on four case study sites located in the Italian Northern Apennines. The quantification of the overall spatial and temporal accuracy, instead, focused on the Dorgola Valley, a landslide-prone catchment in the Province of Reggio Emilia. The assessment of the overall spatial accuracy involved a comparison between remotely sensed and field survey data, as well as an innovative fuzzy-like analysis of a multi-temporal landslide inventory map. Long- and short-term landslide temporal persistence, on the other hand, was appraised over a period of 60 years with the aid of 18 remotely sensed image sets. These results were eventually compared with the current Territorial Plan for Provincial Coordination (PTCP) of the Province of Reggio Emilia.

The outcome of this work suggested that geomorphologically detected and mapped landslides, represented as well defined polygons, are a significant approximation of a more complex reality. In order to convey to the end-users this intrinsic uncertainty, a new form of cartographic representation is needed. In this sense, a fuzzy raster landslide map, like the one prepared for this work, may be an option. With regard to land-use planning, landslide inventory maps, if appropriately updated, confirmed to be essential decision-support tools. This research, however, proved that their spatial and temporal uncertainty discourages any direct use as zoning maps, especially when zoning itself is associated to statutory or advisory regulations.

# ACKNOWLEDGMENTS

First and foremost, I wish to express my sincere gratitude to my advisor, Prof. Enzo Farabegoli. This wonderful journey would not have been possible without his encouragement and guidance. Prof. Farabegoli has been an extraordinary mentor; our endless conversations were always priceless sources of inspiration for my research as well as for my life. He was supportive, but he also gave me the freedom to pursue my ideas and projects allowing me to grow as a science researcher.

I would also like to thank my co-advisor, Giuseppe Onorevoli, for his valuable support and for his patience in handling my stubbornness during our many brainstorming sessions. He was a perfect teammate for the emotional roller coaster that was my PhD research.

I am deeply grateful to my Kiwi hosts at GNS Science and at the University of Canterbury, in particular to Sally Dellow and Prof. Tim Davies, for their co-operation and the stimulating learning experience.

Special thanks to Prof. Riccardo Rigon, Department of Civil, Environmental and Mechanical Engineering, University of Trento, whose comments helped improve and clarify this manuscript.

This doctoral dissertation was possible with the help of several people. In particular, I would like to acknowledge the staff of all the authorities, agencies, institutions, and companies that collaborated to this research by providing data and technical support. Special thanks to Marina Albertelli, Luigi Doria, Stefania Errico, Alessandro Flamini, Luca Grulla, Emanuele Mandanici, Matteo Nardo, and Simone Poggiali.

A heartfelt thanks to my partner, Gianni, for his unconditional love. Without him, I would not have been able to balance my doctoral research with the rest of my life. Thank you for joining me in this amazing adventure. I could not have accomplished this feat without you by my side. I am also incredibly grateful to my beloved Matteo and Marco for their support and the innumerable sacrifices. Thanks also to my parents who have always shared my decisions, even the hardest ones.

Finally, I would like to thank all my friends who have always stood by me along the way. Thanks to Martina, who with her lively enthusiasm has always brought light into the darkness.

# Table of contents

## CHAPTER 1: Introduction

1.1. Background and significance of the research study	2
1.2. Research aims	4
1.3. Structure of the dissertation	6

## CHAPTER 2: Methodology

2.1. Introduction	8
2.2. Data quality	9
2.2.1. Geospatial data quality	9
2.2.2. Geospatial data quality components	10
2.2.3. Definition of the quality parameters of a landslide inventory map	14
2.3. Data collection	19
2.3.1. Selection of the case study sites	20
2.3.1.1. Castelnovo né Monti	21
2.3.1.2. Guiglia	29
2.3.1.3. Zattaglia	30
2.3.1.4. Castrocaro Terme	30
2.3.2. Field investigations and interviews	31
2.3.3. Acquisition of GeoEYE satellite images	34
2.3.4. Historical data	34
2.4. Data processing	34
2.4.1. Image processing	35
2.4.2. Landslide detection and processing	37
2.5. Conclusions	44

## CHAPTER 3: Accuracy of data geographic positioning

3.1. Introduction	47
3.2. <i>Datum</i> and map projections	48
3.2.1. Coordinate Reference Systems adopted in Italy	49
3.2.2. Emilia-Romagna Region Coordinate Reference System	52
3.3. <i>Datum</i> transformation	54
3.3.1. Transformation algorithms	55
3.3.2. Transformation software	56
3.4. Methodology	58
3.5. Analysis and discussion	61
3.5.1. Transformation reversibility	61
3.5.2. Comparison between the transformed files and the original WGS84 file	62
3.5.3. Comparison among files transformed with different software	67
3.6. Conclusions	69

<b>CHAPTER 4: Spatial accuracy of landslide detection and mapping</b>	
4.1. Introduction	72
4.2. Landslide detection and mapping techniques: a comparison between remotely sensed and field survey data	73
4.2.1. Analysis and results	76
4.2.1.1. Descriptive statistics	77
4.2.1.2. Landslide abundance	80
4.2.1.3. Correspondence of landslide areas	83
4.2.1.4. Time and cost evaluation	86
4.2.2. Discussion	87
4.2.2.1. Limiting factors of the detection and mapping techniques	87
4.2.2.2. Data interpretation	90
4.3. Spatial accuracy of a multi-temporal landslide inventory map	91
4.3.1. Analysis and results	92
4.3.2. Discussion	100
4.4. Conclusions	102
<b>CHAPTER 5: Landslide temporal persistence</b>	
5.1. Introduction	105
5.2. Multi-temporal landslide inventory map of the Dorgola catchment	106
5.2.1. Analysis and results	106
5.2.1.1. Descriptive statistics	106
5.2.1.2. Correspondence of landslide areas	111
5.2.2. Discussion	112
5.3. Characterization of new and undetected landslides	115
5.3.1. Analysis and results	117
5.3.1.1. Descriptive statistics	117
5.3.1.2. New detection size	119
5.3.1.3. New detection location	122
5.3.2. Discussion	122
5.4. Temporal persistence of landslide footprints	126
5.5. Conclusions	128
<b>CHAPTER 6: Landslide inventory maps and land-use planning</b>	
6.1. Introduction	131
6.2. Land-use planning in landslide-prone areas	132
6.2.1. The landslide problem in Italy and in the Emilia-Romagna region	132
6.2.2. The planning process and setting	134
6.2.3. Landslide susceptibility, hazard, and risk zoning	139
6.2.4. Landslide management in the Emilia-Romagna region	143
6.3. Limits and applications of a landslide inventory map to land-use planning. The case study of the Dorgola catchment.	145
6.3.1. Analysis and results	146
6.3.1.1. Descriptive statistics and landslide abundance	146
6.3.1.2. Correspondence of landslide areas	150
6.3.1.3. Spatial and temporal accuracy assessment of the 2010 PTCP inventory map	150

6.3.2. Discussion	152
6.4. Conclusions	157
<b>CHAPTER 7: Conclusions and recommendations</b>	
7.1. General conclusions	160
7.2. Research limits and recommendations	164
<b>REFERENCES</b>	167
<b>APPENDIX A</b>	178
<b>APPENDIX B</b>	185

# List of acronyms

AGEA	Agency for funds Distribution in Agriculture ( <i>Agenzia per le Erogazioni in Agricoltura</i> )
AGS	Australian Geomechanics Society
API	Area of Potential Instability
CRS	Coordinate Reference System
CTR	Regional Technical Map ( <i>Carta Tecnica Regionale</i> )
DEM	Digital Elevation Model
DI	Detection Index
ETRS89	EUREF Terrestrial Reference System 1989
IGM	(Italian) Geographic Military Institute ( <i>Istituto Geografico Militare</i> )
IFFI	Inventory of the Landslides Events in Italy ( <i>Inventario dei Fenomeni Franosi in Italia</i> )
GBO	Western zone of the Gauss-Boaga projection ( <i>Gauss-Boaga Ovest</i> )
GIS	Geographic Information System
GPS	Global Positioning System
GCP	Ground Control Point
GSUEG	Research Group on Geomorphology of the Universities of Emilia ( <i>Gruppo di Studio delle Università Emiliane per la Geomorfologia</i> )
INSPIRE	Infrastructure for Spatial Information in Europe
IOGP	International association of Oil & Gas Producers (ex European Petroleum Survey Group - EPSG)
ISO	International Organization for Standardization

JTC-1	Joint Technical Committee on Landslides and Engineered Slopes
LL	Lazarus landslide
LR	Regional Law ( <i>Legge Regionale</i> )
PGA	Peak Ground Acceleration
PTCP	Territorial Plan for Provincial Coordination ( <i>Piano Territoriale di Coordinamento Provinciale</i> )
RDN	National Dynamics Network ( <i>Rete Dinamica Nazionale</i> )
RMS	Root Mean Square
RPC	Rational Polynomial Coefficient
UIE	Elementary Hydromorphological Unit ( <i>Unità Idromorfologiche elementari</i> )
UNISDR	United Nations Office for Disaster Risk Reduction
UTM	Universal Transverse Mercator
VHR	Very High Resolution
WGS84	World Geodetic System 1984
WMS	Web Map Service

Note:

Italian acronyms were translated in English by the author. This translation does not imply any official recognition by Italian public authorities or agencies.

# CHAPTER 1

## Introduction

- 1.1. Background and significance of the research study
- 1.2. Research aims
- 1.3. Structure of the dissertation

# 1. Introduction

## 1.1. Background and significance of the research study

Landslides are a worldwide problem and represent a major threat to human life, properties, and activities (Brabb, 1991). In most mountainous and hilly regions landslides cause casualties and millions of Euros worth of damage. Indeed, they affect communities directly, in terms of loss of lives and properties (*e.g.* damages to buildings, vehicles, transport routes, utilities, *etc.*), but also with important, and sometimes long-term, side-effects (*e.g.* disruptions of transport routes and of utility supplies, floods due to river damming, loss of forest, *etc.*). According to the United Nations Office for Disaster Risk Reduction (UNISDR), from 1980 to 2008 366 landslides affected 7,031,523 people causing 20,008 fatalities and about 6 billion US\$ economic damages (UNISDR, 2014). Nevertheless, landslide socio-economic impact is generally underestimated as mass movements are often overshadowed by their triggering events (*e.g.* earthquakes, volcanoes, storms, floods, and heavy rains). Unfortunately, this misperception contributes to reduce the general awareness and concern about landslide social, economic, and political consequences (Brabb, 1991).

Despite the United Nations efforts to reduce their impacts, landslide hazard and risk are growing and, indeed, more landslides are expected as a consequence of climate change and demographic pressure (Cascini *et al.*, 2005; Schuster and Highland, 2007; Fell *et al.*, 2008a). Among European countries, Italy is the one that has suffered the greatest human and economic losses due to landslides. Only in the 20<sup>th</sup> century 7,799 casualties (including 5,831 deaths, 108 missing people, and 1,860 injured people) were recorded, while the number of affected people is uncertain but probably exceeds 100,000 (Guzzetti, 2000).

A sound policy with legal and institutional foundations is an essential element to build sustainable and landslide resilient communities. In this sense, land-use planning proved to be a valuable and powerful tool for the management, the reduction, and the mitigation of landslide hazard and risk (Cascini *et al.*, 2005; Greiving *et al.*, 2006; Greiving and

Fleischhauer, 2006; Saunders and Glassey, 2007; AGS, 2007a; Schuster and Highland, 2007; Fell *et al.*, 2008a; Fell *et al.*, 2008b; Leventhal and Kotze, 2008; Glavovic *et al.*, 2010; Guillard and Zezere, 2012). Due to the peculiarity of the background and scenario of each country, several planning approaches have been applied worldwide (Cascini *et al.*, 2005). One of the most common is zoning, which effectively allows to represent homogeneous areas or domains according to their degrees of actual or potential landslide susceptibility, hazard, or risk. Furthermore, in order to be more effective, zoning is usually associated to specific regulations which govern acceptable and unacceptable uses and can basically be advisory or statutory. Hence, the importance of land-use planning is due to both its success as a planning tool and the legal effects of its application. Indeed, an inadequate or erroneous land-use planning may threaten community safety with serious, if not tragic, social, and economic consequences. Meanwhile, its legally binding regulation may lead to litigations between private and public subjects. In fact, on one hand, regulatory restrictions on private properties are often perceived as a form of expropriation. On the other hand, however, landslide victims, finding themselves financially unable to rebuild their houses, seek to recover their losses through lawsuit other potentially involved subjects (Schwab *et al.*, 2005). As a consequence, it is fundamental that planning documents can rely on a sound scientific background. In particular, if statutory constraints are to be imposed on the basis of landslide zoning, it is essential that the type, the scale, and the level of zoning itself is comparable to the required usage, as well as to the quantity, quality, and resolution of the available input data (AGS, 2007a; Fell *et al.*, 2008a).

In Italy land-use plans are acts of public authorities and represent the “*certezza pubblica*” (public certainty). In this regard, according to Giannini (1960), “*tra la realtà rappresentata e la rappresentazione fornita dall’atto di certezza sussiste, anzi deve sussistere, corrispondenza; tuttavia lo scopo dell’atto di certezza non è quello di fondare una verità, ma di fornire un’utilità che possa essere accettata, in quanto è plausibile che sia rispondente alla realtà*” (between reality and its representation on the act of legal certainty there must be correspondence. However, the goal of the legal act is not to define “truth”, but rather to supply a tool that likely resembles reality). In this context, if reality proves the inconsistency of the legal certainty, the most powerful tool to review the legal act is the legal process.

In this context, the role of landslide inventory maps is crucial. Indeed, by describing landslide location, abundance, characteristics, and pattern distribution, they provide a valuable reference background for planning and decision-making. Furthermore, landslide inventory maps are also key input parameters for susceptibility and hazard assessment and validation (Galli *et al.*, 2008; van Westen *et al.*, 2008; Guzzetti *et al.*, 2012). In this sense, it can be stated that landslide inventory maps are the cornerstone of land-use planning.

The Emilia-Romagna Region was among the first Italian local governments to invest resources on geological and landslide mapping, so that today it can rely on a valuable database. At the same time, since its territory is remarkably prone to landslides, the Emilia-Romagna Regional Authority has also given a wide prominence to land-use planning. Indeed, most of its Provincial Administrations already have two generations of land-use plans. Despite these efforts, however, mass movements are still an important social and economic issue due to the intense interaction between landslides and man activities and structures. Although human casualties are fortunately uncommon, according to Bertolini and Pizziolo (2008), in a five years time frame about 390 million Euros were invested by national and regional governments in reconstructions, village relocations, consolidation works, and monitoring activities. These costs, however, are not sustainable and call for a careful analysis about the current land-use planning system which is, indeed, essentially based on landslide inventory maps. For this reason, their quality assessment is a fundamental step.

### **1.2. Research aims**

Understanding slope failure distribution and characteristics is necessary for reducing future landslide-related losses. In this sense, landslide inventory maps are essential decision-support tools for land-use planning and management (Galli *et al.*, 2008; van Westen *et al.*, 2008; Guzzetti *et al.*, 2012). Notwithstanding this, to this day, there are no standards, best practises, or operational protocols for their preparation, validation, and update. Furthermore, no absolute criteria have been proposed to assess their quality and reliability (Guzzetti *et al.*, 2000; Galli *et al.*, 2008; Trigila *et al.*, 2010; Guzzetti *et al.*, 2012). In modern Earth Science, however, the lack of standards and shared protocols sets significant

restrictions to data credibility and usefulness with negative effects also on the derivative products and analysis (Guzzetti *et al.*, 2006).

Given the importance of landslide inventory maps for the success and the legal effects of land-use planning, this research focuses on their quality assessment with respect to their possible applications within land-use planning. In particular, I address the following questions:

- ✓ Which parameters better define the quality of a landslide inventory maps?
- ✓ What is the spatial and temporal accuracy of a landslide inventory map?
- ✓ According to its limits, what are the possible applications of a landslide inventory map within the land-use planning context?

In order to answer these questions, I carried out the following tasks:

- detailed literature survey about the meaning of the term “quality” and its application to landslide inventory maps;
- identification and field investigation of four case study sites in the Northern Apennines (Emilia-Romagna Region, Italy) to be used as test and training areas;
- definition and quantitative analysis of the quality parameters of a landslide inventory map;
- appraisal of the landslide inventory map of the Reggio Emilia Territorial Plan for Provincial Coordination (*Piano Territoriale di Coordinamento Provinciale – PTCP*) applied to the case study area of the Dorola catchment.

### **1.3. Structure of the dissertation**

In addition to this Chapter, which introduces the background, significance, and aims of the research, this dissertation presents six chapters organised in the following way:

- CHAPTER 2. After introducing the concept of quality and its application to landslide inventory maps, I describe the four test areas, data collection, and the methodology used for data processing.
- CHAPTER 3. The specific Coordinate Reference System (CRS) adopted by the Emilia-Romagna Region calls for attention on *datum* transformation as a crucial conditioning factor of data geographic positioning. In this chapter, I present the effects of *datum* transformations on the landslide inventory maps of the four test areas.
- CHAPTER 4. I analyse and discuss the spatial accuracy of the landslide inventory map of the Dorgola catchment by comparing two different landslide detection and mapping techniques (ground- and remote-based) and by quantifying the overall spatial accuracy of a remote-based multi-temporal landslide inventory map.
- CHAPTER 5. In this chapter, I focus on landslide short- and long-term temporal persistence through the analysis of the multi-temporal landslide inventory map of the Dorgola catchment. I also outline the main characteristics of new and undetected landslides.
- CHAPTER 6. After a review of land-use planning processes and settings in landslide-prone areas, I evaluate the efficiency of the landslide inventory map of the 2010 Territorial Plan for Provincial Coordination (PTCP) of the Reggio Emilia Province on the basis of the results of the previous chapters.
- CHAPTER 7. I draw the general conclusions and the research limits, and I propose some recommendations for land-use planning practices in landslide-prone areas.

## CHAPTER 2

### Methodology

- 2.1. Introduction
- 2.2. Data quality
  - 2.2.1. Geospatial data quality
  - 2.2.2. Geospatial data quality components
  - 2.2.3. Definition of the quality parameters of a landslide inventory map
- 2.3. Data collection
  - 2.3.1. Selection of case study sites
    - 2.3.1.1. Castelnovo né Monti
    - 2.3.1.2. Guiglia
    - 2.3.1.3. Zattaglia
    - 2.3.1.4. Castrocaro Terme
  - 2.3.2. Field investigations and interviews
  - 2.3.3. Acquisition of GeoEYE satellite images
  - 2.3.4. Historical data
- 2.4. Data processing
  - 2.4.1. Image processing
  - 2.4.2. Landslide detection and processing
- 2.5. Conclusions

## 2. Methodology

### 2.1. Introduction

The definition of “quality” and the identification of quality parameters represent an essential step for this research as they ascertain the reference framework against which quality itself has to be assessed. Defining the term “quality”, however, is not an easy task. In particular, defining the quality of a dataset is even more challenging as, unlike manufactured goods, data do not have any physical characteristics and their quality has to be assessed as a function of intangible properties such as “completeness” and “consistency” (Veregin, 1999). The widespread use of landslide inventory maps demands for special attention to the user awareness as far as tool restrictions are concerned. An incomplete or unclear knowledge of data limitations may actually lead to misuses and ultimately to faulty decision-making with significant social, legal, and economic consequences (Devillers *et al.*, 2002; Devillers *et al.*, 2005). Landslide detection and mapping are difficult, tedious, time-consuming, and error-prone operations with an intrinsic uncertainty. For this reason, it is essential that the end users (planners, decision-makers, but also landslide specialists) clearly understand that, even if landslides are mapped with sharp boundaries, they are not well-defined entities discriminating safe and unsafe land surface (Ardizzone *et al.*, 2002).

In this chapter, I introduce the meaning of the term “quality” and I try to define the quality parameters of a landslide inventory map. In addition, I describe the four study sites, as well as data collection and processing. The final goal is to present and explain the method and the techniques that were adopted for the quantification of landslide spatial and temporal accuracy.

## 2.2. Data quality

In 1986 the International Organization for Standardization (ISO) described quality as "the totality of features and characteristics of a product or service that bears on its ability to meet a stated or implied need" (ISO 8402, 1986), but the more recent ISO 9000 (2005) defined it as the "degree to which a set of inherent characteristics fulfils requirements". Quality, however, was also defined by other authors as "value" (Abbott, 1955; Feigenbaum, 1951), "conformance to specifications" (Gilmore, 1974; Levitt, 1972), "conformance to requirements" (Crosby, 1979), and "fitness for use" (Juran, 1974). By looking at the different definitions of the term "quality", it is worth noting that there is a certain ambiguity about it. Data producers and data users may indeed view quality from different perspectives (ISO 19114, 2009); while producers refer to it as consistency with the product specifications, users tend to assess quality on the basis of their expectations (Kahn and Strong, 1998).

### 2.2.1. Geospatial data quality

The production, processing, and use of geospatial data have changed significantly in the past decades. Historically, they were produced and used by geospatial experts within the same organization, usually governmental agencies (Veregin, 1999; Devillers *et al.*, 2002; Devillers *et al.*, 2005). In this context, knowledge about data production processes and characteristics, including quality, was more implicit (*i.e.*, organizational memory) than explicit (*i.e.*, metadata) (Devillers *et al.*, 2005). The introduction of internet and digital data, as well as the easier access to Geographic Information System (GIS) applications, encouraged the sharing, interchange, and use of geospatial data. In their work, Devillers *et al.* (2002) stated that geospatial data are becoming a "mass product". Indeed, they are now used in many fields often as a decision-support tool (Devillers *et al.*, 2002). However, most geospatial data users are not familiar with the basic concepts of geographical information and many of them are not aware of the uncertainty that digital data may contain (Guptill & Morrison, 1995; Fisher, 1999). To this end, Goodchild (1995) asserted that "GIS is its own worst enemy: by inviting people to find new uses for data, it also invites them to be

irresponsible in their use.”

Although the widespread availability and use of geospatial data increased the concern about their quality, the definition of data quality remains uncertain. In the literature, authors generally refer to “internal” and “external quality”. The former restricts quality to dataset internal characteristics, *i.e.* the intrinsic properties resulting from data production methods. “External quality”, instead, follows the definition of “fitness for use” according to which quality is defined as the level of fitness between data characteristics and user needs. As a consequence, “external quality” is a relative concept that requires also information about “internal quality” (Devillers *et al.*, 2005). The need of the consumer to assess whether a database meets the requirements of a particular application led to the “truth-in-labelling” paradigm. “Truth-in-labelling” considers errors as inevitable and interprets data quality issues in terms of misuse caused by an incomplete knowledge of data limitations (Goodchild, 1995; Veregin, 1999). Although challenging, documenting and communicating data quality information is essential, not only for the reliability of data representation and interpretation, but also for their effectiveness and for the evaluation of decision alternatives (Buttenfield and Beard, 1991; Goodchild, 1995). To this end, data producers provide metadata, *i.e.* “data about data”. Metadata, however, still present some disadvantages (Devillers *et al.*, 2002):

- they are usually stored in files that are independent from their related data; if data are modified, changes are not automatically recorded in their associated metadata;
- due to their static nature, metadata are not particularly useful for dynamic operations when using a GIS;
- metadata are usually related to the entire dataset, so that they do not represent data quality heterogeneity or granularity (Devillers *et al.*, 2005);
- they usually provide technical descriptions that are hermetic to non-expert users.

To be more effective, data quality communication should overcome all these limitations.

### **2.2.2. Geospatial data quality components**

Like physical processes, geospatial data are multidimensional and relate essentially to spatial, temporal, and thematic components. Intuitively, space is the dominant parameter of

geospatial data analysis. Without space there is nothing geographical about data (Veregin, 1999). Time as well, however, is a crucial variable in understanding and measuring data quality. Indeed, perceived quality is time-dependent, and a product that exceeds user expectations at one point in time may be judged as inadequate at another point in time (Reeves and Bednar, 1994; Rivest *et al.*, 2001). In particular, physical processes have to be understood not as entities that exist at some location but as events that appear and disappear in space and time (Peuquet, 1999; Raper, 1999; Veregin, 1999). That being stated, space and time have to be intended as a framework on which a theme is measured. Without attributes geospatial data would only be geometries; theme itself has to be considered an essential component of data dimension. As a consequence, in order to assess geospatial data quality, quality parameters, where possible, have to be identified for each dimension: spatial, temporal, and thematic (Veregin, 1999).

Standards organizations and academic researchers suggested several parameters for defining quality. Listed below are the main ones (Veregin, 1999; Devillers *et al.*, 2005; ISO 19114, 2009):

- accuracy;
- precision;
- consistency;
- completeness;
- lineage.

#### Accuracy

“Error” refers to the discrepancy between a measured value and the true value (Buttenfield and Beard, 1991; Fisher, 1999; Veregin, 1999). “Accuracy”, instead, is defined as the closeness of agreement between a measured value and the true one, where the latter is substituted by an accepted reference (ISO 5725, 1994, Mark and Csillag, 1989). This definition of “error” implies that there is an objective reality with which measured values can be compared to (Fisher, 1999). However, the requirement that “truth” exists and that it can be observed raises some issues (Veregin, 1999):

- truth may not be observable, *e.g.* historical data;
- truth observation may be infeasible, *e.g.* for costs or technical limitations;

- there might be multiple truths since several natural phenomena tend to be variable. In these cases, inexactness is a fundamental property of spatial data (Goodchild, 1995; Veregin, 1999).

Given the complexity of physical processes, geospatial data can at best approximate reality through a model that implies generalization and abstraction. This conceptual model (or database “specification”) is itself a distorted and abstracted view of reality, interposed between the real world and the database (Goodchild, 1993; Goodchild, 1995; Veregin, 1999) (Fig. 2.1). Goodchild (1993) defined as “source errors” those that exist in the source document (conceptual model) with respect to ground truth and as “processing errors” those between the source document and the database. The former are generally more substantial than processing errors due to the way a source document represents the reality. Models, indeed, allow to express complex phenomena in the form of relatively simple objects but at the cost of decreasing accuracy. For example, a continuous variation of a parameter may be represented by a simple line or sharp discontinuity; in this case, however, the attribute assigned to the corresponding polygon do not in fact apply homogeneously to all the polygon (Goodchild, 1993).

As mentioned above, in order to assess the quality of geospatial data, accuracy has to be identified for each data dimension: spatial, temporal, and thematic. Regarding the spatial components, various metrics were developed for points, whereas for lines and areas accepted metrics have not yet been developed (Veregin, 1999). Temporal accuracy is often underestimated, despite the omission of temporal information has significant implications for features with a high frequency of change (Veregin, 1999). Metrics of thematic accuracy vary with the measurement scale, and they are different for quantitative attributes and for categorical data (Veregin, 1999).

### Precision

According to Veregin (1999) “precision refers to the amount of detail that can be discerned” and affects the degree to which a database is suitable for a certain purpose. Indeed, all data have limited resolution because no measurement system is infinitely precise. Furthermore, conceptual models are generalized by definition since they imply elimination and merging, reduction in detail, smoothing, thinning, and aggregation of classes.

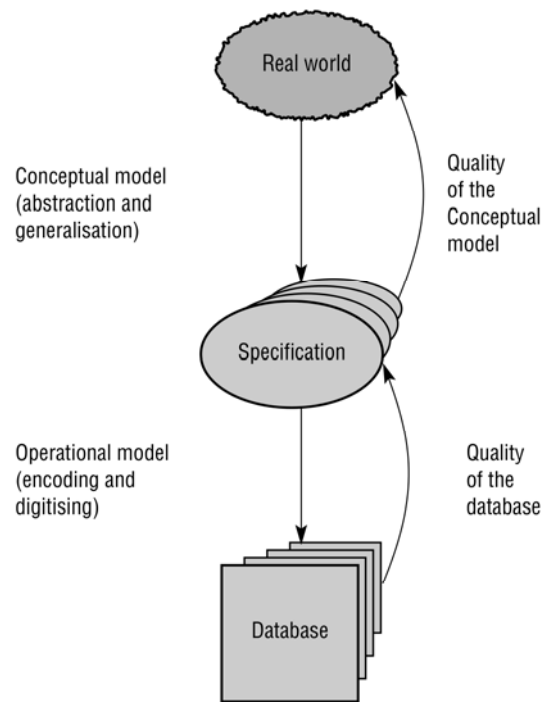


Fig. 2.1: Correlation among real world, database specification (conceptual model), and database (operational model) (Veregin, 1999).

With regard to remote sensed and raster images, spatial resolution refers to the ground dimensions of pixels which determine the minimum size of objects that can be detected (Mark and Csillag, 1989). Temporal precision deals with the discernible duration of an event, and it depends from the duration of the recording interval and the rate of change of the event. Temporal precision, though, should not be confused with the sampling rate. While the former refers to the time collection interval, sampling rate refers to the frequency of acquisition (Veregin, 1999).

#### Consistency

Consistency refers to the absence of apparent contradictions, and it may be considered as a measure of internal validity. With regard to geospatial data, consistency usually refers to topological properties that are normally checked during GIS processing routines.

#### Completeness

Completeness should be intended as an error of omission but also as an error of

commission (Veregin, 1999). With regard to Fig. 2.1, it may refer to both the database and the conceptual model. The database completeness is assessed between the database and its specification, while the model (or specification) completeness refers to the discrepancies between the model itself and the real world. The former is application-independent whereas the latter is application-dependent. For this reason, the model completeness has to be considered for the “fitness for use” analysis (Veregin, 1999).

### Lineage

For data quality assessment it is essential to store, handle, and report data historical information such as acquisition scale and resolution, date of creation, previous processing, *etc.*. To this end, it is worth noting that, while source data may be well documented, derived or second generation data are frequently lacking any information about their processing history.

### **2.2.3. Definition of the quality parameters of a landslide inventory map**

The generation of a landslide inventory represents a challenging effort to minimise the intrinsic uncertainty of landslide detection and mapping. In particular, a landslide inventory is a conceptual model used to generate a simplified knowledge of mass movements (Fig. 2.1). In this context, the reference source of the model is not reality *sensu stricto*, but it is the ground truth. Ground truth, however, is itself affected by uncertainty due to the spatial and temporal complexity of landslide phenomena and to the subjective nature of reality perception. At the same time, a landslide inventory is also the database (digital and/or cartographic) where all the detected landslides and their related data are gathered and mapped. That being so, what stated about the quality assessment and quality parameters of geospatial data may be applied also to landslide inventory maps.

The quality of the conceptual model depends on the capability of understanding and portraying the ground truth in the most reliable way. This intent, however, is inevitably conditioned by landslide active nature and complexity (*e.g.* spatio-temporal landslide interaction, landslide age and freshness, coexistence and interaction of different type of movements, persistence of landslide scars, *etc.*), as well as from the geological, geomorphological, and land-use setting. Conversely, the quality of the database relies on the

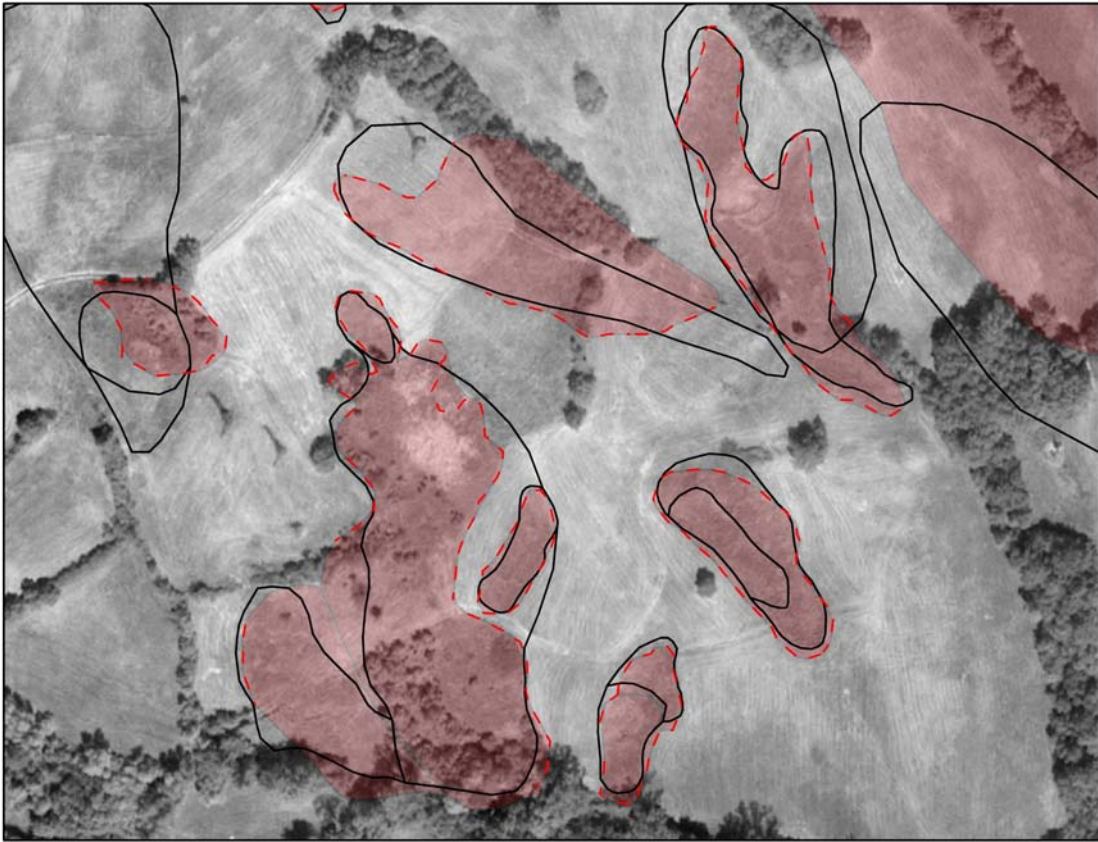


*Fig. 2.2: Comparison between the field based inventory (solid red hatch) and the remotely sensed inventory prepared on the 2012 GeoEYE satellite image (black line). The dashed red lines are the GPS tracks.*

ability of mapping the detected landslides. Realistically, it is impossible to distinguish between the conceptual model and the database quality. Therefore, in this work, I treated the two concepts together.

Several factors affect quality (Carrara *et al*, 1993; Guzzetti *et al*, 2000; Malamud *et al*, 2004; Galli *et al*, 2008; van Westen *et al*, 2008; Trigila *et al*, 2010; Guzzetti *et al*, 2012):

- investigator skills and experience;
- subjective perception of the ground truth;
- detection techniques and supports (scale, date, and quality of aerial photographs or characteristics of satellite images; type, scale, and quality of the base map; instrument type and precision);

- completeness, type, and reliability of the available information;
- data processing and manipulation (digitizing and scanning processes, raster-to-vector and vector-to-raster conversions, transformations of Coordinate Reference Systems, planar projection, *etc.*);
- final purpose.

In the literature, quality is generally associated to accuracy and completeness (Trigila *et al*, 2010; Guzzetti *et al*, 2012), and most commonly, it is assessed in relative or statistical terms, *e.g.* by comparing different landslide inventories (Carrara *et al*, 1993; Ardizzone *et al*, 2002; Wills and McCrink, 2002; Galli *et al*, 2008) or through frequency-area statistics (Malamud *et al*, 2004; Galli *et al*, 2008; Trigila *et al*, 2010). With regard to completeness, it is worth noting that it is a space and time dependent variable. Indeed, landslides are complex events that take place in space and time and whose scars persist on the territory for variable periods. Landslides may not be detected for three main interrelated reasons:

- failure of the detection technique;
- landslide ambiguous and undefined nature;

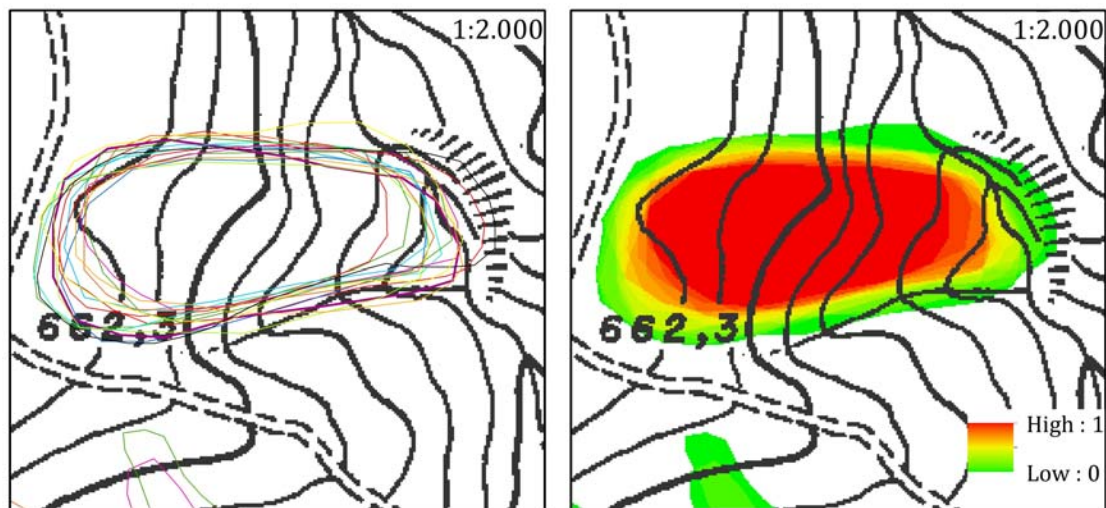


*Fig. 2.3: Fuzzy spatial logic may be a good method for handling spatial data inherent uncertainties. On the left, the results of landslide mapping related to 14 snapshots from 1981 to 2013; on the right, the related fuzzy-like analysis. The overall spatial accuracy is expressed by normalised pixel values ranging from 0 (low spatial persistence) to 1 (high spatial persistence).*

- inappropriate temporal sampling rate.

Landslide inventory maps are ultimately cartographic products. As a consequence, given the importance of spatial and temporal dimensions, I focused on their spatial and temporal accuracy. In order to do this, I identified three key factors:

- positional accuracy in relation to Coordinate Reference System (CRS) transformations;
- spatial accuracy *sensu stricto*, namely the definition of landslide shape and size;
- long-term and short-term<sup>1</sup> temporal accuracy, *i.e.* landslide temporal persistence.

In this context, in order to keep subjectivity as constant as possible, I conducted all the investigations (field and remote surveys) by myself. Notwithstanding this, the variability of interpretation remained an issue as my experience as a geomorphologist progressively increased with time.

#### Accuracy of data geographic positioning

Data geographic positioning is an inherent characteristic of spatial accuracy. Although this topic was widely debated in a country with a long and important cartographic history like Italy, it still represents a source of significant errors.

As argued in Chapter 3, I did not take into consideration absolute positioning. The widespread use of satellite survey techniques and Global Positioning Systems (GPS) emphasise the need of transformation between local CRS's and the World Geodetic System 1984 (WGS84). For this reason, I focused on *datum* transformations and on different transformation algorithms and software tools (Fig. 3.3).

#### Spatial accuracy of landslide detection and mapping

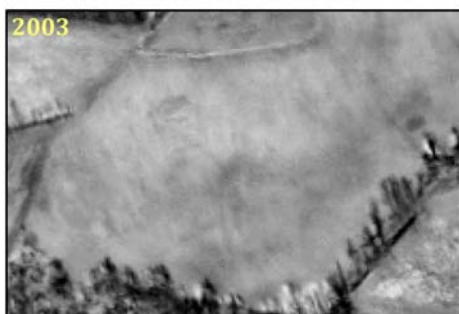
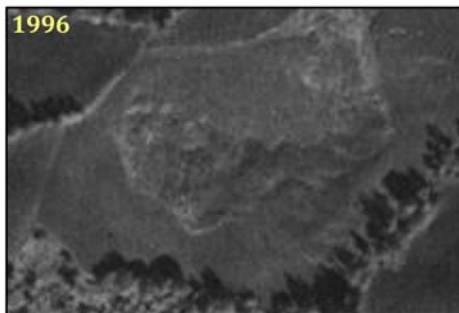
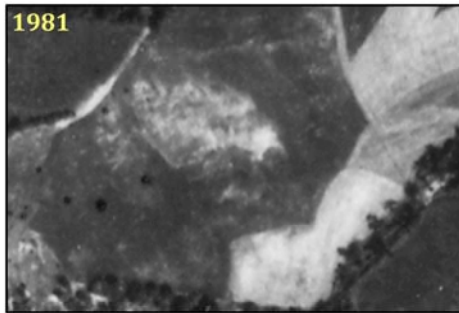
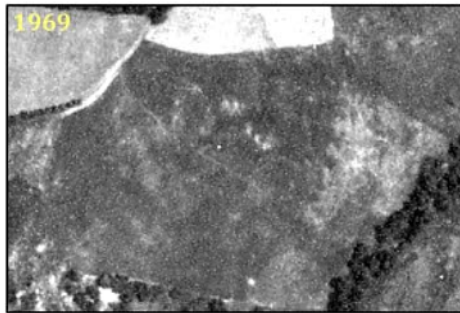
In this work, with the term “spatial accuracy” I meant the definition of landslide shape and size. Since I tried to control subjectivity, spatial accuracy depends basically on two factors:

- detection techniques and supports;

*Fig. 2.4: Landslides that develop in farmland generally show a low temporal persistence due to agricultural activities (ploughing in particular). This example portrays the same cultivated field and its evolution in 10 snapshots analysed for the Dorgola catchment study site (scale 1:3.000).*

---

<sup>1</sup> In this work, “short-term” is referred to image sets acquired in two consecutive years, although the time lag between them may be more than 12 months. These image sets are 2004, 2008, 2012, 2013, and 2014.



- data processing and manipulation.

To evaluate the first point, I compared two different detection techniques (see Chapter 4): a detailed field survey and the visual interpretation of a very high resolution (VHR) orthorectified satellite image (Fig. 2.2). The choice of the compared detection methods was made according to land-use planning goals, resources, and scale.

On the other hand, I assessed the overall spatial accuracy of landslide detection and mapping, as well as the consequences of data and support processing and manipulation, through a fuzzy-like analysis of a multi-temporal landslide inventory (Fig. 2.3) (see Chapter 4). Fuzzy spatial logic is, indeed, an effective method for handling the uncertainties related to spatial data, and it proved to be particularly efficient when dealing with boundary imprecision.

#### Landslide temporal persistence

The temporal dimension is an essential element for the quality assessment of a landslide inventory map due to the natural and anthropogenic evolution of landscape. Indeed, despite the techniques used for landslide detection and mapping, one of the most challenging issue is the temporal validity of the detected data (Fig. 2.4). In this sense, one of the aims of this research was to assess the temporal reliability of landslide inventory maps. At the same time, since landslides are detected through a series of snapshots, I also tried to determine an acceptable time interval between two consecutive images. In fact, if the sampling rate is not suitable for landslide activity, some events or changes may remain undetected (Dragicevic and Marceau, 2000).

### **2.3. Data collection**

Four case study sites were chosen in the Italian Northern Apennines within four different Provincial Administrations of the Emilia-Romagna Region (Reggio Emilia, Modena, Ravenna, and Forlì-Cesena) (Fig. 2.5). For each of them, I collected or acquired the following material:

- topographic, thematic, and historical maps;
- all available aerial photographs and high resolution satellite images (GeoEYE and



*Fig. 2.5: Location of the four case study sites with respect to the Emilia-Romagna Region and its Provincial Administrations (RE – Provincial Administration of Reggio Emilia, MO - Provincial Administration of Modena, RA - Provincial Administration of Ravenna, FC - Provincial Administration of Forlì-Cesena).*

IKONOS);

- specifically acquired VHR GeoEYE satellite images (for only two areas);
- past and current land-use plans;
- detailed field surveys specifically performed with the aid of a high precision GPS;
- public archival documents and data about landslides and landslide consolidation works.

### **2.3.1. Selection of case study sites**

Test areas were essentially used as training fields in order to exercise and improve my skills to detect and characterise landslides in various geological, geomorphological, and land-use settings. All of the areas were used to quantify the accuracy of data geographic positioning. On the other hand, given the high precision and time-consuming operations involved in their assessment, I evaluated the spatial and temporal accuracy only for one area.

The case study sites were chosen according to the following criteria:

Tab. 2.1: Approvals of the Territorial Plans for Provincial Coordination of the four Provinces under investigation.

	Reggio Emilia	Modena	Ravenna	Forlì-Cesena
1° PTCP	RCR n° 769 05/25/1999	RCR n° 1864 10/26/1998 (RCR n° 2489 12/21/1999)	RCR n° 94 02/01/2000	RCR n° 1595 07/31/2001
1° PTCP (modification)	-	PCR n° 107 07/21/2006	RCR n° 2663 12/03/2001	-
2° PTCP	PCR n° 124 06/17/2010	PCR n° 46 03/18/2009	PCR n° 9 02/28/2006	PCR n° 68886/146 09/14/2006
2° PTCP (modification)	-	-	-	PCR n° 70346/146 07/19/2010

RCR Regional Committee Resolution  
PCR Provincial Committee Resolution

- every area had to be in a different Provincial Administration and possibly within different Municipalities, in order to meet heterogeneous land-use planning rules. All of the Provincial Administrations under investigation have two generations of Territorial Plan for Provincial Coordination (PTCP) (Tab. 2.1);
- different geological, geomorphological, and land-use settings;
- higher availability of archival aerial photographs and satellite images;
- proximity to pluviometric gauges.

The final aims were to avoid *a priori* biases and to select representative areas of the regional natural and administrative context.

### 2.3.1.1. Castelnovo né Monti

The Castelnovo né Monti study site is located in the homonymous municipality of the Provincial Administration of Reggio Emilia in the western sector of the Emilia-Romagna region. This area is the main case study site because it was used for the analysis of spatial accuracy and landslide temporal persistence.

The test area corresponds to the catchment of the Dorgola Creek, a left tributary of the Secchia River, and it extends over an area of approximately 16 km<sup>2</sup>. The first human traces



*Fig. 2.6: With its sheer drops and massive presence the mesa-like feature of the Pietra di Bismantova overlooks the entire Dorgola Valley.*

in the area are dated back to the Upper Palaeolithic (Tirabassi, 2011). Ever since, man presence has been basically constant and mostly concentrated around the Pietra di Bismantova, a religious but also historical military site. Today the area is sparsely populated with no significant industrial sites. Castelnuovo né Monti, located on the northern part of the area, is the only medium size village in the surroundings. Nevertheless, small (mostly historical) settlements are scattered around the catchment.

The landscape is characterised by forested terrain, cultivated fields, and permanent meadows. The scenery is dominated by the Triassic Gypsums and by the massive presence of the Pietra di Bismantova (Fig. 2.6), a characteristic landform with a sheer drop of over 100 m. For the beauty and uniqueness of its natural features, in 2010 part of the area was included in the Appennino Tosco-Emiliano National Park.

The Northern Apennines are a fold-and-thrust belt built up by a complex multiphase convergence that started in the Upper Cretaceous with the closing of the Tethyan Sea and evolved in the Neogene with the Apennine Orogeny *sensu stricto* still active at present. In general terms, this convergence involved two continental blocks: the European Plate and the Adriatic (micro)Plate once part of the African Plate. This complex plate tectonic setting formed a thrust nappe system generally divided into three distinct paleogeographic domains (Bettelli and De Nardo, 2001):

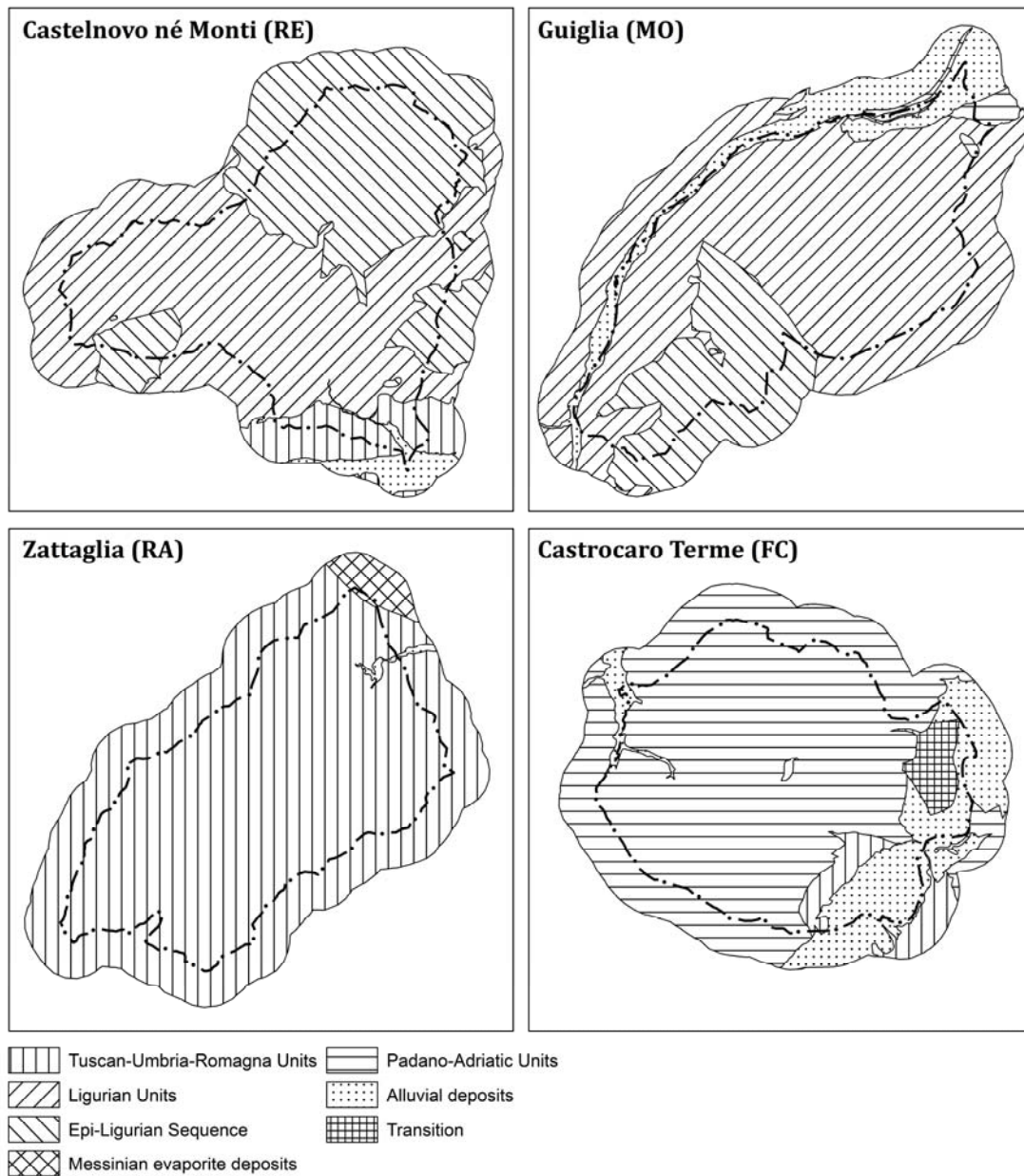


Fig. 2.7: Geological Domains (scale 1:100,000) (modified from Regione Emilia-Romagna, 2013).

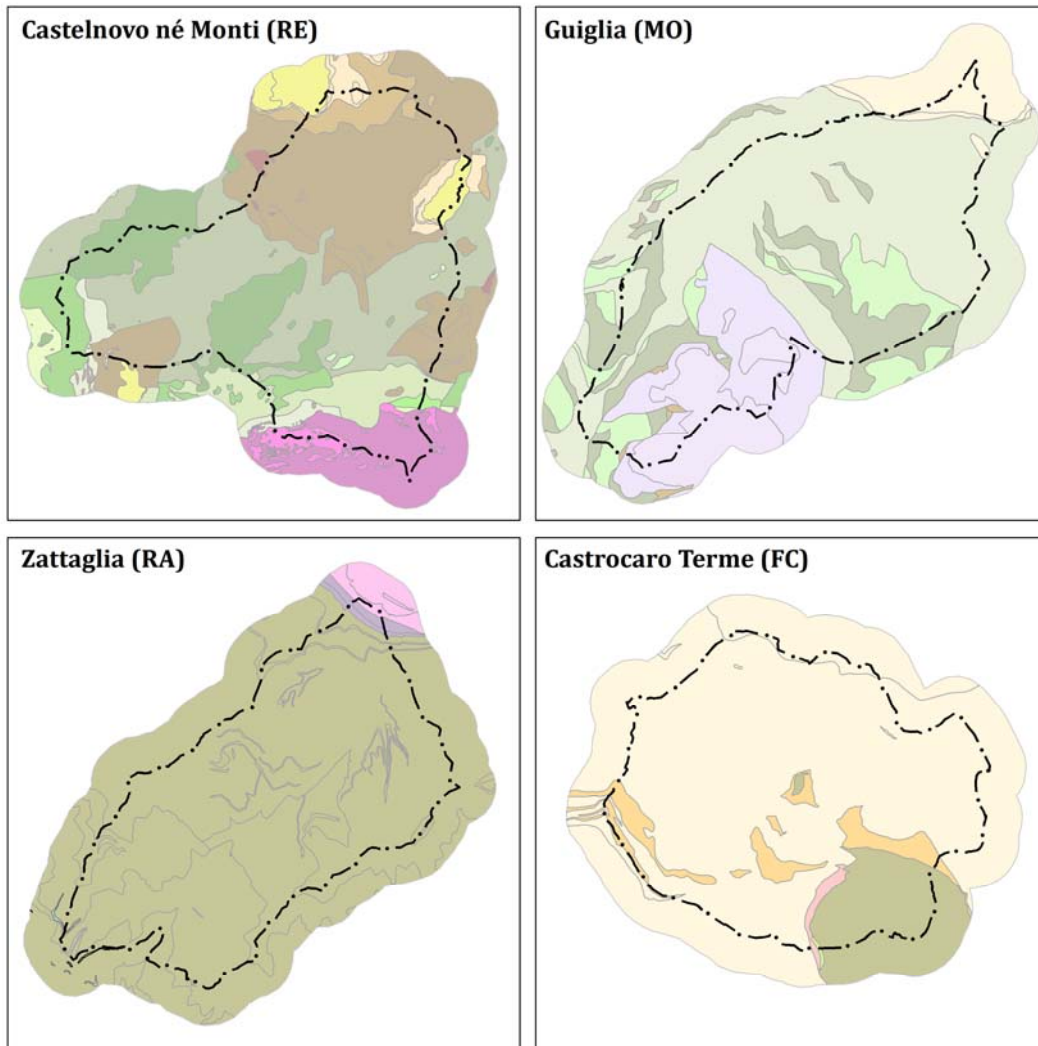
- Tuscan-Umbria-Romagna Units;
- Sub-Ligurian Units;
- Ligurian Units.

The Tuscan-Umbria-Romagna and the Ligurian Units with their Tertiary cover (Epi-Ligurian Sequence) are both present in the Dorgola catchment (Fig. 2.7). The Tuscan-Umbria-Romagna Units outcrop in the south part of the study area in correspondence of the Secchia Valley. There, the escarpments of Mt. Rosso and Mt. Merlo, carved in Late Triassic evaporates, create distinct geomorphological features. The Ligurian Units were overthrust on top of the Tuscan-Umbria-Romagna Units during the collision stage of the Apennine orogenesis (Bettelli and De Nardo, 2001). In the Dorgola Valley they correspond essentially to the Upper Cretaceous deep-water shaly and clayey units of the Argille Varicolori di Cassio, Argille Variegate di Grizzana Morandi, and Argille a Palombini and to the calcareous and arenaceous turbidite basins of the Monte Cassio Flysch and Monte Venere Formation. The Epi-Ligurian Sequence was deposited during the Early-Middle Eocene tectonic phase. In the Dorgola Valley it is separated from the underlying Ligurian Units by tectonic boundaries (Bettelli and De Nardo, 2001; Borgatti and Tosatti, 2010), and it is represented by the arenaceous and marly Ranzano (Upper Eocene-Lower Oligocene) and Antognola Formations (Upper Oligocene-Lower Miocene) and by the biocalcarenes of the Pantano Formation (Mid-Lower Miocene), which forms the Bismantova relief (Borgatti and Tosatti, 2010) (Fig. 2.8).

The Northern Apennines are an active convergent orogenic wedge (GSUEG, 1976). According to the Hazard Maps of Albarello *et al.* (1999), the Peak Ground Acceleration (PGA) values vary between 0.15 and 0.3 g, the latter with a 10% probability of exceedance in 50 years (475-year return period). The strongest historically documented earthquake (6.5 M) is dated 1920 and its epicentre was located just south of the regional border in the Lunigiana-Garfagnana area (Dipartimento di Protezione Civile, 2014).

During the Würmian glacial period the area around the Pietra di Bismantova was characterized by a periglacial morphoclimatic environment. According to the *Gruppo di Studio delle Università Emiliane per la Geomorfologia* (GSUEG) (GSUEG, 1976), at that time a vast *glacis* topographical surface radiated from the Pietra di Bismantova. This landform was the result of gelifluction and frost weathering processes that took place on gentle slopes

*Fig. 2.8: Geological maps of the four study sites (scale 1:100,000) (modified from Regione Emilia-Romagna, 2012 and 2013).*



with little or no vegetation. With time the *glacis* has been eroded by the drainage system, so that it now appears as gently sloping terraces like those near the settlements of Ginepreto, Case Merlo, Piastre, and Bellaria (GSUEG, 1976). After the last glacial period the area was covered by forests and the Secchia River started to deepen its bed. Eventually, the geomorphic system evolved again during the Holocene basically due to climatic changes (GSUEG, 1976).

Nowadays, from a geomorphological point of view, in correspondence to the Ligurian Units the Dorgola Valley is essentially characterised by a gentle hilly landscape. Indeed, their clayey and shaly deposits dip gently (usually 10°-20°) in contrast with the overlying Epi-Ligurian Sequence that may locally form sub-vertical slopes (Fig. 2.9) like in the mesa-like feature of the Pietra di Bismantova, whose summit corresponds to a lithologic-structural surface.

Due to their clayey and structurally complex nature, Ligurian Units are more prone to landslides than the Epi-Ligurian Sequence (GSUEG, 1976; Bertolini and Pellegrini, 2001, Servizio Geologico Sismico e dei Suoli, 2006). Nevertheless, with the exception of the area of Castelnuovo né Monti, landslides are pretty common all over the Dorgola catchment. In this context, some large landslides dominate on entire slopes (from the watershed to the valley bottom) creating what Crozier (2010) defined a “landslide morphology”. These large landslides can be detected from geomorphological features (*e.g.* through hummocky morphology, drainage pattern, damages and misalignments of natural and man-made features) but they cannot be precisely characterized without more detailed investigations. Furthermore, some of these mass movements had a complex and composite evolution. Indeed, after the last glaciations, they were initially triggered as multi-phase earth flows and then evolved into new earth flows during the rainiest period of the Holocene (Bertolini *et al.*, 2005; Bertolini and Pizziolo, 2008). The biggest landslide in the study area is the Bondolo landslide that extends from the SE sector of the Pietra di Bismantova to the bottom of the Dorgola Valley, close to the Secchia River. In this massive landslide, which strongly contributed to shape the local landscape, large boulders from the Pietra di Bismantova float or are buried into the clayey debris derived from the Ligurian Units (GSUEG, 1976).

The rocky cliffs of the Pietra di Bismantova, instead, are subject to lateral spread, topples, and falls, which overtime accumulated a large amount of debris (from large boulders with

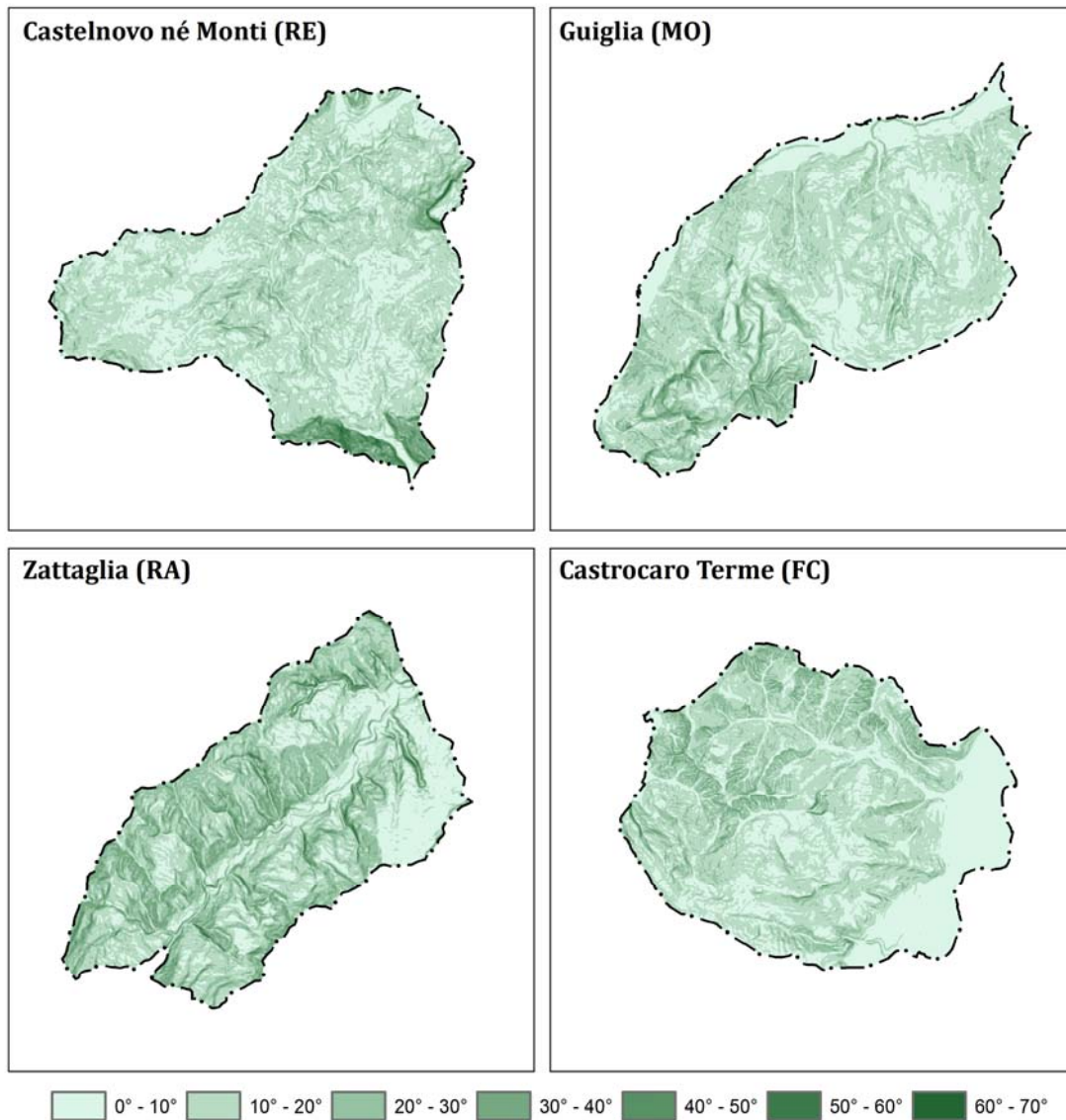


Fig. 2.9: Slope maps realised with Esri®ArcMap™ 10.1 (scale 1:100,000).

volume up to  $10^3 \text{ m}^3$  to small blocks) at the foot of the slopes (Borgatti and Tosatti, 2010). In some cases this material was then mobilised by earth slides and flows affecting the underlying formations (*e.g.* in the Bondolo landslide). Borgatti and Tosatti (2010) estimated that the maximum bounce height is 22 m, whereas the maximum run-out is 110 m from the profile starting point, which is 45 m from the foot of the slope. According to this study, the areas most susceptible to landsliding are the SE, NE and NW faces of the Pietra di

Bismantova. Here rock parameters are poorer and the degradational processes are particularly intense.

Some badlands, nowadays only partially active, can be observed in the upper part of the Dorgola Valley in the marly sediments of the Ranzano Formation. These badlands are basically concentrated close to the valley bottom and their evolution is related to the creek erosion.

The high instability of the Dorgola catchment is the result of various interrelated factors. The geological characteristics of the area (weak and weathered materials, material combination and permeability contrasts, joint sets, *etc.*) are the main predisposing and preparatory factors for landslides. Intense and prolonged rainfall, as well as snow-melt, are, instead, the most important triggering factors (Garberi *et al.*, 1999; Basenghi and Bertolini, 2001; Bertolini *et al.*, 2005; Pizziolo *et al.*, 2008; Rossi *et al.*, 2010; Montrasio *et al.*, 2012), although according to some authors (GSUEG, 1976, Bertolini and Pellegrini, 2001;



*Fig. 2.10: An example of artificial slope built by local farmers in order to improve slope stability. These slopes, whose height generally ranges from 1 to 3 m, are often covered by vegetation so that they cannot be easily detected on remote sensed images.*

Tosatti *et al.*, 2008) earthquakes should be considered as well. Furthermore, another important component for slope instability is human activity. In the study area, indeed, men have strongly contributed to alter and to accelerate the natural evolution of landscape through (GSUEG, 1976):

- deforestation;
- road constructions;
- farming.

In particular, it was a common practice for local farmers to build small artificial slopes to decrease the slope angle (Fig. 2.10). Moreover, the intense agricultural activity (especially ploughing) contributed to soil creep and to accumulate rock stockpiles along the sides of cultivated fields (GSUEG, 1976). Human activities have been particularly significant in the area of Castelnovo né Monti where the original topography was extensively levelled to allocate buildings. Nevertheless, slope stability was not affected by these important processes because of the geological setting of that particular area (GSUEG, 1976).

#### **2.3.1.2. Guiglia**

This study site takes its name after the municipality of Guiglia although it extends on two different municipalities: Guiglia and Savignano sul Panaro, both located in the Provincial Administration of Modena.

The study site extends for about 16 km<sup>2</sup> over the right bank of the Panaro River and includes few minor tributary basins. The small town of Guiglia is the only significant urban area of the study site, which is essentially characterised by small scattered settlements. Apart from few forested terrain, the landscape is basically anthropogenic, and it consists of cultivated fields and badlands. Man influence is significantly evident on rivers and streams that are mostly engineered. In particular, the Panaro River was heavily depleted by gravel extraction.

Guiglia study site falls within the Ligurian Units and their Tertiary cover (Epi-Ligurian Sequence) (Fig. 2.7). The former corresponds essentially to the Cretaceous deep-water shaly and clayey units of the Argille Varicolore di Cassio and Argille a Palombini and to the arenaceous turbidite basin of the Arenarie di Scabiazza. The Epi-Ligurian Sequence, instead, is composed of Miocene sandstones and marls, respectively from the Pantano and

Cigarelo Formation (Fig. 2.8).

#### **2.3.1.3. Zattaglia**

Zattaglia study site is located in the municipalities of Brisighella and Casola Valsenio in the Provincial Administration of Ravenna (eastern sector of the Emilia-Romagna Region).

The original test area is a small section (about 5 km long) of the Sintria Valley, and it extends for approximately 14 km<sup>2</sup>. However, due to the winter season, only 7 km<sup>2</sup> on the right riverbank were actually field surveyed (from the settlement “Il Tre” to the village of Zattaglia). In the study site there are no significant residential areas but only scattered houses. The landscape is characterised by steep slopes often ending in deep canyon-like features. Olive tree cultivation is more frequent than sowable fields, whereas wide areas are covered by young forests.

Zattaglia test area is entirely included in the Tuscan-Umbria-Romagna Units (Fig. 2.7) and is composed by different members of the Marnoso-Arenacea Formation: Miocene marly and arenaceous turbidites (Fig. 2.8).

From a geomorphological point of view, the succession of clayey and arenaceous layers plays a key role in shaping the landscape. Gentle slopes are generally present on the backslopes of crests (in correspondence of dip slopes), whereas on the frontslopes of such crests there are usually sheer drops or cliffs. Nearby the village of Zattaglia the monotonous stratification crop out in impressive canyon-like features up to 100 m deep.

#### **2.3.1.4. Castrocaro Terme**

This study site takes its name after the municipality of Castrocaro Terme and Terra del Sole, located in the Provincial Administration of Forlì-Cesena (eastern sector of the Emilia-Romagna Region).

Castrocaro Terme study site extends over an area of approximately 16 km<sup>2</sup> including two different catchments (the Cozzi-Converselle Creek and the Zanetta-Pietra Brook) and a small section of the right bank of the larger Samoggia basin. Apart from the small town of Castrocaro Terme, which lies in the alluvial plain of the Montone River, the study site has no significant urban areas but only some scattered houses. Human presence, though, may be dated back at least as far as the Lower Palaeolithic and, nowadays, the entire area is heavily affected by human activities. Indeed, the landscape is dominated by cultivated fields

(especially cereals, olive trees and vineyards) and badlands. It is worth noting that in the area there used to be two pig breeding farms both with few thousands animals. One is still active, whereas the other was dismissed after it was severely damaged by a landslide in the late 1990'.

The Castrocaro Terme study site is dominated by the Neogenic-Quaternary Sequence (Fig. 2.7) that in the area consists essentially in the Argille Azzurre Formation (Lower Pliocene-Lower Pleistocene) (Fig. 2.8). These pelagic clayey and marly-clayey deposits are rich in foraminiferous and subordinately in macrofossils like gasteropods and bivalves. Among the Argille Azzurre there is a peculiar rock that consist of an organogenic limestone referred to as Spungone. These two types of deposits create a sharp contrast in the landscape. A gentle hilly morphology, with frequent badlands basins, is indeed typical of the Argille Azzurre, whereas the Spungone generates cliff-dominated morphology characterised by NW-SE oriented crests. Landslides, in the form of mud and earth flows, are essentially concentrated in badland catchments.

### **2.3.2. Field investigations and interviews**

I conducted a detailed geomorphological field investigation for all test areas. The survey campaign started in July 2012 and, delayed by the winter season, finished in April 2013 (Tab. 2.2). I also carried out expeditious supplementary field reconnaissances in spring 2013 (Guiglia and Castrocaro Terme) and spring 2014 (Guiglia). The 2012 surveys focused not only on evident landslides (deposits and source areas) but were also aimed to recognise areas of potential instability. Hummocky topography, as well as topographic anomalies, consolidation works, infrastructure and building damages, superficial drainage systems, anomalous patterns, and ponds, badlands, particular land-uses, and water-demanding vegetation were all surveyed and reported on maps.

During field investigations, I identified landslides visually and then I located and mapped them on the Regional Technical Map (CTR) at 1:5,000 scale, which I employed as reference base support. To this regard, it is worth noting that the original survey used to generate this topographic map dates back to the 1970s (only buildings and infrastructures were occasionally updated) and, therefore, quite frequently it pre-dates landslides. As remarked

Tab. 2.2: Dates of the survey campaigns.

	2012	2013	2014
<b>Castelnovo né Monti</b>	10/01 to 11/13 (23 days)	05/19	
<b>Guiglia</b>	07/20 to 08/14 (13 days)	05/28	06/02
<b>Zattaglia</b> (not completed)	11/26 to 04/17 (18 days)		
<b>Castrocaro Terme</b>	08/21 to 09/26 (18 days)	05/14	

by Santangelo *et al.* (2010) this was an issue especially where the base map did not show clear, or sufficient, landmarks or topographic reference points to locate and map landslides, *e.g.* where pre- and post-failure topography were completely different from each other. At the same time, field investigations were also conducted with a high precision GPS (Garmin Montana 650T). In particular, the GPS receiver was carried along landslide perimeters including, and if possible differentiating, source areas and deposits. This operation was relatively simple when dealing with small to medium recent fresh landslides. On the contrary, old dormant landslides could not be identified and mapped with the same certainty because they were significantly concealed by either intense farming activities or thick forests. In this cases the definition of landslide perimeters was not straightforward and univocal. In fact, it was extremely subjective, and it implied a high uncertainty with both visual reconnaissance and GPS survey. Consequently, small to medium fresh landslides were essentially detected on the basis of GPS tracks, while old dormant landslides required also the aid of the contour lines of the base map (drainage pattern anomalies and deviations, concave/convex slope features, valley morphology, lobate landforms) (Soeters and van Westen, 1996; Santangelo *et al.*, 2010).

I completed field investigations with interviews to the local population in order to acquire more information about historical slope failures, farming common practices, land uses, and landscape evolution. The interaction with local communities represented also a chance to analyse people perception about landslides and man-landslide interaction.

The principal aim of the survey campaign was to acquire a complete and robust knowledge about local land instability and mass movements (*e.g.* warning signs, movement types, degree of activity, causes and triggers, local lithological settings, man interaction and common consolidation practices, damages and costs, *etc.*). Moreover, ground surveys were also used as training fields to exercise and improve my skills with regard to landslide detection and characterization in various geological, geomorphological, and land-use settings. Finally, survey operations represented an important occasion for valuable considerations about field survey difficulties, limitations, subjectivity, and cost-benefit analyses.

For the Castelnovo né Monti study site, I scanned and georeferenced the field survey map in order to prepare a detailed geomorphological landslide inventory map. To this end, for landslide detection and mapping I basically used the field data and the CTR. No remotely sensed data were used in this context and, in the same way, the regional landslide inventory map<sup>2</sup> was intentionally ignored. Landslides were classified according to Cruden and Varnes (1996) and their characteristics (type of movement, age, estimated degree of activity and depth, potential causes and triggers) were determined on the local geomorphological and geological context, general appearance, setting, and, where available, on historical and archival information. In particular, I inferred the relative age of the mass movement from the degree of morphological freshness and vegetation colonization. Where possible, I generally mapped the crown area separately from the deposit together with other significant features (*e.g.* tension cracks, damages to natural or man-made features, topographic anomalies, consolidation works, drainage ponding, major escarpments, *etc.*). Ultimately, in this inventory I also introduced an extra class to identify areas where no landslides were clearly detected, but where morphological (*e.g.* hummocky or generally irregular or anomalous morphology, drainage pattern anomalies, semicircular features and escarpments, *etc.*) and vegetation elements suggested probable or imminent slope failures. These areas, that I named API (Areas of Potential Instability), may be the results of landslide natural or anthropogenic evolution and/or stabilisation. In order to be precisely characterized, these areas require more detailed investigations.

---

<sup>2</sup> The regional landslide inventory map is the same one reported in the Territorial Plan for Provincial Coordination (PTCP), which will be analysed in Chapter 6.

### **2.3.3. Acquisition of GeoEYE satellite images**

VHR panchromatic and multispectral GeoEYE images were acquired for the areas of Castelnovo ne' Monti and Castrocaro Terme. Panchromatic (black and white) images present a 0.5 m resolution, whereas multispectral images have a 2 m resolution. All images were provided resampled with the Cubic Convolution method. On the whole, three sets of images for each area were captured from 2012 to 2014. In particular, the 2012 images were acquired respectively in August and July, the aims for these acquisitions were:

- to have a VHR support to prepare a remotely sensed inventory to be compared with the coeval geomorphological field inventory;
- to build up annual sequences of VHR images. In this sense, the three sets of GeoEYE images were added to the 2011 digital aerial photographs of the *Agenzia per le Erogazioni in Agricoltura* (AGEA). This allowed to have remote sensed annual data from 2011 to 2014.

### **2.3.4. Historical data**

Historical data play a key role in the reconstruction of landslide and landscape evolution. For this reason, the acquisition of all available historical data (*e.g.* consolidation works, infrastructure and building damages, previous studies and/or inventories, historical landslides, *etc.*) was an important stepping stone of the research.

The search involved different public administrations and agencies, and it aimed to collect a wide dataset. Particular attention was given to the land-use planning setting (*e.g.* past and current land-use plans) and to the acquisition of all available remote sensed images (both aerial and satellite) in order to acquire the most complete series of historical data.

## **2.4. Data processing**

Since they had been generated and managed by various producers and agencies, data had different CRS's. Therefore, in order to use them all together, they had to be transformed into a unique CRS. Nevertheless, CRS transformations, and particularly *datum* transformations, are not trivial tasks and may lead to errors and positional inaccuracies.

Indeed, geographic positioning is an important factor for data spatial accuracy, and it is treated in detail in Chapter 3.

### 2.4.1. Image processing

The aerial photographs and satellite images used for this work are summarized in Tab. 5.1. Orthorectification is the process of removing the distortion within an image caused by terrain relief and by the camera (Exelis VIS, 2013). Indeed, aerial photographs show geometric errors in the representation of features due to the effects of tilts and relief displacement. Objects are not represented in their correct planimetric position and, as a consequence, images cannot be used for accurate measurements without being first orthorectified (Campbell and Wynne, 2012). GeoEYE and IKONOS images were orthorectified by e-geos<sup>3</sup> but no information are available about the method and software that were used for this purpose. E-geos also performed the pan-sharpening process<sup>4</sup>, *i.e.* the panchromatic imagery was combined with the multispectral bands to create a 0,5 m resolution colour image. With regard to the positional accuracy, the GeoEye Product Guide (2009) reports a CE90<sup>5</sup> equal to 5 m for the 0,5 m resolution images. Conversely, according to their metadata, the aerial photographs accessible as Web Map Service (WMS) from the Geoportale Nazionale (see Tab. 5.1) were georeferenced by using the vertices of the geodetic network IGM95 and additional GPS points available in official databases. Then they were orthorectified and mosaicked with internationally recognized software. Except for the 1996 aerial photographs, for which there are no available data, the overall declared positional accuracy for these images is 4 m. Also the 2008 and 2011 AGEA aerial photographs (accessible in WMS from the Geoportale of the Emilia-Romagna Region) have the same positional accuracy. However, they were orthorectified by using the 5 m Digital Elevation Model (DEM) and the photographic points derived from the CTR. The aerial photographs supplied by the Emilia-Romagna Region and by the Geographic Military

---

<sup>3</sup> One of the two certified resellers of Digital Globe in Italy.

<sup>4</sup> Pansharpening was performed with the commercial software ERDAS IMAGINE® (e-geos, personal communication, August 21<sup>st</sup>, 2013).

<sup>5</sup> Circular error at 90% confidence which basically indicates that the actual location of an object is represented on the image within the stated accuracy for 90% of the points (GeoEYE Product Guide, 2009).

Institute (IGM) (Tab. 5.1) were neither orthorectified nor georeferenced. Unfortunately, with the technology available for this work, the 1973 and the 1978 images could not be orthorectified. Indeed, due to the low flying altitude, the study area was covered by several overlapping snapshots. In this case, orthorectification and mosaicking should be performed simultaneously for all snapshots and not one snapshot at a time as with ENVI software. For this reason the 1973 and 1978 aerial photographs were only georeferenced with the aid of the CTR using Quantum GIS, Version 1.8.0-Lisboa<sup>6</sup>. The same was done for the 1954 imagery for which the IGM could not provide the camera calibration certificate.

The high flying altitude of the remaining aerial photographs allowed to perform a two steps single-image orthorectification with ENVI 4.8 software. The first step consisted in the computation of the Rational Polynomial Coefficients (RPCs), whereas the second step was the RPC orthorectification. In order to build the sensor geometry and compute RPCs, the ENVI Build RPCs tool requires to determine the interior and the exterior orientation. The former establishes the relationship between the camera and the aerial photograph image, and it needs the camera focal length and the tie points between the aerial photographs and the camera fiducial marks (Exelis VIS, 2013). To this end, I used the camera calibration certificates provided by the IGM and by CGR Spa, who acquired the aerial photographs on behalf of the Emilia-Romagna Regional Authority. Exterior orientation, on the other hand, determinates the position and angular orientation parameters associated with the image (Exelis VIS, 2013). For its definition, it requires Ground Control Points (GCPs) with their relative elevation. In this case, since no GCPs were available, I detected them on the 2013 orthorectified pansharpened GeoEYE image and manually entered them into ENVI. I did the same also with their elevation, which I extracted from the CTR. These operations were quite challenging. Indeed, due to the different age of the base map, the base image, and the different aerial photographs, identifying reliable equivalent points was not a trivial task. Moreover, in this way, the image orthorectification was affected by the positional and geometric accuracy of the base supports. Also the number, distribution, and type of GCPs can affect the accuracy of the orthorectification (Zanutta *et al.*, 2006; Aguilar *et al.*, 2008; Hughes *et al.*, 2006). To this end, I scattered GCPs around the edges of the image but also

---

<sup>6</sup> Also historical maps were georeferenced in the same way.

across the image itself (Hughes *et al.*, 2006). This, however, in a scarcely populated and forested area, like the one under study, was not an easy task. With regard to GCPs type, as suggested by Hughes *et al.* (2006), I used only hard points with sharp edges or corners, *i.e.* building corners and road interactions, bearing in mind that even buildings and roads may have altered over time. About 40 GCPs were used for each image with an average RMS (Root Mean Square) residual<sup>7</sup> <0,5 pixel. Finally, the RPC orthorectification was applied. To perform it, the 5 m DEM of the Emilia-Romagna Region was used and both, the DEM and the aerial photographs, were processed using cubic convolution resampling.

#### **2.4.2. Landslide detection and processing**

In order to represent landslide evolution through space and time, I prepared a multi-temporal landslide inventory map for the Castelnovo né Monti study site. Given the high level of complexity involved, the realization of this kind of product is challenging and particularly time-consuming. Indeed, it requires multiple sets of aerial photographs for the same area and a high degree of experience in order to detect small morphological changes related to slope movements. Moreover, landslide detection always demands to have a clear idea of what to identify and map. In this specific case, I used the term “landslide” to define the slope failure, *i.e.* the sliding action and not the deposit. To this end, I identified and mapped the affected area (depletion and accumulation zones) of each single mass movement including all levels of reactivations of major landslides.

Landslides can be detected and mapped using different techniques and tools (Guzzetti, 2006; van Westen *et al.*, 2008). For several reasons (*e.g.* cost/benefit ratio, working scale, reliability, *etc.*), one of the most used methods is the visual interpretation of remotely sensed images (airborne and satellite) (Rib and Liang, 1978; Turner and Shuster, 1996; Guzzetti, 2006; van Westen *et al.*, 2008). In this regard, photo-interpretation and digital mapping from orthorectified images can be a good substitute of 3D vision or stereoscopic techniques (Fernandez *et al.*, 2006). The multi-temporal landslide inventory map of the Dorgola catchment was prepared using visual interpretation of orthorectified remotely

---

<sup>7</sup> The Root Mean Square (RMS) residual represents the difference in location between the GCPs on the transformed and on the original image (Hughes *et al.*, 2006), and it is generally used to provide a measure of the fit of the entire set of GCPs to the rational polynomial model.

sensed images, and it took me about 4 months to complete it. Since I had conducted the field survey as well, this inventory was inevitably influenced by my field experience. Overall, 15 to 18 sets of aerial photographs and satellite images were used for landslide detection and mapping (Tab. 5.1)<sup>8</sup>, and they were analysed both separately and in combination with each others. Landslide identification was based on the recognition of peculiar morphological, vegetation, and drainage terrain features like those reported in Tab. 2.3. In this way, landslide detectability depended essentially on the contrast with the surroundings. In particular, the distinction between stable and unstable areas was determined by specific image characteristics like *e.g.* tone, texture, pattern, and shape variations or differences. According to Soeters and van Westen (1996) this contrast is affected by:

- the time lapse between the failure and the detection, since with time erosion and vegetation colonization tend to conceal landslide distinctive features;
- the severity with which the landsliding affected morphology, vegetation, and drainage.

After identification, I digitally mapped landslides as polygons using Esri®ArcMap™ 10.1. Since each landslide was outlined on every image set, in order to connect the same landslide through time, I labelled each one with a unique ID number<sup>9</sup>. This operation was particularly time-consuming and error-prone since it had to be carried out manually according to an heuristic method. Indeed, the recognition of the same landslide in different images requires complex evaluations that could not be substituted by automated procedures based on simple geometric and spatial relations. At the same time, I used a second digital code (ID\_landslide) to define the geometric and spatial correlations among different reactivations. This allowed to differentiate up to 6 different hierarchical levels of geometric and spatial associations (Fig. 2.11).

Furthermore, I also classified landslides according to the following elements:

- landslide type, according to Cruden and Varnes (1996);
- location, *i.e.* the name of the nearest toponym;

---

<sup>8</sup> Georeferenced images (1954, 1973 and 1978) were used for landslide detection but not for mapping. In this way, the temporal analysis could rely on 18 image sets spanning over a 60-year time frame (from 1954 to 2014), while for the fuzzy-like analysis were used only the 15 orthorectified images (from 1981 to 2014).

<sup>9</sup> The same ID number was used to define both the original landslide and its reactivations. The latter were, indeed, differentiated by using the detection index.

Tab. 2.3: Morphological, vegetation, and drainage terrain features used for the remote detection of landslides (modified from Soeters and van Westen, 1996).

<b>TERRAIN FEATURES</b>	<b>RELATION TO SLOPE INSTABILITY</b>
<b>Morphology</b>	
Concave/convex slope features	Landslide niche and associated deposit
Steplike morphology	Retrogressive slinding
Semicircular backscarp and steps	Head part of slide outcrop of failure plane
Back-tilting of slope facets	Rotational movement of slide blocks
Hummocky and irregular slope morphology	Microrelief associated with shallow movements or small retrogressive slide blocks
Infilled valleys with slight convex bottom, where V-shaped valleys are normal	Mass movement deposit of flow-type form
<b>Vegetation</b>	
Vegetational clearances on steep scarps, coinciding with morphological steps	Absence of vegetation on headscarp or on steps in slide body
Irregular linear clearances along slope	Slip surface of translational slides and track of flows and avalanches
Disrupted, disordered, and partly dead vegetation	Slide block and differential movements in body
Differential vegetation associated with changing drainage conditions	Stagnated drainage on back-tilting blocks, seepage at frontal lobe, and differential conditions on body
<b>Drainage</b>	
Areas with stagnated drainage	Landslide niche, back-tilting landslide blocks, and hummocky internal relief on landslide body
Excessively drained areas	Outbulging landslide body (with differential vegetation and some soil erosion)
Seepage and spring levels	Springs along frontal lobe and at places where failure plane outcrops
Interruption of drainage lines	Drainage anomaly caused by head scarp
Anomalous drainage pattern	Streams curving around frontal lobe or streams on both sides of body



*Fig. 2.11: Geometric and spatial correlations among landslides were expressed with the use of the ID\_landslide code. In this way, 1° Level landslides represent the main unit; 2° Level landslides are reactivations inside 1° Level landslides; 3° Level landslides are reactivations located inside 2° Level landslides and so forth according to a hierarchical structure.*

- hydromorphic basin, following the Emilia-Romagna Region classification;
- geology, after the 1:10,000 scale geological map of the Emilia-Romagna Region;
- area, as measured by Esri@ArcMap™ 10.1;
- perimeter, as measured by Esri@ArcMap™ 10.1;
- state of activity; the definition provided by the UNESCO Working Party (WP/WLI, 1993) and by Cruden and Varnes (1996) raises significant issues especially as far as the classification of active landslides is concerned. Indeed, a geomorphological survey cannot detect an ongoing movement which requires proper instrumental measurements. To this end, I adopted the following specific definitions:

- 1 “active” landslides are those that moved within the last annual cycle of seasons. To be strictly congruous with this definition, these landslides were defined only where images from two consecutive years were available (2004, 2008, 2012, 2013 and 2014) even though the overall period was more than 12 months;
- 2 “suspended” landslides are those that moved more than one annual cycle of seasons ago, but they still show a fresh aspect with clear signs of recent activity (*e.g.* bare ground or little or no vegetation, irregular morphology, well preserved crown areas and scarps, cracks, *etc.*);
- 3 “dormant” landslides are those that show no evidences of recent movements. In this sense, they appear intensively colonised by a developed or fully-developed vegetation and sometimes also intensively settled by human activities.

In this work the use of the term “relict” was discouraged. Indeed, although some ancient landslides developed under different morphoclimatic conditions, hundreds if not thousands of years ago, they may still reactivate as reported by Bertolini and Pizziolo (2008) on the basis of recent and past events.

- pre- and post- land-use; I visually identified the following categories:
  - 1 bare ground (*e.g.* fresh scarps);
  - 2 cultivated fields and grassland;
  - 3 scrub;
  - 4 wood;
  - 5 mixed (*e.g.* in large landslides);
- landslide age; in order to estimate landslide age, land-use was used as a proxy. On the basis of the above listed categories, landslides were classified into: recent (land-use categories 1 and 2), relatively recent (land-use category 3) and old (land-use category 4). On the other hand, land-use category 5 indicate an undefined age since, according to the different combinations of land-uses and to the type of landslide, it can include landslides from recent to old and very old.

In order to assess landslide temporal persistence, I used all available snapshots including 1954, 1973 and 1978 image sets. For this analysis an additional index, that I named Detection Index (ID), was applied to each landslide for every available image set. The final aim was to quantify both the number of “new” landslides and the number of disappearing

landslides for each year of investigation. Particular care was taken in distinguishing those landslides that were truly new mass movements (namely the results of an actual activation or reactivation) from those that were reappearances of temporarily concealed existing landslides, *e.g.* due to the presence of clouds, shadow areas, or other impending factors. As in palaeontology a Lazarus taxon is a taxon that disappears from the fossil record for a certain period to appear again later (Fara, 2001), I named these landslides Lazarus Landslides (LL). The detection index was given the following values:

- NULL: whenever the landslide was not identified;
- 0: when the landslide was detected and apparently unchanged (no significant and evident reactivations took place);
- ##: the double digit stands for a “new” mass movement. In particular, the first number indicates the current “new” appearance, while the second shows the total number of activations/reactivations, *e.g.* 11 stands for the first and only one activation, 34 stands for the third out of four “new” detections, *etc.*. LL’s were further differentiated to be distinguished from truly new mass movements;
- -##: the negative double digit stands for disappearing landslides according to a criteria similar to the one for new landslides;
- -99: this number stands for a landslide that was erased by the activation or reactivation of a bigger mass movement.

DIs were processed automatically with an Excel worksheet.

Landslide detection and mapping are affected by an intrinsic uncertainty due to their active, and sometimes undefined, nature. Further imprecisions are also introduced by data and base support (*e.g.* maps and images) processing and manipulation (*e.g.* digitizing and scanning processes, CRS transformations, orthorectification or georeferencing, vector-to-raster and raster-to-vector transformations, *etc.*). In order to avoid misuses, it is of primary importance that this spatial uncertainty is correctly communicated to the end-users as part of data limitations. To this end, I tried to quantify the overall spatial accuracy of a landslide inventory through a fuzzy-like analysis (Fig. 2.3), which I performed according to the following step-by-step procedure:

- 1) in order to avoid spatial alterations related to new mass movements, unchanged

landslides were selected using the DIs. In particular, LL's were always considered unchanged, whereas, where a landslide had multiple reactivations, I chose to maintain the longest period of persistence and, as a second chance, the most recent one. In this case, landslides were selected manually;

- 2) using the ID\_landslide, the selected items were further subdivided accordingly to their geometric and spatial correlations in order to eliminate any spatial overlapping among different landslides. This expedient, however, could not remove partial overlapping among landslides of the same level detected from different images. Moreover, due to the low number of landslides, level 5 and 6 were not considered statistically significant, and therefore, they were not used in the following steps;
- 3) each group of landslides was transformed from features to raster (cell size 0.5 m) giving the value 1 to unstable areas and the value 0 to stable areas;
- 4) the "Cell Statistics" command of Esri®ArcMap™ 10.1 was applied to sum up the rasters of the 15 snapshots used for this analysis. The outcomes were four raster maps, one for every level of geometric and spatial connection, with integer pixel values ranging from 1 (for unstable areas that had been detected and mapped once on 15 snapshots) to 15 (for unstable areas that had been always detected and mapped);
- 5) the four output rasters were then normalised by dividing them by 15, so that the final outcomes presented floating pixel values ranging from 0 (low spatial persistence) to 1 (high spatial persistence). However, since floating values do not allow to quantify Counts, rasters were eventually reclassified into equal intervals in order to re-transformed pixel values into integers. In this way, ten classes with a 0.1 bin width were created.

These rasters purposely aim to quantify the overall spatial accuracy of a landslide inventory map over a certain period of time. Consequently, fuzzy indexes were provided only for those pixels where a landslide had been detected at least once. All the other pixels of the raster map, which anyhow could not be considered free of mass movements, were classified as "no data". To this regard, it is worth noting that in this work the term "fuzzy analysis" was used to define this type of output, although it may differ from more rigorous interpretations.

The same procedure was also used to produce a different map that could be adopted as a

proxy to quantify the temporal persistence of mass movements on the territory. To this end, all landslides (both unchanged and reactivated) were included into the analysis and, at step 4, all the rasters were summed up together. The outcome was one single map with a potential maximum pixel value of 60 (15 snapshots multiplied by 4 different levels). In relation to the period of time covered by the available images, a normalised value close to 0 stands for a low frequency of failure, whereas a value close to 1 is indicative of a high frequency.

Since it is strictly related to its analysis, the methodology used for the assessment of data geographic positioning, as well as the related data processing, are directly presented in Chapter 3.

## 2.5. Conclusions

In this work “quality” was intended as “fitness for use” (Juran, 1974), *i.e.* as the capability of data characteristics to fulfil user needs and purposes. In this sense, the lack of suitable information about the quality of a landslide inventory map represents a significant limitation to its use and, with respect to land-use planning, raises serious questions about misuses with potentially dramatic implications.

The identification of quality parameters defined the context against which quality itself has to be quantified and evaluated. In this regard, landslide data were considered multidimensional and related to spatial, temporal, and thematic components. This work, in particular, focused on the spatial and temporal accuracy, and to this end, I identified three factors:

- positional accuracy in relation to CRS transformations;
- spatial accuracy *sensu stricto*, namely the definition of landslide shape and size;
- long-term and short-term temporal accuracy, *i.e.* landslide temporal persistence.

In this context, in order to control subjectivity, which strongly conditions uncertainty, I was the only geomorphologist to conduct the field and remote surveys.

Four test areas, located in the Northern Apennines, were used to exercise and improve my skills to detect and characterise landslides in different geological, geomorphological, and

land-use settings. The same areas were also used to quantify the accuracy of data geographic positioning, while, due to time constraints, the investigations on spatial and temporal accuracy were conducted only on one area, *i.e.* the Dorgola catchment in the Municipality of Castelnovo né Monti (Reggio Emilia Province).

In order to evaluate spatial accuracy, two factors were considered essential:

- detection techniques and supports;
- data processing and manipulation.

In relation to the first point, I compared a detailed geomorphological inventory, based on a field survey, to a visual remotely sensed inventory realised on a coeval VHR satellite image. The choice of the detection techniques to be used as comparison was made according to land-use planning goals and resources. Conversely, in order to assess the overall spatial accuracy of landslide detection and mapping, I realised a fuzzy-like analysis on a multi-temporal inventory. Fuzzy spatial logic is, indeed, a valuable method for handling spatial data inherent uncertainties. Finally, I used all available snapshots to quantify landslide temporal persistence over an interval of 60 years. In particular, to investigate changes on a shorter time scale, three sets of GeoEYE satellite images were purposely acquired and then added to the AGEA 2011 digital aerial photographs in order to have remote sensed annual data from 2011 to 2014.

## CHAPTER 3

# Accuracy of data geographic positioning

- 3.1. Introduction
- 3.2. *Datums* and map projections
  - 3.2.1. Coordinate Reference Systems adopted in Italy
  - 3.2.2. Emilia-Romagna Region Coordinate Reference System
- 3.3. *Datum* transformation
  - 3.3.1. Transformation algorithms
  - 3.3.2. Transformation software
- 3.4. Methodology
- 3.5. Analysis and discussion
  - 3.5.1. Transformation reversibility
  - 3.5.2. Comparison between the transformed files and the original WGS84file
  - 3.5.3. Comparison among files transformed with different software products
- 3.6. Conclusions

## 3. Accuracy of data geographic positioning

### 3.1. Introduction

Geographic positioning is an inherent aspect of data spatial accuracy, and consequently, it represents an essential component of data quality. In particular, in landslide studies it is essential to rely on a constant geographic positioning in order to evaluate, with periodic measurements, potential displacements.

The wider availability of Global Positioning Systems (GPS) and of remote sensing data on a global scale demands more frequent transformations between local geodetic systems and the World Geodetic System 1984 (WGS84) (Featherstone, 1997; Surace, 1998; Iliffe, 2000; Travaglini, 2004; Chen e Hill, 2005; Kwon *et al.*, 2005; You e Hwang, 2006). Notwithstanding this, due to the intrinsic distortions of local geodetic networks, there is not a comprehensive transformation algorithm that can be applied worldwide (Chen e Hill, 2005). Furthermore, every *datum* transformation implies approximations (Maseroli e Nicolodi, 2002). The development of Geographic Information Systems (GIS) and the increasing exchange of data on a global scale also highlights the need to relate data with different CRS's, and at the same time, it emphasises the necessity to raise the general awareness of this issue, especially with those GIS operators who do not have an adequate geodetic background (Surace, 1998; Travaglini, 2004; Chen e Hill, 2005). Ultimately, on the one hand, since in a computerised environment there are no physical limits for measurements, the advent of digital data solved the problem of errors due to graphic signs. On the other hand, however, despite the introduction of metadata, it represented a deterioration of the historical record of processing and manipulation of the data.

The history of Italian cartography started before 1861<sup>1</sup>. Today, though, this outstanding heritage, with all its approximations and limitations, must deal with modern satellite techniques. In this context, the transformation between local and global geodetic systems is

---

<sup>1</sup> Unification of Italian states.

not an easy task. Indeed, it implies a compromise between the historical national standards<sup>2</sup> still in use and the accuracy and precision of satellite systems. In the case of the Emilia-Romagna region there is also an additional issue since the Regional Authority adopted, as standard for all regional cartography, an exclusive reference system.

In this chapter, I analyse the accuracy of geographic positioning with regard to a landslide inventory map. In particular, I focus on *datum* transformations rather than on absolute positioning. Indeed, as already remarked, potential displacements are usually detected by means of repeated measurements and, therefore, a continuous positioning is an essential prerequisite. Nevertheless, data are frequently provided with different CRS's so that it is crucial to assess the precision of the algorithms and software products used for the *datum* conversions.

### **3.2. *Datums* and map projections**

In order to locate an object on the earth surface, a geodetic system is required, *i.e.* a coordinate system (usually Geographic or Cartesian) associated with a reference framework. The latter is called a geodetic *datum*, or simply a *datum*, and it basically consists of a spatial reference against which measurements are made (Soler e Hothem, 1988). By definition a *datum* is a conventional entity defined by 8 parameters: two of shape and size and six of position and orientation. In order to be used, a *datum* must be first “realised”, *i.e.* it requires a reference network represented by a certain number of physical monuments of known coordinates that are used as references for any mapping or survey operations (Surace, 1998; Iliffe, 2000). Most *datums*, however, are realised by national reference networks that, although rigorously defined, are often affected not only by important local deformations but also by the measurement errors and computational approximations of the original survey (Surace, 1998; Donatelli *et al.*, 2002; Maseroli and Nicolodi, 2002; You and Hwang, 2006). In Italy, for example, most geodetic control points were realised at the beginning of the XX century if not even before (Donatelli *et al.*, 2002; Maseroli and Nicolodi, 2002). According to the dimensions involved, a *datum* can be planimetric

---

<sup>2</sup> Historical standards were widely used, among others, for legal purposes.

(horizontal *datum*), altimetric (vertical *datum*), or tridimensional (Soler and Hothem, 1988; Surace, 1998). In consideration of the goals of this research, I do not consider vertical *datum*.

In classical geodesy (up to the 1960s), the computations regarding positioning are referred to a mathematical surface that approximates the shape of the geoid and is actually named “reference ellipsoid”. This reference surface is generally defined by its semi-major axis, semi-minor axis, and flattening. These parameters alone, however, are not sufficient to define a *datum*. Indeed, the ellipsoid needs to be oriented by fixing its origin. This orientation can either be local (local *datum*) or regional (regional *datum*). The former is generally used at a national scale, while the latter is applied to wider areas like, for example, continents.

The advent of satellite geodesy required a tridimensional *datum* related to a geocentric ellipsoid with a global orientation (global *datum*) and an earth-centred earth-fixed set of cartesian coordinates (Soler and Hothem, 1988).

Ultimately, there is an additional factor to be taken into consideration: time. Indeed, due to astronomical precession and plate tectonics, reference monuments, as well as the coordinates of a given point, change with time. As a consequence, geodetic *datum* must be related to a specific year (Surace, 1998; Iliffe, 2000).

Positioning, however, is only part of the problem. Indeed, in order to facilitate computations and to produce simple cartographic representations, data need to be displayed on a flat surface. To this end, map projections are effective tools to represent the surface of an ellipsoid on a plane. Nevertheless, all map projections produce distortions that, according to the final purpose, can be acceptable or not. In this sense, different projections produce distinct deformations and preserve different properties (*e.g.* area, shape, distance, *etc.*).

### **3.2.1. Coordinate Reference Systems adopted in Italy**

Three different *datums* (ROMA40, ED50, and WGS84/ETRF89/ETRF2000) and two map projections (Gauss-Boaga and the Universal Transverse Mercator) are suitable for use in Italy (Surace, 1998; Baiocchi *et al.*, 2002; Donatelli *et al.*, 2002; Travaglini, 2004; Cima *et al.*, 2013;) although, historically, an additional geodetic *datum* was applied to cadastral

maps. The latter is the GE02 *datum* associated to the Bessel 1841 ellipsoid and to the Cassini-Soldner projection (Surace, 1998; Condorelli, 2010), while for geospatial data the following CRS's (Tab. 3.1) are used:

– *ROMA40 Geodetic Reference System*

This system is associated with an International ellipsoid 1924 (or Hayford ellipsoid), and it is oriented in Roma Monte Mario (Surace, 1998; Travaglini, 2004). The ROMA40 system, which uses a Gauss-Boaga projection, is also named the National System as it is the official system in use in Italy for geodetic and topographic purposes. Indeed, most of the Italian cartography, as well as the 1° order IGM triangulation network, are referred to this system (Donatelli *et al.*, 2002; Cima *et al.*, 2013).

– *ED50 (European Datum 1950) Reference System*

The ED50 reference system, created in order to connect European national geodetic networks, uses an International ellipsoid 1924 centred in Potsdam (Germany) and a Universal Transverse Mercator (UTM) projection. Latitude and longitude are calculated respectively from the equator and from the Greenwich meridian. The system, however, presents a low accuracy and, for this reason, in Italy it is applied only for cartographic purposes (Surace, 1998; Donatelli *et al.*, 2002; Cima *et al.*, 2013).

– *WGS84 (World Geodetic System 1984) Reference System*

The WGS84 is a globally consistent system that adopts a *datum* surface (WGS84 ellipsoid) centred at the Earth's centre of mass (geocentric system) and a UTM projection. As a standard geodetic system for the whole world, the WGS84 is currently the reference system being used by GPS's and satellite data. In Europe this system was substituted by the ETRS89 (EUREF Terrestrial Reference System 1989) and now by the ERTF2000 (Donatelli *et al.*, 2002; Cima *et al.*, 2013). The WGS84 was realised in Italy by a high precision tridimensional geodetic network named IGM95. In addition, the new *Rete Dinamica Nazionale* (RDN) was recently introduced; this realization includes 100 GPS permanent stations homogeneously scattered on the Italian territory.

CHAPTER 3

Tab. 3.1: Main characteristics of the Coordinate Reference Systems used in Italy (modified by Surace, 1998).

	<b>GE02</b>	<b>ROMA40</b>
Ellipsoid	Bessel 1841	International 1924 or Hayford
Orientation	Genoa, IIM (1902) f = 44° 25' 08.235" L = 0° azimuth on M. del Telegrafo a = 117° 31' 08.91"	Rome, M. Mario (1940) f = 44° 25' 08.235" l = 0° (12° 27' 08.4" E of Greenwich) azimuth on M. Soratte a = 6° 35' 00.88"
Realization	Fundamental IGM geodetic network implemented by the cadastral triangulation network.	Fundamental IGM triangulation network (1908 - 1919) implemented by the high density geodetic network.
Map projection	Cassini-Soldner	Gauss-Boaga The Italian territory is divided into two zones (West and East) 6° wide. Scale factor: 0,9996 False easting: 1.500 km (West zone) 2.520 km (East zone)
	<b>ED50</b>	<b>WGS84</b>
Ellipsoid	International 1924 or Hayford	WGS84
Orientation	Medium European orientation (European Datum 1950), Potsdam (Germany) Greenwich is the prime meridian	Geodetic system centred at the Earth's centre of mass and with the Z-axis parallel to the Earth's rotation axis.
Realization	Since it was introduced for cartographic purposes, it has no physical realization.	In Italy it was realised by the IGM95 geodetic network and by the <i>Rete Dinamica Nazionale</i>
Map projection	Universal Transverse Mercator The Italian territory is divided into three zones (32, 33, and 34) about 6° wide. Scale factor: 0,9996 False easting: 500 km	Universal Transverse Mercator The Italian territory is divided into three zones (32, 33, and 34) about 6° wide. Scale factor: 0,9996 False easting: 500 km

### 3.2.2. Emilia-Romagna Region Coordinate Reference System

According to the INSPIRE (Infrastructure for Spatial Information in Europe) project, the Emilia-Romagna Regional Authority is now starting to apply the ETRF2000 (ETRS89/UTM32N, EPSG:25832) as its official system for cartography and data exchange (Cima *et al.*, 2013). Until today, however, a local reference system has been adopted for the entire regional territory (Del. del Consiglio Regionale n° 484, 2003; Cima *et al.*, 2013). This system, specifically created for the Emilia-Romagna Region, is known as UTMA or UTM\* or UTM *asteriscato*<sup>3</sup>, and historically, it has been used as the official CRS for the regional cartographic database (*e.g.* CTR, thematic maps, spatial, land-use, and urban plans, *etc.*). Recently, the UTMA was implemented as a new regional system named UTMRER.

This exclusive reference system was introduced in order to solve the following issues (ConvER3 "GPS7", 2013; Cima *et al.*, 2013):

- bypass of zone subdivision;
- possibility to perform simple, although approximated, *datum* transformations;
- use of coordinates with fewer digits in order to be managed by old calculators with a reduced precision and memory.

To this end, however, it is worth noting that Surace (1998) states that the discontinuity introduced by zones cannot be eliminated by simply extending a zone over the next one. Indeed, this artifice violates two fundamental principles indicated by Gauss: the symmetry of the representation and the minimization of the longitudinal extension. In addition, it leads to increasing deformations along the longitudinal direction and a non homogeneous precision between those parts of the territory that are included in the extended zone and those that are not (Surace, 1998).

The local reference systems used by the Emilia-Romagna Region were developed from the *Gauss-Boaga Ovest* (GBO)<sup>4</sup> as shown in Fig. 3.1. In particular, the UTMA was derived from the GBO by means of two sets of translations. The first one, however, replaced a *datum* transformation and, consequently, the result was an approximated ED50 *datum* which

---

<sup>3</sup> Star.

<sup>4</sup> Western zone of the Gauss-Boaga projection, also known as Monte Mario/Italy zone 1 or Rome 1940/Italy zone 1.

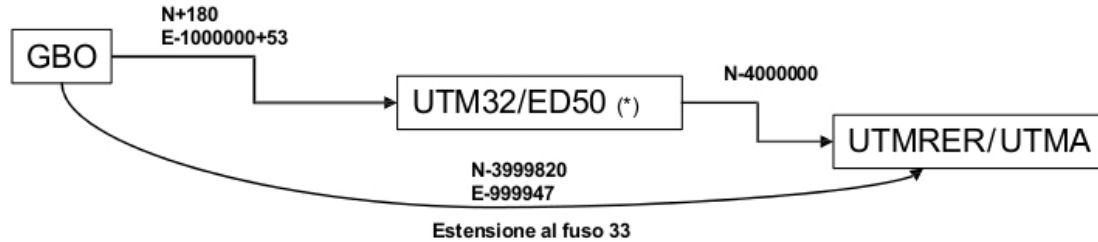


Fig. 3.1: Origin of the UTMA and UTMRER systems from the GBO. The UTMA has an UTM32/ED50\* datum derived from the GBO by means of two sets of translations rather than a proper datum conversion. The UTMRER, instead, has a ROMA40 (Monte Mario) datum and, therefore, implied no datum transformation but just a simple translation (modified from Cima *et al.*, 2013).

was denominated *UTM32/ED50\** or *UTM32CTR*; the second set, on the other hand, basically aimed to reduce the latitude coordinate digits. Moreover, zone 32 was extended on that part of the regional territory included in zone 33 (Conver3 "GPS7"; Cima *et al.*, 2013). The UTRER, instead, was introduced only recently, and, as shown in Fig. 3.1, it shares the same origin of the UTMA. In this way a given point is identified by the same coordinates in both reference systems which basically differ from each other because the UTMRER uses a ROMA40 (Monte Mario) *datum*, whereas the UTMA uses an approximated ED50\* *datum*<sup>5</sup>. This factor is irrelevant for the transformation between UTMA and UTMRER<sup>6</sup>, but it becomes particularly important for *datum* conversions like, for example, for the transformation to WGS84. In this case, it is actually recommended to use the UTMRER, although until recently the UTMA was the only reference system available<sup>7</sup>.

<sup>5</sup> I use this term to indicate the approximated ED50 *datum* created by the Emilia-Romagna Region and denominated UTM32/ED50\* or UTM32CTR.

<sup>6</sup> For the transformation between UTMA and UTMRER shapefiles, the Emilia-Romagna Regional Authority suggests to simply substitute the related PRJ files without using any software (Cima *et al.*, 2013).

<sup>7</sup> If directly used for *datum* transformations, due to its origin, the UTMA would inevitably introduce an approximation.

### 3.3. Datum transformation

Historically, many countries developed their own national *datum*. The advent of satellite geodesy, however, introduced more precise positioning techniques that, due their accuracy, continuity, and efficiency, represent a standard method for establishing networks and constructing a basis for spatial data (Surace, 1998; Kwon *et al.*, 2005). Furthermore, the increasing use of GPS's and GIS's demands more attention to the transformations between local and global geodetic systems (Featherstone, 1997; Iliffe, 2000; Travaglini, 2004; Chen e Hill, 2005; Kwon *et al.*, 2005; You e Hwang, 2006). Choosing the CRS for a GIS project is, indeed, a fundamental step for its preparation since the available data may have been acquired using different methods and techniques and, therefore, may present different *datums*, projections, and coordinate systems (Chen e Hill, 2005). In this sense, only the definition of a single CRS may guarantee a proper data overlay and a correct application of all GIS tools and commands (Condorelli, 2010). The required transformations may be simple operations within the same *datum* or may involve more complex computations to convert one *datum* into another. According to the research aims, I focused only on the latter and, in particular, on the mutual conversions between: ROMA 40, ED50\*, and WGS84.

Due to the inherent distortions of the classical geodetic networks, there is no optimal transformation algorithm that can be adapted to all cases (Chen e Hill, 2005). In fact, effective correlations, *i.e.* the comparison of points whose coordinates are known in both systems, can be carried out only locally and must be limited to areas with similar distortions (Vanicek e Steeves, 1996; Donatelli *et al.*, 2002; Maseroli e Nicolodi, 2002). Furthermore, Maseroli and Nicolodi (2002) stated that the conversion of GPS data to the Italian local reference system necessary implies a corruption of the GPS accuracy. Indeed, in order to adapt to the official standards, satellite geometry must align to a reference system that is inevitably affected by errors<sup>8</sup>. For this reason, Maseroli and Nicolodi (2002) recommended to avoid *datum* transformations whenever they are not necessary and specifically in those studies that appraise relative movements on the basis of repeated

---

<sup>8</sup> In Italy the difference between the precision of the historical network (20-30 cm) and that of the IGM95 (about 2.5 cm) is one order of magnitude (Maseroli and Nicolodi, 2002).

measurements like, for example, in the analysis of slope failures. Notwithstanding this, with regard to landslide hazard and risk, it is quite unlikely to bypass *datum* conversions since the available data often present different *datum*. In this specific work, for example, it was necessary to correlate data with a WGS84 *datum* (GPS's records and satellite images) and data that use the regional reference systems UTMA and UTMRE (e.g. CTR, land-use plans, rain gauge location, etc.).

### 3.3.1. Transformation algorithms

According to Collier and Steed (2001), the essential conditions to perform a *datum* transformation are simplicity, efficiency, uniqueness, and rigor. In this sense, the 7-parameter transformations (e.g. the Bursa-Wolf and the Molodensky-Badekas) are among the most widely used conversion methods (Maseroli and Nicolodi, 2002; Chen and Hill, 2005; Kwon *et al.*, 2005). Essentially, they handle the *datum* conversion as a three-dimensional Cartesian coordinate transformation with three translations (origin offset), three rotations (axis orientation), and one scale factor. The 7-parameters (dx, dy, dz, rx, ry, rz and one scale factor) are appraised by applying the method of the least squares to a given number of points whose coordinate are known in both systems. Ideally, if control networks had no distortions, the residuals would be null. This, however, is not the case and, as a consequence, the transformations are not precise. The Bursa-Wolf and the Molodensky-Badekas transformations basically differ for their application point. Indeed, the former is specifically suited to satellite *datum* on a global scale, while the latter is more suitable to the transformation between terrestrial and satellite *datums* (Featherstone, 1997; Deakin, 2006).

The Molodensky-Badekas, in particular, had been adopted by the IGM for the ROMA40-WGS84 transformation. To this end, the 7-parameters were set for the surrounding (10-15 km) of each IGM95 control point. Despite few advantages, the consequent subdivision of the national territory presented, however, evident problems of continuity and ambiguity (Donatelli *et al.*, 2002). For this reason the IGM introduced a new empirical transformation method based on a matrix (*grigliati*<sup>9</sup>) made up by the differences between the coordinates

---

<sup>9</sup> Grids.

of homologous points. This matrix was eventually integrated into a specific software tool (IGM software Verto) that provides interpolated but continuous and univocal results<sup>10</sup>. With regard to the ED50 – WGS84 *datums*, the IGM performed the transformation in an indirect, although analogous, way through the conversions ROMA40-ED50 and ROMA40-WGS84 (Donatelli *et al.*, 2002).

### 3.3.2. Transformation software

Three independent studies were realised by Baiocchi *et al.* (2002), Del Moro and Lancia (2007), and Travaglini (2004) to test the performance of different software tools with regard to *datum* transformation. Some of the tested products, which include dedicated software and GIS's, are available only in Italy (CartLab, TN-ShArc e Transpunto) while others are commercial international software (ArcGIS e MapInfo Professional). According to these studies, Transpunto<sup>11</sup> and CartLab show the most precise results. In particular, for the ROMA40–WGS84 conversion, they provide values that are generally less than 1 m and that, especially for CartLab, present a quite homogeneous distribution (Del Moro e Lancia, 2007). Conversely, the precision of the other software is rather variable and ranges from 1 m to a few tens of metres. For Del Moro and Lancia (2007), this discrepancy is due to a *datum* conversion based on a simple mathematical transformation without the use of any physical control point

Despite the UTM RER was officially entered in the IOGP's EPSG Geodetic Parameter Dataset (EPSG:5659), it has not yet been introduced in the most common software tools and GIS's<sup>12</sup>. As a consequence, although there are plenty of products for *datum* transformation, for this work the choice was limited by the specific CRS's and the type of files (shapefiles of polygons). Ultimately, three software tools were used as comparison: the freeware ConvER3-GPS7<sup>13</sup>, purposely produced by the Emilia-Romagna Region, and the Blue Marble

---

<sup>10</sup> See Donatelli *et al.* (2002) for more details about the *grigliati* method.

<sup>11</sup> A freeware produced by the Italian Ministry of Environment.

<sup>12</sup> Some GIS's, like for example Esri@ArcMap™, allow to manage unconventional reference systems. This, however, requires complex geodetic settings that go beyond the purposes of this work.

<sup>13</sup> This work did not test the 2013 version of the software, because it was not possible to solve some doubts and issues about it.

programs Global Mapper 13 EN and Global Mapper 14 ITA<sup>14</sup> which both allow to transform unconventional CRS's through a simple PRJ file. The difference between the English and the Italian version of Global Mapper is that the former is conceived to be used worldwide, while the latter is specifically dedicated to the Italian territory. The default transformations applied by Global Mapper 13 EN are the 3-parameter Molodensky-Badekas for the ED50 and the 7-parameter Bursa-Wolf for the ROMA40 (see Tab. 3.2) (Blue Marble, personal communication, April 1<sup>st</sup>, 2014). On the other hand, according to the Italian company that manages the software on behalf of Blue Marble, Global Mapper 14 ITA adopts a conversion method similar to that used by IGM, *i.e.* the *grigliati* method (Global Mapper Italia, personal communication, April, 2013). With regard to ConvER3-GPS7, it adopts a transformation algorithm very similar to that of the IGM software Verto described by Donatelli *et al.* (2002).

Tab. 3.2: Parameters used by Global Mapper 13 EN for the 3-parameter Molodensky-Badekas and the 7-parameter Bursa-Wolf transformations.

Datum Name	ED50 (ITALY)	ROME40 (M. MARIO) (GREENWICH)	ROME40 (M. MARIO) (ROME)
EPSG Code	6230	6265	6806
Ellipsoid Name	International 1909 (Hayford/Intl 1924)	International 1909 (Hayford/Intl 1924)	International 1909 (Hayford/Intl 1924)
dX (m)	-87.00	-104.10	-104.10
dY (m)	-98.00	-49.10	-49.10
dZ (m)	-121.00	-9.90	-9.90
rX (as)	N/A	0.9710	0.9710
rY (as)	N/A	-2.9170	-2.9170
rZ (as)	N/A	0.7140	0.7140
Scale (x 10 <sup>-6</sup> )	N/A	-11.68000	-11.68000

<sup>14</sup> During the research, Blue Marble released new versions of both software. In order to test compatibility, I performed an expeditious comparison between the used versions and the new ones (Global Mapper 15 EN and Global Mapper 15 IT). Results proved that the transformation algorithms had not been revised and that, therefore, the outcomes of this work may be extended also to the newest versions of Global Mapper.

In this sense, it can run both the IGM *grigliati*<sup>15</sup> and the related version prepared by the Emilia-Romagna Region on the basis of the GPS 7 km regional network (ConvER3 "GPS7", 2013). The outcomes of *datum* conversion inside the regional borders differ from the IGM values of few cm in planimetry and of few dm in height (ConvER3 "GPS7", 2013).

### 3.4. Methodology

The data collected for this work refer to three different *datums*. Consequently, *datum* transformations are an essential step for a proper analysis. In particular, I focused on the conversions between the unconventional regional reference systems (UTMA/ED50\* and UTMRER/ROMA40) and the WGS84, whereas the transformation between UTMA/ED50\* and UTMRER/ROMA40 was not tested (see par. 3.2.2. for details). With regard to the software tools, instead, this work was bound to three programs (see par. 3.3.2. for details).

The conventional method used to appraise the geodetic performance of a software tool requires a network of control points equally distributed on the territory and whose coordinates are known in different reference systems (Baiocchi *et al.*, 2002; Travaglini, 2004; Del Moro e Lancia, 2007). Nevertheless, in order to test directly the effects of *datum* transformations on a landslide inventory map, in this work I used landslide polygons as references<sup>16</sup>. It was, therefore, necessary to have a landslide inventory map available in all three reference systems. To this end, I downloaded the shapefiles "*Coperture quaternarie*" (Quaternary deposits) from the regional website *Catalogo dei Dati Geografici* (catalogue of geographic data) (Regione Emilia-Romagna, 2013) with the following CRS's:

- EPSG: 202032                      UTMA/ED50\*
- EPSG: 202003/5659             UTMRER/ROMA40
- EPSG: 32632                     WGS84/UTM Zona 32N

According to their metadata, however, these files were all acquired with an ED50 UTM32N\*RER (false North = -4.000.000 m)<sup>17</sup> CRS; therefore, only the EPSG:202032 UTMA/ED50\* file has a truly "original" *datum*. Notwithstanding this, since these data were

---

<sup>15</sup> The IGM *grigliati*, however, are not included in the software tool.

<sup>16</sup> I used polygon shapefiles instead of points in order to appraise potential areal distortions.

<sup>17</sup> In April 2014 the same metadata were changed into UTMRER (MONTE MARIO / UTMRER).

provided by an official and reliable source, I assumed that they were adequately verified and that the declared CRS was, indeed, correct.

In consideration of the research aims, and in order to reduce the processing times, I focused only on the landslide polygons included in the four study sites so that I could select complete features identified by a unique GISID<sup>18</sup>. The three shapefiles with the different CRS's were then transformed one into the other by using the above mentioned software tools (see par. 3.3.2.). To this end, it is worth noting that while ConvER3-GPS7 could distinguish the regional reference systems both Blue Marble products could not perform the conversion directly, but, instead, they had to use the "UTMA.prj" and "UTMRER.prj" files provided by the Emilia-Romagna Region (Tab. 3.3).

*Tab. 3.3: Details of the PRJ files of the UTMA and UTMER systems.*

<b>UTMA.prj</b>	<b>UTMRER.prj</b>
PROJCS["ED_1950_UTM_Zone_32A"]	PROJCS["UTMRER"]
GEOGCS["GCS_European_1950"]	GEOGCS["GCS_Monte_Mario"]
DATUM["D_European_1950"]	DATUM["D_Monte_Mario"]
SPHEROID	SPHEROID
["International_1924",6378388.0,297.0]	["International_1924",6378388.0,297.0]
PRIMEM["Greenwich",0.0]	PRIMEM["Greenwich",0.0]
UNIT["Degree",0.0174532925199433]	UNIT["Degree",0.0174532925199433]
PROJECTION["Transverse_Mercator"]	PROJECTION["Transverse_Mercator"]
PARAMETER["False_Easting",500000.0]	PARAMETER["False_Easting",500053.0]
PARAMETER["False_Northing",-4000000.0]	PARAMETER["False_Northing",-3999820.0]
PARAMETER["Central_Meridian",9.0]	PARAMETER["Central_Meridian",9.0]
PARAMETER["Scale_Factor",0.9996]	PARAMETER["Scale_Factor",0.9996]
PARAMETER["Latitude_Of_Origin",0.0]	PARAMETER["Latitude_Of_Origin",0.0]
UNIT["Meter",1.0]	UNIT["Meter",1.0]

---

<sup>18</sup> Since the study areas were identified on watersheds, the landslide polygons within them are essentially complete features.

After the conversion, all the shapefiles with the same CRS were visualised with Esri®ArcMap™ 10.1. This expeditious comparison highlighted a discrepancy not only with regard to the original file, *i.e.* the file that was not involved in any transformations, but also between the files converted with different software tools (Fig. 3.2.). In order to appraise these differences in quantitative and spatial terms, the different shapefiles were imported into Vectorworks and the landslide polygons with the same GISID were connected with each other. Next, for each feature the minimum, maximum, and average values of the most significant descriptive parameters of the offset vector were calculated, *i.e.*:

- absolute magnitude ( $d$ );
- longitude component ( $\Delta x$ );
- latitude component ( $\Delta y$ ).

These data, determined for landslide barycentres as well as for each vertex of landslide

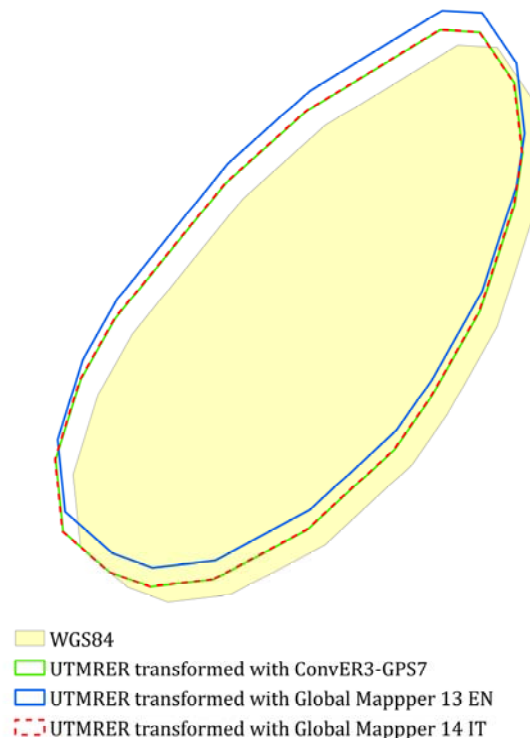


*Fig. 3.2: Comparison between transformed landslide polygons (using ConVER3-GPS7, Global Mapper 13 EN, and Global Mapper 14 IT) and the original untransformed polygon in WGS84.*

Tab. 3.4: Outline of the comparisons realised in this work. The orange hatches indicate the comparisons with the original WGS84, while the green hatches refer to the comparisons of the results obtained with different software tools.

	WGS84	ConvER3-GPS7	Global Mapper 13 EN	Global Mapper 14 IT
WGS84	-			
ConvER3-GPS7		-		
Global Mapper 13 EN			-	
Global Mapper 14 IT				-

polygons, were eventually imported into an Excel worksheet.

Ultimately, in order to quantify both the absolute and the relative accuracy of each program, I compared the transformed files with the original one and with each other (Tab. 3.4). In particular, to analyse the offset spatial distribution and to evaluate if it shows a peculiar trend, the data of every single vertex were elaborated and interpolated<sup>19</sup> with Surfer 11. The Surfer grid was then used by Esri®ArcMap™ 10.1 to elaborate offset isolines with an interval of 1 cm. The related contour maps are shown in Appendix A and B, while Tab. 3.5 and Tab. 3.7 show the numerical values related to landslide barycentres.

## 3.5. Analysis and discussion

### 3.5.1. Transformation reversibility

According to the OGP, the EPSG:5659 has a reversible conversion. However, since this is a local reference system with implicit approximations, I decided to appraise the veracity of this statement. To this end, I performed a forward transformation and then a reverse one, *i.e.* from UTMA/UTMRER to WGS84 and backwards. The results show that for the UTMER the difference is <1 mm when using ConvER-GPS7 and Global Mapper 14 IT, whereas is one order of magnitude higher for Global Mapper 13 EN. With regard to the UTMA, instead, ConvER3-GPS7 and Global Mapper 13 EN present an unchanged precision, while Global

<sup>19</sup> For the interpolation was used the Kriging method.

Mapper 14 IT increases its difference of one order of magnitude.

At the same time, I compared the outcomes of single opposite transformations (*e.g.* UTMA→WGS84 and WGS84→UTMA) which, if completely reversible, should return vectors with an equal magnitude. In this sense, Tab. 3.5 shows that ConvER3-GPS7 has an imprecision <1 mm, while for the Blue Marble products it is in the order of the millimetre. These differences almost certainly arise from rounding in the finite precision representation of the transform parameters and the coordinates. Nevertheless, according to the aims of this work and in consideration of the order of magnitude of these differences, this approximation can be considered acceptable. As a consequence, in the following paragraphs I present only the results of the transformations from UTMER/UTMA to WGS84 considering the inverse conversions as homologous.

### **3.5.2. Comparison between the transformed files and the original WGS84 file**

The maps contained in Appendix A show the spatial representation of the effects of the transformations from UTMER/UTMA to WGS84. Their analysis reveals that the offset progressively increases eastward (average gradient <1 m) with the exception of the conversions performed with ConvER3-GPS7 which present a minimum offset in correspondence of the Guiglia study site. This latter trend cannot be explained, at least apparently, by the spatial distribution of the vertexes of the GPS 7 km network (Fig. 3.3), though, it may be interpreted as a consequence of the different transformation method used by the software. Given the aims of this work, however, the in-depth analysis of this issue should be addressed by further researches. Conversely, the fact that the offset increases eastward is compatible with the approximations introduced by both local reference systems which include all the Emilia-Romagna territory in zone 32 (Gauss-Boaga western zone). An approximation that voluntarily introduces an error in those areas that would be in zone 33 (Gauss-Boaga eastern zone).

The analysis of the maps in Appendix A also shows that, within each single study site, the offset is in the order of the centimetre with an approximate SW-NE trend. Local fluctuations, especially in the area of Guiglia, may be affected by the different transformation

Tab. 3.5: Descriptive parameters of the offset vector between the transformed UTM RER/UTMA files and the original WGS84 file. These values (in metres) were calculated with respect to the barycentre of landslide polygons. Dmin/max/average - absolute magnitude of the offset vector;  $\Delta x$ min/max/average - longitude component;  $\Delta y$ min/max/average - latitude component.

UTMRER	ConvER3-GPS7		Global Mapper 13 EN		Global Mapper 14 IT	
	A	B	A	B	A	B
Dmin	1.0892	1.0890	1.7627	1.7611	1.1618	1.1624
Dmax	1.9739	1.9738	3.2162	3.2147	2.0203	2.0216
<b>Dmean</b>	<b>1.5387</b>	<b>1.5385</b>	<b>2.4401</b>	<b>2.4385</b>	<b>1.5203</b>	<b>1.5207</b>
$\Delta x$ min	0.1654	0.1654	0.2486	0.2490	0.1409	0.1417
$\Delta x$ max	1.4803	1.4804	1.3236	1.3236	1.5330	1.5341
<b><math>\Delta x</math>mean</b>	<b>0.9380</b>	<b>0.9380</b>	<b>0.8143</b>	<b>0.8143</b>	<b>0.9322</b>	<b>0.9325</b>
$\Delta y$ min	1.0258	1.0255	1.7369	1.7353	0.9233	0.9228
$\Delta y$ max	1.3263	1.3261	2.9406	2.9390	1.3286	1.3292
<b><math>\Delta y</math>mean</b>	<b>1.1631</b>	<b>1.1629</b>	<b>2.2831</b>	<b>2.2815</b>	<b>1.1323</b>	<b>1.1325</b>

UTMA	ConvER3-GPS7		Global Mapper 13 EN		Global Mapper 14 IT	
	A	B	A	B	A	B
Dmin	1.0892	1.0890	2.1464	2.1472	2.1464	2.1472
Dmax	1.9739	1.9738	2.6313	2.6324	2.6313	2.6324
<b>Dmean</b>	<b>1.5387</b>	<b>1.5385</b>	<b>2.4033</b>	<b>2.4040</b>	<b>2.4033</b>	<b>2.4040</b>
$\Delta x$ min	0.1654	0.1654	1.3848	1.3829	1.3848	1.3829
$\Delta x$ max	1.4803	1.4804	1.8094	1.8077	1.8094	1.8077
<b><math>\Delta x</math>mean</b>	<b>0.9380</b>	<b>0.9380</b>	<b>1.6305</b>	<b>1.6287</b>	<b>1.6305</b>	<b>1.6287</b>
$\Delta y$ min	1.0258	1.0255	1.6024	1.6051	1.6024	1.6051
$\Delta y$ max	1.3263	1.3261	2.0142	2.0169	2.0142	2.0169
<b><math>\Delta y</math>mean</b>	<b>1.1631</b>	<b>1.1629</b>	<b>1.7628</b>	<b>1.7655</b>	<b>1.7628</b>	<b>1.7655</b>

A - UTM RER/UTMA  $\rightarrow$  WGS84  
 B - WGS84  $\rightarrow$  UTM RER/UTMA

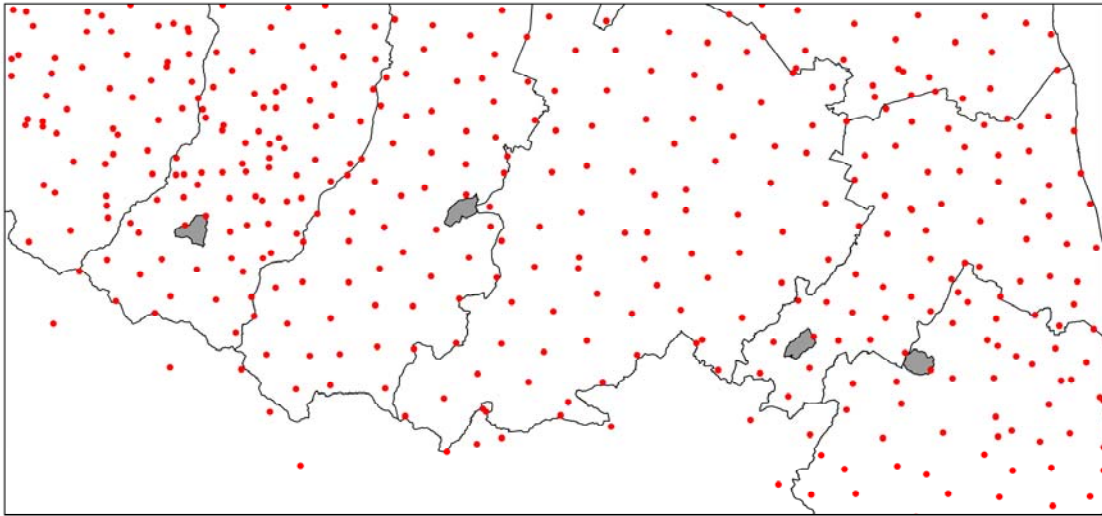


*Fig. 3.3: Spatial distribution of the vertexes (red dots) of the GPS 7 km network realised by the Emilia-Romagna Region.*

algorithms<sup>20</sup> as well as by the spatial relationship among the four study sites and by the quantity and the spatial distribution of the data used for this study. Indeed, while the algorithm and the grid used for the contouring are the same for all the four areas, the spatial distribution of landslide polygons and the concentration of the related vertexes (digit/m) are not homogeneous (Fig. 3.4 and Tab. 3.6).

This work revealed that the total offset, due to the conversion from UTM RER/UTMA to WGS84, is in the order of a metre. In particular, as highlighted by the maps in Appendix A, ConvER3-GPS7 provides the minimum values (1,10 m - 1,97 m) whereas Global Mapper 13 EN presents the highest ones (UTMRER: 1,77 m - 3,21 m; UTMA: 2,15 m - 2,63 m). Global Mapper 14 IT, on the other hand, shows contrasting values. Indeed, for the UTM RER system it provides results similar to those of ConvER3-GPS7 (1,17 m - 2,02 m), while for the UTMA system it is more in agreement with Global Mapper 13 EN (2,15 m - 2,63 m). Similar outcomes emerge also from Tab. 3.5 that shows the absolute magnitude and the longitude and latitude components of the offset vector calculated with respect to the barycentre of landslide polygons.

In this specific case, the differences between the transformed UTM RER/UTMA files and the

<sup>20</sup> The trend changes from software to software.

original WGS84 file emphasise the importance of an additional factor: data lineage, *i.e.* data historical information (see par. 2.2.2.). Indeed, as already remarked (see par. 3.4.), the metadata provided by the *Catalogo dei Dati Geografici* report that the data used for this work were initially acquired as ED50 UTM32N\*RER (false North = -4.000.000 m)<sup>21</sup>, therefore,

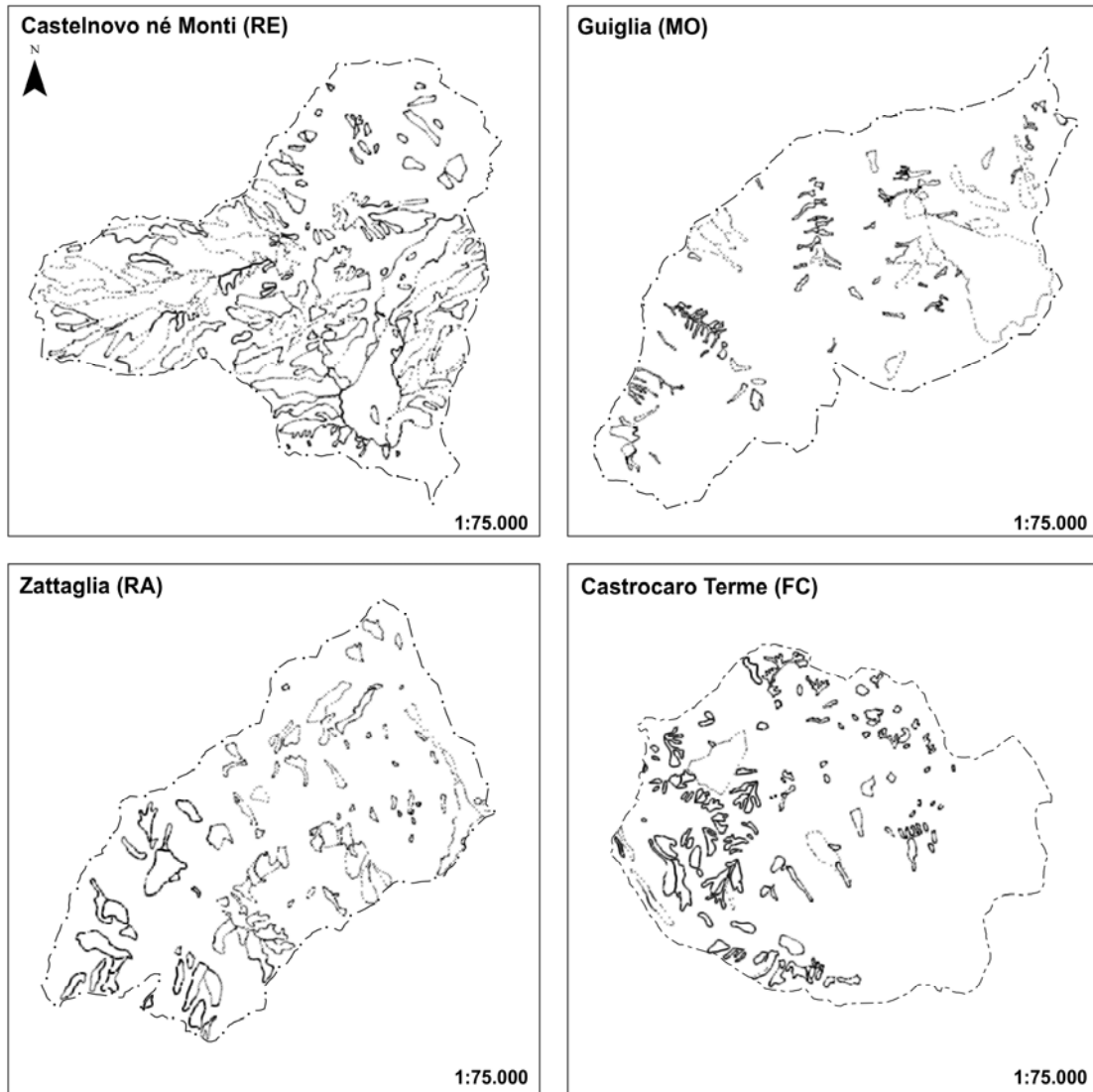


Fig. 3.4 – Spatial distribution of landslide polygons and of the related vertexes within the four study sites.

<sup>21</sup> In April 2014 the same metadata were changed. The new metadata report that data were initially acquired as UTMRER (MONTE MARIO / UTMRER).

Tab. 3.6: Concentration of landslide polygons and of their related vertexes in the four study sites.

	Landslide polygons		Points		Points/Polygons
	#	%	#	%	
<b>Castelnovo né Monti (RE)</b>	121	28	8,774	36	73
<b>Guiglia (MO)</b>	93	22	3,573	15	38
<b>Zattaglia (RA)</b>	92	21	5,102	21	55
<b>Castrocaro Terme (FC)</b>	122	29	6,679	28	55
<b>Tot.</b>	<b>428</b>		<b>24,128</b>		

the WGS84 file was inevitably involved in at least another *datum* transformation<sup>22</sup>. The data, however, are lacking any information about their processing history, in particular, as far as previous *datum* transformations are concerned (algorithm and software). Consequently, it is impossible to know whether this conversion was correctly performed with the support of the UTMRE or if it was performed directly from the UTMA that is from an unconventional and approximated ED50 *datum* (see par. 3.2.2. for details). Briefly, I cannot exclude that the data used for this work are affected by a problem due to the historical evolution of the regional CRS, *i.e.* by the approximated transformation from GBO to ED50\*. In this sense, although the introduction of the UTMRE system technically solved this issue, the uncontrolled spread of UTMA data and their conversion to other *datums*, together with the lack of information about data lineage, introduced a possible set of errors.

Finally, it is worth noting that while ConVER3-GPS7 achieved the same results for both UTMA and UTMRE, the Blue Marble programs generated different outcomes for the two reference systems. Once again, this discrepancy demonstrates that ConVER3-GPS7 was specifically created to manage the Emilia-Romagna regional systems. In fact, this software takes into consideration the system origin and approximations (Cima *et al.*, 2013). In particular, when converting the UTMA system with ED50\* *datum* into WGS84, ConVER3-

<sup>22</sup> From UTMA to WGS84.

GPS7 operates both a translation and an appropriate *datum* transformation<sup>23</sup>. Conversely, since they do not recognise the distinctiveness of the ED50\* *datum*, the Blue Marble software tools treat it as if it were a conventional ED50 *datum* introducing important approximations into the computational process.

### 3.5.3. Comparison among files transformed with different software products

The offset values between the barycentre of landslide polygons transformed with different software tools are shown in Tab. 3.7, whereas Appendix B contains the contour maps with the spatial representation of the offset values referred to each single vertex of landslide polygons.

Despite the different transformation method, for the UTMA Global Mapper 13 EN and Global Mapper 14 ITA provided the same results since both of them could not recognise the peculiarity of this system (Tab. 3.7). On the other hand, in absolute terms, the offset between the outcomes of the Blue Marble software and ConvER3-GPS7 range from 0.72 m in the Castrocaro Terme area to 2.25 m in the Castelnovo né Monti site (Appendix B).

With regard to the UTRER, instead, Global Mapper 14 ITA performed quite similarly to ConvER3-GPS7. In fact, although spatially irregular, the offset between these two programs barely exceeded 20 cm with the highest values concentrated in the area of Castelnovo né Monti. Conversely, with respect to ConvER3-GPS7, Global Mapper 13 EN shows offset values that range from 0.76 m in the Castrocaro Terme area to 1.66 m in the Castelnovo né Monti site.

It is worth noting that, in both cases, the offset within the same area never exceeds 10 cm. The analysis of the contour maps of Appendix B reveals also that the offset generally increases westward with the exception of the comparisons between ConvER3-GPS7 and Global Mapper 13 EN, and Global Mapper 14 ITA and Global Mapper 13 EN for the UTRER. The explanation of these trends, however, exceeds the aims of this work and should be investigated by more detailed geodetic analyses.

In general, I suggest that the discrepancies highlighted by this study may be essentially

---

<sup>23</sup> ConvER3-GPS7 recognises the ED50\* for what it is, *i.e.* an unconventional approximated *datum* developed from the GBO by means of a simple translation (see par. 3.2.2.). Consequently, it operates the correct transformation.

Tab. 3.7: Descriptive parameters of the offset vector between files transformed with different software tools. A) refers to UTMER, while B) refers to UTMA. Values (in metres) were calculated with respect to the barycentre of landslide polygons.  $D$  min/max/average – absolute magnitude of the offset vector;  $\Delta x$  min/max/average - longitude component;  $\Delta y$  min/max/average - latitude component.

A)

$D_{min}$	ConvER3-GPS7	Global Mapper 13 EN	Global Mapper 14 IT
ConvER3-GPS7	-	0.75	0.02
Global Mapper 13 EN	0.75	-	0.73
Global Mapper 14 IT	0.02	0.73	-

$\Delta x_{min}$	ConvER3-GPS7	Global Mapper 13 EN	Global Mapper 14 IT
ConvER3-GPS7	-	0.00	0.01
Global Mapper 13 EN	0.00	-	0.02
Global Mapper 14 IT	0.01	0.02	-

$\Delta y_{min}$	ConvER3-GPS7	Global Mapper 13 EN	Global Mapper 14 IT
ConvER3-GPS7	-	0.59	0.00
Global Mapper 13 EN	0.59	-	0.65
Global Mapper 14 IT	0.00	0.65	-

$D_{max}$	ConvER3-GPS7	Global Mapper 13 EN	Global Mapper 14 IT
ConvER3-GPS7	-	1.66	0.22
Global Mapper 13 EN	1.66	-	1.65
Global Mapper 14 IT	0.22	1.65	-

$\Delta x_{max}$	ConvER3-GPS7	Global Mapper 13 EN	Global Mapper 14 IT
ConvER3-GPS7	-	0.50	0.08
Global Mapper 13 EN	0.50	-	0.43
Global Mapper 14 IT	0.08	0.43	-

$\Delta y_{max}$	ConvER3-GPS7	Global Mapper 13 EN	Global Mapper 14 IT
ConvER3-GPS7	-	1.66	0.21
Global Mapper 13 EN	1.65	-	1.64
Global Mapper 14 IT	0.21	1.64	-

$D_{mean}$	ConvER3-GPS7	Global Mapper 13 EN	Global Mapper 14 IT
ConvER3-GPS7	-	1.18	0.10
Global Mapper 13 EN	1.18	-	1.20
Global Mapper 14 IT	0.10	1.20	-

$\Delta x_{mean}$	ConvER3-GPS7	Global Mapper 13 EN	Global Mapper 14 IT
ConvER3-GPS7	-	0.24	0.05
Global Mapper 13 EN	0.24	-	0.25
Global Mapper 14 IT	0.05	0.25	-

$\Delta y_{mean}$	ConvER3-GPS7	Global Mapper 13 EN	Global Mapper 14 IT
ConvER3-GPS7	-	1.12	0.08
Global Mapper 13 EN	1.12	-	1.15
Global Mapper 14 IT	0.08	1.15	-

B)

$D_{min}$	ConvER3-GPS7	Global Mapper 13 EN	Global Mapper 14 IT
ConvER3-GPS7	-	0.75	0.02
Global Mapper 13 EN	0.75	-	0.73
Global Mapper 14 IT	0.02	0.73	-

$\Delta x_{min}$	ConvER3-GPS7	Global Mapper 13 EN	Global Mapper 14 IT
ConvER3-GPS7	-	0.00	0.01
Global Mapper 13 EN	0.00	-	0.02
Global Mapper 14 IT	0.01	0.02	-

$\Delta y_{min}$	ConvER3-GPS7	Global Mapper 13 EN	Global Mapper 14 IT
ConvER3-GPS7	-	0.59	0.00
Global Mapper 13 EN	0.59	-	0.65
Global Mapper 14 IT	0.00	0.65	-

$D_{max}$	ConvER3-GPS7	Global Mapper 13 EN	Global Mapper 14 IT
ConvER3-GPS7	-	1.66	0.22
Global Mapper 13 EN	1.66	-	1.65
Global Mapper 14 IT	0.22	1.65	-

$\Delta x_{max}$	ConvER3-GPS7	Global Mapper 13 EN	Global Mapper 14 IT
ConvER3-GPS7	-	0.50	0.08
Global Mapper 13 EN	0.50	-	0.43
Global Mapper 14 IT	0.08	0.43	-

$\Delta y_{max}$	ConvER3-GPS7	Global Mapper 13 EN	Global Mapper 14 IT
ConvER3-GPS7	-	1.66	0.21
Global Mapper 13 EN	1.65	-	1.64
Global Mapper 14 IT	0.21	1.64	-

$D_{mean}$	ConvER3-GPS7	Global Mapper 13 EN	Global Mapper 14 IT
ConvER3-GPS7	-	1.18	0.10
Global Mapper 13 EN	1.18	-	1.20
Global Mapper 14 IT	0.10	1.20	-

$\Delta x_{mean}$	ConvER3-GPS7	Global Mapper 13 EN	Global Mapper 14 IT
ConvER3-GPS7	-	0.24	0.05
Global Mapper 13 EN	0.24	-	0.25
Global Mapper 14 IT	0.05	0.25	-

$\Delta y_{mean}$	ConvER3-GPS7	Global Mapper 13 EN	Global Mapper 14 IT
ConvER3-GPS7	-	1.12	0.08
Global Mapper 13 EN	1.12	-	1.15
Global Mapper 14 IT	0.08	1.15	-

attributed to the following causes:

- different *datum* transformation method (*e.g. grigliati* method vs 3- or 7-parameters roto-translation);
- use of local parameters acquired from physical geodetic control points;
- origin of the ED50\* *datum* (see par. 3.2.2.);
- inherent imprecision of the UTMA and UTMRE systems (especially zone extension).

The first two causes can be considered intrinsic factors of software tools, while the others are related to the peculiarity of the Emilia-Romagna reference systems with respect to which ConvER3-GPS7 and the Blue Marble software products behave differently. Indeed, ConvER3-GPS7 was intentionally created to be used only within the Emilia-Romagna region and with the specific purpose of managing the unconventional regional system. On the other hand, Global Mapper 13 EN is an international commercial software system and, for this reason, it must adopt a more generic transformation algorithm which does not imply the use of local parameters (see par. 3.3.1. and 3.3.2. for more details). To this end, it is worth noting that, according to Donatelli *et al.* (2002), in most of the Italian territory, the differences between the results of the *grigliati* method and those of the 7-parameters transformation, performed on the basis of the IGM95 control points, are generally <10 cm. In this sense, it is likely that the discrepancy between ConvER3-GPS7 and Global Mapper 13 EN is due to the use of local parameters based on physical geodetic control points rather than to the transformation method itself. The importance of the “geodetic contextualization” of the conversion algorithm is underlined by the results provided by Global Mapper 14 ITA, which, as reported in par. 3.3.2., was adapted to the Italian territory.

### **3.6. Conclusions**

Given the importance of geographic positioning for landslide studies, this work aimed to assess, in quantitative and spatial terms, the effects of *datum* transformations in relation to the software tools, and the algorithms, used for the conversion. The final goal, however, was not to appraise their overall geodetic efficiency but rather to quantify the fallouts of these transformations on a landslide inventory map. To this end, I tested three different software tools with respect to the WGS84 and the unconventional reference systems adopted by the

Emilia-Romagna Regional Authority (UTMRER and UTMA).

In general, this work proved that, with regard to the landslide inventory maps of the study sites, the offset associated to *datum* conversion may be of the order of metric length, *i.e.* one order of magnitude higher than the resolution of a VHR satellite image (0.50 m). It also confirmed that there is no comprehensive transformation algorithm that can be applied worldwide as, instead, would require international software products. Indeed, *datum* conversions are affected by the intrinsic distortions of local geodetic networks and, as a consequence, it is advisable to use software tools based on local parameters calculated on physical control points.

On this basis, whenever possible, in order to preserve the benefits of the high precision of satellite data, it is recommended to avoid *datum* transformations by acquiring data with the same CRS. Otherwise, *datum* conversions should be performed by using only one software product so as to keep the offset as constant as possible; an essential condition for multi-temporal studies. In addition, the magnitude of this uncertainty should be correctly quantified and taken into consideration for the assessment of potential data uses. In particular, as far as landslide inventory maps are concerned, an imprecision of the order of metric length should discourage any rigid application of landslide polygons.

Finally, this work underlined the unsuitability as well as the difficult and complex management required by unconventional reference systems. To this regard, it particularly emphasised the importance of data lineage as an essential parameter to define quality especially for derived or second hand data.

## CHAPTER 4

# Spatial accuracy of landslide detection and mapping

- 4.1. Introduction
- 4.2. Landslide detection and mapping techniques: a comparison between remotely sensed and field survey data
  - 4.2.1. Analysis and results
    - 4.2.1.1. Descriptive statistics
    - 4.2.1.2. Landslide abundance
    - 4.2.1.3. Correspondence of landslide areas
    - 4.2.1.4. Time and cost evaluation
  - 4.2.2. Discussion
    - 4.2.2.1. Limiting factors of the detection and mapping techniques
    - 4.2.2.2. Data interpretation
- 4.3. Spatial accuracy of a multi-temporal landslide inventory map
  - 4.3.1. Analysis and results
  - 4.3.2. Discussion
- 4.4. Conclusions

## 4. Spatial accuracy of landslide detection and mapping

### 4.1. Introduction

In this Chapter, I address spatial accuracy, *i.e.* the definition of landslide size and shape, from two different points of view: landslide detection and mapping techniques and the overall spatial accuracy of a landslide inventory map.

Landslide data can at best approximate the complexity of physical reality (see par. 2.2.3.). In this sense, landslide detection method is the basic tool through which reality is perceived and, therefore, it decisively affects the conceptual model that is ultimately realised in a landslide inventory map. In order to appraise this aspect, I carry out a comparison between two different detection techniques: remote sensing and field investigation. To this end, I prepared two inventories (both realised on the 2012 status) that I compared on the basis of their descriptive statistics, landslide abundance, correspondence of landslide areas, time, and cost/benefit ratio.

Conversely, to quantify and effectively communicate the overall spatial accuracy of landslide detection and mapping, I perform a fuzzy-like analysis on a multi-temporal inventory. In this sense, spatial persistence and boundary reliability are used as proxies for spatial accuracy.

This study is conducted on the catchment of the Dorgola Creek, *i.e.* on the Castelnovo né Monti site (see par. 2.3.1.1.). Despite its natural aspect, this area had been, and it still is, severely modified by human activities so that anthropogenic processes must always be considered when dealing with slope stability.

With regard to landslides, in this work the use of the terms “cancel”, “erase”, or similar are discouraged. Indeed, geomorphological surveys are limited to superficial analysis and do not provide any subsurface information. As a consequence, they do not supply any real evidences that a given mass movement was actually removed or stabilised and not merely concealed or just partially slowed down.

## **4.2. Landslide detection and mapping techniques: a comparison between remotely sensed and field survey data**

The quality of a landslide inventory relies on several factors (see par. 2.2.3.). Among others, for example, detection techniques and supports strongly influence the inventory completeness and the overall accuracy of landslide identification and mapping. Landslide inventory maps can be prepared using different methods and tools, however, most of these techniques could not be effectively used in this context due their cost, time commitment, and tested reliability. In the last decades, visual interpretation of remotely sensed images became a substantial support to field investigations and one of the most frequently used method for landslide detection and mapping (Rib and Liang, 1978; Turner and Schuster, 1996; Guzzetti, 2006). Remote sensing techniques present, indeed, important advantages:

- coverage of large areas;
- possibility to investigate the temporal dimension;
- sufficient to excellent resolution;
- good cost/benefit ratio.

In particular, until recently, aerial photographs were the most common type of remotely sensed data (Mantovani *et al.*, 1996). Nowadays, thus, the cost, availability, resolution, and knowledge of satellite images and techniques considerably improved so that they became an effective alternative to aerial photographs. The GeoEye-1 satellite is a commercial remote sensing system launched on 6<sup>th</sup> September 2008. It provides images at nadir with 0.5 m panchromatic (black & white) and 2 m multispectral resolution. The GeoEYE-1 is a polar-orbiting sun-synchronous satellite that orbits the Earth 15 times per day at an altitude of 681 km and with a 10:30 a.m. equator crossing (E-geos.it, 2014).

According to the research aims, I tried to assess the efficiency of two of the most used landslide detection and mapping techniques. To this end, I compared a remotely sensed inventory (Fig. 4.1), prepared on a VHR orthorectified panchromatic GeoEYE image, with a detailed geomorphological field-based inventory (Fig. 4.2). For this comparison the time issue was disregarded (see Chapter 5), since the two inventories were prepared on new coeval data: the GeoEYE image acquired on August 2012 and the field survey conducted in October-November 2012. Furthermore, in order to control the effects of subjectivity, I

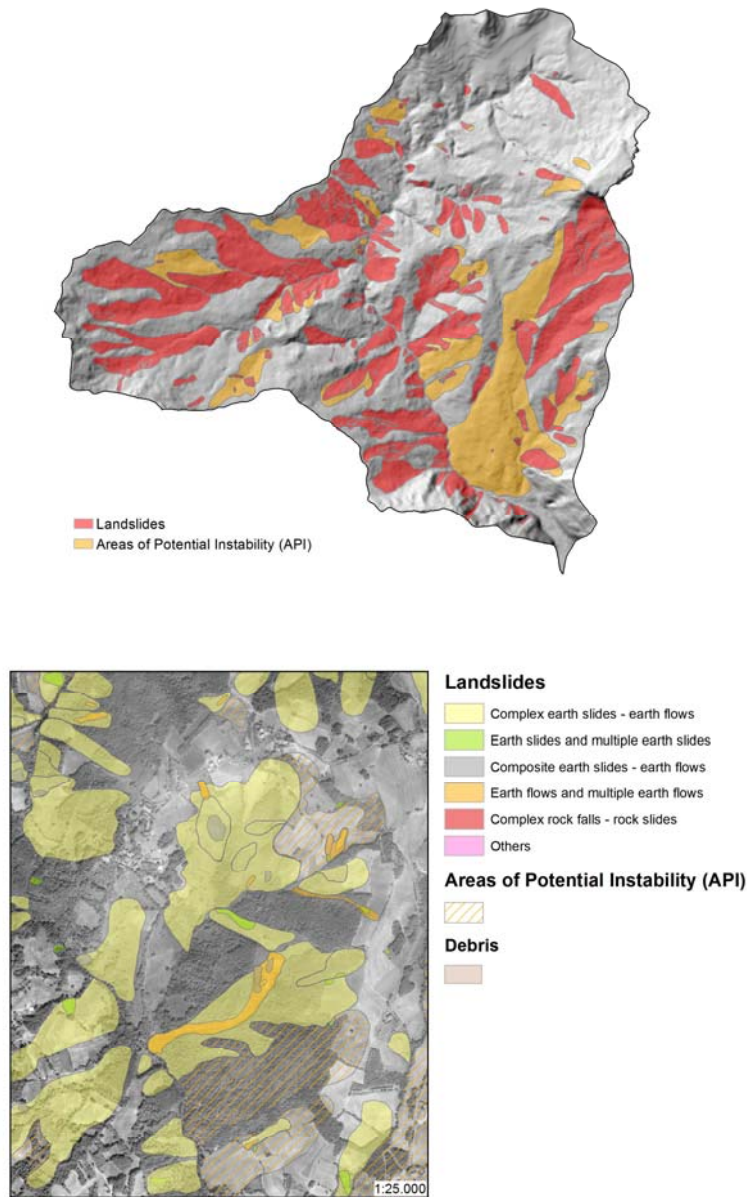


Fig. 4.1: Remotely sensed landslide inventory map of the Dorgola catchment. This inventory, which includes also areas of potential instability, was prepared with visual interpretation and digital mapping from an orthorectified satellite image. In this specific case, a panchromatic GeoEYE-1 image with a 0.5 m resolution was used for the purpose. The 11-bit image, interpolated with a Cubic Convolution method, was acquired on 3<sup>rd</sup> August 2012 at 10:13 GMT.

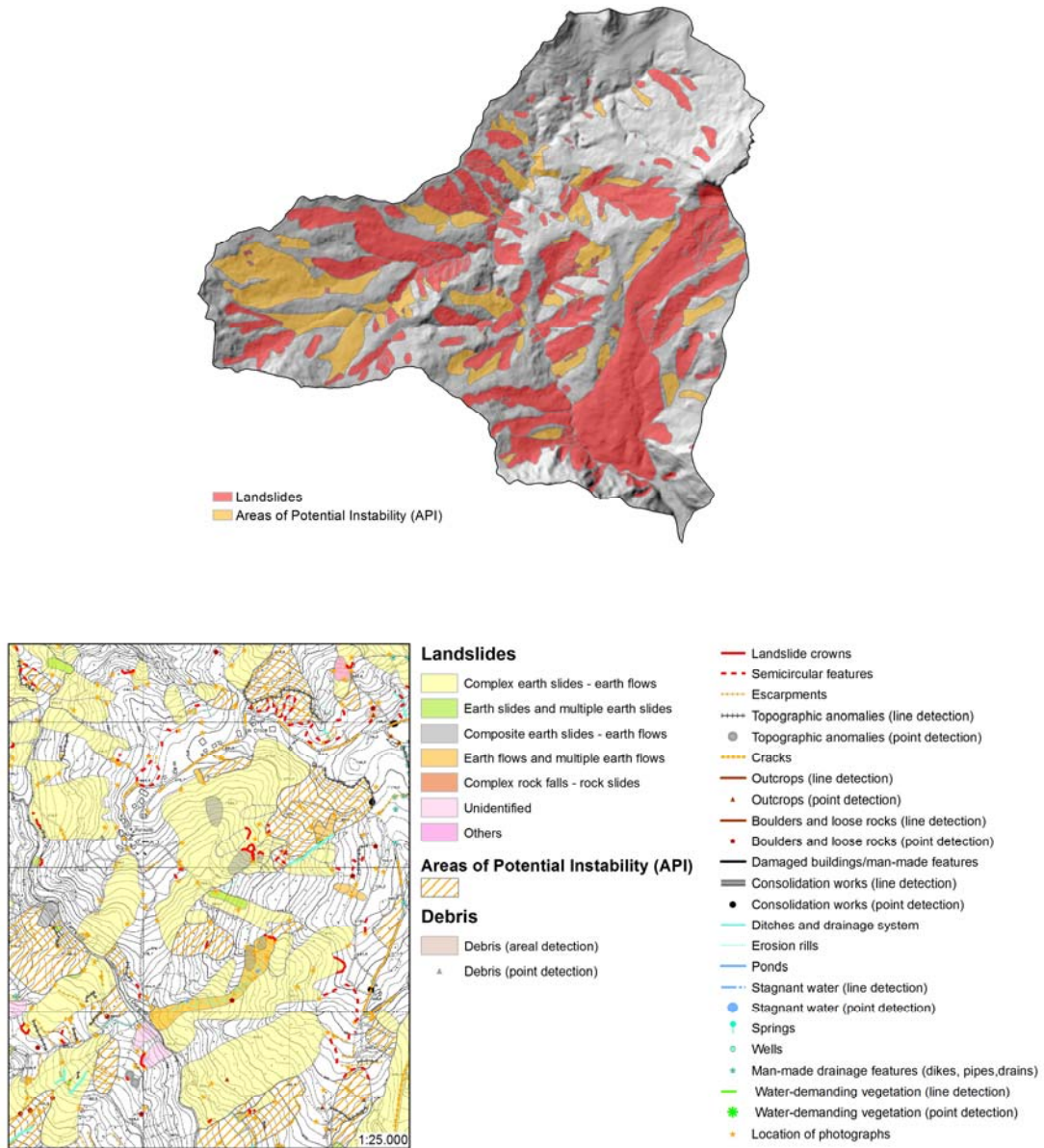


Fig. 4.2: Ground-based geomorphological landslide inventory map of the Dorgola catchment. The survey campaign was conducted over a non-continuous period from the 1<sup>st</sup> October to the 13<sup>th</sup> November 2012 for a total amount of 23 working days. Field investigations focused not only on evident landslides (deposits and source areas), but they also detected areas of potential instability and hummocky topography, as well as topographic anomalies, consolidation works, infrastructure and building damages, superficial drainage systems, ponds, and anomalous patterns, badlands, anthropogenic features, particular land-uses, and water-demanding vegetation.

prepared both inventories by myself. This comparison did not involve the thematic dimension. Indeed, the assessment of the attribute accuracy cannot disregard the connection with other interpreters, and it requires a solid base for comparison, *i.e.* a shared definition of landslide attributes (classification, state, distribution, and style of activity, *etc.*). Moreover, a geomorphological analysis, although integrated with ancillary data (lithology, bedding, *etc.*), is rarely sufficient for a complete and accurate characterization of many landslides, which would require more detailed subsurface investigations (Basenghi and Bertolini, 2001).

#### 4.2.1. Analysis and results

The most common types of landslides in the Dorgola catchment, according to the Cruden and Varnes (1996) classification, are complex earth slides–earth flows, earth slides, composite earth slides–earth flows, and earth flows (Fig. 4.3). All together they represent about 90% of all landslides. Despite the different nomenclature, these results are consistent with those of the IFFI Project (*Inventario dei Fenomeni Franosi in Italia*) database (Bertolini and Pellegrini, 2001; Servizio Geologico, Sismico e dei Suoli, 2006). The higher incidence of complex rock falls–rock slides is due to the peculiar geomorphological context of the Dorgola Valley, dominated by the outstanding rocky cliffs of the Pietra di Bismantova and by the

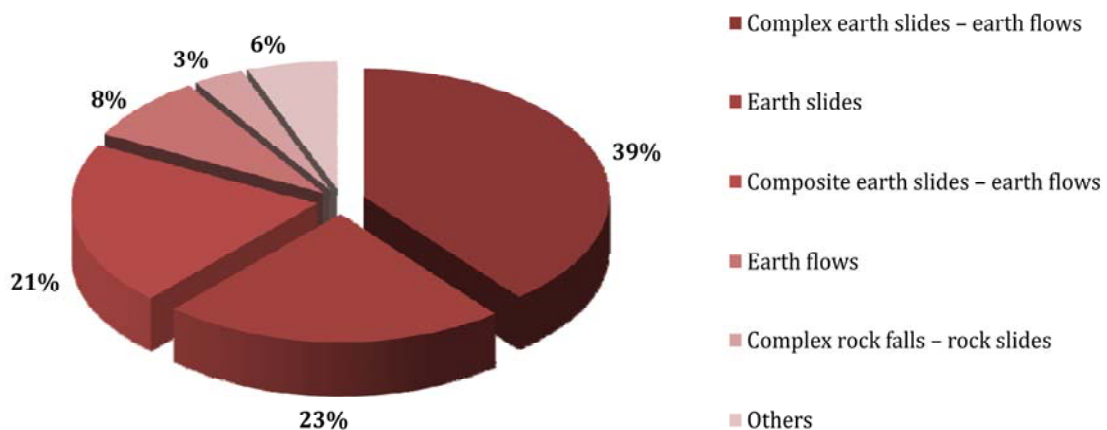


Fig. 4.3: Landslide type distribution in the Dorgola catchment. The nomenclature is the one proposed by Cruden and Varnes (1996).

Tab. 4.1: Landslide indexes for the geological domains of the Dorgola Valley.

	Area of geological domains (m <sup>2</sup> )	Landslide areas (m <sup>2</sup> )			
		Field inventory 2012		GeoEYE 2012	
Tuscan-Umbria-Romagna Units	774,766	168,852	22%	87,416	11%
Ligurian Units	9,036,696	4,099,235	45%	3,454,267	38%
Epi-Ligurian Sequence	6,319,482	1,095,183	17%	819,739	13%

steep slopes of the Sassalbo Triassic Gypsums.

Both inventories confirmed the higher landslide index of the Ligurian Units with respect to the Tuscan-Umbria-Romagna Units and to the Epi-Ligurian Sequence (Tab. 4.1). At the same time, as shown in Tab. 4.2, they also present a percentage of landslide index consistent with the one indicated by the IFFI Project and the Emilia-Romagna Regional Authority that, for the same municipality, report values of 20%÷30% (Servizio Geologico, Sismico e dei Suoli, 1999 and 2006).

In order to identify those areas where no landslides were clearly detected but where morphological and vegetation elements suggested probable or potential instability, in the geomorphological field-based inventory I distinguished an extra class: API (see par. 2.3.2.). To be fully compared with each other, I then introduced the same distinction also in the GeoEYE 2012 inventory.

#### 4.2.1.1. Descriptive statistics

According to the descriptive statistics reported in Tab. 4.2, the inventory prepared on the basis of the panchromatic GeoEYE image presents 35.7% more landslides than the field inventory. Instead, with regard to the total area of mapped landslides and to the total area covered by landslides, the latter shows values respectively 24.6% and 18.7% higher than those of the GeoEYE 2012 inventory. This discrepancy is associated with the biggest landslide mapped in the geomorphological inventory. This landslide, that extends over an area of 1,492 km<sup>2</sup>, was not detected in the remote-based inventory and in the database it actually represents an exceptional feature. If this landslide is removed from the dataset, both areas are slightly higher in the GeoEYE 2012 inventory than in the ground-based inventory.

The same consideration is valid also for the smallest landslide of the field inventory (28 m<sup>2</sup>) which represents an isolated value. Moreover, despite their different meanings, mean, median, and mode areas are all higher in the ground-based inventory than in the GeoEYE 2012 inventory. This indicates that the two maps diverge from each other not only for the total amount of landslides but also as far as the mapped landslide size is concerned. In particular, small landslides are more abundant in the remotely sensed inventory. This is also confirmed by the area frequency distribution shown in Fig. 4.4 A. This histogram was prepared by using an area class bin width progressively increased according to a log5 scale in order to display in a proper way all the area range. The histogram shows that, with respect to the field survey 2012, the most frequent class of the GeoEYE 2012 corresponds to smaller areas. Indeed, it is evident that the discrepancy in the total number of landslides

*Tab. 4.2: Descriptive statistics of the ground-based and remote-based inventories. The values in parentheses do not consider the Bondolo landslide.*

		<b>Field inventory 2012</b>	<b>GeoEYE 2012</b>
Number of landslides	#	224*	304
Total area of mapped landslides	Km <sup>2</sup>	6.245 (4.752)	5.039
Total area covered by landslides	Km <sup>2</sup>	5.37 (4.193)	4.365
% of landslide area	%	33.12 (25.86)	26.92
Landslide density	#/Km <sup>2</sup>	13.81	18.75
Area of smallest landslide	m <sup>2</sup>	28	79
Area of biggest landslide	m <sup>2</sup>	1,492,740 (434,995)	392,681
Landslide average area	m <sup>2</sup>	27,880	16,577
Landslide median area	m <sup>2</sup>	4,622	2,522
Most abundant landslide area	m <sup>2</sup>	~300	~200

\* The total number of landslides was generally considered to be 223 since two of them were recognized in the GeoEYE inventory as a single object.

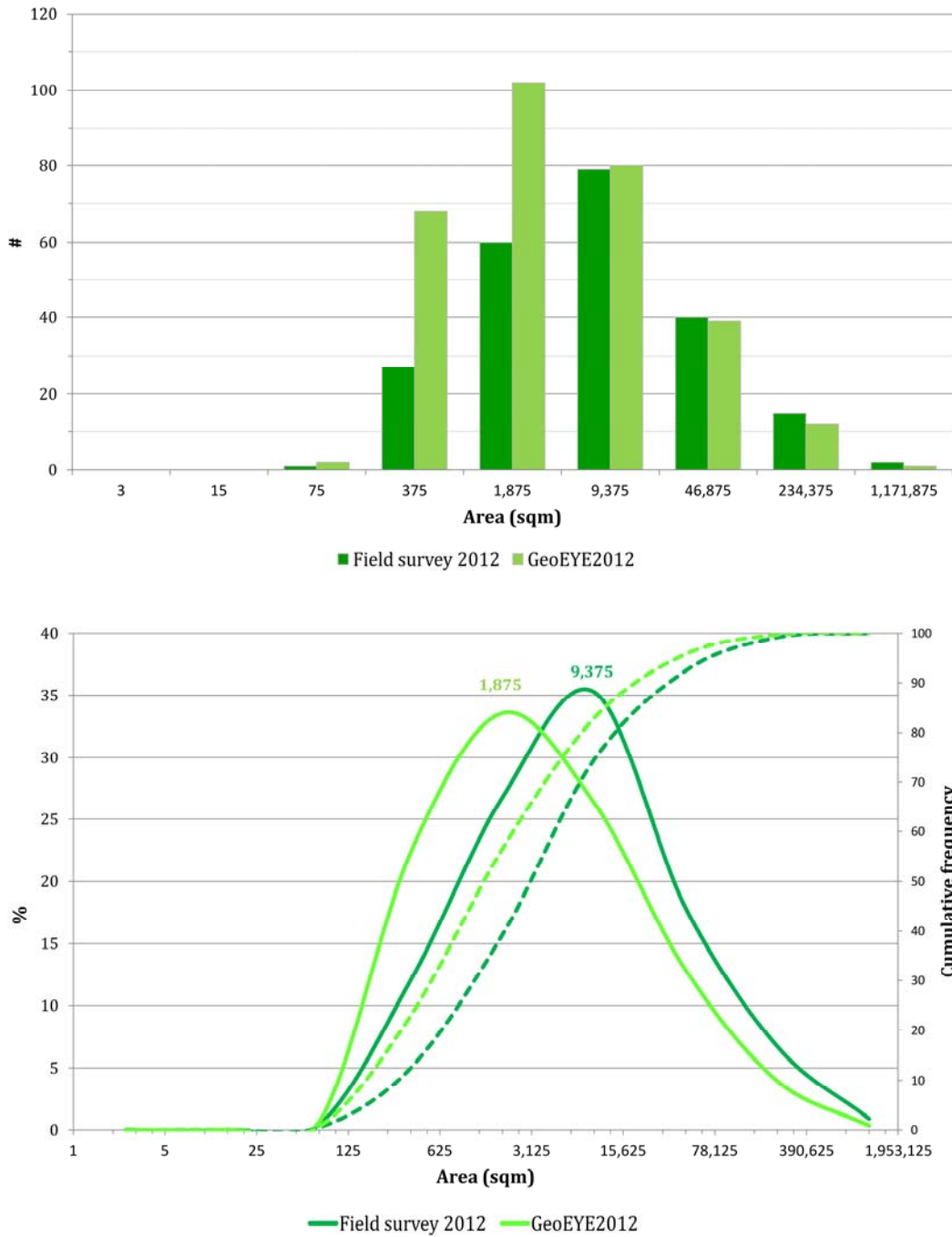


Fig. 4.4: Landslide area frequency distribution for the ground-based and the remote-base inventories. In order to display all the area range, area class bin width were progressively increased according to a log5 scale. A) The histogram represents the absolute number of landslides in each area class represented by the bin central value. B) The diagram shows both the cumulative and the non-cumulative curves related to landslide percentage.

between the two inventories is to be related basically to landslides with an area  $\leq 3,125 \text{ m}^2$ <sup>1</sup>. The same outcome appears in Fig. 4.4 B where the central value of the area class bin width is plotted against landslide percentage.

#### **4.2.1.2. Landslide abundance**

The two inventories share 169 landslides, *i.e.* 75.8% of the ground-based map and 55.6% of the remote-based inventory. These landslides were detected with both methods and were identified with the same ID. In the ground-based inventory 139 (82.2%) of these mass movements were mapped with the aid of a GPS from 3.3% to 100% of their total perimeter; in particular, most of them (55%) were GPS tracked for about 10÷40% (Fig. 4.5 A). The analysis of Fig. 4.5 B shows that there is no relationship between GPS tracks and slope failure areas, even though most of the GPS records seem to be concentrated in landslides with areas in the order of thousands and tens of thousands square meters.

With respect to the remotely sensed inventory, the field survey missed 135 slope failures, whereas 54 landslides were not identified from the visual interpretation of the GeoEYE 2012 satellite image. In reality, as far as the ground-based inventory is concerned, 6 (4.4%) of the missing landslides had been only partially detected, not as polygons but just as linear features (crown areas or semicircular potential crown areas). For these landslides the remotely sensed perspective offered a better point of view that allowed the recognition of the entire landslide. More generally, 120 (88.9%) of the undetected landslides were included in the geomorphological inventory as part of bigger slope movements or API. With regard to the GeoEYE 2012 inventory, 14 (25.9%) of the 54 undetected landslides were completely included in forested areas, whereas 12 (22,2%) were located in cultivated fields and their recognition, due to man interventions, was not straightforward even on the ground. Furthermore, 15 missed landslides were actually mapped in the remotely sensed inventory as API. One outstanding example is the Bondolo landslide, a complex earth slide-earth flow which intensively contributed to shape the local landscape (Fig. 4.6). This massive slope failure formed in different morpho-climatic conditions and at present it does not show any evident signs of activity. During field investigations, it was detected mainly on the basis of the Pietra di Bismantova boulders. Indeed, most of them are concentrated in the Dorgola

---

<sup>1</sup> Area class upper limit.

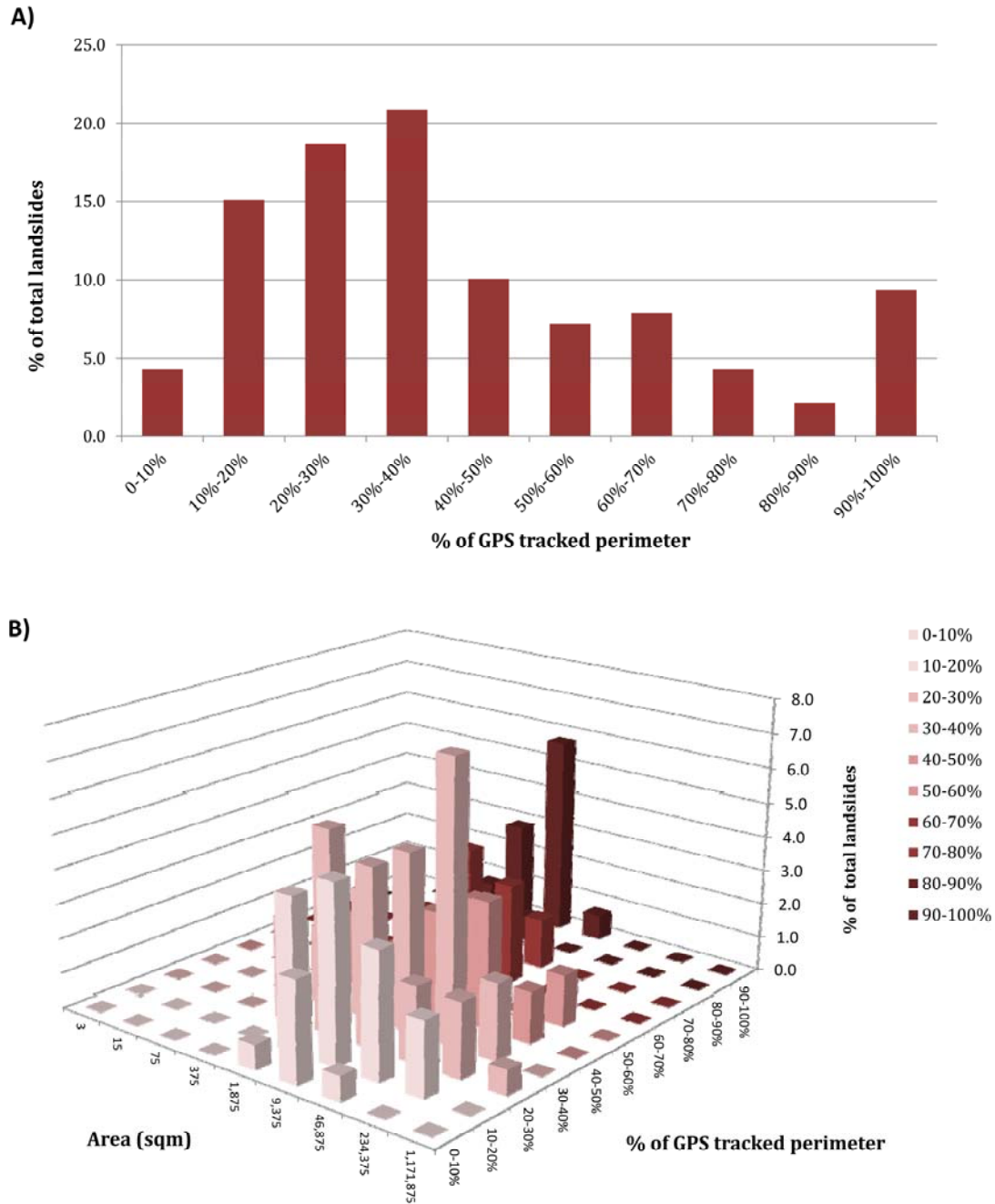
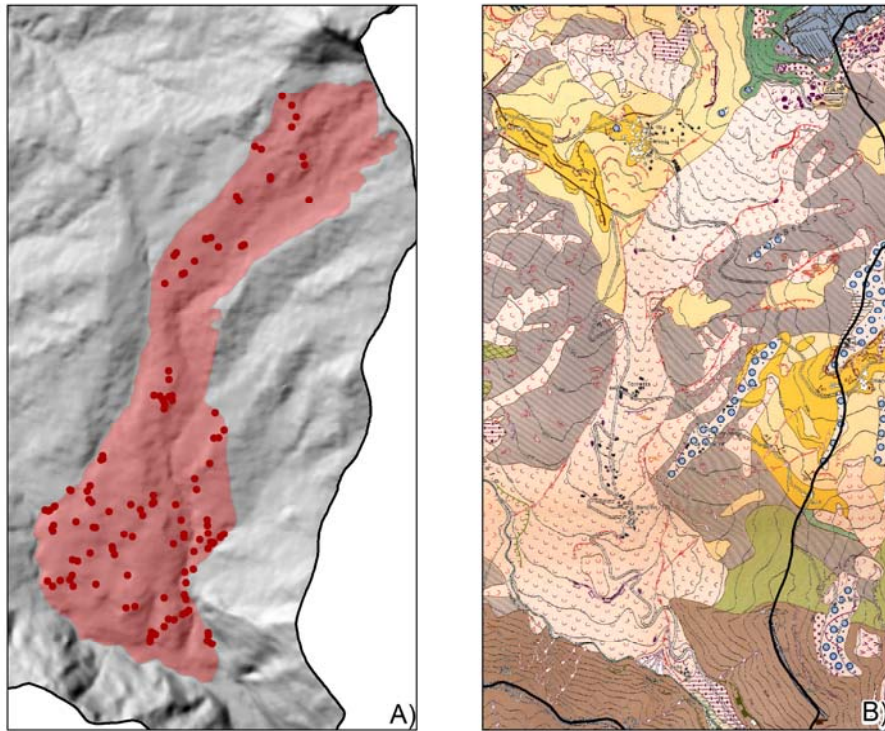


Fig. 4.5: These 2D and 3D histograms display the relationship between GPS records and landslides percentage (A) and among GPS records, landslides percentage, and area (B) which is indicated by the class bin upper value.

riverbed along the margin of the landslide toe (about 3 km from the Pietra di Bismantova), but many others are scattered all over the entire landslide deposit. Furthermore, the convex lobate shape of the run-out area was clearly detectable on the CTR and on the shaded relief raster created by Esri@ArcMap™ 10.1 from the CTR 5 m DEM. On the other hand, with just few isolated exceptions, boulders, mostly hidden by vegetation, could not be seen on the satellite image (Fig. 4.7) making the landslide identification more challenging. Indeed, the Bondolo landslide is remotely detectable only on the basis of its landform. This, however, was not recognised both for its massive dimensions<sup>2</sup> and because with time the source area was partially concealed and eroded by successive, and at least partially still active, mass



*Fig. 4.6: The Bondolo landslide extends over an area of approximately 1,5 km<sup>2</sup>, from the Pietra di Bismantova to the Dorgola riverbed. A) The landslide as it was identified and mapped during the 2012 field survey. Red dots represent some of the Pietra di Bismantova boulders that had been GPS mapped over the landslide deposit. B) The Bondolo landslide as it was mapped by the GSUEG (1976).*

<sup>2</sup> In a way, the Bondolo landslide is not part of the landscape, but it is itself the main landscape feature.

movements. To this end, a 3D/stereoscopic vision would have probably helped the recognition. Eventually, on the GeoEYE 2012 image the Bondolo landslide was not mapped as a mass movement, but it was identified as an API basically due to the characteristic shape of its toe.

The area frequency distribution of the missing landslides in the two inventories is represented in Fig. 4.8. Undetected landslide sizes confirm that the ground-based inventory missed more small landslides than the remotely sensed one, which instead seem to partially fail on medium to large landslides.

#### 4.2.1.3. Correspondence of landslide areas

In order to quantify the degree of cartographic matching between the two maps, the overall mapping error was calculated according to the method proposed by Carrara *et al* (Carrara *et al*, 1993) as modified by Galli *et al* (2008):

$$E = \frac{(A1 \cup A2) - (A1 \cap A2)}{(A1 \cup A2)} \quad 0 \leq E \leq 1 \quad (1)$$

where  $A1$  and  $A2$  are the total landslide area in the two inventories, whereas  $\cup$  and  $\cap$  are respectively the cartographic union and intersection of the two maps automatically computed by Esri®ArcMap™ 10.1. From Eq (1) Galli *et al* (2008) obtained the matching index:

$$M = 1 - E, \quad 0 \leq M \leq 1 \quad (2)$$

Ideally if two maps match perfectly the error index would be 0 and, consequently, the degree of matching would be 1. On the contrary, if two maps do not overlap at all the error index would be 1 and the matching index 0. Eq. (1) shows the overall mismatch as it encompasses landslide identification, positioning, and mapping.

The comparison between the ground- and the remote-based landslide maps of the Dorgola catchment shows an error index value of 0,54 (54%), *i.e.* a matching index of 0,46 (46%). However, if the comparison is extended also to the API mapped in both inventories, the error index decreases to 0,36 (36%) which corresponds to a rather satisfying matching index of 0,64 (64%). The cartographic matching was computed also for every single landslide that had been mapped in both inventories (169 landslides). In this case, the error index ranges from a maximum of 0.90 ( $M=0.10$ ) to a minimum of 0.16 ( $M=0.84$ ), with a



*Fig. 4.7: Boulders from the Pietra di Bismantova included in the Bondolo landslide. In spite of their large dimensions (up to  $10^3 \text{ m}^3$ ), these boulders cannot be easily remotely detected generally due to vegetation canopy. A) a boulder is included into an historical rural building. B) a huge boulder, although partially hidden by vegetation, is remotely detectable. However, the use of a colored or B/W image considerably influence its recognition.*

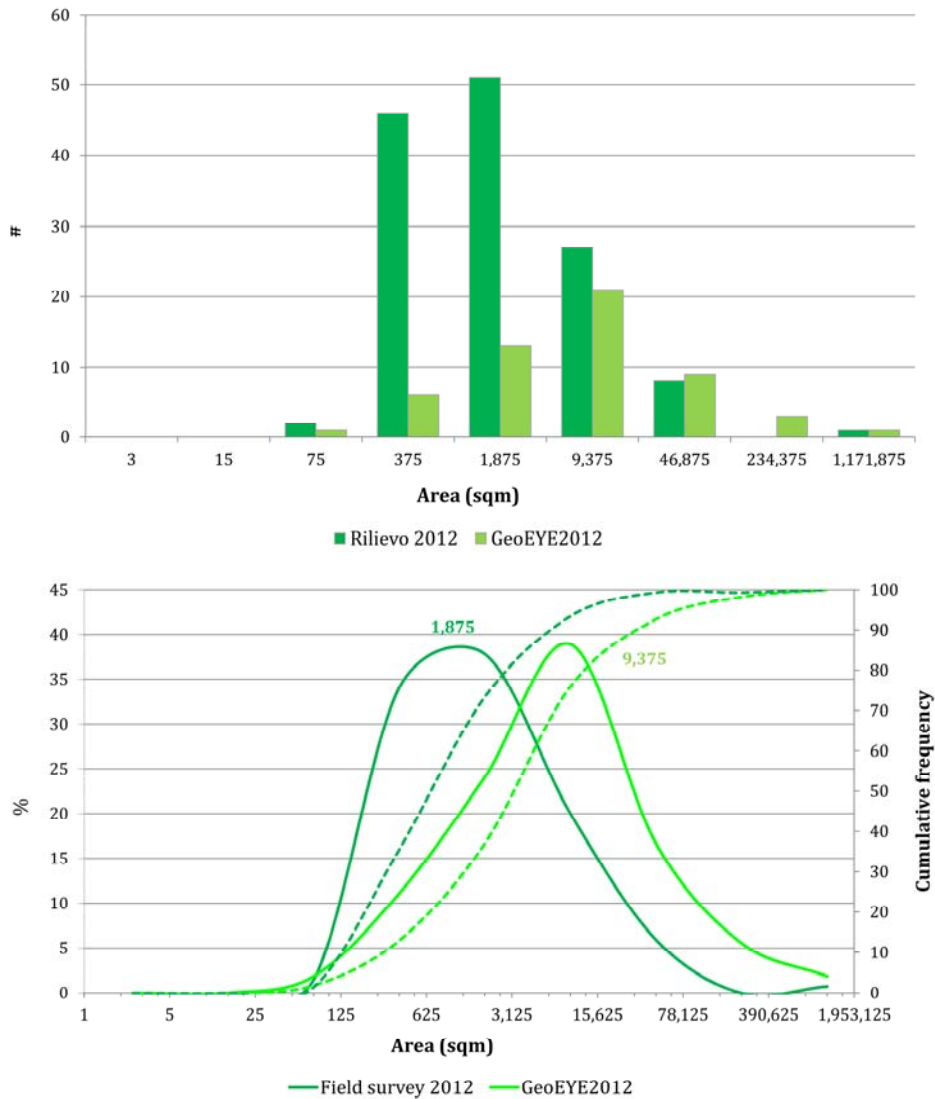
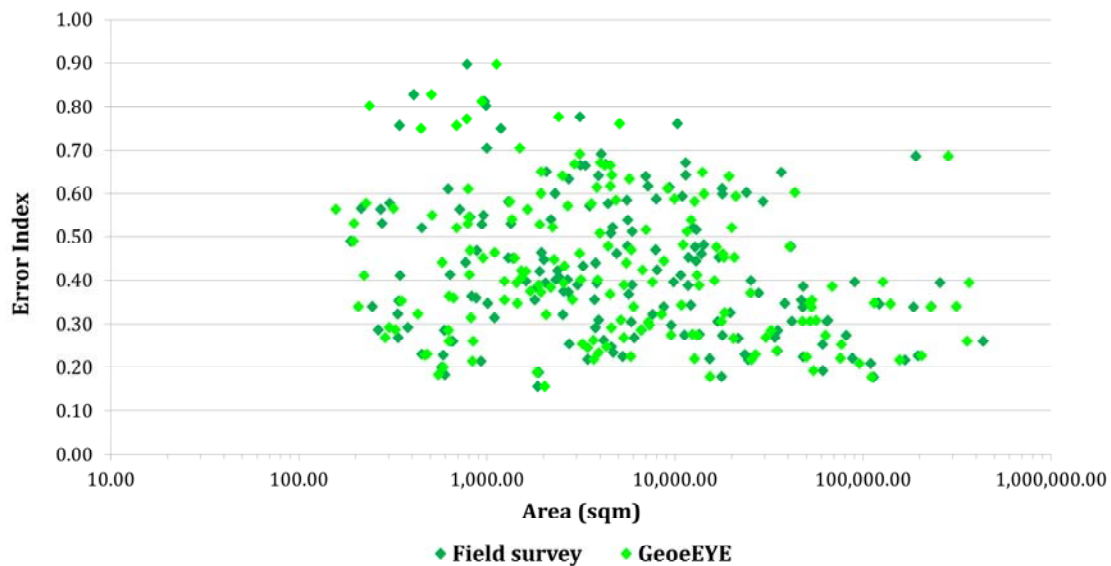


Fig. 4.8: Area frequency distribution of missing landslides in the two inventories. In order to display all the area range, area class bin width were progressively increased according to a log5 scale. A) The histogram represents the absolute number of landslides in each area class represented by the bin central value. B) The diagram shows both the cumulative and the non-cumulative curves related to landslide percentage.

median value of 0.4 ( $M=0.6$ ). The analysis of Fig. 4.9 shows that apparently there is no relationship between the error index and the landslide areas. Indeed, the lack of high values of error index in correspondence to larger landslides may be a consequence of their reduced frequency.

#### 4.2.1.4. Time and cost evaluation

The survey campaign (see Chapter 2 for details) was realized during a non-continuous period from the 1<sup>st</sup> October to the 13<sup>th</sup> November 2012 for a total amount of 23 working days (Tab. 2.2). Data processing for the realization of the geomorphological landslide inventory required 10 extra working days for a total of 33 days (Tab. 4.3). There was no need to buy support material or any specific instrumentation (the CTR and the GPS were both already available to the geomorphologist) so that costs (about 687,98 euro) are ascribable only to transports to and from the survey area<sup>3</sup>. Conversely, the GeoEYE image was tasked on the 26<sup>th</sup> June 2012 and acquired on the 3<sup>rd</sup> August 2012. The time lapse between the image tasking and acquisition depends on weather conditions and satellite availability. According to the producer Delivery Terms (GeoEYE, 2009) for areas <500 km<sup>2</sup> GeoEYE-1 images are delivered within 60 days. The realization of the landslide inventory required 5 extra working days (Tab. 4.3). The minimum order size for Geo image is 100 km<sup>2</sup> and the cost for it with an Academy Licence (-30%) is 1.522,50 euro+VAT.



*Fig. 4.9: In this diagram the error index values, calculated for each single landslide detected in both inventories, are plotted against the two sets of landslide areas.*

<sup>3</sup> For time and resource optimisation, during weekdays I decided to stay at the study area instead of daily commuting. Accommodation costs, however, are not included in the total expense.

Tab. 4.3: Time and cost of the two inventories prepared for the Dorgola catchment.

		Field inventory 2012	GeoEYE 2012
Survey period	days	23	(38)*
Processing time	days	10	5
Costs	euro	687,98	1,522.50+VAT**

\* Time lapse between image tasking and acquisition.

\*\* This cost is referred to 100 km<sup>2</sup> and it does not include orthorectificatio; the proportional expense for 16 km<sup>2</sup> is about 348 euro including orthorectification.

Orthorectification operations were later performed by e-geos at the cost of 6,50 euro/km<sup>2</sup> <sup>4</sup> (Tab. 4.3).

## 4.2.2. Discussion

### 4.2.2.1. Limiting factors of the detection and mapping techniques

Some the major limiting factors of both detection techniques under study are common to both of them (weather/cloud cover, cost/benefit ratio, surveyor experience), while others are more specifically connected to one method or the other (Tab. 4.4). Generally, the importance of each factor is basically related to the landscape and the morphology of the area, so that it is improper to list them according to an absolute relevance.

As far as field survey is concerned, area inaccessibility can be due to different causes: steep or impervious slopes, risky areas, impenetrable vegetation, and prohibited areas (fenced-in private properties, hunting areas, military zones, *etc.*). Most of these issues were encountered during the survey of the Dorgola catchment. Another relevant factor is the surface detail of the survey, *i.e.* the surveyor trekking intensity with respect to local morphology, landslide size and land-use. Indeed, in order to be detected, a small landslide in a forested area with an irregular morphology requires a more intense wander than a similar landslide located in an open field with little or no vegetation and a more regular morphology. To this end, it is evident that this factor is strictly related to the available time as well as to

<sup>4</sup> In this case, the minimum order size of 100 Km<sup>2</sup> can be subdivided among different areas.

Tab. 4.4: Limiting factors of the data quality for field survey and for the visual interpretation of orthorectified satellite images.

Field survey	Visual interpretation of orthorectified satellite images
area inaccessibility	forest and snow canopy
surface detail of the survey with respect to local morphology, landslide size and land-use	shadow areas
weather	cloud cover
available time	image illumination
lack of perspective	lack of 3D/stereoscopic vision
cost/benefit ratio	cost/benefit ratio
surveyor experience	surveyor experience
land-use	image bands (colour vs B/W) and resolution
Landslide drafting and digitizing	positional and orthorectification accuracy

the actual feasibility to walk and see everywhere. In this sense, the lack of perspective from different points of view, *e.g.* from the opposite slope or from a higher position, represents another significant restriction to the data quality of field survey. Land-use can be a further limiting factor. Indeed, different land-uses imply different challenges. Nevertheless, also the same land-use in a different season or a different time of the day can either facilitate or prevent landslide detection. This, for example, is the case of cultivated fields where old dormant medium to large landslides can be more easily detected when the crop just started to grow rather than before harvest or just after ploughing. Young plants tend actually to be healthier on the landslide moist deposit than in the soil depleted source area. In this sense, it is evident that the season is an important, although not necessary limiting<sup>5</sup>, aspect of field

<sup>5</sup> Every season, indeed, presents some advantages and some disadvantages.

survey not only for the total amount of daylight<sup>6</sup> but also for the growth of both natural and cultivated vegetation. Finally, the quality of the field survey data is also affected by landslide drafting and digitizing. In particular, landslide drafting can be quite challenging and error-prone if the topographic support pre-dates the mass movement.

With regard to remote sensing, most of the limiting factors affecting data quality are quite straightforward, and they do not require a particular explanation (forest and snow canopy, cloud cover, shadow areas, *etc.*). According to the geographic position and altitude of the study area, a useful expedient to reduce some of these issues is to acquire satellite images in a particular season. In the case of the Dorgola Valley, springtime and late autumn proved to be the best moments of the year since forest and snow canopies are generally absent. Unfortunately, in the Northern Apennines these are also the rainiest periods of the year and, besides, snow-melt itself is considered as one of the most important landslide causes. Indeed, 48% of mass movements take place between March and May, whereas 29% of landslides occur between October and December (Bertolini & Pellegrini, 2001). This suggests that an image captured in spring may miss some mass movements, while in autumn some landslides may have been concealed by summer farming activities. A compromise between these two factors is, therefore, necessary. The quality of remote sensed data also depends on image bands and resolution. Along with the interpreter personal sensibility towards coloured and B/W images, there are also more objective situations when one type of image is more effective than the other like, for example, in the case of the Pietra di Bismantova boulder represented in Fig. 4.7 B. Image resolution, on the other hand, determines the minimum dimensions of the smallest detectable object. However, when more image sets are compared or related to each other, like *e.g.* in a multi-temporal inventory map, high precision may be corrupted by a poor orthorectification or positional accuracy (see Chapter 3). In fact, both of these terms, as well as image resolution itself, should be as constant as possible throughout the different image sets in order to provide an homogeneous basis for comparisons and overlays. Image illumination may also be a limiting factor for the detection of particular landslides. Indeed, without the support of a 3D/stereoscopic vision, a vertical intense illumination can flatten the image making it more

---

<sup>6</sup> During short winter days the total number of hours with an optimum illumination is lower than in summer.

difficult to recognised hummocky morphology and topographic concavities and convexities. The cost/benefit ratio, instead, may be generally considered an advantage of remote sensing, although if the area of interest is very small it may be worth reconsidering other survey options.

#### **4.2.2.2. Data interpretation**

The ground- and the remote-based inventories share a significant amount of landslides, respectively 75.8% and 55.6%. Furthermore, according to the literature (Carrara *et al*, 1993; Ardizzone *et al*, 2002; Galli *et al*, 2008; Santangelo *et al*, 2010), they present also a satisfactory cartographic matching index of 0,64 (64%). Hence, overall, the two detection techniques provide quite analogous outcomes. Notwithstanding this, there is still a reasonable disagreement about the total number, as well as about the size, of the detected and mapped landslides. Furthermore, since both techniques present advantages and disadvantages, it is worth considering which one did better appraise “truth”. Field survey is generally considered the most reliable term of comparison, although several factors may influence its accuracy and soundness (see par. 4.2.2.1.). In particular, the coexistence and interaction of these elements generate more degrees of outcome quality, thus offering different “ground truths”. Nevertheless, despite some great advantages, also remote sensing can produce different results on the basis of different preconditions.

The field survey realised in the Dorgola catchment was conducted in details with an average surveyed area of about 0,7 km<sup>2</sup> per day and a total amount of GPS records of about 185 km. Data quality, however, was partially reduced by both area inaccessibility and surface detail of the survey. Conversely, in many cases the airborne perspective offered a better point of view and was more efficient in detecting the contrast between stable and unstable areas, especially with respect to reactivations of major landslides with little or no vegetation.

At the same time, however, this comparison revealed that, although not completely essential, the visual interpretation of remotely sensed images should be associated with 3D/stereoscopic vision in order to improve the identification of large dormant landslides that, in certain conditions, may be missed (e.g. Bondolo landslide). Indeed, although this kind of massive slope failures had contributed to shape the local landscape, the recognition of their distinctive features (e.g. concave and convex slope morphology) basically relies on a

3D vision so that, without the support of a detailed topographic map, an unsuitable illumination may prevent or make their identification more challenging. On the other hand, field survey, especially if supported by large scale (1:5.000 to 1:10.000) topographic maps, allowed a prompt identification for large dormant landslides and, in addition, it supplied more detailed information about the overall geomorphological and hydrological context as well as about specific issues (e.g. damages to buildings and infrastructures, consolidation works, localised cracks and failures, etc).

Finally, as far as the cost/benefit ratio is concerned, ground survey detail came at a cost as it proved to be a particularly time-consuming technique, whereas, apart from the time lapse between image tasking and acquisition, remote sensing represented a faster and over wide areas even cost-effective landslide detection method (about 15.23 euro/km<sup>2</sup> for non orthorectified images).

### **4.3. Spatial accuracy of a multi-temporal landslide inventory map**

In order to quantify and effectively communicate the overall spatial accuracy of landslide detection and mapping, a fuzzy-like analysis was conducted on a multi-temporal landslide inventory map specifically prepared for the Dorgola catchment. This inventory was entirely prepared by using only one detection method (remote sensing) but with changing surrounding conditions (*e.g.* image resolution, date and time, sensor, *etc.*) (see par. 2.4.2.). As a consequence, it basically presents all the advantages and disadvantages reported in the previous paragraph.

Fuzzy logic was introduced by Zadeh (1965) with the fuzzy set theory. In contrast with classical set theory, in which the membership of an element in a set is stated in binary terms (either it belongs or it does not belong to the set), fuzzy set theory implies gradual degrees of membership expressed with a membership function valued in the interval [0,1]. Fuzzy logic is, therefore, a form of many-valued logic which can be considered as an extension of Boolean logic. Among experts, there is an open debate about whether fuzzy logic is to be considered by itself or as part of probability theory. This research, however, cannot take any position in this controversy. In this context, fuzzy logic was just considered

more suitable to express the uncertainty of landslide detection and mapping than probability theory which, in turn, is usually associated to slope susceptibility to sliding.

In the fuzzy raster landslide map specifically conceived for this work pixel values correspond to the degree of membership of a single pixel to a landslide polygon (see par. 2.4.2.). In this sense, membership may be 1, 0, or any gradual value in between. Hence, this type of representation does not show a clear separation between what is in and what is out of the landslide polygon as it does instead a sharp linear boundary. On the contrary, it displays to what extent a certain pixel belongs or does not belong to a landslide pixel set. More specifically, spatial persistence was here meant as the repeated membership of a pixel to a landslide polygon. In this way, if a landslide was detected in every image pixel values is equal to 1, whereas if it could be identified and mapped only in a few images pixel membership is close to 0. It is worth noting, however, that if a landslide was detected and mapped even only once, there are no doubts that it existed at some point in time. As a consequence, a low degree of membership does not indicate that there are few chances that there is a landslide. On the contrary, it means that that particular mass movement may had been poorly identified from a spatial point of view since its recognition and mapping were based only on one or just a few images. Indeed, where a landslide was detected in more snapshots, it was never mapped in the same way so that in the fuzzy raster landslide map its boundary is not sharp and well defined, but instead it is “fuzzy”. Fundamentally, while the pixels of the central part of the mapped landslide present high values of membership, those in the external part are characterised by decreasing membership values from the inside toward the outside (Fig. 2.3). On this basis, it is clear that spatial persistence is strictly related to time. However, in this context, the two variables cannot be basically separated. Indeed, a “*short -lasting*” landslide has less chances to be captured in several images and, therefore, the opportunities to check its size and shape are fewer.

#### **4.3.1. Analysis and results**

In this study, I used spatial persistence and boundary reliability as proxies for spatial accuracy, *i.e.* the definition of landslide shape and size. To this end, I prepared a multi-temporal landslide inventory map where each landslide was outlined on every available

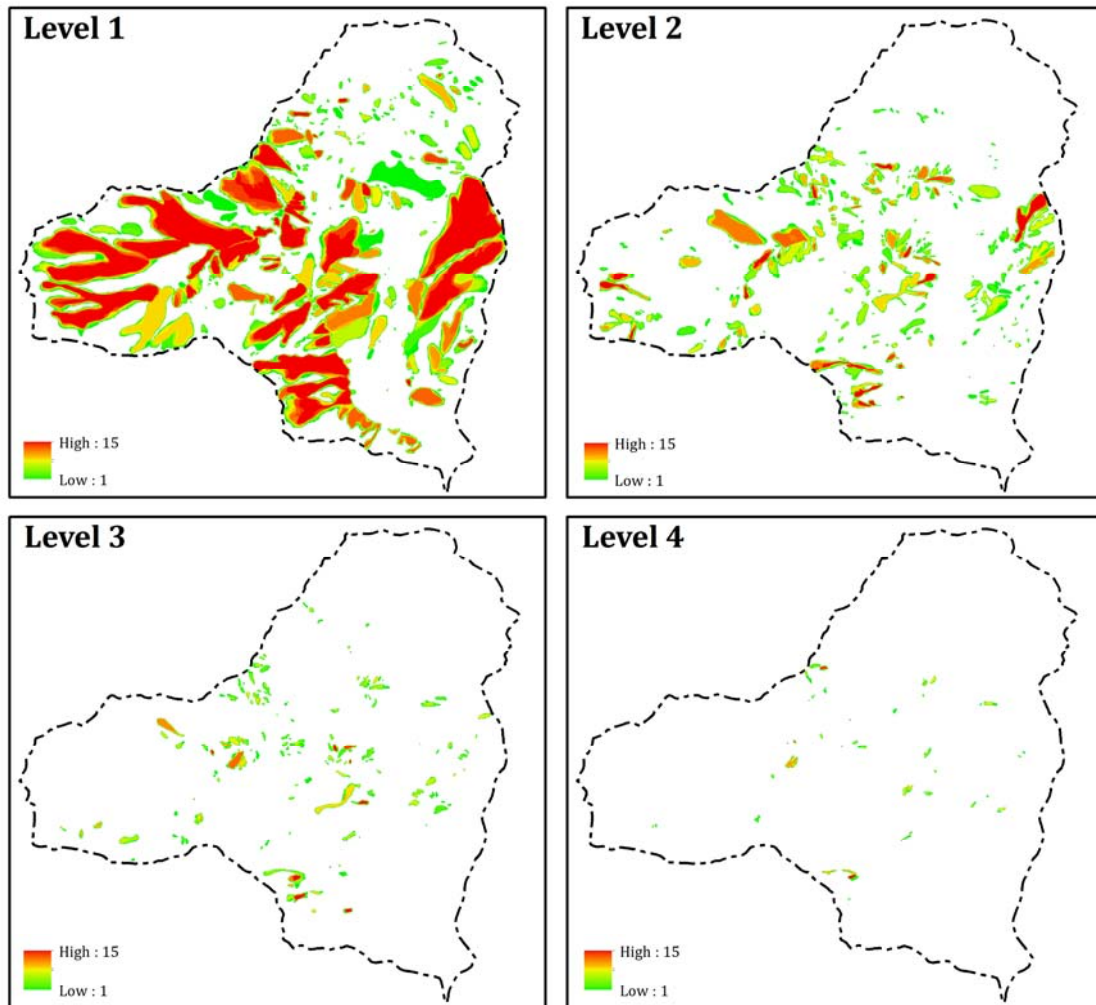


Fig. 4.10: Output of the fuzzy-like analysis performed for the Dorgola catchment. Results are expressed in relation to the total number of image sets used for the analysis.

orthorectified image. Overall, I used 15 image sets spanning over an approximately 30 year<sup>7</sup> time interval with an average temporal sampling rate of about 2 years. In order to avoid spatial alterations related to new sliding movements, for the fuzzy-like analysis I used only unchanged landslides, *i.e.* only those that did not undergo any substantial and detectable reactivation (see par. 2.4.2.). The final results are displayed in Fig. 4.10 and Fig. 4.11. The former shows an absolute value with respect to the 15 snapshots used for the

<sup>7</sup> For the fuzzy-like analysis were used only the image sets from 1981 to 2014.

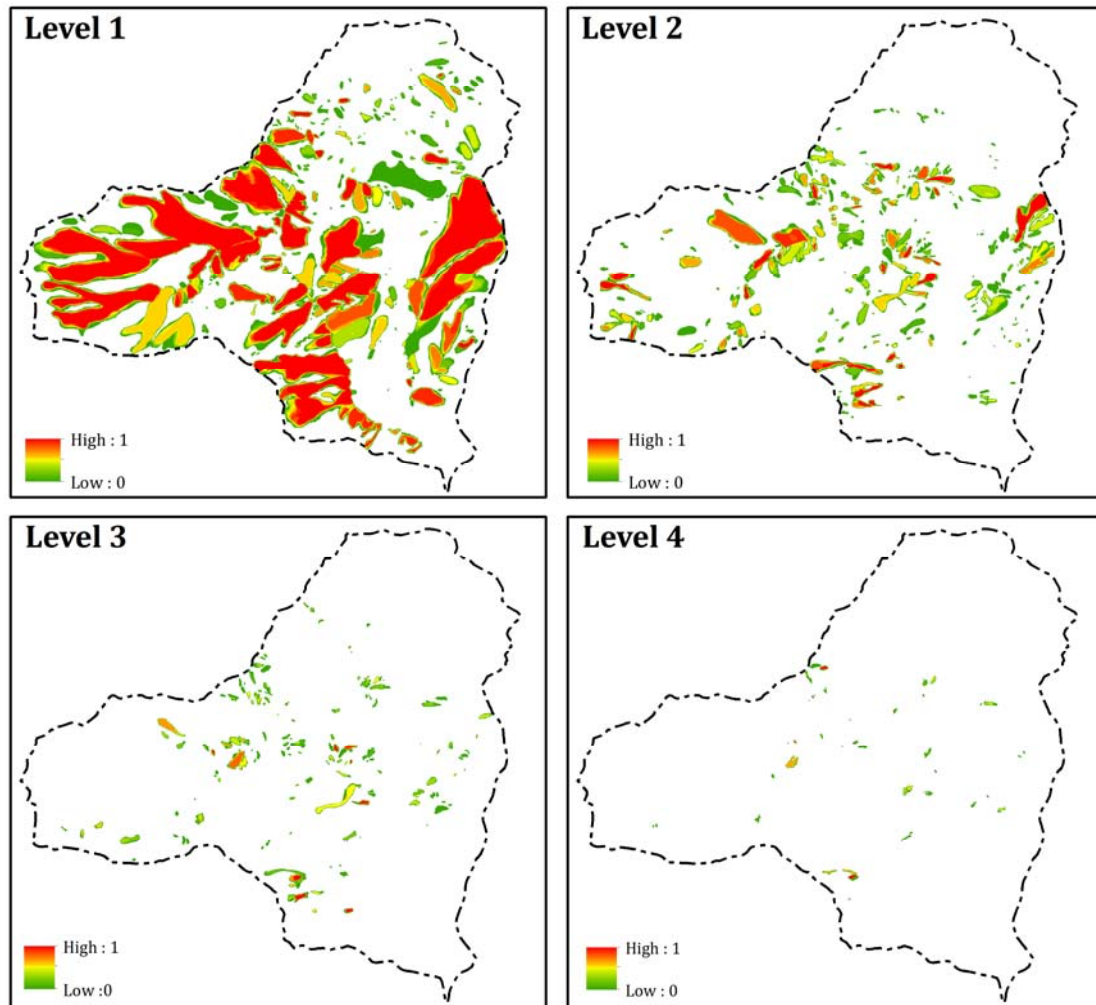


Fig. 4.11: Final output of the fuzzy-like analysis performed for the Dorgola catchment. Results are expressed through a fuzzy index valued in the interval  $[0,1]$ .

analysis, whereas the latter represents the same results according to a normalised fuzzy index.

Before proceeding with the fuzzy-like analysis, in order to avoid any spatial overlapping among different mass movements, I subdivided landslides into 6 six different levels. This classification is based simply on geometrical and spatial bonds, so that a 1° level landslide may contain a 2° level landslide, which in turn may contain a 3° level and so on according to a hierarchical structure (Fig. 2.11). This expedient was essential to avoid merging of different overlapping mass movements (*e.g.* smaller reactivations of larger landslides)

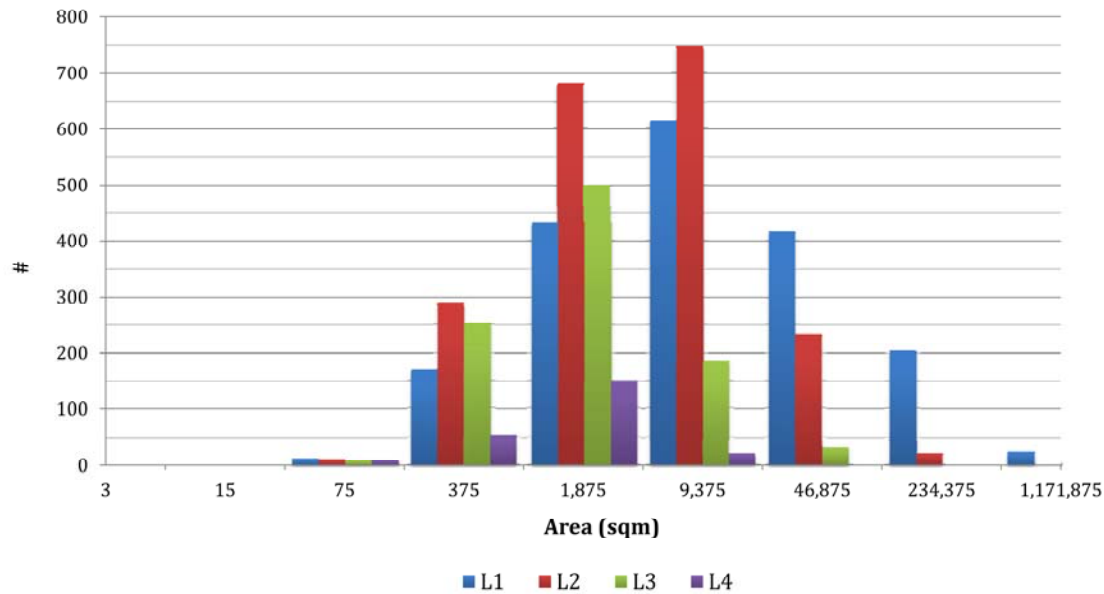


Fig. 4.12: Landslide area frequency distribution for the four levels used for the fuzzy-like analysis. This subdivision, based essentially on geometrical and spatial bonds, was adopted in order to avoid merging of overlapping mass movements during the vector-to-raster transformation.

during the vector-to-raster transformation. Due to the low number of landslides, 5° and 6° levels were not considered statistically significant and, therefore, were not used for the fuzzy-like analysis. The area frequency distribution of the first four levels is shown in Fig. 4.12. In general, this histogram suggests that the 1° and 2° levels contain more landslides and that these mass movements are more heterogeneous and larger than those of the 3° and 4° levels (see also Tab. 4.5).

Overall, the multi-temporal landslide inventory of the Dorgola catchment contains 1.105<sup>8</sup> landslides. About 14.5% (160) of these slope failures were identified as LL's, *i.e.* as mass movements that temporarily disappeared from the record to reappear again without any apparent reactivation (see par. 2.4.2. for details). This temporary concealment was basically caused by different impending factors, mainly: clouds, vegetation, shadow areas, and more generally image scale and illumination. As a consequence, this lapse of time was conceived as a "black-out period" due to the detection method and not to the landslide true evolution.

<sup>8</sup> This number does not include reactivations which, as already remarked, were classified with the same ID number of the original landslide.

*Tab. 4.5: Descriptive statistics for the landslide levels used for the fuzzy-like analysis. For this purpose were used only those landslides that did not undergo any substantial and detectable reactivations.*

	Level 1	Level 2	Level 3	Level 4
Number of landslides*	1.881	1.989	981	234
% of total number of landslides	37,0	39,1	19,3	4,6
Total area covered by landslides	7.082.375	4.970.672	509.890	91.663
Area of smallest landslide	54,19	65,70	54,66	73,03
Area of biggest landslide	474.010	403.442	27.906	5268
Median	7.585	3.238	1.293	1.190

\* As remarked in the text, in the multi-temporal inventory each landslide was outlined on every image set. This value includes the overall number of detected mass movements, which means also the same landslide mapped in different images.

In the specific case of the Dorgola Valley, the 160 LL's were so divided:

- 121 (75.6%) were temporary concealed due to image illumination, tone and bands (color vs B/W images);
- 25 (15.6%) were included in woody areas;
- 14 (8.8%) were covered by shadows.

Since theoretically they do not imply any real reactivations and, therefore, any new mass movements, in the fuzzy-like analysis I considered LL's as a whole, including their "black-out periods". On the other hand, with regard to reactivated landslides, I chose to maintain only the longest period of persistence or, as a second chance, the most recent one.

The histogram in Fig. 4.13 shows the pixel (counts) frequency distribution in the four output rasters representing the fuzzy index classes. In particular, the class bins were obtained by dividing the interval [0,1] by 0.1, whereas the pixel number of each level was plotted as a percentage of the counts of the total area covered by landslides. Despite the

unequal magnitude, the histogram shows that 1° and 2° levels present pixels with both low and high membership degree, *i.e.* areas with low and high spatial persistence, whereas in 3° and 4° levels low fuzzy indexes are more common. These trends are better displayed in Fig. 4.14 where every single level is plotted alone.

The histogram of the 1° level is quite irregular probably due to the heterogeneity of this group, which is basically made up of two different categories of mass movements:

- old dormant landslides;
- small to medium isolated landslides.

Old dormant landslides have been intensively colonised both by natural and anthropogenic processes. They usually involve the entire slope, and they could be identified only at smaller scale. However, their imprinting on the local landscape is so intense that, if remotely detectable, they could always be identified regardless of image capturing conditions. In this case, all the uncertainties about their mapping were concentrated along the boundaries. As a consequence, these large landslides, concentrated mainly in the Ligurian Units, are responsible for the high fuzzy index values (0.8÷1.0), but to some extent they are also

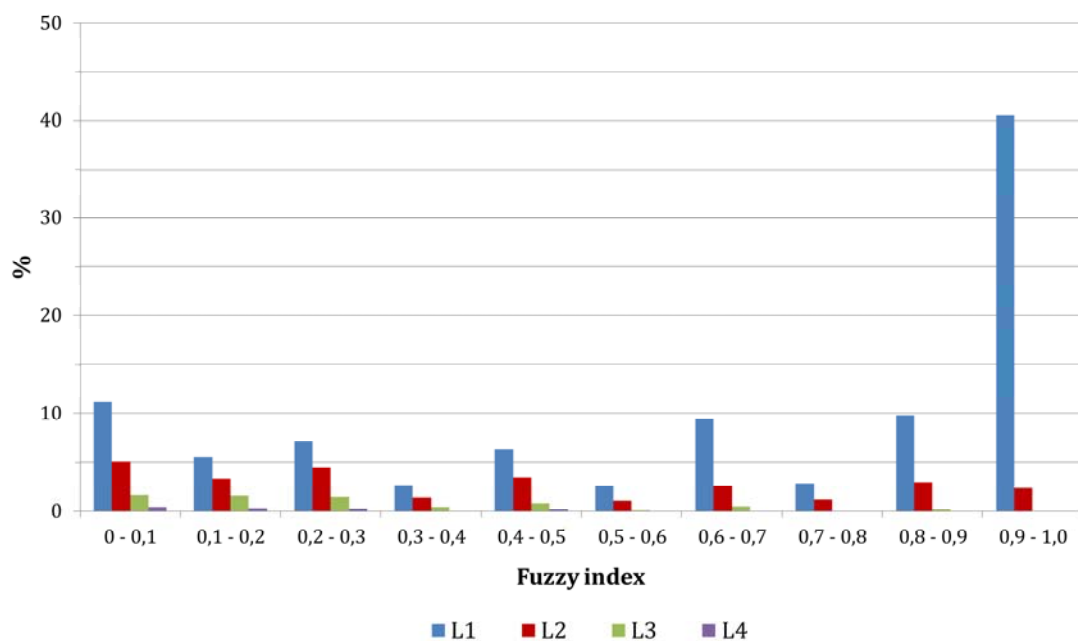


Fig. 4.13: Pixel frequency in fuzzy index classes for the four landslide levels.

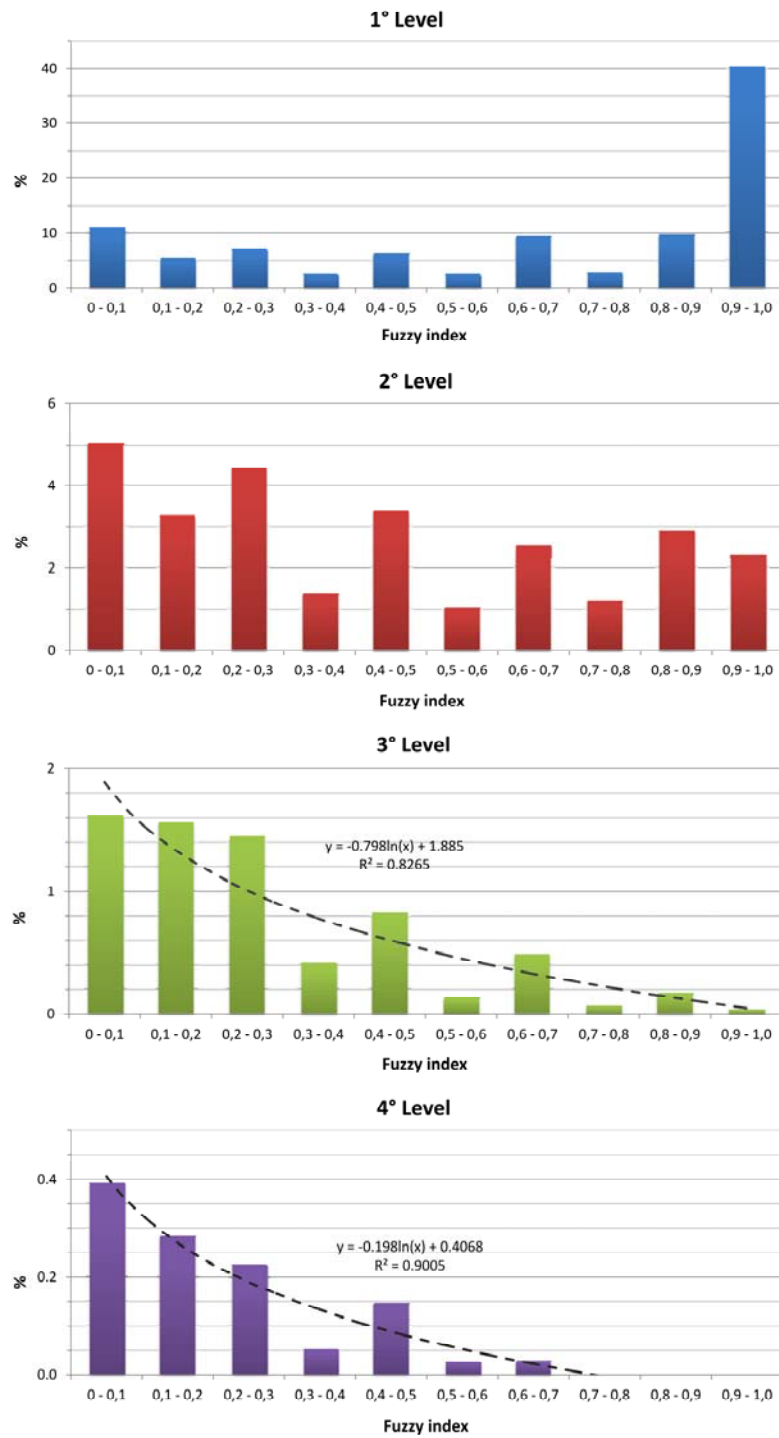


Fig. 4.14: Pixel frequency in fuzzy index classes for each of the four landslide levels.

related to lower values as far as their marginal parts are concerned. The second category contains stand-alone landslides. Most of them are included in the Epi-Ligurian Sequence, and they generally differ from the previous ones for age, depth, and spatial persistence. In this case, the low fuzzy index values ( $0 \div 0.3$ ) can be related to a truly short "*lifetime*", to challenging optimal detection conditions, or to a low inactivity, which indeed increases the detection complexity. It is not a chance that this category includes many Lazarus landslides.

The 2° level histogram is quite irregular as well, but its landslides are a bit different from those of the 1° level. Indeed, in this case mass movements can be attributed to the following categories:

- active and suspended portions of bigger landslides;
- small to medium reactivations of bigger landslides.

Due to their fresh and persistent aspect, mass movements from the first category could be detected basically in every image set and, therefore, are responsible for the high fuzzy index values ( $0.8 \div 1.0$ ). In this case, like for bigger landslides, only boundary areas are affected by a significant uncertainty. Low to medium fuzzy index values ( $0 \div 0.5$ ) are due to these areas and to small to medium reactivations of bigger landslides. Although generally unrelated from a genetic point of view, small landslides take place within bigger ones and disappear quite quickly due to man activities (especially farming) and further overlapping slope failures. Medium size landslides, instead, are inactive parts of bigger landslides. Indeed, inactivity and the consequent colonization by plants increase the detection complexity by concealing landslide original shape.

With respect to the 1° and 2°, the 3° and 4° levels contain more homogeneous and smaller landslides included in bigger ones. Probably due to landslide homogeneity, both histograms show a distinct trend that highlights a clear abundance of low fuzzy index values ( $0 \div 0.3$ ) (Fig. 4.14). This complies with the fact that small landslides can be easily concealed by natural and/or anthropogenic processes or completely masked by new reactivations.

### 4.3.2. Discussion

In this work, a fuzzy raster landslide map was used to quantify and display the spatial accuracy of a landslide inventory map. Although in a rigorous fuzzy analysis the membership function is valued in the interval  $[0,1]$ , in this context I referred also to the absolute value related to the total number of image sets. Indeed, this is an important piece of information for the end-users since the spatial accuracy of a landslide inventory map strongly relies on the number and characteristics of the images used to prepare it. In this sense, a landslide inventory map prepared on the basis of 15 different snapshots with an average temporal sampling rate of about 2 years basically presents a higher overall accuracy than a landslide inventory map that could rely on fewer image sets separated by a longer time interval.

Apparently, relating landslide spatial persistence and, hence, spatial accuracy to the number of image sets used to prepare the inventory may not seem appropriate. Indeed, one single snapshot, if acquired in the right moment and in the right conditions, may be sufficient to define landslide spatial attributes in the most accurate way. To this end, adding more data may generally worsen the overall landslide mapping accuracy since with time the landslide boundary tends to be concealed or altered by natural and/or anthropogenic processes. Notwithstanding this, chances to catch a landslide just after it had happened are little especially with a high temporal sampling rate. In this way, in most cases, the first time a landslide is detected and mapped it is difficult to prove that it actually displays its original size and shape. Furthermore, a new mass movement may conceal an older one. In this case, if detection conditions are not advantageous, relict parts of the previous slope failure can be confused with the more recent landslides altering its original size and shape. As a consequence, for most landslides, spatial persistence proves to be a good proxy for the definition of their spatial accuracy. For this purpose, more data are available the better it is. In this sense, a fuzzy raster landslide map, like the one prepared for this work, is a tool that needs to be continuously implemented.

In the specific case of the Dorgola catchment, old large dormant landslides could be detected constantly in nearly all image sets regardless of the quality of the image used as support

and of the general capturing conditions. Indeed, these landslides had such a relevant role in the definition of landscape and local morphology that unlikely their distinctive features (*e.g.* concave and convex slope morphology, lobate run-out areas, drainage pattern deviations, irregular morphology, *etc.*) could be concealed by natural or anthropogenic processes. In this case, the fuzzy-like analysis confirmed that these landslides present a high spatial persistence and, therefore, are characterised by high fuzzy index values with the exception of the outer parts. Indeed, external boundaries are affected by a significant uncertainty and their accurate identification strictly depends on several factors. Smaller landslides (< 10.000 m<sup>2</sup>), on the other hand, generally present a poor spatial persistence and are actually defined by low fuzzy index values. This means that their mapping is affected by a high uncertainty. The main issue about these landslides is that they usually have a short “lifetime”, *i.e.* they present a low temporal persistence (see Chapter 5). As a consequence, they have few chances to be captured in several image sets, and, hence, their mapping accuracy relies entirely on the quality, capturing conditions, and landslide appearance of those few snapshots.

Ultimately, another landslide category that proved to be particularly challenging for mapping are LL's. A disadvantageous set of images, for example, may cause these landslides to be completely undetected. For this reason, although certain capturing conditions may appear better than others, their continuous application must be carefully evaluated. Indeed, if they lead to some sort of bias (*e.g.* repeated shadows or forest cover over the same areas) they may constantly prevent the detection of some mass movements. If this is the case, options should be analysed.

On the basis of this work, landslide spatial accuracy depends on extrinsic and intrinsic factors. Basically extrinsic factors can be related to:

- orthorectification accuracy;
- geographic positioning accuracy (see Chapter 3);
- scale and resolution of image sets;
- image capturing conditions (date, time, azimuth, weather, *etc.*).

With the exception of image capturing conditions, which could have a higher magnitude, the effects of these aspects on spatial accuracy are of the order of metric length. As a

consequence, their influence is proportionally more significant for smaller landslides than for larger ones. In this particular case, geographic positioning accuracy could be assessed separately, whereas the remaining variables were appraised all together. Efforts should be made to quantify and improve every single aspect, *e.g.* by creating a protocol for orthorectification method, limitations, and software.

Landslide spatial accuracy is controlled also by several intrinsic variables like for example:

- landslide natural stabilization, revegetation, and progressive concealment;
- inherent uncertainty related to landslide geomorphological survey<sup>9</sup>;
- landslide active nature, so that a landslide can be strongly affected or even completely concealed by other sliding movements or by significant reactivations;
- anthropogenic processes that can both stabilise (consolidation works) or conceal (*e.g.* farming activities) the original mass movements<sup>10</sup>.

In general, these factors affect spatial accuracy in the order of tens of meters. Moreover, also in this case, the separation of every single contribute is quite challenging, because it is specifically related to each individual landslide.

#### **4.4. Conclusions**

This Chapter focused on the spatial accuracy of a landslide inventory map. In particular, this subject was addressed from two different points of view: landslide detection and mapping techniques, and the overall spatial accuracy.

I carried out a comparison between a remotely sensed inventory, prepared on a VHR orthorectified GeoEYE image, and a detailed geomorphological field-based inventory. This work ultimately proved that neither of these two detection methods provided a complete inventory map, consequently, they should be considered complementary. Indeed, field survey is an essential and efficient method to develop a detailed reference framework, while the visual interpretation of orthorectified satellite images represents a precise, cost-effective, and quick method not only to complete, but also to monitor and implement the

---

<sup>9</sup> Geomorphological survey is generally limited to the superficial analysis of landforms.

<sup>10</sup> Man-induced modifications should probably be considered as extrinsic factors, but since they modify directly the landslide appearance, I decided to list them among intrinsic variables.

initial framework and keep it constantly updated.

In order to quantify the overall spatial accuracy of landslide detection and mapping, I performed a fuzzy-like analysis on a multi-temporal landslide inventory specifically prepared for the Dorgola catchment. In this context, spatial persistence and boundary reliability were used as proxies to assess the uncertainty related to slope failure mapping. This analysis demonstrated that old large dormant landslides generally present a very good spatial persistence, while smaller landslides (< 10.000 m<sup>2</sup>) are generally affected by a high mapping uncertainty expressed by low fuzzy indexes. In this sense, this work proved that mapping accuracy strongly relies on the “lifetime” of a landslide footprint as well as on the image quality and capturing conditions. The former, in particular, emphasises the importance of the time variable. Image quality and capturing conditions, instead, should be carefully evaluated as they may prevent the detection of certain slope failures like, for example, when they lead to some sort of bias (*e.g.* repeated shadows or forest cover over the same area). Ultimately, the fuzzy-like analysis demonstrated that representing landslides with sharp boundaries is a significant simplification of a more complex and uncertain situation. According to the “truth-in-labelling” paradigm, the fuzzy raster landslide map is an effective tool not only to quantify but also to display and convey information about the inherent uncertainty and spatial accuracy of landslide detection and mapping. For wide and heterogeneous areas, it would be actually awkward to resume spatial accuracy in a unique number. In this sense, a map is a much more efficient metadata to convey punctual as well as spatial information.

In conclusion, this research appraised that landslide identification and mapping are affected by a significant uncertainty. This confirmed that the conceptual model that is ultimately realised in a landslide inventory is a merely approximation and a generalization of reality. This consideration, however, must not reduce the importance of landslide inventories as decision-support tools. Indeed, as widely argued, it is not the tool but rather the use that can be potentially erroneous. In this sense, in order to avoid any possible misuses, it is essential to convey to the end-users all the limitations of a landslide inventory map in the most accurate way possible.

## CHAPTER 5

### Landslide temporal persistence

- 5.1. Introduction
- 5.2. Multi-temporal landslide inventory map of the Dorgola catchment
  - 5.2.1. Analysis and results
    - 5.2.1.1. Descriptive statistics
    - 5.2.1.2. Correspondence of landslide areas
  - 5.2.2. Discussion
- 5.3. Characterization of new and undetected landslides
  - 5.3.1. Analysis and results
    - 5.3.1.1. Descriptive statistics
    - 5.3.1.2. New detection size
    - 5.3.1.3. New detection location
  - 5.3.2. Discussion
- 5.4. Temporal persistence of landslide footprints
- 5.5. Conclusions

## 5. Landslide temporal persistence

### 5.1. Introduction

In order to be a reliable and effective reference tool for land instability, a landslide inventory map has to record every single mass movement. In the literature, completeness is actually considered as a fundamental element for quality assessment (Trigila *et al.*, 2010; Guzzetti *et al.*, 2012). Completeness, however, is a space-time dependent variable as landslides are complex events that take place in space and time.

In general, for a landslide inventory map used within the land-use planning context, a landslide is forever. In particular, although its deposit may be stabilised, concealed, or even completely removed (*e.g.* landslide deposits along road cuts) or eroded (*e.g.* landslide deposits along riverbeds), the fact that a slope failure had happened in a certain place in a certain moment is an important piece of information that a landslide inventory map, prepared for planning purposes, cannot ignore or miss. Indeed, this event is indicative of a potential, albeit not necessarily current, sliding susceptibility and is essential for a complete and detailed framework of landslide activity. In this sense, it is fundamental to map a mass movement when it is still well recognizable and, in order to determine a proper data acquisition frequency, to assess for how long a landslide can be identified.

In this chapter, I deal with landslide activity and with the temporal persistence of landslide footprints. In particular, I carefully analyse the multi-temporal inventory prepared for the Dorgola catchment in order to evaluate potential temporal trends and to characterise new detected and undetected landslides, *i.e.* those landslides that disappear from the records. The ultimate purpose is to investigate the temporal reliability of a landslide inventory map.

## **5.2. Multi-temporal landslide inventory map of the Dorgola catchment**

The temporal evolution of the active landscape of the Dorgola catchment was portrayed by a multi-temporal landslide inventory specifically prepared for this purpose (see par. 2.4.2.). For the temporal analysis I used all available image sets (18 spanning from 1954 to 2014) including those that were just georeferenced but not orthorectified.

### **5.2.1. Analysis and results**

Most of the image sets used for this work are aerial photographs, while the remainings consist of VHR satellite images (GeoEYE and IKONOS) (Tab. 5.1). With regard to the time frame, most images were acquired between June and September as they were tasked for agricultural purposes. In this part of the Apennine Range, however, 48% of slope failures take place between March and May, and 29% between October and December (Bertolini and Pellegrini, 2001). Unfortunately, just 5 image sets were captured in the first period and only 1 in the second. On the other hand, as far as sampling rate is concerned, the first 30 years are not particularly well represented as they rely only on 4 image sets with a significant 19-years time lag between the first (1954) and the second (1973) snapshot. From 1986 onward, instead, the acquisition frequency became smaller with an average of about 2 years (min: 1 year, max: 6 years).

#### **5.2.1.1. Descriptive statistics**

On the whole, the multi-temporal landslide inventory contains 1,105<sup>1</sup> landslides. The average number of mass movements without LL's for each snapshot is about 334<sup>2</sup>. However, in order to get a more realistic distribution, the histogram of Fig. 5.1 displays the total number of mass movements including hidden LL's, which were added to those image sets where, although undetected, they were likely present. In particular, data from Tab. 5.2 show that 1996, 1998, 2000, 2003, 2007, and 2008 are the most affected image sets. Major landslide peaks were recorded in 1981, 1996, 2003, 2011, and 2013, while conversely the 1954,

---

<sup>1</sup> See footnote # 8 in Chapter 4.

<sup>2</sup> If considering LL's the average is 356.

CHAPTER 5

*Tab. 5.1: Main characteristics of the image sets used in this work. Since they could not be orthorectified, the 1954, 1973 and 1978 image sets were used only for landslide detection but not for landslide mapping. As a consequence they were considered for the temporal persistence, but they were not included in the fuzzy-like analysis.*

Supplier	Producer	Type	Altitude (m)	Photo scale	Year	Month	Day	Time	Flight line	Photo
<b>IGM</b>	IGM	B&W aerial photograph	10.000	55.000	<b>1954</b>	07	08	09:37	51	1182
<b>RER</b>	CGR Spa	B&W aerial photograph	2.142	14.000	<b>1973</b>	07/08	n/a	14:16	n/a	RER69_13_49_2803
						07/08	n/a	14:15	n/a	RER69_13_49_2804
						07/08	n/a	11:10	n/a	RER69_13_50_2925
						07/08	n/a	11:11	n/a	RER69_13_50_2927
<b>RER</b>	CGR Spa	Color aerial photograph	2.050	13.500	<b>1978</b>	06	05	12:18	n/a	RER76_13a_13_7834
						06	05	12:18	n/a	RER76_13a_13_7835
						06	05	12:18	n/a	RER76_13a_13_7836
						06	05	12:19	n/a	RER76_13a_13_7837
						06	05	12:06	n/a	RER76_13a_14_7797
						06	05	12:05	n/a	RER76_13a_14_7799
						06	05	11:16	n/a	RER76_13a_15_7744
<b>IGM</b>	IGM	B&W aerial photograph	4.500	28.000	<b>1981</b>	07	27	11:24	XIVA	346
<b>RER</b>	CGR Spa	B&W aerial photograph	3.825	25.000	<b>1986</b>	09	06	13:00	n/a	RER85_15c_014

## Landslide temporal persistence

<b>Supplier</b>	<b>Producer</b>	<b>Type</b>	<b>Altitude (m)</b>	<b>Photo scale</b>	<b>Year</b>	<b>Month</b>	<b>Day</b>	<b>Time</b>	<b>Flight line</b>	<b>Photo</b>
<b>IGM</b>	IGM	B&W aerial photograph	5.100	28.000	<b>1988</b>	11	05	11:28	12	201
<b>IGM</b>	IGM	B&W aerial photograph	5.750	33.000	<b>1994</b>	06	06	10:39	9	6071
<b>Geoportale/AGEA</b>	CGR Spa (AGEA)	B&W aerial photograph	6.000	40.000	<b>1996</b>	08	14	n/a	n/a	n/a
<b>Geoportale</b>	CGR Spa	Color aerial photograph	6.000	40.000	<b>1998</b>	07	10	n/a	n/a	n/a
<b>IGM</b>	IGM	B&W aerial photograph	5.500	36.000	<b>2000</b>	06	15	11:22	44	256
<b>GISItalia/e-geos</b>	Digital Globe	IKONOS PAN satellite image	n/a	n/a	<b>2003</b>	02	15	10:37	n/a	n/a
<b>IGM</b>	IGM	B&W aerial photograph	7.200	47.000	<b>2004</b>	05	21	09:13	262	9195
<b>Geoportale</b>	n/a	Color aerial photograph	5.500	35.000	<b>2007</b>	05	10	n/a	n/a	n/a
<b>RER/AGEA</b>	n/a	Color aerial photograph	n/a	n/a	<b>2008</b>	06	23	n/a	n/a	n/a
<b>RER/AGEA</b>	CGR Spa (AGEA)	Color digital aerial photograph	n/a	n/a	<b>2011</b>	05	28-29	n/a	n/a	n/a
<b>GISItalia/e-geos</b>	Digital Globe	GeoEYE PAN satellite image	n/a	n/a	<b>2012</b>	08	03	10:13	n/a	n/a
<b>GISItalia/e-geos</b>	Digital Globe	GeoEYE pansharpened satellite image	n/a	n/a	<b>2013</b>	04	18	10:11	n/a	n/a
<b>GISItalia/e-geos</b>	Digital Globe	GeoEYE pansharpened satellite image	n/a	n/a	<b>2014</b>	03	20	10:16	n/a	n/a

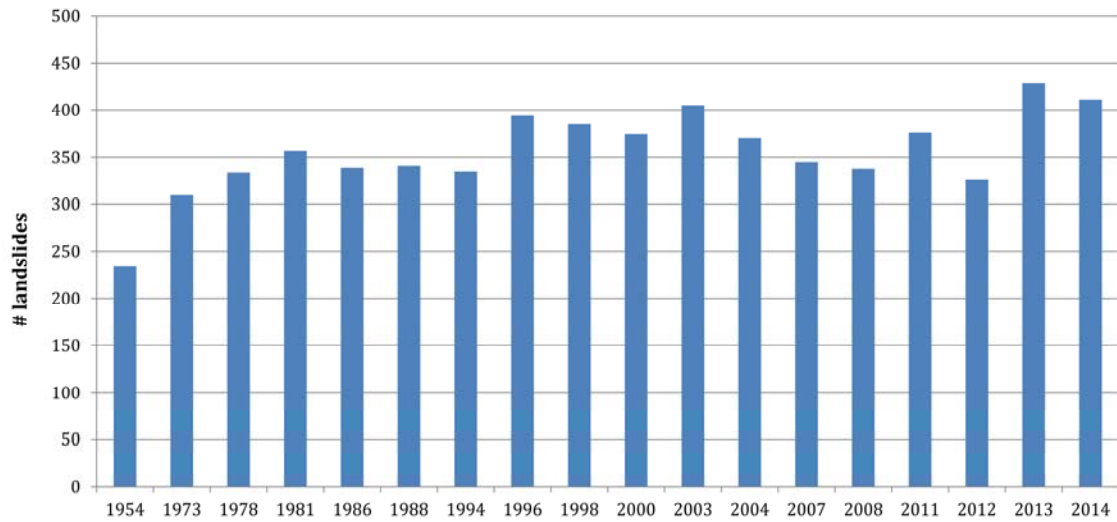


*Fig. 5.1: Landslide frequency distribution in the multi-temporal inventory of the Dorgola catchment. The histogram displays the total number of slope failures per year including hidden LL's. These mass movements, that disappear from the records to reappear later without any evident reactivation, were, indeed, added to those image sets where, although undetected, they were likely present. This correction allowed to reduce the effects of detection limits and to obtain a more realistic and comparable number of landslides.*

1994, 2008, and 2012 image sets represent the lows. A correction regarding LL's should be performed also for areas. Nevertheless, spatial accuracy is affected by an intrinsic uncertainty which is a function of several variables (see Chapter 4). Therefore, for each landslide the area is not a unique value but it changes from snapshot to snapshot. Consequently, as far as areas are concerned, data with no correction were used as proxies.

In general, the total area covered by mass movements, as well as landslide smallest, biggest, and median areas, all diminish with time particularly after 1988 (Fig. 5.2). Furthermore, according to the total area, also landslide indexes, with values included between 25.8% and 36.2%, basically decrease with time (Tab. 5.2). Altogether, higher values belong to the 1988 inventory, whereas lower ones are those of the 2008 inventory. Indeed, although the 1988 image set presents very similar characteristics to those of 1981 and 1986 (*e.g.* flight altitude and photo scale, resolution, B/W, *etc.*), its detection potential is higher. This image was actually acquired in early November and, due to the different illumination in this season, the long shadows allowed to highlight hummocky morphologies more effectively. As a

Tab. 5.2: Descriptive statistics of the 18 inventories that form the multi-temporal inventory of the Dorgola catchment from 1954 to 2014. The values in parenthesis include hidden LL's.

		<b>1954</b>	<b>1973</b>	<b>1978</b>	<b>1981</b>	<b>1986</b>	<b>1988</b>
Number of landslides	#	234 (234)	306 (310)	328 (334)	345 (357)	321 (339)	325 (341)
Total area of mapped landslides	km <sup>2</sup>	-	-	-	6,197	6,591	7,128
Total area covered by landslides	km <sup>2</sup>	-	-	-	4,990	5,284	5,864
% of landslide area	%	-	-	-	30,8	32,6	36,2
Landslide density	#/km <sup>2</sup>	-	-	-	21,3	19,8	20,0
Area of smallest landslide	m <sup>2</sup>	-	-	-	145	75	278
Area of biggest landslide	m <sup>2</sup>	-	-	-	454.501	441.908	474.010
Landslide average area	m <sup>2</sup>	-	-	-	17.963	20.534	21.932
		<b>1994</b>	<b>1996</b>	<b>1998</b>	<b>2000</b>	<b>2003</b>	<b>2004</b>
Number of landslides	#	311 (335)	346 (394)	353 (385)	341 (376)	368 (405)	348 (377)
Total area of mapped landslides	km <sup>2</sup>	6,201	6,356	5,827	6,025	6,345	6,250
Total area covered by landslides	km <sup>2</sup>	5,126	5,153	4,722	4,889	5,095	5,133
% of landslide area	%	31,6	31,8	29,1	30,2	31,4	31,7
Landslide density	#/km <sup>2</sup>	19,2	21,3	21,8	21,0	22,7	21,5
Area of smallest landslide	m <sup>2</sup>	158	188	125	149	88	93
Area of biggest landslide	m <sup>2</sup>	448.952	440.502	400.072	422.612	397.602	409.994
Landslide average area	m <sup>2</sup>	19.938	18.369	16.507	17.669	17.243	17.959
		<b>2007</b>	<b>2008</b>	<b>2011</b>	<b>2012</b>	<b>2013</b>	<b>2014</b>
Number of landslides	#	304 (345)	290 (338)	350 (376)	304 (326)	429 (429)	411 (411)
Total area of mapped landslides	km <sup>2</sup>	4,834	4,571	5,405	5,039	5,501	5,453
Total area covered by landslides	km <sup>2</sup>	4,184	3,977	4,528	4,365	4,587	4,527
% of landslide area	%	25,8	24,5	27,9	26,9	28,3	27,9
Landslide density	#/km <sup>2</sup>	18,7	17,9	21,6	18,7	26,5	25,3
Area of smallest landslide	m <sup>2</sup>	66	73	73	79	54	55
Area of biggest landslide	m <sup>2</sup>	384.010	398.199	403.442	392.681	395.219	393.225
Landslide average area	m <sup>2</sup>	15.903	15.761	15.443	16.577	12.823	13.236

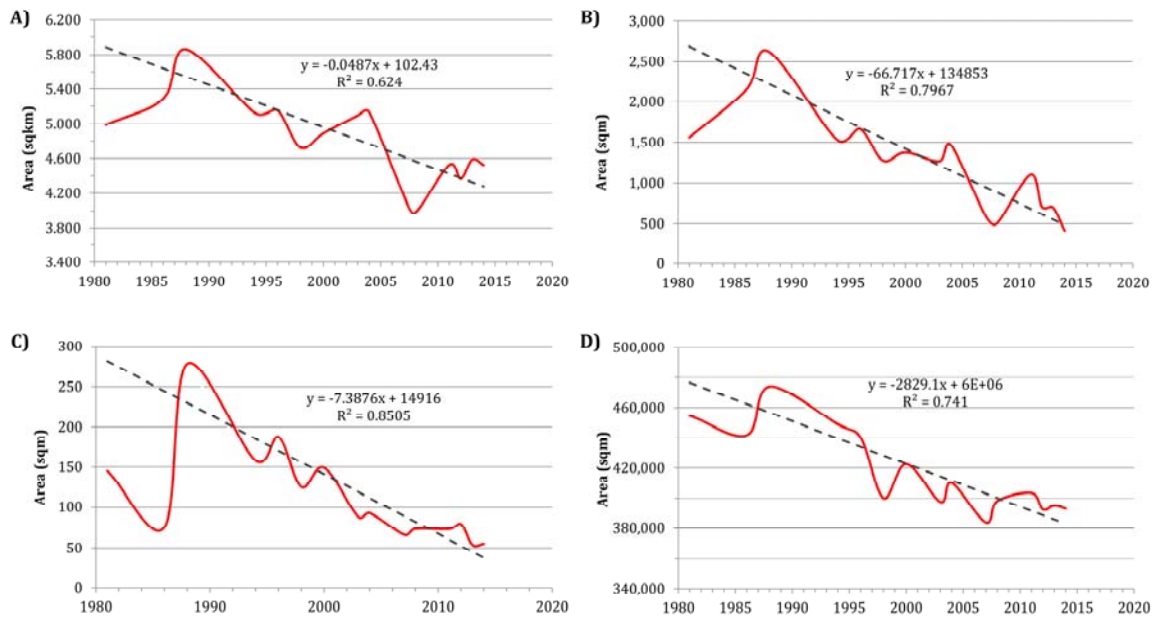


Fig. 5.2: Temporal trends of the total area covered by landslides (A) and of landslide median (B), smallest (C), and biggest (D) areas. These data could not be corrected as far as LL's are concerned since landslide areas are not unique values but they change from snapshot to snapshot. Therefore, data with no correction were used as proxies.

consequence, some large dormant landslides, unrecognised in the other image sets, were detected. In the same way, despite its very high resolution, the 2008 image set shows a low detection potential due to capturing conditions, especially season and illumination.

#### 5.2.1.2. Correspondence of landslide areas

The cartographic matching between each pair of inventories was calculated according to the method proposed by Carrara *et al* (1993) as modified by Galli *et al* (2008) (see par. 4.2.1.3.). Results concerning the error index are displayed in Fig. 5.3 where darker colours indicate higher values. This matrix highlights how the error index increases with time, *i.e.* as the time lag between two inventories becomes bigger. In this sense, there is a good correspondence between two inventories realised from two consecutive image sets. In particular, in the short-term (time lag from 1 to 2 years) the error index is between 10% and 20%, while for longer periods (about 10÷15 years) an increasing mismatch with an error index  $\geq 30\%$  is observed.

	1981	1986	1988	1994	1996	1998	2000	2003	2004	2007	2008	2011	2012	2013	2014
1981	-	18.9	26.6	27.0	28.9	29.3	26.0	28.9	28.4	34.6	37.4	35.3	36.8	35.9	36.7
1986		-	21.5	24.1	25.3	26.3	25.6	25.5	25.2	33.3	36.9	32.8	34.1	32.7	33.2
1988			-	24.6	24.1	29.0	26.8	26.1	25.9	36.8	40.1	33.5	34.8	33.6	34.5
1994				-	21.9	19.7	20.5	22.6	22.2	30.0	34.0	28.3	29.5	29.2	30.3
1996					-	24.4	24.2	19.9	21.5	31.4	36.6	29.0	30.4	31.7	31.4
1998						-	18.4	23.7	22.9	28.2	32.5	28.7	29.6	29.6	30.6
2000							-	22.3	20.8	29.0	31.7	28.3	29.5	29.4	30.1
2003								-	17.4	28.6	33.6	26.2	28.2	28.5	28.4
2004									-	26.4	31.1	24.2	26.6	27.5	27.3
2007										-	20.8	20.4	22.8	26.2	26.5
2008											-	23.4	26.7	28.0	27.7
2011												-	14.5	20.4	21.3
2012													-	16.7	18.2
2013														-	10.5
2014															-

Fig. 5.3: Error index matrix. The correspondence of landslide areas was calculated according to the method proposed by Carrara et al. (1993) as modified by Galli et al. (2008). Darker colours indicate higher values of cartographic mismatch between each pair of inventories.

### 5.2.2. Discussion

The total number of landslides in each snapshot is a ready-reference but its interpretation is not so straightforward. First of all, one issue is represented by LL's. Indeed, these mass movements exist even in those "black-out periods" when they cannot be detected. As a consequence, adding LL's to those effectively recognised and mapped in a certain image set is a way to reduce the effects of the detection method limits and to obtain a more realistic and comparable number of landslides. The 1996, 1998, 2000, 2003, 2007, and 2008 image sets are those with the highest number of hidden LL's with values ranging from 32 to 48

items (Tab. 5.2). On the basis of these image sets, possible causes for LL's include image illumination, vegetation, and shadowed areas (see par. 4.3.1.). Indeed, with the exception of the 2003 image, all the other were acquired from May to August, *i.e.* when the vegetation canopy is present and farming is particularly active. The capturing time, on the other hand, is not always available but it is strictly related to illumination which affects landslide detection. In this sense, high illumination angles increase shadows which, on one hand, may obscure some landslides but on the other hand may emphasise hummocky morphologies.

Despite LL's correction, the total number of landslides must still be interpreted with care since it is the result of two further time-dependent and partially contrasting forces: the intrinsic activity and evolution of landslides, and anthropogenic processes. The variable trend of slope failure distribution shown in Fig. 5.1 is the result of these two factors. The intrinsic activity and evolution of mass movements act toward an increase (new activations/reactivations) and a decrease (natural concealment operated by vegetation) of the total number of landslides. Conversely, anthropogenic processes basically lead to a decrease of this number<sup>3</sup> as they contribute to the concealment of landslides both with (*e.g.* consolidation works) or without (*e.g.* ploughing) any real improvement in the slope stability. Peaks in Fig. 5.1 correspond to landslide climaxes<sup>4</sup>, whereas lows are probably correlated to periods of minor activity when the anthropogenic component takes over slope failures reducing their overall number. The overall value alone, however, does not give any precise information about the respective contribution of the two variables. To this end, more detailed analysis on the number of new detections (new activations and reactivations) and undetected landslides are essential.

The progressive decrease with time of the total area covered by landslides, as well as that of landslide smallest, biggest, and median areas, became particularly evident after 1988. Indeed, from 1988 onward a linear decrease can be observed for all the four terms. This means that mapped landslides became generally smaller. Given that minor fluctuations may

---

<sup>3</sup> As potential causes of mass movements, anthropogenic processes are included in landslide activity and evolution.

<sup>4</sup> For the Emilia-Romagna region, the correlation between landslides and rainfalls is not straightforward. Indeed, as remarked by Basenghi and Bertolini (2001), the relationship between causes and effects is anything but simple and, for this reason, its analysis was not included in this work.

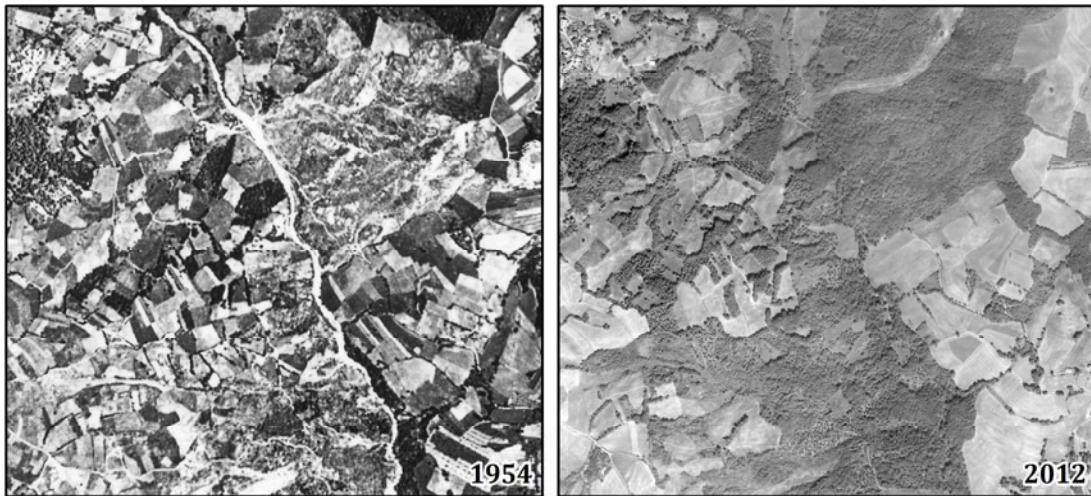


*Fig. 5.4: Comparison between the 1954 and the 2012 image sets (scale 1:20,000). The increase of forested and scrubby areas is evident and it proves the general revegetational processes that took place in the Dorgola Valley in this time lag.*

be ascribed to landslide and anthropogenic activities, the general trend can be explained by two main factors:

- improvement of image set resolution. In fact, a better resolution, besides allowing to recognise smaller landslides, improves mapping definition;
- natural and anthropogenic revegetation. As shown in Fig. 5.4, since 1954 the Dorgola Valley has been significantly reforested and naturally revegetated. This process was, at least partially, directly induced by man through tree planting, but it was also due to the relinquishment of some areas that were progressively recolonised by the vegetation. Although it potentially improved local slope stability, the presence of wider forested areas and scrublands worsened landslide detection conditions by preventing or reducing the recognition of some landslides.

In this dataset, however, image resolution does not improve linearly. On the contrary, the transition is rather sharp with the introduction in 2008 of VHR (0.5 m) digital aerial photographs and satellite images. This may suggest that revegetation had a more significant role than image resolution.

The correspondence of landslide areas reveals that the error index increases with the time lag between two image sets. Although this value may be affected by detection issues (*e.g.*

2008 image set), it suggests that data temporal quality undergoes a progressive deterioration both in the short- ( $10\% \leq \text{error index} \leq 20\%$ ) and long-term ( $\text{error index} \geq 30\%$ ). As a consequence, periodic updates are essential in order to guarantee a reliable reference frame. Indeed, landslide activity and evolution depend on several time-dependent variables:

- triggering factors (intensive rainfall, snow-melt, earthquakes, *etc.*);
- hydrologic and hydrogeologic setting;
- anthropogenic processes;
- vegetation and vegetation evolution;
- local characteristics that change after each slope failure (*e.g.* soil thickness).

The analysis of the multi-temporal landslide inventory of the Dorgola catchment confirmed that time is an important dimension of landslide data and, therefore, is a fundamental component of its quality assessment. However, in order to understand how much a landslide inventory map is affected by time and what are the characteristics of the involved landslides, it is essential to distinguish new detections as well as those landslides that each year disappear from the records (*e.g.* shallow landslides).

### **5.3. Characterization of new and undetected landslides**

In the previous paragraph the multi-temporal landslide inventory of the Dorgola catchment was considered as a whole. Here below, I analyse new detections and undetected landslides separately in order to assess their main characteristics like location and size. In particular, I subdivided new detections into three groups: new activations, reactivations, and LL's. New activations are those landslides that are detected for the first time within the time frame of the multi-temporal landslide inventory, whereas reactivations represent a further activity of already detected landslides. In general, this distinction is quite questionable since there is no way to ascertain whether in the past a certain area was involved in a mass movement or not. Undetected landslides, on the other hand, are those slope failures that disappear from the records because they were concealed either by natural (*e.g.* consolidation of the vegetation) or anthropogenic (*e.g.* farming) processes.

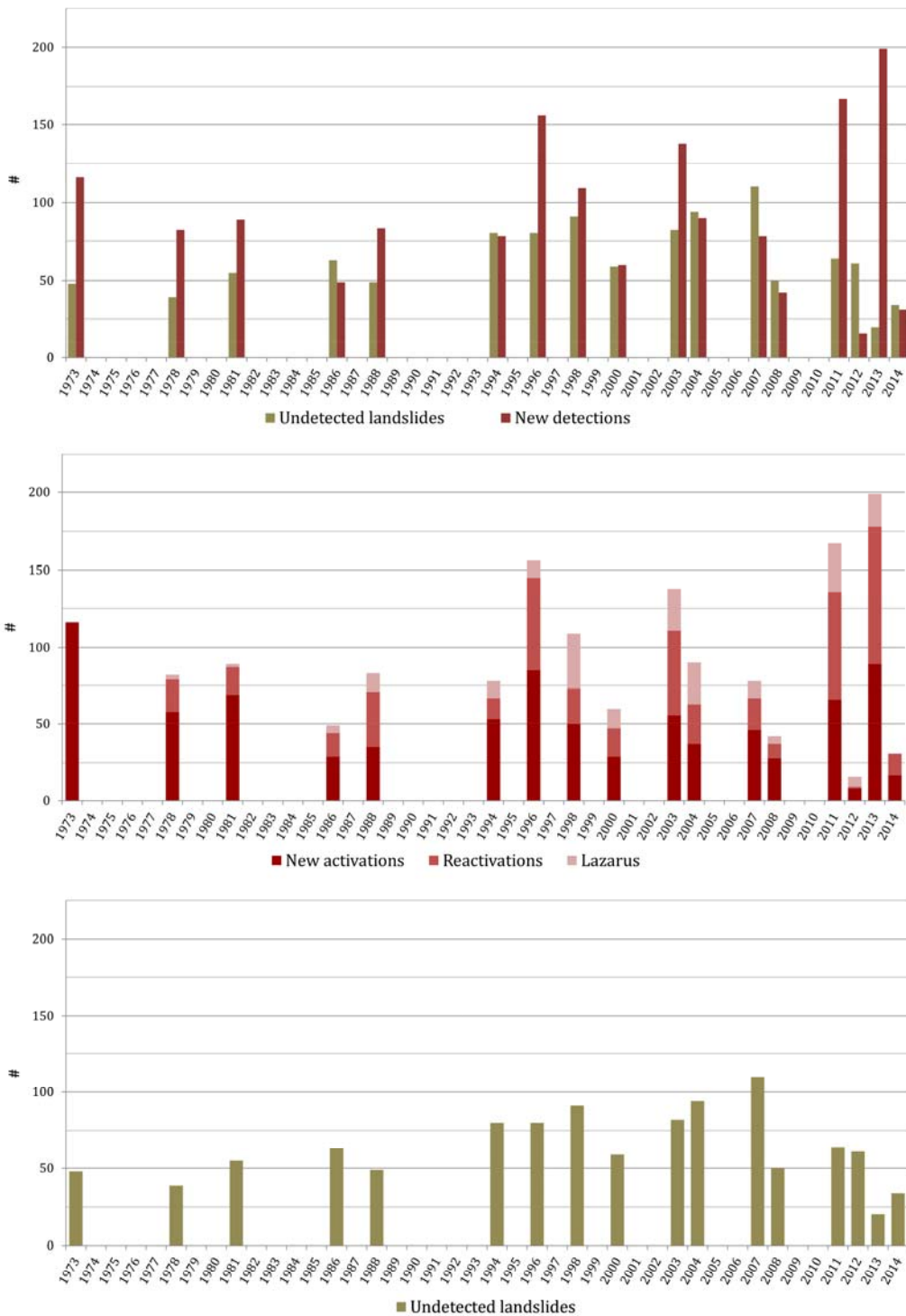


Fig. 5.5: Frequency distribution of new detected and undetected landslides in the multi-temporal inventory of the Dorgola catchment.

### 5.3.1. Analysis and results

#### 5.3.1.1. Descriptive statistics

New detections and undetected landslides for each image set are listed in Tab. 5.3, whereas Fig. 5.5 shows their frequency distribution. In general, these data confirm that the total number of landslides in an inventory has to be treated with care as it is the result of three main factors: detection issues, slope failure activity and evolution, and anthropogenic processes.

Since 1954, the total number of new detections (new activations, reactivations, and LL's) is 1,583 with yearly values ranging from 42 (2008) to 199 (2013). In order to get a representative average, I divided the number of new detections of each image set by the number of years of the time lag with the previous snapshot. In this way, for the entire period from 1978 to 2014<sup>5</sup>, I calculated an average of about 48,6 new mass movements per year with values ranging from a minimum of 9.8 #/y (1986) to a maximum of 199.0 #/y (2013) (Tab. 5.4). On the other hand, for the short-term the average is 75.6 #/y with values ranging from 16.0 #/y (2012) to 199.0 #/y (2013) (Tab. 5.4). Due to the reduced data sample, this average is particularly high because is strongly affected by the 2013 extreme event. In general, the analysis of the frequency histogram of Fig. 5.5 shows that there are several highs and lows. The years with the highest numbers of new detections are 1973, 1996, 2003, 2011, and 2013 for which more than a 100 new landslides were detected. The 1973 peak, however, is probably a fake as, most likely, it is the result of a resolution contrast with the previous image set (1954). Conversely, the 1996, 2003, 2011, and 2013 peaks likely indicate sliding climaxes. For 1996, for example, data from the literature confirm that in 1995 landslide events had been particularly intense in the Reggio Emilia Province (Basenghi and Bertolini, 2001). The high number of reappearing LL's in 1998, 2003, 2004, 2011, and 2013 (all exceeding 20 events) is due, instead, to the favourable detection conditions of these image sets<sup>6</sup> (season, colour, time, illumination, *etc.*).

---

<sup>5</sup> The 1954 was not considered both for its low quality and for the long time lag with the successive snapshot.

<sup>6</sup> As previously stated, 1998 and 2003 image sets are characterised by some detection limiting factors which account for the high number of hidden LL's. The former, in particular, presents a

Tab. 5.3: List of new detections and undetected landslides. All values are calculated with respect to the previous image set. New detections are subdivided into new activations, reactivations, and LL's. New activations are those slope failures that supposedly appear for the first time, whereas reactivations represent a further activity of already detected mass movements. Undetected landslides, on the other hand, are those slope failures that apparently disappear from the records due to vegetation consolidation or to man activities.

		1954	1973	1978	1981	1986	1988
<b>New detections:</b>	#	-	116	82	89	49	83
new activations		-	116	58	69	29	35
reactivations		-	0	21	18	15	36
Lazarus		-	0	3	2	5	12
<b>Undected landslides</b>	#	-	48	39	55	63	49

		1994	1996	1998	2000	2003	2004
<b>New detections:</b>	#	78	156	109	60	138	90
new activations		53	85	50	29	56	37
reactivations		14	60	23	18	55	26
Lazarus		11	11	36	13	27	27
<b>Undected landslides</b>	#	80	80	91	59	82	94

		2007	2008	2011	2012	2013	2014
<b>New detections:</b>	#	78	42	167	16	199	31
new activations		46	28	66	8	89	17
reactivations		21	9	70	1	89	14
Lazarus		11	5	31	7	21	0
<b>Undected landslides</b>	#	110	50	64	61	20	34

With regard to undetected landslides, their overall number is 1,079 with yearly values ranging from 20 #/y (2013) to 110 #/y (2007) (Tab. 5.3). The long-term average<sup>7</sup> turned out to be 33.4 #/y with values ranging from 11.0 #/y (1981) to 94.0 #/y (2004), whereas for the short-term is 51.8 #/y with values ranging from 20.0 #/y (2013) to 94.0 #/y (2004)

disadvantageous scale and season of acquisition, whereas the latter has an unfavourable illumination. Both image sets, however, are more effective for the recognition of certain mass movements due respectively to colour and to the season of acquisition.

<sup>7</sup> Long-term and short-term averages were calculated as for new detections.

Tab. 5.4: Averages of new detected and undetected landslides expressed as number of landslides per year. The values in parenthesis do not consider LL's.

		New detections	Undetected landslides
Total	#	1,583	1,079
Long-term average	#/year	48.6 (40.9)	33.4
min.	#/year	9.8 (8.8)	11.0
max.	#/year	199.0 (178.0)	94.0
Short-term average	#/year	75.6 (63.6)	51.8
min.	#/year	16.0 (9.0)	20.0
max.	#/year	199.0 (178.0)	94.0

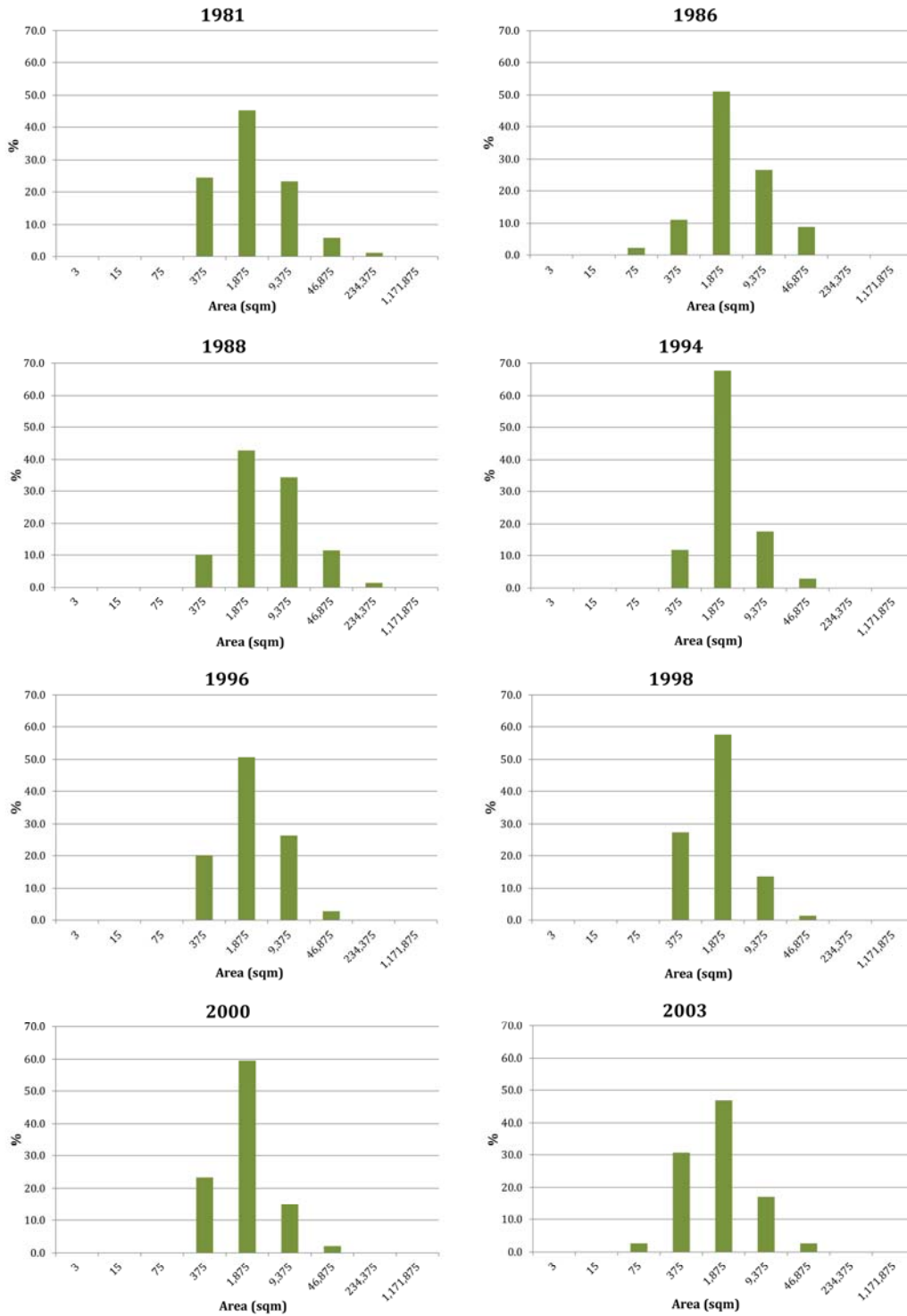
(Tab. 5.4). Also in this case, however, the analysis of the histogram of Fig. 5.5 shows that there are several highs and lows. The two most outstanding peaks correspond to 1998 and 2007 image sets respectively with 91 and 110 undetected landslides. On the other hand, the year with the lowest number is 2013 with 20 mass movements that were not detected with respect to 2012. In particular, 10 of these landslides were not detected because they had been overlapped by other slope failures. Finally, it is also worth noting that 21.3% (230) of the undetected landslides reappeared as LL's, 40.8% (440) underwent successive reactivations, while, at least for the moment, 59.2% (639) did not reappear.

### 5.3.1.2. New detection size

Histograms in Fig. 5.6 represent the area frequency distribution of the new landslides (both new activations and reactivations) that were detected in the Dorgola catchment since 1981<sup>8</sup>. In order to have a more realistic characterization of the areas of new detections, these histograms do not include LL's.

Besides highlighting the image sets with the highest number of new detections, Fig. 5.6 shows that until 2004 the most frequent area class is that of 1,875 m<sup>2</sup>. However, with the exception of the 2011 image set, from 2007 onward 375 m<sup>2</sup> becomes the most frequent

<sup>8</sup> The 1954, 1973, and 1978 image sets were not used for this analysis, since they were not orthorectified.



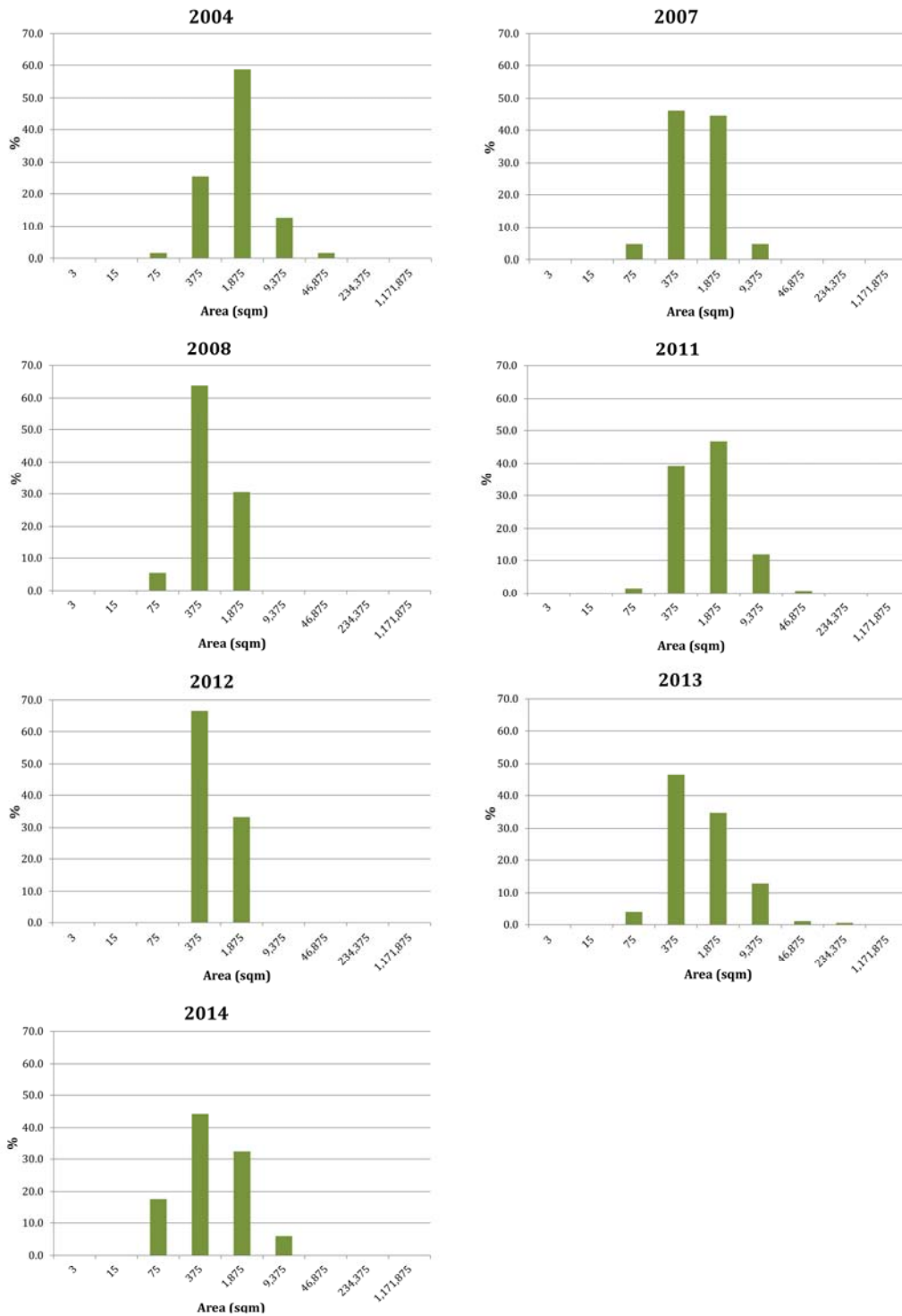


Fig. 5.6: Area frequency distribution of new detected landslides (new activations and reactivations). For their particular nature LL's were not considered.

*Tab. 5.5: Cluster analysis of landslide centroids. The frequency of landslide centroids is calculated with respect to the total number of landslide centroids in each cluster.*

# of landslides per cluster	% of total landslides
≥5	83,7%
≥10	72,1%
≥15	60,1%
≥20	50,0%

one.

### 5.3.1.3. New detection location

About 1.8% of new detections is within the Tuscan Units, 36.2% within the Epi-Ligurian Sequence, and 62.1% within the Ligurian Units, which confirm to be the most susceptible to landsliding. With regard to previous image sets, on average, 63.2% of new detections fall within existing landslides.

In order to investigate any possible spatial relationship among new detections, I performed a rough cluster analysis with Esri@ArcMap™ 10.1. To this end, landslide centroids were used as proxies for landslide location. All new detection centroids were gathered in a unique shapefile and buffered with a buffer distance of 50 m. The relative polygons were then dissolved together in order to create clusters. Results proved that 50% of new detections fall within clusters with a total number of landslides centroids  $\geq 20$  (Tab. 5.5). Indeed, as shown in Fig. 5.7, landslide activity seems to concentrate in particular areas. To this end, more detailed studies should be carried out in order to understand this arrangement.

### 5.3.2. Discussion

The cumulative number of mass movements increases with time as shown in Fig. 5.8. Although, the distinction between new activations and reactivations is quite questionable, the plotted values were calculated by adding first detections to the total number of landslides of the previous year. According to  $R^2$ , data points fit a linear, a 3° polynomial, and a power-law

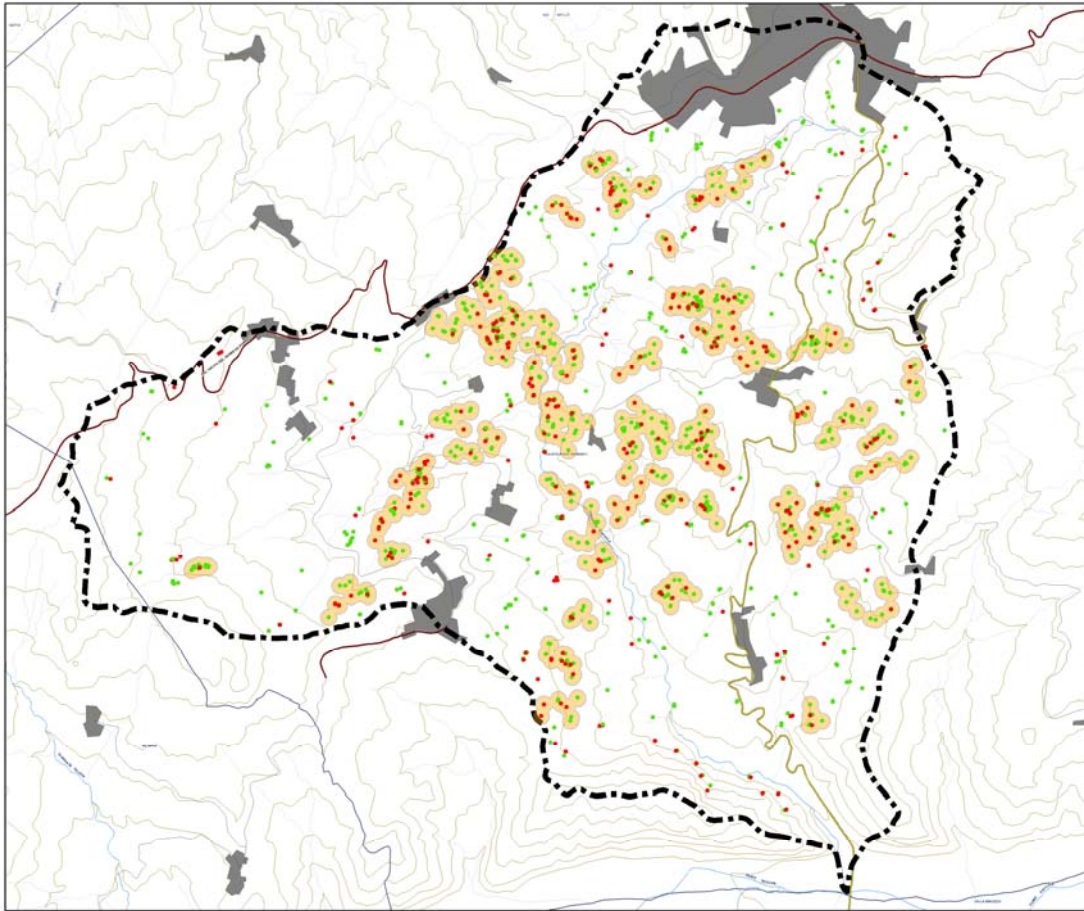


*Fig. 5.7: New landslide centroid distribution. Coloured areas are those clusters that contain a number of landslide centroid  $\geq 10$ . Clusters were obtained by buffering each centroid with a buffer distance of 50 m. Green dots represent long-term, while red dots refer to short-term new detections. In this work, "short-term" is referred to image sets (2004, 2008, 2012, 2013, and 2014) acquired in two consecutive years, although the time lag between them may be more than 12 months.*

curve. The latter, however, represents an unlikely model as it would probably overestimate the increasing number of landslides. Conversely, data dispersion around the linear regression suggests a more complex trend. Indeed, from 1996 to 2012 landslide total number increases at a higher rate than from 1973 to 1994, and apparently it increases even further from 2013. This trend, together with the good fit for the 3<sup>o</sup> polynomial curve, indicates that most likely the increase is linear but with different gradients. This kind of evolution is consistent with the fact that landslide activity, triggered by occasional events, develops

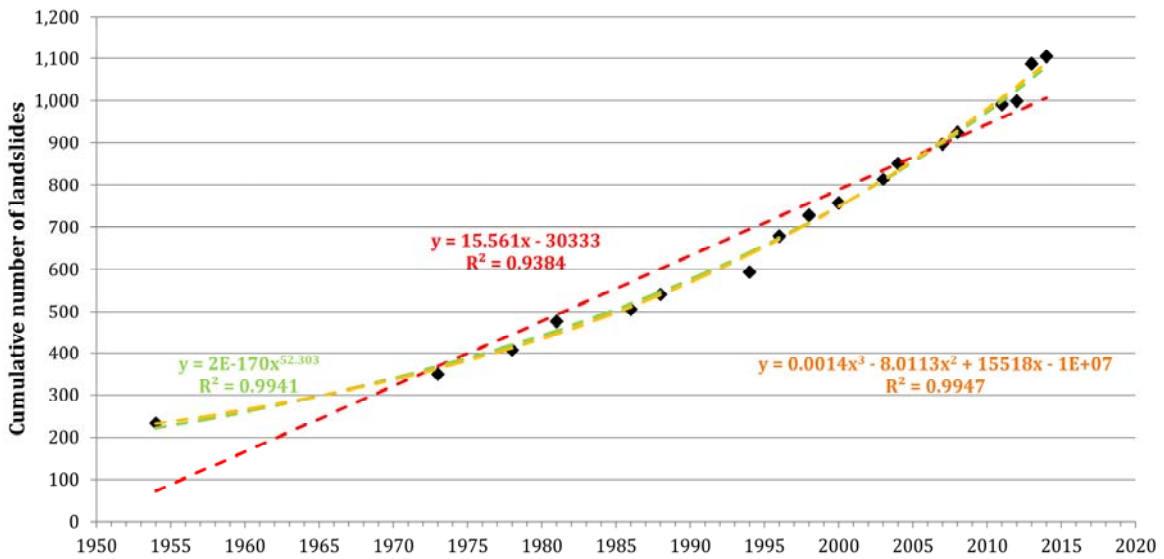


Fig. 5.8: Cumulative number of landslides for the multi-temporal inventory of the Dorgola catchment. The plotted values were calculated by adding first detections to the total number of landslides of the previous year. Red = linear regression; green = power-law curve; orange = 3<sup>o</sup> polynomial curve.

according to a steplike rather than a constant trend. The improvement of image resolution probably contributed to increase the gradient by lifting the most recent end and by underestimating the other end. However, image resolution and the related chance to recognise smaller slope failures cannot account completely for the general increasing trend. Indeed, theoretically, in an undisturbed context, a system would be in equilibrium. In reality, occasional triggering events (generally tectonics and extreme climatic events) disturb the system and force it to find a new equilibrium through an increase of landslide activity. As a consequence, in a natural context a system is more likely characterised by a metastable equilibrium that could be represented by a steplike trend. In this sense, the constant increase shown in Fig. 5.8 may be interpreted as a part of a wider cycle, *i.e.* as a response to some triggering events with long-term effects (*e.g.* climatic changes) or it may be the sign of a constantly unstable system. To this end, it is worth remembering that the Dorgola Valley cannot be considered a natural system as it had been populated by men for centuries. Man presence and activities, however, are important landslide predisposing and triggering factors, and consequently, their constant action cannot be excluded as a possible

explanation for the landslide trend of Fig. 5.8. Indeed, further researches should be done in order to investigate if in the future this increasing trend, under continuous anthropogenic solicitations, will remain constant or if, being part of some sort of natural cycle, it will eventually lead to equilibrium. Furthermore, it would also be interesting to compare different areas to evaluate if the increasing gradient may be considered as a quantification for this disequilibrium.

On the basis of Fig. 5.8, the total number of landslides in a multi-temporal inventory is expected to progressively increase with time. This, however, in the case of the Dorgola catchment does not happen as landslide distribution presents a quite variable trend (Fig. 5.2). In fact, although the Dorgola Valley is not intensively populated, man activities are particularly intense, and they effectively influence landslide footprints. In this sense, as already remarked, landslide distribution is the result of two antagonistic forces. In particular, according to Fig. 5.5, man efforts to overcome landslides apparently become more relevant and intense after slope instability climaxes like, for example, in 1986, 1998, 2004, 2007, 2008, 2012, and 2014. As a consequence, landscape is always changing in one sense or the other.

Data about new and undetected landslides revealed that, generally, new detections are more abundant than those landslides that each year apparently disappeared from the records. Indeed, according to the intensity of triggering factors, the number of new detections may be in the order of tens or hundreds of mass movements per year, whereas, on the other hand, slope failures seem to disappear at a lower rate, in the order of tens of landslides per year (Tab. 5.3).

With regard to the location of new detections, this study proved that in the Dorgola Valley they are not scattered randomly but rather they tend to be clustered in specific areas and within existing landslides. In the same way, new detections also present characteristic dimensions. Indeed, new landslides show quite small areas (from 125 to 3,125 m<sup>2</sup>) which become even smaller with time probably due to the improvement of image resolution.

### 5.4. Temporal persistence of landslide footprints

The definition of the persistence of a landslide scar is an essential information for the assessment of the temporal reliability of a landslide inventory map and a fundamental element for the determination of a proper data acquisition frequency.

To quantify the persistence on the territory of landslide footprints, I analysed the image sets from 1973 to 2014. I excluded the 1954 image set in order to reduce the time range between two successive snapshots since in this interval landslide presence had to be interpolated. In this sense, if a slope failure appeared in the oldest image set I considered it present, at least, until the successive snapshot. Landslide persistence was calculated as the ratio between the number of years in which a landslide had been recognised or interpolated divided by the overall time frame (42 years), as simplified in Fig. 5.9. In order to avoid float results, these values were then reclassified according to integer numbers, *i.e.* persistence classes that are equal to the total number of years in which a certain mass movements supposedly existed. The histogram in Fig. 5.10 displays the landslide frequency distribution with respect to these persistence classes. In particular, this histogram shows that, although

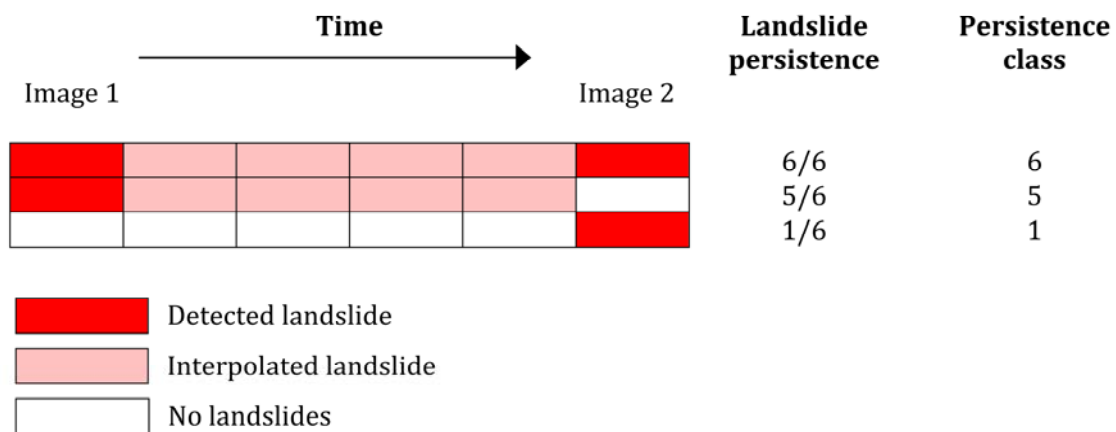


*Fig. 5.9 – A simplified description of the procedure used to interpolate landslides and define landslide persistence and persistence classes. This method could be used since the time lag between two successive image sets is quite short and generally constant. It is worth noting that the persistence class is basically equal to the number of years in which a landslide was detected or interpolated.*

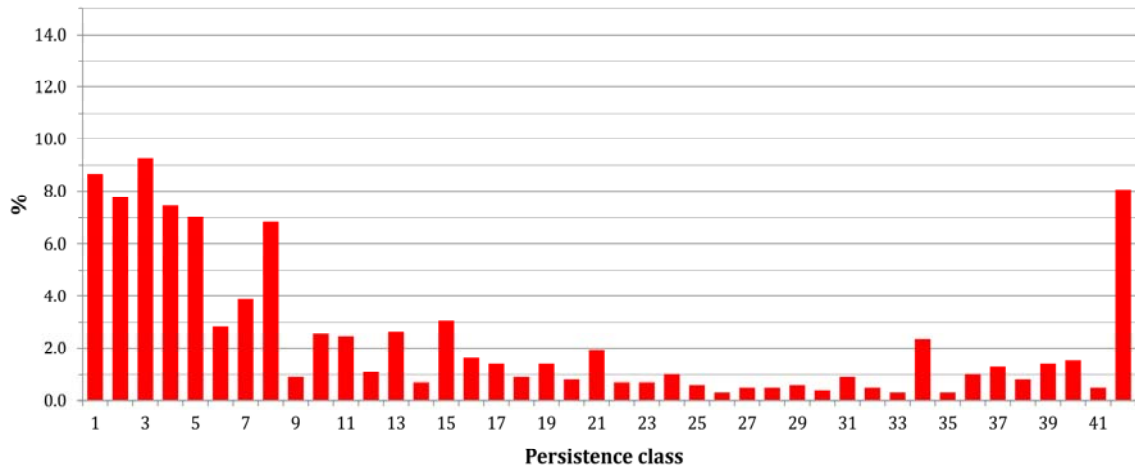


Fig. 5.10: Landslide frequency distribution with respect to persistence classes (see Fig. 5.9 for a simple explanation of persistence classes).

about 18% of mass movements scars resist on the territory for time periods  $\geq 30$  years, the frequency of landslide footprints generally decreases with increasing persistence classes. In particular, about 23% of landslide scars (247) shows a temporal persistence  $\leq 2$  years, while 61% of them (647) seem to persist for periods  $\leq 10$  years.

It is worth noting, however, that these results are affected by the intrinsic characteristics of the study area like, for example, the geo-morphological setting, the sampling rate of the dataset, and the frequency and intensity of the triggering factors and of man activities during the considered time frame. Furthermore, in Fig. 5.10 “old” landslides, *i.e.* landslides that had time to evolve and eventually disappear, were plotted together with “young” landslides, *i.e.* recently appeared landslides. This is clearly an approximation which almost certainly lead to an overestimation of the lowest persistence classes. Notwithstanding this, these results proved that in the Dorgola catchment landslide footprints disappear with time and, at least apparently, they disappear quite swiftly. Indeed, apart from a reduced group of mass movements whose scars have a relative high temporal persistence<sup>9</sup>, most of them (61%) cannot be detected after 10 years from their appearance. As a consequence, in order to record all of them properly and produce a complete reference frame of landslide activity,

<sup>9</sup> As already remarked in Chapter 4, these landslides fundamentally include old large dormant landslides.

it is essential to adopt a high data acquisition frequency. Although these results may be overestimated, a reasonable sampling rate is once a year or maximum every 2 years. Finally, it is worth remembering that these outcomes require to be tested also in different geo-morphological contexts and, if possible, for longer time periods.

## 5.5. Conclusions

The time variable is an essential aspect of landslide inventory maps and a fundamental component of their quality assessment. The realization of a multi-temporal inventory allowed to partially reconstruct the evolution of the Dorgola catchment in the last 60 years. An overall analysis of this multi-temporal inventory revealed that data temporal quality underwent a progressive deterioration both in the short- and long-term. In particular, this work highlighted that with time mapped landslides became generally smaller. A possible explanation for this may be the evolution of the landscape, *i.e.* the progressive natural and anthropogenic revegetation of the Dorgola catchment. Indeed, the spread of forested and scrubby areas worsened landslide detection conditions by preventing or reducing the recognition of some landslides that, anyhow, are still present. According to land-use planning goals, for which unstable areas are probably more significant than the overall number of landslides, this is a valuable piece of information. To this regard, however, a careful correlation analysis between land-uses (forested and scrubby areas in particular) and the evolution of landslide areas should be addressed by further researches.

This work proved that the cumulative number of landslides increased with time according to multiple linear gradients. To this end, further researches and monitoring programs should investigate future developments to assess whether this trend could be the consequence of some sort of existing triggering factors with long-term effects or the response to the constant anthropogenic action. Moreover, given that the total number of landslides in each inventory did not raise, this study remarked that landslide frequency is the result of two antagonistic forces: landslide activity *sensu stricto* and anthropogenic processes. In this sense, the total number of mass movements in an inventory is a ready-reference, but it has to be interpreted with care as the territory is an ever-changing reality

that reacts to different and opposing solicitations.

This work also revealed that new landslides are basically quite small and tend to be concentrated in specific areas and within existing landslides. This confirms that, at least for some types of mass movements, modelling and susceptibility maps may be valuable tools for landslide prediction and forecasting.

Ultimately, with regard to the persistence of landslide footprints, an approximated evaluation revealed that only 18% of all mass movements insist on the territory for time periods  $\geq 30$  years, whereas about 61% of them, although most likely present, cannot be detected after 10 years from their appearance. This outcome calls for greater attention to the time variable and to the potential uses and applications of a landslide inventory map especially as far as land-use planning is concerned. With regard to landslide inventory completeness, this work suggested that, in order to record all mass movements properly, it is essential to adopt a high data acquisition frequency. Although these data may be overestimated, a reasonable sampling rate is once a year or maximum every two years. However, given that these results are restricted to a particular geomorphological, climatic, and anthropogenic context, as well as to a defined time frame, further researches should extend the study to different and wider data sets.

## CHAPTER 6

# The land-use planning process and the possible applications of a landslide inventory map

- 6.1. Introduction
- 6.2. Land-use planning in landslide-prone areas
  - 6.2.1. The landslide problem in Italy and in the Emilia-Romagna region
  - 6.2.2. The planning process and setting
  - 6.2.3. Landslide susceptibility, hazard, and risk zoning
  - 6.2.4. Landslide management in the Emilia-Romagna region
- 6.3. Limits and applications of a landslide inventory map to land-use planning. The case study of the Dorgola catchment.
  - 6.3.1. Analysis and results
    - 6.3.1.1. Descriptive statistics and landslide abundance
    - 6.3.1.2. Correspondence of landslide areas
    - 6.3.1.3. Spatial and temporal accuracy assessment of the 2010 PTCP inventory map
  - 6.3.2. Discussion
- 6.4. Conclusions

## **6. The land-use planning process and the possible applications of a landslide inventory map**

### **6.1. Introduction**

Worldwide landslides cause fatalities, environmental degradation, and millions of Euros worth of damage to buildings, transport routes, utility supplies, and more generally, to human activities. In order to build sustainable and landslide resilient communities, it is essential to invest into a solid policy with a legal, institutional, and scientific foundation. Land-use planning is a powerful tool to reduce territory mismanagement and to sustain an effective risk reduction and mitigation. However, an inadequate or erroneous land-use plan, that disregards its goal and the societal requests, may lead to serious consequences in terms of community safety and of legal conflicts. To this end, a realistic understanding of the type, accuracy, and limitations of zoning boundaries is a key issue.

Landslide inventory maps are essential tools for land-use planning and for decision-making regarding territory management. Nevertheless, as widely argued in the previous chapters, they are affected by spatial and temporal uncertainties. Furthermore, landslide inventory maps are not continuous in space as they do not provide any information where landslides were not detected. Indeed, these areas remain unclassified as they cannot be considered free of mass movements, but rather they represent “blind” areas with no available data (Guzzetti and Cardinali, 1989; Cardinali *et al.*, 1990; Antonini *et al.*, 1993; Cardinali *et al.*, 2001; Guzzetti, 2006). This, however, makes a significant difference for land-use planning purposes.

Planners can rely on a wide range of tools and mechanisms, like for example, regulatory planning documents (Schuster and Highland, 2007; Glavovic *et al.*, 2010). In all the land-use plans investigated in this study, landslide inventory maps were used as reference frame to describe landslide distribution and characteristics. At the same time, however, they were also adopted as zoning maps, *i.e.* landslide polygons were used as spatial constraints for

regulating compatible and incompatible land-uses.

First of all, in this chapter I propose a general overview of land-use planning practices and issues in landslide-prone areas. Then, on the basis of the results of this research, I analyse the limits and applications of a landslide inventory map to land-use planning for the Dorgola study site.

## **6.2. Land-use planning in landslide-prone areas**

### **6.2.1. The landslide problem in Italy and in the Emilia-Romagna region**

Much of the Italian territory consists of hilly and mountainous areas. Consequently, mass movements are a common natural hazard and landslide risk represents a significant social and economic issue (Guzzetti, 2000; Cardinali et al., 2002; Salvati *et al.*, 2010).

A landslide database spanning from 1279 to 1999 was compiled by Guzzetti (2000) from a variety of different sources. According to these data, Italy yearly average of dead or missing people is the highest in Europe and among the highest worldwide. More than 10,000 people died in a total of 840 landslides events. In particular, probably due to the better completeness of the catalogue, in the 20<sup>th</sup> century 7,799 casualties (comprising 5,831 deaths, 108 missing people, and 1,860 injured people) were recorded for an average of 59.4 victims per year. On the other hand, the number of homeless or evacuated people is uncertain, but it probably exceeds 100,000. Fast-moving landslides (*e.g.* rockfalls, rockslides, soil slips, debris flows, and rock avalanches) were responsible for more than 80% of deaths and injuries, while slow-moving landslides (*e.g.* deep seated and earth flows) resulted in a large number of homeless and evacuated people but not in fatalities (Guzzetti, 2000). Ultimately, it is worth noting that two of the largest landslide disasters of the 20<sup>th</sup> century (Vajont and Stava) were directly influenced by human activity (Chandler and Tosatti, 1995; Semenza and Ghirotti, 2000; Genevois and Ghirotti, 2005; Fondazione Stava 1985 onlus, 2014).

The Emilia-Romagna region is particularly prone to landslides. Some of its municipalities are covered by landslides for about 40% and, in some cases, up to 50% of their territory

*Table 6.1: Damages and costs of the two landslide events that took place in the Emilia-Romagna region in March-April 2013 and from November 2013 to March 2014 (Pizziolo et al., 2014a; Pizziolo et al., 2014b).*

	Mar-Apr 2013	Nov 2013 - Mar 2014
Destroyed residential buildings and residential buildings with irreparable damages	33	30*
Destroyed or highly damaged production activities	36	n/a
Evacuated people	130	50
Road disruptions	38	n/a
Damaged roads	>800	>370
Estimated economic losses (Euros)**	>200 million	n/a

\* Total number of evacuated buildings, of which 20 were seriously damaged

\*\* Damages, estimated after the Ordinance n° 130 22/11/2013, include those to private properties and to public infrastructures, as well as hydraulic damages

(Servizio Geologico, Sismico e dei Suoli, 1999). A main issue is represented by ancient dormant landslides. Indeed, due to their long periods of inactivity and to their gentle morphology, these mass movements were “colonised” by men and man activities as they were considered suitable for human settlements (Bertolini and Pizziolo, 2008; Bertolini and Pizziolo, 2012). In general, 1,608 settlements lie on dormant landslides, whereas 281 are located on or are affected by active slope failures. Furthermore, 16% of the total road network passes through existing mass movements, so that it is threaten and periodically affected by their activity. Although human casualties are fortunately uncommon, economic losses are extremely high. In a five years time frame about 390 million Euros were actually invested by national and regional governments in reconstructions, village relocations, consolidation works, and monitoring activities (Bertolini and Pizziolo, 2008).

Even during this research the Emilia-Romagna region was involved in two important landslide events. The first one took place in the period between March and April 2013, and it is well documented by this study. The other one took place from November 2013 to

March 2014. The respective damages and costs are reported in Tab. 6.1 (Pizziolo *et al*, 2014a; Pizziolo *et al*, 2014b). These results undoubtedly highlight the intense interaction between landslides and men, and the socio-economic impact of mass movements in the region. Most of all, however, they call for a careful consideration about the current land-use planning system.

### **6.2.2. The planning process and setting**

According to Greiving *et al* (2006), until the mid-1990s natural hazards were mainly addressed by emergency management and sectorial planning. In this sense, land-use planning has represented a significant improvement. Indeed, on the basis of long-term economic, social, and environmental goals, land-use planning identifies, evaluates, and decides on the different options concerning the use of the land. Although it is undertaken by public authorities, it usually involves communities and interest groups. Land-use planning goals are achieved with the promulgation of plans that state the permitted and acceptable uses.

In general, mass movements represent a potential issue where one or more of these elements are present (AGS, 2007a; Fell *et al*, 2008a; Fell *et al*, 2008b):

- existing landslides including inactive ones;
- topographic, geological, and geomorphological predisposing factors;
- forestry works and agricultural land clearing;
- anthropogenic features and structures with cut or filled slopes (*e.g.* dams, mine waste dumps, retaining walls, loose silty-sandy fills, *etc.*).

Indeed, land-use planning concentrates not only on existing or known landslides but also on potential slope failures which can be reasonably predicted on the basis of geology, geometry, and slope forming processes (Fell *et al*, 2008a). Furthermore, human activities may contribute to destabilise slopes that otherwise could have endured much longer if left undisturbed (Schwab *et al*, 2005; Schuster and Highland, 2007). These alterations include (Olshansky, 1996; Schuster and Highland, 2007):

- slope undercutting and modification by construction of roads, railways, buildings, *etc.*;
- slope overload;

- redirection of storm runoff on unprepared slopes;
- increase of pore water pressure (*e.g.* leaking pipes);
- vegetation removal.

In this sense, land-use planning must consider all the territory, *i.e.* unstable and apparently stable areas. In particular, for the latter the possible effects of future developments should be evaluated (*e.g.* future building areas).

Due to the various scenarios and backgrounds related to every country, no single land-use planning approach can be applied (Cascini *et al.*, 2005). Nevertheless, zoning proved to be an effective tool in order to manage and reduce landslide hazard and risk (Cascini *et al.*, 2005; Greiving *et al.*, 2006; AGS, 2007a; Schuster and Highland, 2007; Fell *et al.*, 2008a; Fell *et al.*, 2008b). With regard to landslides, according to the Australian Geomechanics Society (AGS) (2007a), this term is to be intended as “the division of land into homogeneous areas or domains and their ranking according to degrees of actual or potential landslide susceptibility, hazard or risk”. Three different types of landslides zoning are identified: susceptibility, hazard, and risk zoning (Cascini *et al.*, 2005; Guzzetti, 2006; AGS, 2007a; Schuster and Highland, 2007; Fell *et al.*, 2008a; Fell *et al.*, 2008b), although landslide inventory maps are sometimes considered as a further type (AGS, 2007a; Fell *et al.*, 2008a; Fell *et al.*, 2008b). Zoning can be carried out at various scales (AGS, 2007a; Fell *et al.*, 2008a):

- regional (1:250,000 to 1:25,000),
- local (1:25,000 to 1:5,000),
- and site-specific (<1:5,000),

and with three different levels of characterization: preliminary, intermediate, and advanced. The type, the scale, and the level of landslide zoning strictly depends on the intended purposes and the land management policy (Tab. 6.2) as well as on other factors like, for example:

- the stage of development of the land-use plan. Susceptibility zoning, for example, should be used in preliminary stages, whereas risk zoning is more suitable for detailed stages. In particular, whereby landslide zoning introduces a more detailed assessment at site scale, susceptibility and preliminary hazard mapping are sufficient to define those areas where more detailed landslide hazard and risk assessment are needed (AGS, 2007a; Fell

The land-use planning process and the possible applications of a landslide inventory map

Table 6.2: Recommended types and scales of zoning maps related to zoning purposes (modified from Fell et al., 2008).

Purpose	Type of zoning				Applicable zoning map scales
	Inventory	Susceptibility	Hazard	Risk	
<i>Regional zoning</i>					1:25,000÷1:250,000
Information	X	X			
Advisory	X	X	(X)		
Statutory	n.r.				
<i>Local zoning</i>					1:5,000÷1:25,000
Information	X	X	X	(X)	
Advisory	(X)	X	X	X	
Statutory		(X)	X	(X)	
<i>Site-specific zoning</i>					1:5,000÷1:1,000
Information	n.r.				
Advisory	n.c.u.				
Statutory		(X)	X	X	
Design		(X)	(X)	X	

Notes: X = applicable; (X) = may be applicable; n.r. = not recommended; n.c.u. = not commonly used

- et al.*, 2008a). To this end, it is worth noting that risk maps generally reflect the current situation of potential damage and, in this sense, non-urbanised areas are often displayed as having a low risk level regardless the level of existing hazard (Cascini *et al.*, 2005);
- the classification, activity, volume, or intensity of landsliding. Risk zoning is usually required where there is a threat to life (e.g. debris flows, rock avalanches, rock falls, etc.), so that it can be determined using life loss risk criteria (AGS, 2007a; Fell et al., 2008a);
  - funds can be a practical constraint to zoning (AGS, 2007a; Fell *et al.*, 2008a);
  - the amount and quality of available information, *i.e.* input data must be appropriate and must have a suitable resolution and quality. Furthermore, in order to prepare an hazard quantitative zoning map, a reliable landslide frequency must be available. This also

means that the input data should be at a larger scale than the zoning map, otherwise the boundary accuracy would just be misleading (Phillips, 2005; AGS, 2007a; Saunders and Glassey, 2007; Fell *et al.*, 2008a; Fell *et al.*, 2008b);

- the required accuracy of zoning boundaries. In particular, where statutory constraints are imposed, large scale maps with an appropriate level of input data must be used (Fell *et al.*, 2008a). Indeed, larger scale zoning must be accompanied by a greater data detail and by a complete understanding of the slope processes (AGS, 2007a; Fell *et al.*, 2008a).

Fundamentally, it is essential to match the type, the scale, and the level of landslide zoning to the required usage, as well as to the land management policy and to the quality, quantity, and resolution of the available input data. More generally, considering the degree of judgement involved in landslide zoning, a balance should be established among the cost of zoning, the consequences of zoning on development costs, and the responsibilities of the parties involved in the process (Leventhal and Kotze, 2008). With regard to the scale, Fell *et al.* (2008a), on behalf of the Joint Technical Committee on Landslides and Engineered Slopes (JTC-1), and the AGS (2007a) propose for the different landslide zoning the applications reported in Tab. 6.3.

In order to be effective and successful, land-use planning must count on a solid policy and a sound legal and scientific framework. In particular, it should rely on regulatory tools (Greiving *et al.*, 2006; Schuster and Highland, 2007; Glavovic *et al.*, 2010). Regulations can basically be advisory or statutory. The latter can point out precluded land uses or operations (*e.g.* building or road construction, irrigation systems, storage or disposal of liquids, *etc.*) and development restrictions (*e.g.* density of development) (Schuster and Highland, 2007). To this end, according to Fell *et al.* (2008a), if statutory constraints are to be imposed on the basis of landslide zoning, zoning should be hazard or risk zoning at a large or detailed scale. Susceptibility maps, instead, are not appropriate as they do not consider the frequency of potential landsliding, while landslide inventory maps are not recommended, or even taken into consideration, for statutory purposes (Tab. 6.2). It is worth noting that Fell *et al.* (2008b) also highlighted that there could be some doubts on the feasibility to take site specific decisions, even at detailed scale, on the basis of zoning maps without ground inspections to define zoning boundaries or without a site specific assessment. Besides regulations, there are several other measures that may be taken into consideration in order

Table 6.3: Landslide zoning mapping scales and their application (Fell et al, 2008).

Scale description	Indicative range of scales	Examples of zoning application	Typical area of zoning
Small	<1:100,000	Landslide inventory and susceptibility to inform policy makers and the general public.	>10,000 km <sup>2</sup>
Medium	1:100,000÷1:25,000	Landslide inventory and susceptibility zoning for regional development or very large scale engineering projects. Preliminary level hazard mapping for local areas.	1,000÷10,000 km <sup>2</sup>
Large	1:25,000÷1:5,000	Landslide inventory, susceptibility and hazard zoning for local areas. Intermediate to advanced level hazard zoning for regional development.  Preliminary to intermediate level risk zoning for local areas and the advanced stages of planning for large engineering structures, roads, and railways.	10÷1,000 km <sup>2</sup>
Detailed	>5,000	Intermediate and advanced level hazard and risk zoning for local and site-specific areas and for the design phase of large engineering structures, roads, and railways.	Several hectares to tens of square kilometres

to discourage new developments in landslide-prone areas. The following proved to be successful in the USA (Schuster and Highland, 2007):

- government acquisition of properties;
- disclosure to potential property buyers of public records on urban land ownership including information on slope failure hazards;
- limiting public investments on infrastructures such as, for example, water and sewer lines;
- public education in order to have the support of the affected population;
- public awareness of legal liabilities;

- posted warning signs;
- tax credits and special assessments;
- denying loans for development or construction;
- prohibitive insurance costs.

According to Fell *et al.* (2008a), as a form of quality control and validation, zoning studies applied to land-use planning should be submitted to a peer review in order to provide an independent judgment of the susceptibility, hazard, and risk assessment. In New Zealand, for example, councils may request an independent peer review of any geological/geotechnical assessments of landslide risk (Saunders and Glassey, 2007).

### **6.2.3. Landslide susceptibility, hazard, and risk zoning**

Landslide inventory maps as well as susceptibility, hazard, and also risk zoning maps provide the technical and scientific support to Local Government politicians, decision-makers, and planners to regulate land management at large scale, but often also to the cadastral scale. For this reason it is essential that these maps are accurate and reliable. The framework of landslide risk assessment is shown in Fig. 6.1. This structure is widely used internationally and it is recommended for all kinds of zoning whether a quantitative or qualitative approach is being taken (AGS, 2007a; Fell *et al.*, 2008a).

The preparation of a landslide inventory is an essential part of the zoning process (Cascini *et al.*, 2005; Guzzetti, 2006; AGS, 2007a; Saunders and Glassey, 2007). It is, indeed, a preliminary step for susceptibility zoning and, consequently, for hazard and risk zoning. However, as partially quantified by this work, this exceptional tool presents some uncertainties and limitations that must be clearly conveyed to the end-users (Guzzetti, 2006; Fell *et al.*, 2008a; Fell *et al.*, 2008b). Moreover, landslide inventory maps do not provide information on all the territory but just where mass movements were detected. This is an important approximation because, as it was proved also by this study, landslide inventory maps are far from being complete. In this sense, landslide density maps, which quantify the spatial distribution of slope failures, represent an improvement with respect to landslide inventory maps as they are fillers of space. Furthermore, they show an improved readability and a reduced cartographic error. Notwithstanding this, also density

The land-use planning process and the possible applications of a landslide inventory map

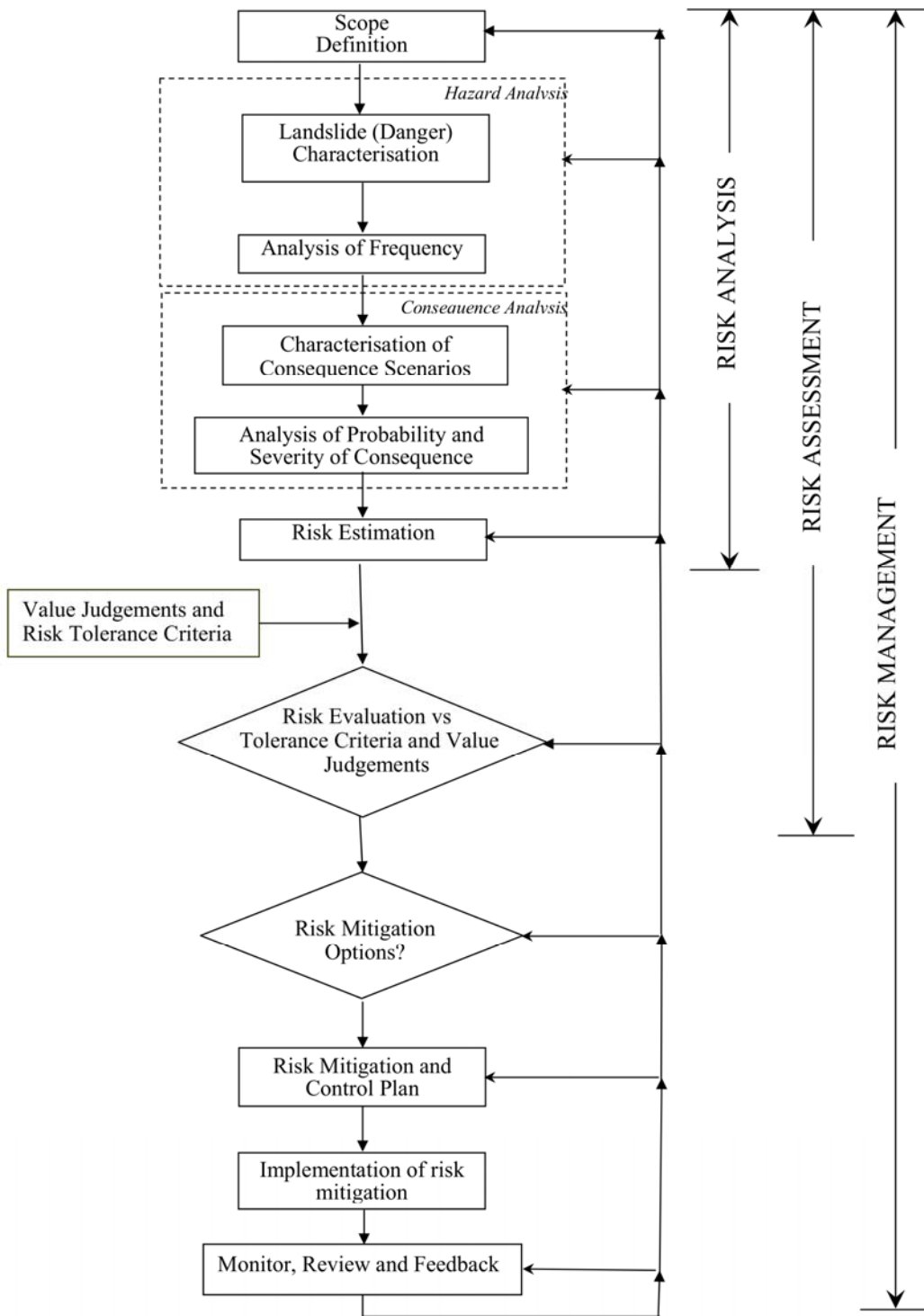


Figure 6.1: Framework for landslide risk management (Fell et al, 2005).

maps have some limitations. Indeed, they do not show landslide location and their accuracy essentially rely on the landslide inventory map quality (Guzzetti, 2006).

The realization of a landslide susceptibility map basically relies on two assumptions that proved to be generally reasonable:

- the past is the key to the future, *i.e.* areas that in the past were involved in landsliding are likely to be involved again in the future (Varnes *et al.*, 1984; Hutchison, 1995; Aleotti and Chowdhury, 1999; AGS, 2007a);
- areas that present similar topographic, geological, and geomorphological characteristics as those that experienced landsliding are likely to be involved in a mass movement as well (AGS, 2007a).

Regardless of existing landslides, susceptibility zoning assesses the propensity of the slopes to be involved in a mass movement including run-out areas and those zones that may be caught up in the regression of the landslide crown area (Fell *et al.*, 2008a). Also susceptibility maps are filler in space, and in general, they represent an improvement with respect to inventory and density maps. In particular, errors in the landslide inventory maps are here compensated for by a reliable susceptibility model (Guzzetti, 2006). However, also susceptibility maps show some limitations. In particular, they do not provide any information about landslide temporal frequency or expected magnitude (Guzzetti, 2006; Fell *et al.*, 2008a; Fell *et al.*, 2008b). Furthermore, they basically rely on deterministic or statistical models whose behaviour must be fully understood before it can be applied for practical uses. In this sense, like any other scientific prediction, susceptibility maps should be accompanied by a quantitative estimate of the associated prediction error (Guzzetti, 2006).

Landslide hazard zoning estimates the frequency of the potential mass movements highlighted by the susceptibility map. This, however, is not a trivial task, and it basically depends on the type of landslide. For small slope failures and for rock falls, hazard is described in terms of the number of sliding events per square kilometre of source area/annum, whereas for large landslides hazard is generally expressed as the annual probability of sliding (Fell *et al.*, 2008a). Furthermore, also hazard zoning must include both landslide source and deposition areas (Cascini *et al.*, 2005; Guillard and Zezere, 2012). Ultimately, it is essential to consider the possible changes produced by buildings and

infrastructures located close to landslide crown or toe, and to understand that development boundaries, established for safety beyond the unstable area, may become obsolete in a short time frame (Feckner, 2002; Cascini *et al.*, 2005). Landslide hazard maps, which are filler of space, rely on a model that incorporates a susceptibility component. For this reason, they basically present the same advantages and disadvantages of susceptibility models and maps (Guzzetti, 2006).

According to Fell *et al.* (2008a) and to the AGS (2007a), risk is “a measure of the probability and severity of an adverse effect to health, property or the environment”. Indeed, on the basis of hazard mapping, risk zoning assesses the potential damage to elements at risk by taking into account their vulnerability and the temporal and spatial probability of the landslide event. Elements at risk are primarily the people and the properties potentially affected by the slope failure because of their location (on, below, and up-slope of the potential landslide). However, they may also include indirect impacts such as environmental damages and reduced economic activities due, for example, to the disruptions of services, utilities, and roads. Given this wide variety of elements, risk is usually simplified in two categories: risk for life loss (individual and societal) and risk for property loss (Cascini *et al.*, 2005; AGS, 2007a; Fell *et al.*, 2008a; Fell *et al.*, 2008b). In particular, according to the International Union of Geological Sciences (IUGS) (1997), the former should be calculated on the basis of the probability of natural death. In this sense, tolerable and accepted values are generally between  $10^{-3}$  and  $10^{-6}$  per annum (Cascini *et al.*, 2005; Bell *et al.*, 2006; Massey *et al.*, 2012). For property loss, on the other hand, risk is usually expressed as the yearly loss value and the annual probability of loss (Fell *et al.*, 2008a). It is, therefore, essential that risk maps are at the right scale of detail and accuracy (essentially site specific), and they also must be easily updatable with regard to both hazard assessment and elements at risk (Cascini *et al.*, 2005).

Hazard zonation requires a deep understanding of landslide processes and, of course, it implies the ability to identify landslide hazard. For this reason hazard zonation is under the responsibility of earth scientists. On the other hand, defining vulnerability and assessing acceptable risks require knowledge of the impact of landslides on people, building areas, and economic activities. As a consequence, the more suitable experts are planners, social scientists, engineers, and ultimately decision-makers (Soeters and van Westen, 1996;

Schuster and Highland, 2007).

Several factors contribute to zoning potential inefficiency (AGS, 2007a; Fell *et al.*, 2008a):

- limitations of the landslide inventory maps;
- limitations in the stability of temporal series;
- limitations in the available level of data detail;
- model uncertainty, *i.e.* limitations of the method used to assess landslide susceptibility and hazard;
- limitations in the skill of the operator that realises the zoning.

Consequently, landslide zoning is not a precise science and its results are only a prediction of performance of the slopes based on the available data.

#### **6.2.4. Landslide management in the Emilia-Romagna region**

In Italy the legal framework for planning was established in 1942. However, in the early 1970s spatial and urban planning were taken in charge by regional authorities that, within the national regulations, promulgated their own laws. Today, in the Emilia-Romagna region spatial and urban planning are regulated by the regional law LR 20/2000 (*Legge Regionale*) which, according to the three levels of governing, identifies three different levels of planning:

- regional,
- provincial,
- and municipal.

In this context, each plan must comply with the upper-tier planning and policy statements. As far as landslides are concerned, the regional plan PAI (*Piano stralcio per l'Assetto Idrogeologico*) is prepared by the River Basin Authority, and it represents the starting point for the Territorial Plan for Provincial Coordination (*Piano Territoriale di Coordinamento Provinciale* - PTCP). This plan, realised by the Provincial Administrations at a local scale and for the entire provincial territory, is the statutory and advisory framework for municipality and site specific plans, which should enhance it and complete it with further investigations. This work focused on the PTCP as it basically establishes the planning standards and techniques for all the subordinate municipal plans.

According to the Attachment of LR 20/2000 (Art. A-2), the PTCP, in line with PAI

provisions, must locate landslides and potentially unstable areas, and with respect to them, it establishes the main compatible and incompatible uses. The regional law also ratifies that the reference frame, which describes and evaluates the territory and its evolution, is part of the planning tool and is essential for the definition of the plan goals and sustainability.

The PTCP's of the four test areas aim to prevent, reduce, and mitigate landslide risk in order to build sustainable and resilient communities. The PTCP planning system relies on zoning and regulations. In particular, these plans supply three different types of regulations with respect to land-use in landslide-prone areas:

- statutory, which directly influence the legal regime of properties by regulating the compatible and incompatible uses;
- directive, which define the arrangements that must be abide by the subordinate plans;
- advisory, which define the arrangements that should be abide by the subordinate plans but with a certain degree of discretion.

All the investigated PTCP's use landslide inventory maps as zoning maps<sup>1</sup>, *i.e.* they apply regulations on the basis of landslide boundaries. Among other restrictions, for example, on dormant landslides it is prohibited to build new constructions, whereas on active landslides it is also forbidden to extend existing buildings and change their urban use classification in order to avoid an increase of landslide risk. The terms “active” and “dormant”, however, imply a certain vagueness. Indeed, in the case of the Reggio Emilia and Modena Provinces dormant landslides are those mass movements that were not evidently active in the last 30 years although they may reactivate anytime; active landslides, instead, are ongoing slope failures or mass movements that showed some kind of activity in the last 30 years. Conversely, no precise definitions for these terms are provided by the Forlì-Cesena and Ravenna Provinces. In the four study sites, landslide inventory maps are also used as zoning maps in the municipal plans at local and site-specific scale, although all the PTCP's under investigation require municipal plans to define safety zones around active landslides. Ultimately, only two out of four plans (Reggio Emilia and Modena) provide a directive regulation that calls for periodic revisions of these landslide inventories.

The Reggio Emilia PTCP was approved by the Provincial Administration in 2010 and its

---

<sup>1</sup> The Ravenna Province adopts also a risk map based on hydromorphological elementary units (*Unità Idromorfologiche Elementari* - UIE).

landslide inventory map, realised in 2008, is an update of a previous version released in 2003. On the whole, the 2008 inventory was prepared on basis of the following data sources:

- regional landslide inventory map released in 1996 and subsequently updated in 2000 (1:10,000);
- regional geological map (1:10,000 and 1:100,000);
- Civil Defence landslide inventory map released by the Reggio Emilia Province;
- study on the seismic hazard of the Reggio Emilia and Modena Provinces released by the Reggio Emilia Province;
- SCAI-CNR and GNDCI database;
- historical landslide dataset of the Emilia-Romagna Region;
- B/W aerial photographs from the 2000 flight realised by the regional Civil Defence Department (1:12,000);
- colour aerial photographs from the 1976-1978 flights realised by the Emilia-Romagna Region (1:13,500);
- in-depths analysis performed by different agencies and authorities in occasion of important landslide events;
- in-depths analysis realised within local and site-specific planning and interventions.

The same resources were used to prepare also the previous PTCP released by the Reggio Emilia Province in 1999.

### **6.3. Limits and applications of a landslide inventory map to land-use planning. The case study of the Dorgola catchment.**

In the previous chapters, I demonstrated that the preparation of a landslide inventory map implies several generalizations, simplifications, and limitations that need to be identified, appraised, and correctly conveyed to the end-users. Fundamentally, uncertainty has to be considered as an inherent and inevitable characteristic of landslide data and, in this sense, the most relevant issue about the quality of landslide inventories concerns their uses and applications.

According to the aims of this research, in this paragraph I test the landslide inventory map

of the current PTCP of the Reggio Emilia Province against the results presented in the previous chapters.

### **6.3.1. Analysis and results**

The method used for the realization of the landslide inventory of the Reggio Emilia PTCP was described in par. 6.2.4.. The final map is quite heterogeneous being the result of the combination of different documents and also of various information sources. In particular, since several operators worked on it, the subjectivity of interpretation must be considered as an additional variable for the final product. Moreover, it is worth noting that the geological map of the Emilia-Romagna Region, which was used as one of the starting points of this landslide inventory, does not show the entire slope failure but only the landslide deposit without the crown area and the main scarp. On the other hand, in this work I used the term “landslide” to define the sliding action and not the deposit (see par. 2.4.2. for details). Consequently, in order to prepare a landslide inventory as complete as possible, I mapped each single slope failure with its affected area (depletion and accumulation zones), including all levels of reactivations of major landslides. These two procedures, neither of which is absolutely correct or wrong, demonstrate the variety of options and issues involved in the realization of a landslide inventory map.

Shown below is a statistical and cartographic comparison among the following landslide inventories realised for the Dorgola catchment: the two generations of PTCP landslide inventories (the 1999 and the current plan approved in 2010), the multi-temporal inventory, the 2012 geomorphological field inventory and the landslide inventory obtained from the VHR GeoEYE 2012 image set. To this end, the comparison between remotely sensed and field survey data, exposed in par. 4.2, is entirely recalled. The final aim is to evaluate the overall reliability and limitations of a landslide inventory map within the context of large scale<sup>2</sup> land-use planning.

#### **6.3.1.1. Descriptive statistics and landslide abundance**

The descriptive statistics for the inventory maps prepared for the Dorgola catchment are

---

<sup>2</sup> According to Fell et al. (2008a) and to the AGS (2007a), large scale range from 1:25.000 to 1:5.000.

CHAPTER 6

*Table 6.4: Descriptive statistics for all the landslide inventories available for the Dorgola catchment. The values in parentheses for the Field survey and the GeoEYE 2012 inventories include API.*

		1999 PTCP	2010 PTCP	Field inventory 2012	GeoEYE 2012	Multi-temporal inventory
Number of landslides	#	49	142	224 (249)	304 (321)	1.105
Total area of mapped landslides	Km <sup>2</sup>	4,814	6,593	6,245 (9,669)	5,039 (8,045)	87,724
Total area covered by landslides	Km <sup>2</sup>	4,814	6,593	5,370 (7,266)	4,365 (6,514)	7,247
% of landslide area	%	29,69	40,66	33,12 (44,81)	26,92 (40,17)	44,69
Landslide density	#/Km <sup>2</sup>	3,02	8,76	13,81 (15,36)	18,75 (19,80)	68,15
Area of smallest landslide	m <sup>2</sup>	11.331	625	28 (28)	79 (79)	54
Area of biggest landslide	m <sup>2</sup>	990.457	974.900	1,492,740 (1,530,351)	392.681 (1,675,594)	474.010
Landslide average area	m <sup>2</sup>	98.235	46.433	27,880 (38,833)	16.577 (25,063)	17.044
Landslide median area	m <sup>2</sup>	59.975	16.768	4,622 (5,983)	2.522 (2,820)	2.870
Most abundant landslide area	m <sup>2</sup>	132.600	7.100	~300	~200	~300

\* Area complessiva = 16,21 Km<sup>2</sup>

summarised in Tab. 6.4, where for the ground-based and the remote-based inventories are reported both values: with and without API areas (see Chapter 4 for details). The analysis of Tab. 6.4 reveals that the total number of landslides increases from the 1999 and the 2010 PTCP inventories to the multi-temporal inventory. In particular, the 1999 PTCP inventory shares 4.4% of the total number of landslides of the multi-temporal inventory and 16.1% of that of the remote-based inventory realised on the GeoEYE 2012 image set. These percentages reduce respectively to 12.9% and 46.7% for the 2010 PTCP inventory, which presents 189.8% more landslides than the previous plan. The higher number of mass movements of the multi-temporal inventory is reflected in the total area of mapped landslide, while, despite the lower number of slope failures, the total area covered by landslides in the 2010 PTCP inventory is similar to those of the ground-based and the remote-based inventories. To this end, it is also worth noting that for both PTCP inventories the total area of mapped landslides is equal to the total area covered by landslides. This factor, together with the low number of mass movements, indicates that these inventories focused only on large landslides without mapping their inner reactivations. According to the geometrical distinction introduced in Chapter 4, it can be stated that the 1999 and the 2010 PTCP inventories show only 1° Level landslides.

The disparity in landslide numbers and areas, reflected also in the different landslide indexes and densities, indicate that differences exist in the average size of the slope failures mapped in the inventories under investigation. Indeed, the median area of the 1999 PTCP map is approximately 10 times larger than that of the field inventory and about 20 times those of the remotely sensed inventories. Proportions are a bit smaller for the 2010 PTCP map but, anyhow, they too reveal a consistent area discrepancy. In particular, the main differences are related to smaller slope failures since bigger ones present similar values, especially if not considering the Bondolo landslide.

The frequency distribution shown in Fig. 6.2 confirms the divergence as far as areas are concerned. In fact, it highlights that not only the 1999 PTCP map has less landslides but that, with the highest recurrence at 46,875 m<sup>2</sup>, they are also generally bigger than those of the other inventories. Conversely, despite the different total amount of landslides, the ground-based and the 2010 PTCP inventories show a similar area distribution with the highest peak at 9,375 m<sup>2</sup>. Ultimately, as already remarked, the remotely sensed GeoEYE inventory

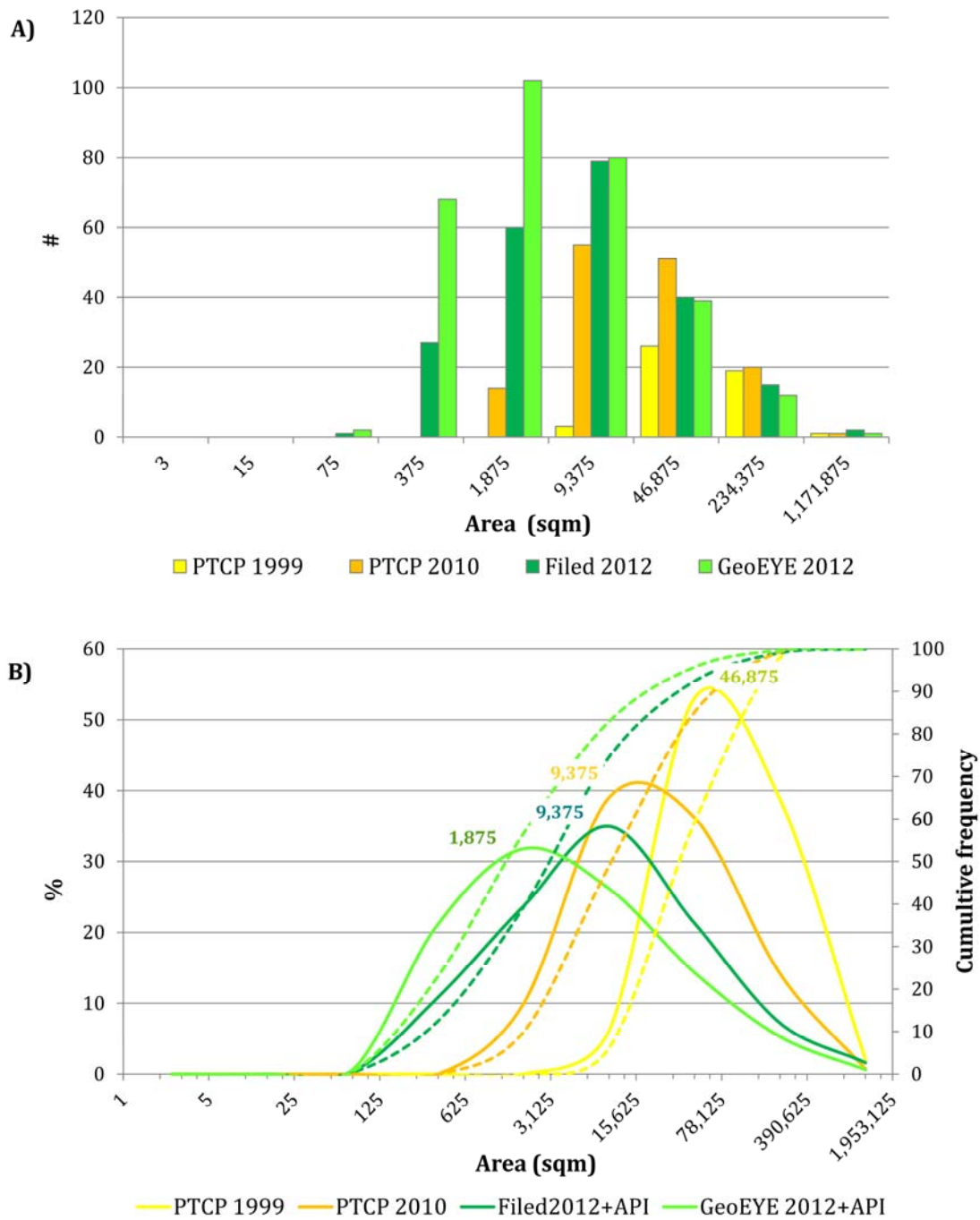


Figure 6.2: Landslide area frequency distribution for the 1999 PTCP, the 2010 PTCP, the ground-based and the remote-base inventories. In order to display all the area range, area class bin width were progressively increased according to a log5 scale. A) The histogram represents the absolute number of landslides in each area class represented by the bin central value. B) The diagram shows both the percentage cumulative and the non-cumulative curves.

presents smaller (1,875 m<sup>2</sup>) and more abundant landslides.

### 6.3.1.2. Correspondence of landslide areas

The cartographic matching was again calculated according to the method proposed by Carrara *et al.* (1993) as modified by Galli *et al.* (2008). Overall, mapping errors range from 30% to 62% (Tab. 6.5). In particular, the two PTCP maps show a rather satisfying matching index (70%) being one the updated version of the other. Conversely, with regard to the other inventories, the 2010 PTCP map shows a mapping error ranging from 39%, (field survey 2012) to 50%, (multi-temporal), whereas the 1999 PTCP map basically presents higher error indexes with values ranging from 49%, (field survey 2012) to 60% (GeoEYE 2012). Furthermore, it is worth noting that the mapping errors of the GeoEYE 2012 and of the multi-temporal inventory maps are quite similar proving their equal detection method.

### 6.3.1.3. Spatial and temporal accuracy assessment of the 2010 PTCP inventory map

This research showed that landslide detection and mapping pose several issues (see Chapter 4 and 5). In order to quantify spatial uncertainty, I introduced a fuzzy raster landslide map (see Chapter 4 for details), which, here below, I use to assess the overall accuracy of the current PTCP by clipping the 1° Level of the fuzzy inventory on the 2010 PTCP map. Results are reported in Tab. 6.6 which reveals that in the 2010 PTCP about 50%

*Table 6.5: Mapping error quantifying the cartographic mismatch of the landslide inventory maps of the Dorgola catchment. The values in parentheses refer to data including API.*

	Field survey 2012	PTCP 1999	PTP 2010
Multi-temporal	54% (41%)	60%	50%
GeoEYE 2012	54% (35%)	62% (50%)	60% (45%)
Field survey 2012	-	55% (49%)	49% (39%)
PTCP 1999	-	-	30%

Table 6.6: Percentage frequency of pixel counts related to fuzzy index classes. Data were obtained by clipping the 1° Level of the fuzzy inventory on the 2010 PTCP map. It is worth noting that 31.5% of the pixels could not be classified since they were not mapped as landslides in the multi-temporal inventory.

Fuzzy index classes	% Counts
0 - 0,1	5.3
0,1 - 0,2	2.9
0,2 - 0,3	3.5
0,3 - 0,4	1.4
0,4 - 0,5	3.6
0,5 - 0,6	1.5
0,6 - 0,7	6.8
0,7 - 0,8	1.8
0,8 - 0,9	6.8
0,9 - 1,0	35.0
Not classified	31.5

of the pixels of the total area covered by landslides presents a fuzzy index  $\geq 0,6$ . Nevertheless, 31.5% of them could not be evaluated since they were not mapped as landslides in the multi-temporal inventory, which conversely was not included in the planning document for about 37.3% of its extension. These data proved that, despite a significant mapping mismatch, landslide areas present a rather satisfying fuzzy index. This, however, is the result of what was probably an *a priori* decision, *i.e.* the 2010 PTCP inventory apparently focused only on larger landslides without taking into consideration small mass movements and, in particular, the inner reactivations inside bigger landslides.

With regard to the temporal reliability of landslide footprints, this study suggested that new activations and reactivations generally present an area ranging from 125 m<sup>2</sup> to 3,125 m<sup>2</sup> according to the image set resolution. These area classes, however, are not well represented, or are not represented at all, in the 2010 PTCP inventory. Consequently, the temporal reliability of this map is only apparent and it comes at a cost of an overall poor

mapping accuracy which, indeed, excludes small slope failures and inner reactivations of larger landslides.

### 6.3.2. Discussion

The 1999 and the 2010 PTCP inventory maps of the Reggio Emilia Province have been both used as planning reference frame as well as zoning maps. The study realised for the Dorgola catchment proved that, with respect to the multi-temporal, the ground-based, and the remote-based inventories, both PTCP inventories present a cartographic matching consistent with those reported in the literature (Carrara *et al.*, 1993; Ardizzone *et al.*, 2002; Galli *et al.*, 2008). In this sense, in addition to those reported and analysed in Chapters 4 and 5, there are several other aspects that contributed to the poor mapping correspondence:

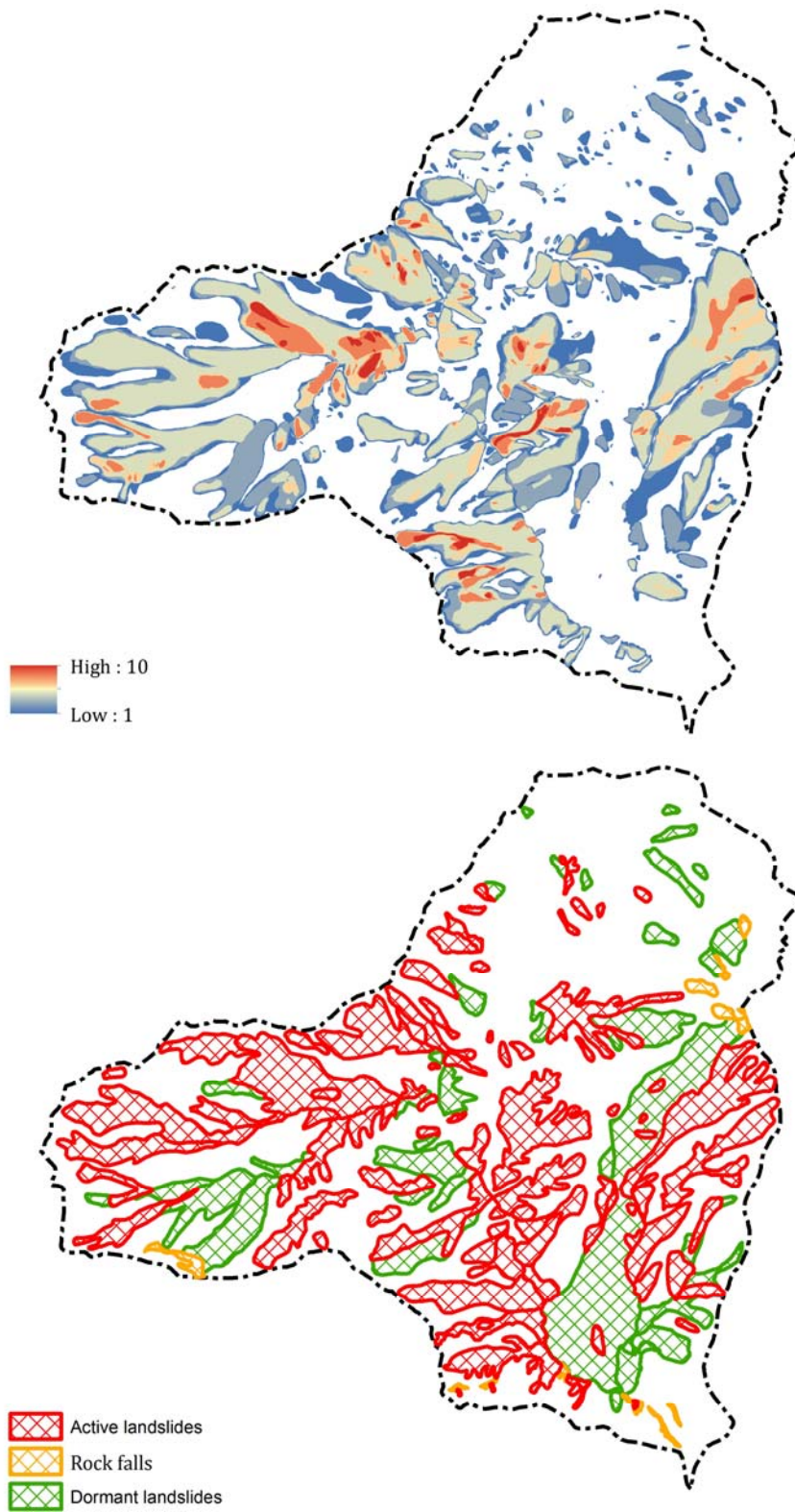
- interpreter's subjectivity. Both PTCP inventories were, indeed, realised in multiple phases and by different organizations and operators;
- specific *a priori* decisions. The geological map of the Emilia-Romagna Region, for example, shows only landslide deposits and not the whole landslide affected area (depletion and accumulation zones). At the same time, although not directly stated, it is likely that some sort of dimensional filter was applied to the mapped landslides<sup>3</sup>;
- heterogeneous information sources. The PTCP inventory maps were realised on the basis of different pre-existing documents realised with various purposes and at different scale.

The 1999 and the 2010 PTCP maps underestimate small slope failures and ignore every

*Figure 6.3: Visual comparison between the fuzzy raster landslide map (above) and the landslide inventory of the 2010 PTCP with regard to the Dorgola catchment (below). In the first map a high fuzzy index (red tones) indicates a substantial spatial and temporal persistence of landslide activity. In this sense, the two maps convey different information. In particular, the fuzzy-like analysis is able to emphasise those areas where the landsliding was more intense during the time frame under investigation.*

---

<sup>3</sup> According to the explanatory notes of the regional landslide inventory map, the cartographic limit adopted for its realization was 1:25.000. In this way, landslides with an area <100 m<sup>2</sup> were not mapped (Regione Emilia-Romagna, 1994).



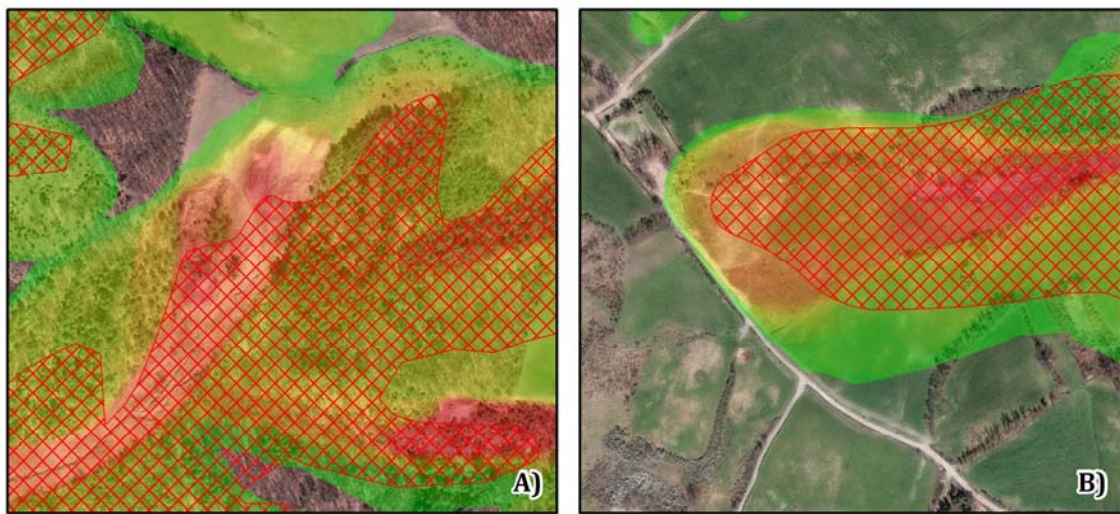
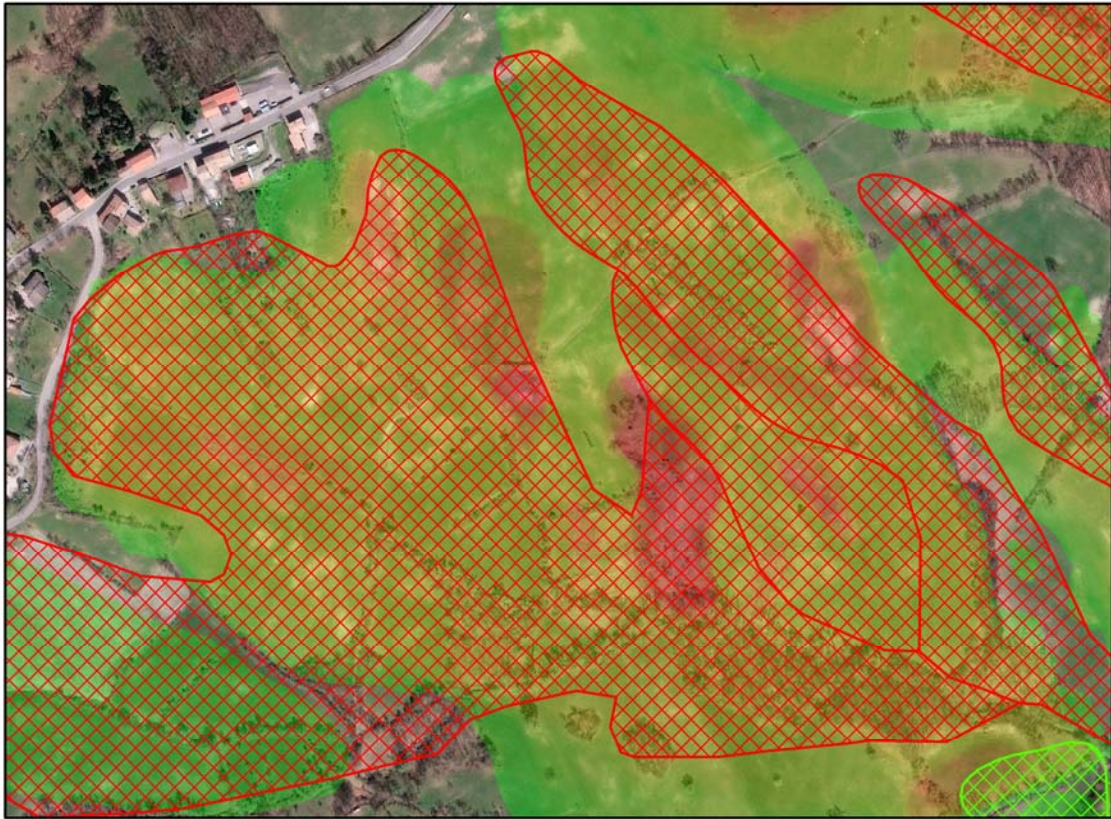


Figure 6.4: Cartographic overlapping between the 2010 PTCP landslide inventory map and the fuzzy raster landslide map. The GeoEYE 2013 image set was used as background. In both cases the PTCP inventory presents a single, well defined, and homogeneously active landslide, whereas the fuzzy raster highlights that the sliding movements are concentrated in specific areas.

partial reactivation located inside bigger mass movements in such a way that large landslide polygons overwrite all the other within them. It was not possible, however, to prove whether this poor mapping accuracy was a choice or not. Apparently this could be a thoughtful decision in order to exclude from planning documents those landslides that proved to be more challenging to detect and map. Indeed, the 2010 PTCP inventory shows a rather satisfying spatial and temporal accuracy. Nevertheless, this outcome is only apparent as it comes at a cost of an overall poor mapping quality. This inventory, like the previous one, actually provides a general and incomplete reference frame as it does not give any information about small landslides and more active areas. This kind of information, together with landslide frequency, represents a basic and essential background for land-use planning and, in particular, for the assessment of landslide hazard and risk. In this regard, Fig. 6.3 shows a visual comparison between the 2010 PTCP inventory map and the raster map realised by performing a fuzzy-like analysis including all landslide levels and both unchanged and reactivated mass movements (see Chapter 2 for details). In the latter, a high fuzzy index (red tones) indicates a substantial spatial and temporal persistence of landslide activity. In this way, this map, which is meant to be an ancillary data for the landslide



*Figure 6.5: Cartographic overlapping between the 2010 PTCP landslide inventory map and the fuzzy raster landslide map. The GeoEYE 2013 image set was used as background. The PTCP inventory basically identifies only a single complex mass movement, while the fuzzy raster gives more details as it distinguishes also several earth slides–earth flows that evolved on the larger landslide.*

inventory *sensu stricto*, not only supplies information about landslide spatial reliability, but it directly highlights those areas that were more active in the time frame under investigation. This information is not efficiently expressed in the 2010 PTCP inventory, where landslides appear as well defined, homogeneous, active or dormant areas regardless of possible localised inner movements. This generalization poses several limits to land-use planning efficiency especially as far as hazard assessment and risk reduction is concerned as shown, for example, in Fig. 6.4. According to the 2010 PTCP, these areas are involved in a single, well defined, and homogeneously active mass movement. The fuzzy raster landslide maps, instead, clearly highlight that the sliding activity is essentially concentrated in specific zones so that it was there that, with time, the retrogressive motion of the mass

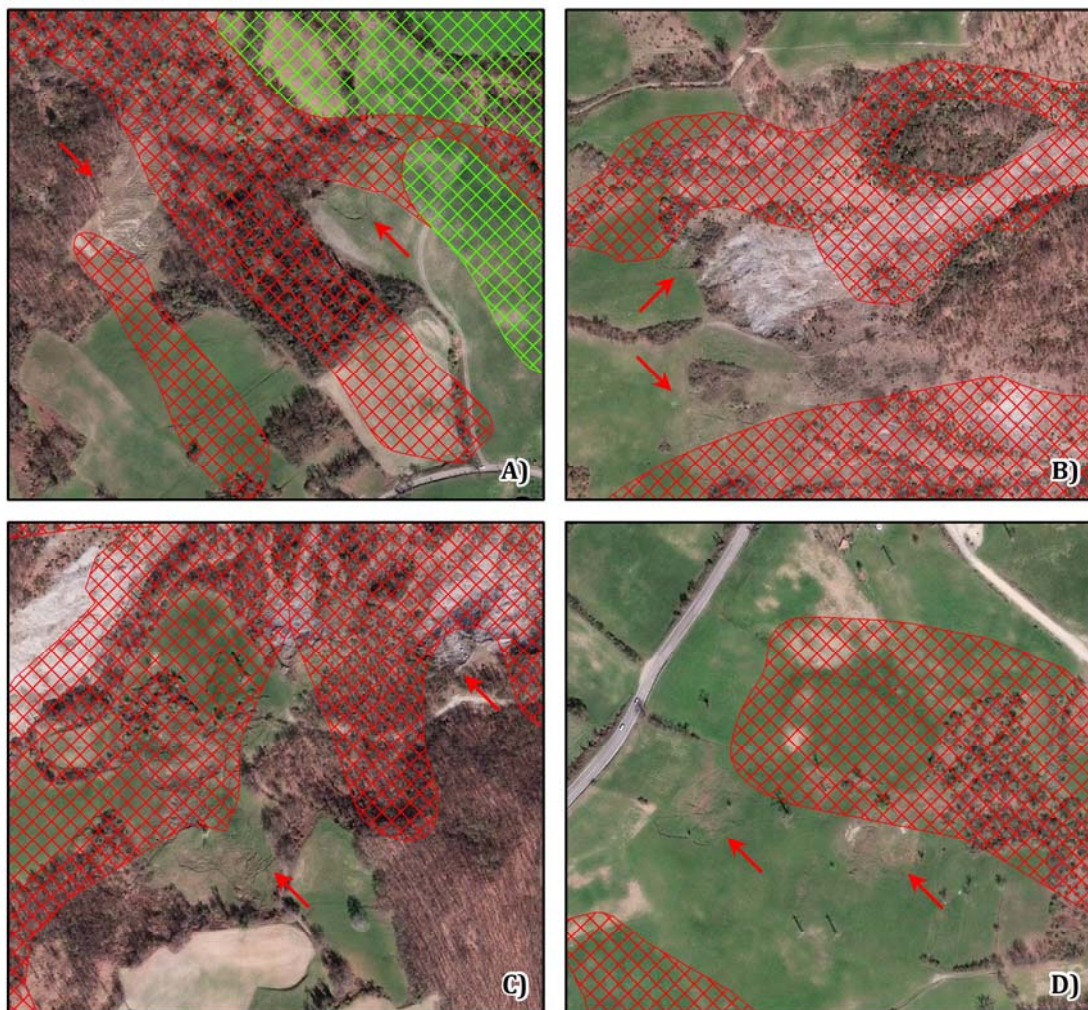


*Figure 6.6: The overlapping of the 2010 PTCP landslide inventory map with the GeoEYE 2013 image set shows that, already after few years from its realization, the planning document needs to be updated as several new landslides evolved outside the detected boundaries.*

movements ended up involving areas that were once considered stable. In order to optimise resources, this information would be essential for planning monitoring and emergency activities, as well as for defining priorities for mitigation strategies.

Furthermore, the overall generalization proposed by the PTCP map does not allow also to separate overlapped sliding movements. This, for example, is the case reported in Fig. 6.5, which shows an area where several earth slides–earth flows evolved on a larger and deeper complex landslide. These are distinct types of mass movements with different frequencies of

occurrence and geomechanical characteristics. Indeed, they pose a different level of threat to life and properties and, therefore, according to land-use planning goals, they should be differentiated from each other and managed separately.

With regard to the temporal accuracy, the 2010 PTCP inventory is characterised by an apparent reliability since new activations and reactivations are not included in the size range of this inventory. This is a significant mapping simplification with important fallouts on the efficiency of the inventory for planning purposes. Moreover, it does not solve the issue of temporal reliability. Indeed, as shown in Fig. 6.6, just after few years from the land-use plan release, the legal landslide reference is outdated posing a series of questions about the possible applications of a landslide inventory map within the land-use planning context.

## 6.4. Conclusions

In the four study sites chosen for this work, landslide inventory maps are used as reference frames and as zoning maps, *i.e.* to impose statutory constraints and advisory regulations to properties and to the subordinate municipal plans.

In general, the use of a landslide inventory map as a reference frame, to portray landslide distribution and characteristics, is advantageous and basically recommended. This work, however, showed the great variety of options and issues involved in the realization of this type of map. Indeed, besides those factors analysed in Chapters 4 and 5, there are several other aspects that affect landslide detection and mapping:

- interpreter's subjectivity;
- specific *a priori* decisions related to the mapping purposes and to the available data;
- heterogeneous information sources in terms of scale, detail, quantity, and purpose.

This work demonstrated that the apparent spatial and temporal accuracy of the landslide inventory map of the 2010 PTCP of the Reggio Emilia Province is the result of a significant mapping simplification with important fallouts on its application and efficiency for planning purposes. For this reason, in order to avoid misunderstandings, and ultimately, misuses and faulty judgments, this study recommends that all the limitations of a landslide inventory are clearly identified, quantified, and correctly conveyed to the end-user. To this regard, a question is raised on who is the ultimate end-user of a landslide inventory map. In the case

of the Emilia-Romagna Region, to this day, the end-users are basically planners and decision-makers. However, since a landslide inventory map should be essentially used as a support to further technical investigations (*e.g.* preparation and validation of susceptibility and hazard maps), the results of this study should be addressed primarily to those landslide specialists that develop landslide modelling, as well as landslide susceptibility, hazard, and risk maps, which, according to the literature, are suitable zoning tools (AGS, 2007a; Saunders and Glassey, 2007; Fell *et al.*, 2008a).

Conversely, according to this work, the application of a landslide inventory map as a zoning map should be discouraged, because, in order to be effective, landslide zoning must involve not only existing or known landslides but also potential slope failures that can be reasonably predicted. In this sense, a landslide inventory is not continuous in space and, as a zoning map, it is incomplete by definition as it represents only recognised landslides. To this regard, this work proved that, besides the inherent spatial and temporal uncertainty, there can be significant discrepancies between different inventories realised for the same area. As a consequence, this work ascertained that landslide boundaries do not represent reliable regulatory constraints.

Statutory and advisory planning tools, like those adopted in the Emilia-Romagna Region, impose significant restrictions to private properties, and consequently, it is essential that they can rely on a sound scientific background. This does not mean that landslide zoning must be based on a “scientific truth”, but that zoning regulations should be proportional to the accuracy and reliability of zoning boundaries. In this sense, the complexity of the geological and geomorphological setting of the Apennines, as well as the peculiar nature of many slope failures, suggests that landslide zoning for statutory and advisory regulations must be performed at the site-specific scale and with a performance purpose, *i.e.* according to the type of intervention. Furthermore, auxiliary measures like, for example, independent peer reviews to planning documents, insurances, disclosure of landslide issues to potential buyers, *etc.*, should be taken into consideration in order to assist zoning and improve land-use planning efficiency.

## **CHAPTER 7**

### **Conclusions and recommendations**

- 7.1. General conclusions
- 7.2. Research limits and recommendations

## 7. Conclusions and recommendations

### 7.1. General conclusions

Landslide inventory maps are essential decision-support tools for land-use planning, a valuable and powerful attempt to build sustainable and landslide resilient communities. Consequently, their quality assessment is a burning issue. In order to investigate it, I addressed three issues.

✓ Definition of the quality parameters of a landslide inventory map

The results of a detailed literature survey about quality and its descriptive components were presented in Chapter 2. In this work, I used the term “quality” to define the “fitness for use” (Juran, 1974), *i.e.* the suitability of data characteristics to user’s needs, and I also adopted the “truth-in-labelling” paradigm (Goodchild, 1995; Veregin, 1999).

In this sense, I investigated the limits and the reliability of the conceptual model and of the database ultimately represented in a landslide inventory.

Like all physical events, landslide data are multidimensional, and consequently, quality parameters have to be identified for each dimension. In particular, I focused on the spatial and temporal accuracy of a landslide inventory map, and in order to do this, I identified and investigated three key factors:

- positional accuracy;
- overall spatial accuracy of landslide detection and mapping with respect to both detection techniques and data processing and manipulation;
- landslide temporal accuracy.

✓ Quantification of the spatial and temporal accuracy of a landslide inventory map

The accuracy of data geographic positioning was analysed for all four test areas and was investigated in Chapter 3. Conversely, given the research time constraints, the overall spatial accuracy and the temporal accuracy were elaborated only for the

Dorgola catchment test area (Castelnovo né Monti – Reggio Emilia) and were the subjects respectively of Chapter 4 and Chapter 5.

Shown below are the general conclusions that can be used for the definition of standards, best practices, and protocols for the preparation of a landslide inventory map.

- Positional accuracy is an important parameter of quality. Its importance does not lie as much in the absolute geographic positing, but rather in the relative one. Indeed, in order to make proper comparison between different landslide inventory maps (*e.g.* to appraise potential relative movements or to quantify spatial differences), a constant geographic positioning is essential. To this end, the end-user must be aware of the errors that can be introduced by *datum* transformation, in particular when using different software tools, *i.e.* different algorithms. In general, I suggest to avoid *datum* transformation, however, if this is not possible, the following tips should be taken into consideration:
  - be aware of the magnitude of the problem in the study area;
  - if possible, always use the same software to keep the error as constant as possible;
  - be aware of data lineage, *i.e.* data history as far as *datum* transformations are concern;
  - the experience of the Emilia-Romagna Region suggests that the adoption of unconventional regional CRS's should be discouraged as it may be inappropriate and lead to gross errors.
- The spatial accuracy of a landslide inventory map is greatly influenced by the detection and mapping technique. This work proved that neither a geomorphological ground survey nor a visual interpretation of remotely sensed images provide a complete landslide inventory map. As a consequence, I recommend a combined use of these techniques. Field investigations are, indeed, essential to develop a detailed reference framework, while remote sensing represents a precise, cost-effective, and quick method to complete, monitor, and update this setting. In the case of the Dorgola catchment, remote sensing was even more efficient than ground survey in recognizing and mapping small landslides, *i.e.* the dimensional category to which most new landslides/reactivations belong to.

- The overall spatial accuracy is a key element of the quality of a landslide inventory map. Indeed, although represented with sharp boundaries, landslides proved to be uncertain and not well defined entities distinguishing safe and unsafe areas. In particular, this work demonstrated that their recognition and mapping depend on both extrinsic and intrinsic variables whose effects may range from metric length to tens of meters and even determine if a certain landslide can or cannot be detected. To this end, in order to reduce or limit these factors, I suggest to adopt the following measures:
  - define a protocol for orthorectification (*e.g.* limitations, software tools, protocols for the definition of ground control points, *etc.*);
  - data scale and resolution (in particular of base support data) should be kept as constant as possible;
  - avoid capturing conditions bias, *e.g.* repeated shadows or forest cover over the same areas as they might constantly prevent the detection of some landslides;
  - control of positional accuracy (see above);
  - in order to reduce map heterogeneities and subjectivity, it would be advantageous for landslide inventory maps to be elaborated and managed by a single agency.

These efforts may help to improve spatial accuracy but they cannot completely solve the issue. In this sense, according to the “truth-in-labelling” paradigm, the type of fuzzy raster landslide maps prepared for this work proved to be valuable tools to convey to the end-user the spatial approximations and limitations of landslide inventory maps.

- The time variable is an essential aspect of landslide inventory maps. This work proved that, due to the progressive deterioration of data temporal quality, these maps need periodic updates especially as far as small landslides are concern. According to the results obtained for the Dorgola catchment, a desirable data acquisition frequency is once a year or maximum every two years. To this end, remote sensing proved to be a suitable and cost-effective tool in order to guarantee high acquisition frequency. In this regard, it is also worth remembering that data acquisition is a form of long-term investment as it basically represents the base for

future researches.

✓ Possible applications and limits of a landslide inventory map to land-use planning

According to the definition given in this work, quality must be judged against a particular application. In this sense, in Chapter 6 I evaluated the spatial and temporal accuracy of the PTCP landslide inventory map of the Dorgola catchment. It turned out that the use of landslide inventory maps as reference frame is generally advantageous and valuable. However, it is essential that their inherent simplifications, generalizations, and ultimately their limitations are correctly conveyed to the end-user in order to avoid misuses and faulty decision-making. To this end, I consider these tasks essential:

- preparation of a fuzzy raster landslide map to convey the spatial mapping reliability;
- definition of the landslide area range with respect to the scale and resolution of the detection method, *i.e.* the imprinting of detection and mapping operations on the landslide area range;
- frequent updates that in the long-term will allow to define the area range affected by new landslides or reactivations;
- realization of a detailed report with, at least, these information: purpose and limitations of the inventory, essential data information (*e.g.* resources, scale, lineage, limits, *etc.*), and an accurate description of the detection and mapping technique.

Conversely, the use of landslide inventory maps as zoning maps, especially when related to regulatory constraints, must be discouraged. Indeed, landslide zoning must involve also potential slope failures that can be reasonably predicted, and besides, zoning regulations must be proportional to the accuracy of zoning boundaries. In this sense, landslide inventory maps not only are not continuous in space but they also represent unreliable boundaries due to their inherent spatial and temporal uncertainty.

## 7.2. Research limits and recommendations

As landslide data, the quality assessment of a landslide inventory map must be multidimensional. This work performed a quantitative evaluation of spatial and temporal accuracy, but it did not investigate landslide attribute that should be addressed by further research. An additional limitation concerns the extension of the investigated site. As far as the land-use is concerned, further investigations should also concentrate on the correlation between the development of forests and scrubs, and the evolution of landslide areas. Furthermore, more research is also needed in order to quantify the interpreter subjectivity. To this end, to properly address this issue, all the other variables (*e.g.* detection method, time, base support material, *etc.*) should be restrained as much as possible. Considering the importance of the detection method and of the interpreter subjectivity, I also recommend that future researches assess the results of this work by applying on the same study site

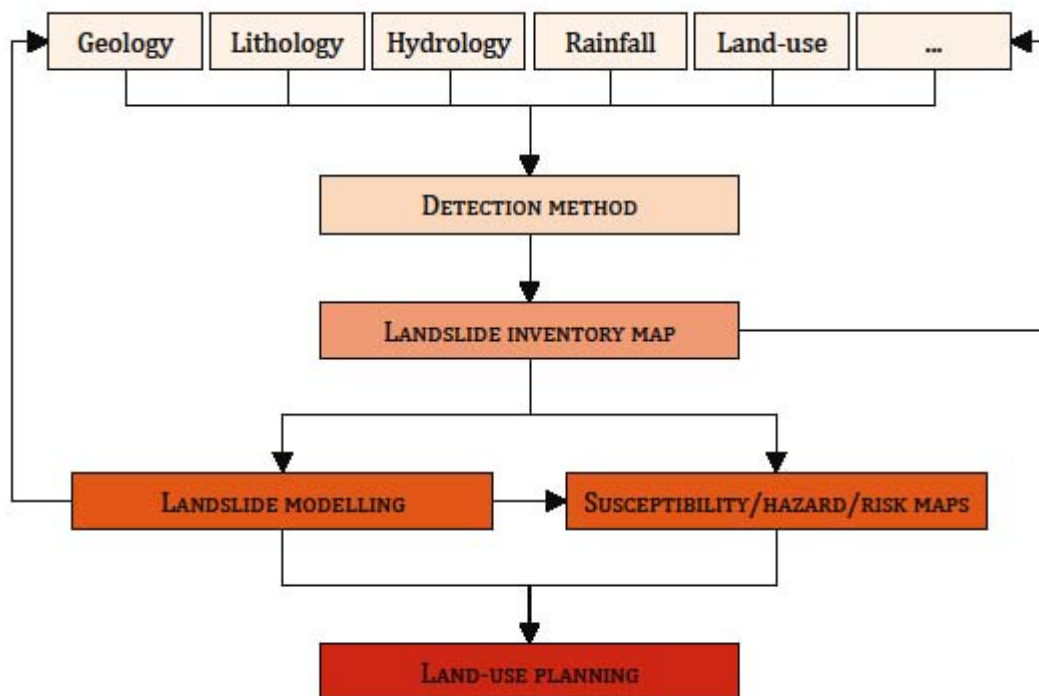


Figure 7.1: Suggested iterative flowchart for land-use planning.

other landslide detection techniques, and in particular, automated and semi-automated detection methods (e.g. LIDAR, SAR interferometry, object-based image analysis, NDVI thresholding, *etc.*).

The use of landslide inventory maps as support to further technical investigations raises some serious questions about the whole range of their possible end-users. Indeed, it would be interesting to test the results of this work, in particular as far as fuzzy raster landslide maps are concerned, on landslide modelling, and more generally, on the preparation and validation of susceptibility and hazard maps.

Ultimately, I suggest to consider a different land-use planning approach for landslide-prone areas in the Emilia-Romagna Region. Indeed, given the complex and challenging geological and geomorphological setting of this territory, the planning approach should be assessed also on the basis of the landslide type. Shallow landslides and old dormant landslides, for example, pose a different hazard to man life and properties, and consequently, they should be managed in a different way. Shallow landslides can likely be predicted on the basis of modelling, whereas, in order to evaluate the frequency and the behaviour of old dormant landslides, historical data and more detailed subsurface investigations are required. More generally, the statutory zoning of the Emilia-Romagna Region should be applied with care at the large scale. Indeed, the constraints imposed by the planning regulation must match the quality, quantity, and resolution of the available data, *i.e.* the zoning boundary reliability. In this sense, at the site-specific scale, statutory zoning must be integrated with detailed ground inspections and geotechnical data. Furthermore, as already applied to the seismic hazard, restrictions should be proportional to the type of intervention. Fundamentally, I recommend to adopt a risk-based approach according to which the realization of a barn, an apartment building, or an hospital implies different planning efforts and restrictions.

Landslide inventory maps are a cornerstone of land-use planning, but they represent only the starting point of the planning workflow, which, indeed, should comprehend other tools and should be iterative with constant data updates and revisions (Fig. 7.1). In general, I suggest that large scale land-use plans (*e.g.* PTCP) provide zoning maps that are finer in space and that include unstable and potentially unstable areas by taking into consideration also the effects of future developments. In this sense, landslide modelling and susceptibility maps are essential to likely predict landslides and landslide behaviour, whereas hazard and

risk maps are crucial to assess the effects, the consequences, and ultimately the economic and the social sustainability of landslides. As a consequence, I strongly recommend to adopt these tools in land-use planning documents.

---

## References

- Abbott, L. (1955), *Quality and competition*, New York: Columbia University Press.
- Aguilar, M.; Agüera, F.; Aguilar, F. & Carvajal, F. (2008), 'Geometric accuracy assessment of the orthorectification process from very high resolution satellite imagery for Common Agricultural Policy purposes', *International journal of remote sensing*, 29(24), 7181-7197.
- Albarelo, D.; Bosi, V.; Brammerini, F.; Lucantoni, A.; Naso, G.; Peruzza, L.; Rebez, A.; Sabetta, F. & Slejko D. (1999), 'Hazard maps 1999. PGA (g) values with a 10% probability of exceedance in 50 years (475-year return period)', Nat. Sism. Service, Rome, Italy.
- Aleotti, P. and Chowdhury, R. (1999), 'Landslide hazard assessment: summary review and new perspectives', *Bulletin of Engineering Geology and the Environment*, 58, 21-44.
- Antonini, G., Cardinali, M., Guzzetti, F., Reichenbach, P. & Sorrentino, A. (1993), 'Carta Inventario dei Fenomeni Franosi della Regione Marche ed aree limitrofe', *CNR Gruppo Nazionale per la Difesa dalle Catastrofi Idrogeologiche*, 580, 2 sheets, scale 1:100,000.
- Ardizzone, F.; Cardinali, M.; Carrara, A.; Guzzetti, F. & Reichenbach, P. (2002), 'Impact of mapping errors on the reliability of landslide hazard maps', *Natural Hazards and Earth System Science*, 2(1/2), 3-14.
- AGS (Australian Geomechanics Society) (2007a), 'Guidelines for landslide susceptibility, hazard and risk zoning for land use planning', [on-line]. Available at: <http://irm.australiangeomechanics.org/other-resources/guidelines/ags-2007/> [Accessed 13 Oct. 2014].
- Baiocchi, V.; Crespi, M. & De Lorenzo, C. (2002), 'Il problema della trasformazione di datum e di coordinate per applicazioni cartografiche: soluzioni informatiche e loro prestazioni', *Documenti del territorio*, 49, 11-18.
- Basenghi, R. & Bertolini, G. (2001), 'Ricorrenza e caratteristiche delle frane riattivate durante il XX secolo nella provincia di Reggio Emilia Appennino settentrionale', *Quad. Geol. Appl.*, 8 (1), 153-162.
- Bell, R.; Glade, T. & Danscheid, M. (2006), 'Challenges in defining acceptable risk levels'. In: *RISK21-Coping with Risks due to Natural Hazards in the 21st Century: Proceedings of the Risk21 Workshop*, Monte Verita, Ascona, Switzerland, 28, 77-87.
- Bertolini, G. & Pellegrini, M. (2001), 'The landslides of the Emilia Apennines (northern Italy) with reference to those which resumed activity in the 1994-1999 period and required Civil Protection interventions', *Quad. Geol. Appl.*, 8(1), 27-74.
- Bertolini, G.; Guida, M. & Pizziolo, M. (2005), 'Landslides in Emilia-Romagna region (Italy):

## References

---

- strategies for hazard assessment and risk management', *Landslides*, 2(4), 302-312.
- Bertolini, G. & Pizziolo, M. (2008), 'Risk assessment strategies for the reactivation of earth flows in the Northern Apennines (Italy)', *Engineering Geology*, 102, 178-192.
- Bertolini, G. & Pizziolo, M. (2012), 'The reactivation of ancient landslides in the Emilia-Romagna Region (Italy): risk-reduction strategies', [on-line].  
Available at: [http://ambiente.regione.emilia-romagna.it/geologia/archivio\\_pdf/dissesto-idrogeologico/reactivation\\_landslides\\_Bertolini\\_Pizziolo.pdf/view](http://ambiente.regione.emilia-romagna.it/geologia/archivio_pdf/dissesto-idrogeologico/reactivation_landslides_Bertolini_Pizziolo.pdf/view) [Accessed January 2015].
- Bettelli, G. & De Nardo, M. (2001), 'Geological outlines of the Emilia Apennines (Italy) and introduction to the rock units cropping out in the areas of the landslides reactivated in the 1994-1999 period', *Quad. Geol. Appl.*, 8(1), 1-26.
- Borgatti, L. & Tosatti, G. (2010), 'Slope Instability Processes Affecting the Pietra Di Bismantova Geosite (Northern Apennines, Italy)', *Geoheritage*, 2(3-4), 155-168.
- Brabb, E.E. (1991), 'The World Landslide Problem', *Episodes*, 14(1), 52-61.
- Butenfield, B. P. & Beard, M. K. (1991), 'Visualizing the Quality of Spatial Information', National Center for Geographic Information and Analysis - Research Initiative# 7, supported by flagrant from the National Science Foundation (SES-88-10917).
- Campbell, J. & Wynne, R. (2012), *Introduction to Remote Sensing, Fifth Edition*, Guilford Publications.
- Cardinali, M., Guzzetti, F. & Brabb, E.E. (1990), 'Preliminary map showing landslide deposits and related features in New Mexico', U.S. Geological Survey Open File Report 90/293, 4 sheets, scale 1:500,000.
- Cardinali, M., Antonini, G., Reichenbach, P. and Guzzetti, F. (2001), 'Photo-geological and landslide inventory map for the Upper Tiber River basin', CNR Gruppo Nazionale per la Difesa dalle Catastrofi Idrogeologiche, 2154, scale 1:100,000.
- Cardinali, M.; Reichenbach, P.; Guzzetti, F.; Ardizzone, F.; Antonini, G.; Galli, M.; Cacciano, M.; Castellani, M.; Salvati, P. & others (2002), 'A geomorphological approach to the estimation of landslide hazards and risks in Umbria, Central Italy', *Natural hazards and earth system science*, 2(1/2), 57-72.
- Carrara, A.; Cardinali, M. & Guzzetti, F. (1993), 'Uncertainty in evaluating landslide hazard and risk', *ITC Jour.*, 2, 101-109.
- Cascini, L.; Bonnard, C.; Corominas, J.; Jibson, R. & Montero-Olarte, J. (2005), 'Landslide hazard and risk zoning for urban planning and development', *Landslide Risk Management*, Taylor and Francis, London, 199-235.

- Chandler, R. J. & Tosatti, G. (1995), 'The Stava tailings dams failure, Italy, July 1985', *Proceedings of the institution of civil engineers, Geotechnical Engineering*, 113, 67-79.
- Chen, W. & Hill, C. (2005), 'Evaluation procedure for coordinate transformation', *Journal of surveying engineering*, 131 (2), 43-49.
- Cima, V.; Olivucci, S. & Zennaro, L. (2013), 'Sistemi di coordinate geografiche e cartografiche in Regione Emilia-Romagna e loro trasformazioni', [on-line]. Available at: <http://geoportale.regione.emilia-romagna.it/it/services/servizi%20tecnici/servizio-di-conversione/conver-2013-software-per-la-conversione-fra-sistemi-di-coordinate-in-emilia-romagna> [Accessed August 2013].
- Collier, P. & Steed, J. (2001), 'Australia's National GDA94 Transformation Grids', *Proceedings of the 42nd Australian Surveyors Congress*, Brisbane, Australia.
- Condorelli, A. (2010), 'Impiego di cartografia catastale in Sistemi Informativi Geografici: problematiche fondamentali e possibili approcci applicativi', *Proceedings of the ASITA XIV National Conference*, Brescia, Italy, 631-636.
- ConvER3 "GPS7" (2013), *Software per la trasformazione di coordinate*, [on-line]. Available at: <http://geoportale.regione.emilia-romagna.it> [Accessed March 2013].
- Crosby, P. (1979), *Quality is free: The art of making quality certain*, New York: New American Library.
- Crozier, M. (2010), 'Landslide geomorphology: An argument for recognition, with examples from New Zealand', *Geomorphology*, 120(1), 3-15.
- Cruden, D. M. & Varnes, D. J. (1996), 'Landslide types and processes', *Landslides: investigation and mitigation*, 247, 36-75.
- Deakin, R. (2006), 'A Note on the Bursa-Wolf and Molodensky-Badekas Transformations', School of Mathematical and Geospatial Sciences, RMIT University, 1-21.
- Del Moro, M. A. & Lancia, F. (2007), 'Disomogeneità territoriale dell'errore nelle trasformazioni fra datum', *Proceedings of the ASITA XI National Conference*, Torino, Italy, 1-6.
- Devillers, R.; Gervais, M.; Bédard, Y. & Jeansoulin, R. (2002), 'Spatial data quality: from metadata to quality indicators and contextual end-user manual', In *OEEPE/ISPRS Joint Workshop on Spatial Data Quality Management*, 21-22.
- Devillers, R.; Bédard, Y. & Jeansoulin, R. (2005), 'Multidimensional management of geospatial data quality information for its dynamic use within GIS', *Photogrammetric Engineering & Remote Sensing*, 71(2), 205-215.

## References

---

- Dipartimento di Protezione Civile (2014), [on-line].  
Available at: <http://www.protezionecivile.gov.it/> [Accessed 22 July 2014].
- Donatelli, D.; Maseroli, R. & Pierozzi, M. (2002), 'Le trasformazioni fra i sistemi di riferimento utilizzati in Italia', *Bollettino di Geodesia e Scienze Affini*, 4.
- Dragicevic, S. & Marceau, D. J. (2000), 'An application of fuzzy logic reasoning for GIS temporal modeling of dynamic processes', *Fuzzy sets and Systems*, 113(1), 69-80.
- E-geos.it (2014), e-GEOS GeoEye-1/IKONOS, [on-line].  
Available at: <http://www.e-geos.it/products/geoeeye.html> [Accessed 24 Aug. 2014].
- Exelis VIS (Visual Information Solutions) (2013), 'ENVI tutorial: orthorectifying aerial photographs'.
- Fara, E. (2001), 'What are Lazarus taxa?', *Geological Journal*, 36(3-4), 291-303.
- Featherstone, W. E. (1997), 'A comparison of existing co-ordinate transformation models and parameters in Australia', *Australian surveyor*, 42 (2), 25-34.
- Feckner, S. (2002), 'Development setbacks from river valley/ravine crests in newly developing areas'. In: R. McInnes and J. Jakeways (eds.). *Instability Planning and Management*, Thomas Telford, 135-142.
- Feigenbaum, A. (1951), *Quality control: Principles, practice, and administration*, New York: McGraw-Hill.
- Fell, R.; Ho, K. K. S.; Lacasse, S. & Leroi, E. (2005), 'State of the Art Paper 1-A framework for landslide risk assessment and management'. In: *Proceedings of the International Conference on Landslide Risk Management*, Vancouver, Canada (31).
- Fell, R.; Corominas, J.; Bonnard, C.; Cascini, L.; Leroi, E. & Savage, W. Z. (2008a), 'Guidelines for landslide susceptibility, hazard and risk zoning for land use planning', *Engineering Geology*, 102, 85-98.
- Fell, R.; Corominas, J.; Bonnard, C.; Cascini, L.; Leroi, E. & Savage, W. Z. (2008b), 'Commentary - Guidelines for landslide susceptibility, hazard and risk zoning for land-use planning', *Engineering Geology*, 102, 99-111.
- Fernandez, T.; Delgado, J.; Cardenal, J.; Irigaray, C.; El Hamdouni, R. & Chacon, J. (2006), 'Improvement of positional accuracy of landslide database using digital photogrammetry techniques', *Proceedings of the 7th International Symposium on Spatial Accuracy Assessment in Natural Resources and Environmental Sciences*, [on-line].  
Available at: <http://www.spatial-accuracy.org> [Accessed 22 July 2014].
- Fisher, P. F. (1999), 'Models of uncertainty in spatial data', *Geographical information systems*,

1, 191-205.

Fondazione Stava 1985 onlus (2014), [on-line].

Available at: <http://www.stava1985.it/> [Accessed December 2014].

Galli, M.; Ardizzone, F.; Cardinali, M.; Guzzetti, F. & Reichenbach, P. (2008), 'Comparing landslide inventory maps', *Geomorphology*, 94(3), 268-289.

Garberi, M.; Palumbo, A. & Pizziolo, M. (1999), *I numeri sulle frane*, Grafiche Damiani.

Genevois, R. & Ghirotti, M. (2005), 'The 1963 Vajont landslide', *Giornale di Geologia Applicata*, 1, 41-52.

GeoEYE (2009), 'GeoEye Product Guide v1.0.1', [on-line].

Geoportale Nazionale, [on-line].

Available at: <http://www.pcn.minambiente.it/GN/> [Accessed from November 2013 to September 2014]

Geoportale della Regione Emilia-Romagna, [on-line].

Available at: <http://geoportale.regione.emilia-romagna.it/it> [Accessed 22 July 2014].

Giannini, M.S. (1960), 'Certeza pubblica', In: Giufré (ed), *Enciclopedia del diritto. Annali*, Milano, 769-792.

Gilmore, H. (1974), 'Product conformance cost', In *Quality progress*, 16-19.

Glavovic, B.; Saunders, W. & Becker, J. (2010), 'Land-use planning for natural hazards in New Zealand: the setting, barriers, 'burning issues' and priority actions', *Natural Hazards*, 54(3), 679-706.

Goodchild, M. F. (1993), 'Data models and data quality: problems and prospects', *Environmental modeling with GIS*, 94-103.

Goodchild, M. F. (1995), *Sharing imperfect data*.

Greiving, S. & Fleischhauer, M. (2006), 'Spatial planning response towards natural and technological hazards', *Natural and technological hazards and risks affecting the spatial development of European regions*, Geological Survey of Finland, Special Paper 42, 109-123.

Greiving, S.; Fleischhauer, M. & Wanczura, S. (2006), 'Management of natural hazards in Europe: the role of spatial planning in selected EU member states', *Journal of environmental planning and management*, 49(5), 739-757.

GSUEG (Gruppo di Studio delle Università Emiliane per la Geomorfologia) (1976), 'Geomorfologia dell'area circostante la Pietra di Bismantova (Appennino reggiano)', *Boll*

## References

---

*Serv. Geol. It.*, 97.

Guillard, C. & Zezere, J. (2012), 'Landslide susceptibility assessment and validation in the framework of municipal planning in Portugal: the case of Loures municipality', *Environmental management*, 50(4), 721-735.

Guptill, S. C. & Morrison, J. L. (1995), *Elements of spatial data quality*, Elsevier Science Oxford, 202.

Guzzetti, F. & Cardinali, M. (1989), 'Carta Inventario dei Fenomeni Franosi della Regione dell'Umbria ed aree limitrofe', *CNR Gruppo Nazionale per la Difesa dalle Catastrofi Idrogeologiche*, 204, 2 sheets, scale 1:100,000.

Guzzetti, F. (2000), 'Landslide fatalities and the evaluation of landslide risk in Italy', *Engineering Geology*, 58(2), 89-107.

Guzzetti, F.; Cardinali, M.; Reichenbach, P. & Carrara, A. (2000), 'Comparing landslide maps: A case study in the upper Tiber River Basin, central Italy', *Environmental management*, 25(3), 247-263.

Guzzetti, F. (2006), 'Landslide hazard and risk assessment', PhD thesis, Mathematisch-Naturwissenschaftlichen Fakultät der Rheinischen Friedrich-Wilhelms-Universität University of Bonn, 389.

Guzzetti, F.; Reichenbach, P.; Ardizzone, F.; Cardinali, M. & Galli, M. (2006), 'Estimating the quality of landslide susceptibility models', *Geomorphology*, 81(1), 166-184.

Guzzetti, F.; Mondini, A. C.; Cardinali, M.; Fiorucci, F.; Santangelo, M. & Chang, K.-T. (2012), 'Landslide inventory maps: New tools for an old problem', *Earth-Science Reviews*, 112(1), 42-66.

Hughes, M. L.; McDowell, P. F. & Marcus, W. A. (2006), 'Accuracy assessment of georectified aerial photographs: Implications for measuring lateral channel movement in a GIS', *Geomorphology*, 74(1), 1-16.

Hutchinson, J.N. (1995), 'Landslide hazard assessment', In: Bell (ed.) *Landslides*, A.A. Balkema, Rotterdam, 1805-1841.

Iliffe, J. (2000), *Datums and Map Projections for remote sensing, GIS, and surveying*, Whittles Publishing Services, Scotland, UK.

ISO/TC 176/SC1 (1986), *ISO 8402 Quality vocabulary*, International Standard Organization, Geneva.

ISO/TC 69/SC6 (1994), *ISO 5725-1:1994 Measurement methods and results - Accuracy (trueness and precision) of measurement methods and results*, International Standard

Organization, Geneva.

ISO/TC 176/SC (2005), *ISO 9000:2005 Quality management systems – Fundamentals and vocabulary*, International Standard Organization, Geneva.

ISO/TC 211 (2009), *ISO 19114:2003 Geographic information – Quality evaluation procedures*, International Standard Organization, Geneva.

IUGS (International Union of Geological Sciences) (1997), 'Quantitative risk assessment for slopes and land-slides – the State of the Art', IUGS Working Group on Landslides, Committee on Risk Assessment. In: *Landslide risk assessment*, Cruden and Fell (eds), Balkema, Rotterdam, 3-12.

Juran, J.; Gryna, F. J. & Bingham, R. (1974), *Quality control handbook*, New York: McGraw-Hill

Kahn, B. & Strong, D. (1998), 'Product and Service Performance Model for Information Quality: An Update', *Proceedings of the Conference on Information Quality*, Massachusetts Institute of Technology, Cambridge, MA.

Kwon, J. H.; Bae, T.-S.; Choi, Y.-S.; Lee, D.-C. & Lee, Y.-W. (2005), 'Geodetic datum transformation to the global geocentric datum for seas and islands around Korea', *Geosciences Journal*, 9 (4), 353-361.

Leventhal, A. R. & Kotze, G. P. (2008), 'Landslide susceptibility and hazard mapping in Australia for land-use planning with reference to challenges in metropolitan suburbia', *Engineering Geology*, 102(3), 238-250.

Levitt, T. (1972), *Production-line approach to service*, Harvard Business Review.

Malamud, B. D.; Turcotte, D. L.; Guzzetti, F. & Reichenbach, P. (2004), 'Landslide inventories and their statistical properties', *Earth Surface Processes and Landforms*, 29(6), 687-711.

Mantovani, F.; Soeters, R. & Van Westen, C. (1996), 'Remote sensing techniques for landslide studies and hazard zonation in Europe', *Geomorphology*, 15(3), 213-225.

Mark, D. M., & Csillag, F. (1989), 'The nature of boundaries on 'area-class' maps', *Cartographica: The International Journal for Geographic Information and Geovisualization*, 26(1), 65-78.

Maseroli, R. & Nicolodi, S. (2002), 'Alcuni metodi per il passaggio dal sistema WGS84 ai sistemi geodetici locali', *Bollettino ASIT*, 32.

Massey, C.; Taig, T. & Webb T. (2012), 'Principles and criteria for the assessment of risk from slope stability in the Port Hills, Christchurch', *GNS Science Consultancy Report*, [online].

## References

---

Available at <http://www.ccc.govt.nz/homeliving/civildefence/chcheearthquake/porthillsgeotech/porthillsgnsreports.aspx> [Accessed 13 Oct. 2014].

Montrasio, L.; Valentino, R. & Losi, G. L. (2012), 'Shallow landslides triggered by rainfalls: modeling of some case histories in the Reggiano Apennine (Emilia Romagna Region, Northern Italy)', *Natural hazards*, 60(3), 1231-1254.

Olshansky, R.B. (1996), *Planning for hillside development*, American Planning Association Planning Advisory Service Report no. 466.

Peuquet, D. (1999), 'Time in GIS and geographical databases', *Geographical information systems*, 1, 91-103.

Phillips, J. (2005), 'Weathering instability and landscape evolution', *Geomorphology*, 67, 255-272.

Pizziolo, M.; Del Maschio, L.; Gozza, G. & Pignone, S. (2008), 'Determinazione di soglie pluviometriche per l'insacco di frane in Emilia-Romagna', *Geol. Emilia-Romagna*, 29, 21-27.

Pizziolo, M.; Bernardi, M.; Daniele, G.; Generali, M. & Piacentini, D. (2014a), 'Rapporto sugli eventi di frana avvenuti nei mesi di Marzo e Aprile 2013 in Emilia-Romagna', Servizio Geologico Sismico e dei Suoli - Regione Emilia-Romagna, [on-line]. Available at: <http://ambiente.regione.emilia-romagna.it/geologia/temi/dissesto-idrogeologico/rapporto-frane-marzo-aprile-2013-1>

Pizziolo, M.; Daniele, G. & Generali, M. (2014b), 'Rapporto sulle frane attivate in Emilia-Romagna nel periodo Novembre 2013 – Marzo 2014', Servizio Geologico Sismico e dei Suoli - Regione Emilia-Romagna, [on-line]. Available at: <http://ambiente.regione.emilia-romagna.it/geologia/temi/dissesto-idrogeologico/rapporto-frane-novembre-2013-marzo-2014>

Porporato, C. (2012), 'Transformation from the Cadastral DATUM to the Roma 1940 and ETRF2000 DATUM', *Territorio Italia*, 1, 107-119.

Provincia di Forlì-Cesena (2001), *Piano Territoriale di Coordinamento Provinciale*.

Provincia di Forlì-Cesena (2006), *Piano Territoriale di Coordinamento Provinciale*.

Provincia di Forlì-Cesena (2010), Variante Integrativa al *Piano Territoriale di Coordinamento Provinciale*.

Provincia di Modena (1999), *Piano Territoriale di Coordinamento Provinciale*.

Provincia di Modena (2006), Variante al *PTCP di adeguamento in materia di dissesto idrogeologico* ai Piani di Bacino dei fiumi Po e Reno.

- Provincia di Modena (2009), *Piano Territoriale di Coordinamento Provinciale*.
- Provincia di Ravenna (2000), *Piano Territoriale di Coordinamento Provinciale*.
- Provincia di Ravenna (1999), *Variante integrativa al PTCP*.
- Provincia di Reggio Emilia (1999), *Piano Territoriale di Coordinamento Provinciale*.
- Provincia di Ravenna (2010), *Piano Territoriale di Coordinamento Provinciale*.
- Raper, J. F. (1999), 'Spatial representation: the scientist's perspective', *Geographical information systems*, 1, 61-70.
- Reeves, C. A. & Bednar, D. A. (1994), 'Defining quality: alternatives and implications', *Academy of management Review*, 19(3), 419-445.
- Regione Emilia-Romagna (1994), *Note illustrative della carta del dissesto geologico attuale*, Firenze.
- Regione Emilia-Romagna (2003), 'DELIBERAZIONE DEL CONSIGLIO REGIONALE 28 maggio 2003, n. 484. Approvazione dell'atto di indirizzo e coordinamento tecnico per l'attuazione della L.R. 24 marzo 2000, n. 20, art. 27, recante "Strumenti cartografici digitali e modalita' di coordinamento ed integrazione delle informazioni a supporto della pianificazione".
- Regione Emilia-Romagna (2012), *Carta geologica della Regione Emilia-Romagna*, [on-line]. Available at: <http://ambiente.regione.emilia-romagna.it/geologia/cartografia/webgis-banchedati/webgis> [Accessed June 2012].
- Regione Emilia-Romagna (2013), *Il Catalogo dei Dati Geografici, Servizio Geologico Sismico e dei Suoli*, [on-line]. Available at: <http://geo.regione.emilia-romagna.it/geocatalogo/> [Accessed March 2013 and April 2014].
- Rib, H. T. & Liang, T. (1978), 'Recognition and identification', *Landslide Analysis and Control*, National Academy of Sciences, Transportation Research Board Special Report, 176, 34-80.
- Rivest, S.; Bédard, Y. & Marchand, P. (2001), 'Toward better support for spatial decision making: defining the characteristics of spatial on-line analytical processing (SOLAP)', *GEOMATICA-OTTAWA*, 55(4), 539-555.
- Rossi, M.; Witt, A.; Guzzetti, F.; Malamud, B. D. & Peruccacci, S. (2010), 'Analysis of historical landslide time series in the Emilia-Romagna region, northern Italy', *Earth Surface Processes and Landforms*, 35(10), 1123-1137.
- Salvati, P.; Bianchi, C.; Rossi, M. & Guzzetti, F. (2010), 'Societal landslide and flood risk in

## References

---

Italy', *Natural Hazards and Earth System Science*, 10(3), 465-483.

Santangelo, M.; Cardinali, M.; Rossi, M.; Mondini, A. & Guzzetti, F. (2010), 'Remote landslide mapping using a laser rangefinder binocular and GPS', *Natural Hazards and Earth System Science*, 10(12), 2539-2546.

Saunders, W., & Glassey, P. (2007), 'Guidelines for assessing planning policy and consent requirements for landslide prone land', *GNS Science Miscellaneous Series 7*.

Schwab J.C.; Gori, P.L. & Jeer S. (2005), *Landslide hazards and planning*, American Planning Association Planning Advisory Service Report no. 533/534, 208.

Schuster, R. L. & Highland, L. M. (2007), 'The Third Hans Cloos Lecture. Urban landslides: socioeconomic impacts and overview of mitigative strategies', *Bulletin of Engineering Geology and the Environment*, 66(1), 1-27.

Semenza, E. & Ghirotti, M. (2000), 'History of the 1963 Vajont slide: the importance of geological factors', *Bulletin of Engineering Geology and the Environment*, 59(2), 87-97.

Servizio Geologico Sismico e dei Suoli - Regione Emilia-Romagna (1999), *I numeri sulle frane*, Regione Emilia-Romagna, 94.

Servizio Geologico Sismico e dei Suoli - Regione Emilia-Romagna (2006), *Progetto IFFI - Relazione Tecnica Regione Emilia-Romagna*, Regione Emilia-Romagna, APAT and Servizio Geologico d'Italia, 26.

Soeters, R. & Van Westen, C. J. (1996), 'Slope instability recognition, analysis and zonation'. In: Turner AK, Schuster RL (eds), *Landslides, investigation and mitigation*, Transportation Research Board, National Research Council, Special Report 247, National Academy Press, Washington, USA, 129-177.

Soler, T. & Hothem, L. D. (1988), 'Coordinate systems used in geodesy: basic definitions and concepts', *Journal of Surveying Engineering*, 114 (2), 84-97.

Surace, L. (1998), 'La georeferenziazione delle informazioni territoriali in Italia', *Bollettino di Geodesia e Scienze Affini*, 57 (2), 181-234.

Tirabassi, I. (2011), 'Preistoria e protostoria nella Valle del Tassobbio', In *La Valle del Tassobbio. La vita nei secoli prima dei Canossa*, Proloco Cortogno, 35-74.

Tosatti, G.; Castaldini, D.; Barbieri, M.; D'Amato Avanzi, G.; Giannecchini, R.; Mandrone, G.; Pellegrini, M.; Perego, S.; Puccinelli, A.; Romeo, R. W. & others (2008), 'Additional causes of seismically-related landslides in the Northern Apennines, Italy', *Revista de geomorfologie*, 10, 5-21.

Travaglini, D. (2004), 'Trasformazioni tra sistemi di coordinate: software disponibili, limiti e potenzialità', *Forest@*, 1 (2), 128-134.

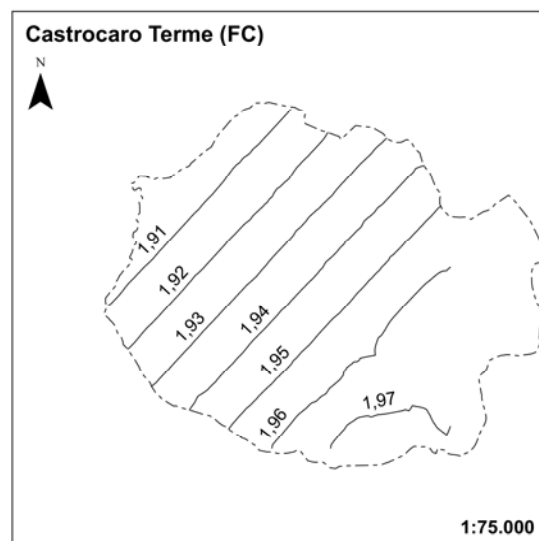
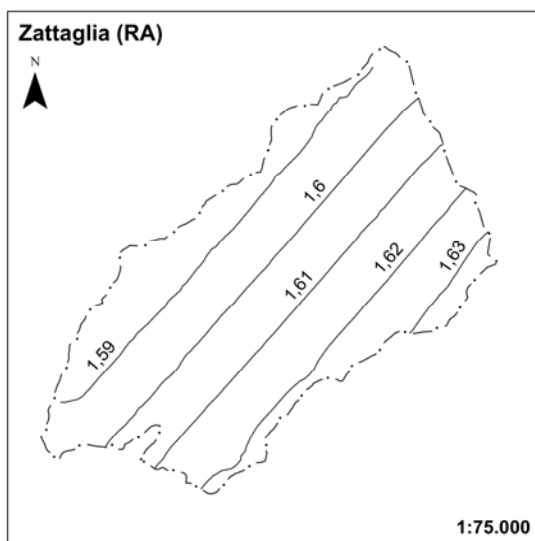
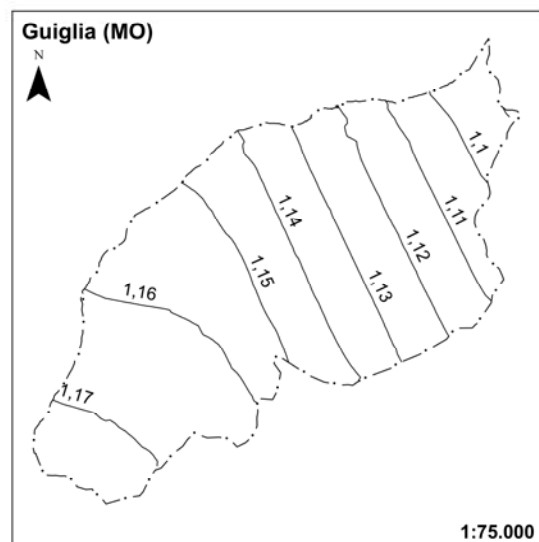
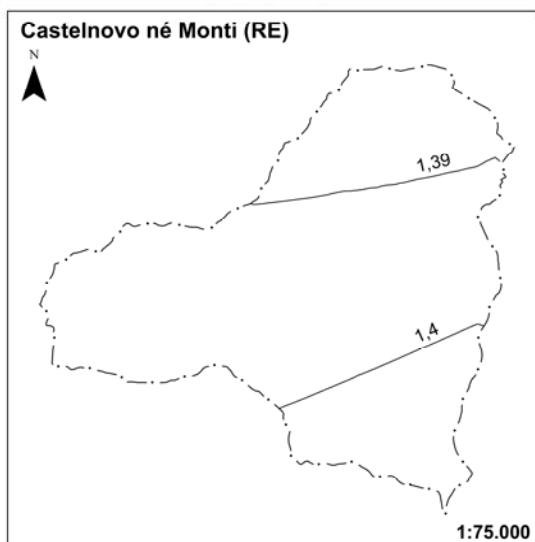
- Trigila, A.; Iadanza, C. & Spizzichino, D. (2010), 'Quality assessment of the Italian Landslide Inventory using GIS processing', *Landslides*, 7(4), 455-470.
- Turner, A. & Schuster, R. (1996), *Landslides*, Washington: National Academy Press, 673.
- UNISDR (United Nations Office for Disaster Risk Reduction) (2014), [on-line]. Available at: <http://www.preventionweb.net/english/hazards/statistics/?hid=65> [Accessed 7 Oct. 2014].
- Vanicek, P. & Steeves, R. R. (1996), 'Transformation of coordinates between two horizontal geodetic datums', *Journal of Geodesy*, 70 (11), 740-745.
- van Westen, C. J.; Castellanos, E. & Kuriakose, S. L. (2008), 'Spatial data for landslide susceptibility, hazard, and vulnerability assessment: an overview', *Engineering geology*, 102(3), 112-131.
- Varnes, D.J. and IAEG Commission on Landslides and other Mass-Movements (1984), *Landslide hazard zonation: a review of principles and practice*, The UNESCO Press, Paris, 63.
- Veregin, H. (1999), 'Data quality parameters', *Geographical information systems*, 1, 177-189.
- Wills, C. & McCrink, T. (2002), 'Comparing landslide inventories: the map depends on the method', *Environmental & Engineering Geoscience*, 8(4), 279-293.
- WP/WLI – International Geotechnical Societies' UNESCO Working Party on World Landslide Inventory (1993), 'A suggested method for describing the activity of a landslide', *Int. Ass. Eng. Geol. Bull.*, 47, 53-57.
- You, R.-J. & Hwang, H.-W. (2006), 'Coordinate transformation between two geodetic datums of Taiwan by least-squares collocation', *Journal of surveying engineering*, 132 (2), 64-70.
- Zadeh, L. A. (1965), 'Fuzzy sets', *Information and control*, 8(3), 338-353.
- Zandbergen, P. A. (2008), 'Positional Accuracy of Spatial Data: Non-Normal Distributions and a Critique of the National Standard for Spatial Data Accuracy', *Transactions in GIS*, 12 (1), 103-130.
- Zanutta, A.; Baldi, P.; Bitelli, G.; Cardinali, M. & others (2006), 'Qualitative and quantitative photogrammetric techniques for multi-temporal landslide analysis', *Annals of Geophysics*, 49(4/5), 1067-1080.

## APPENDIX A

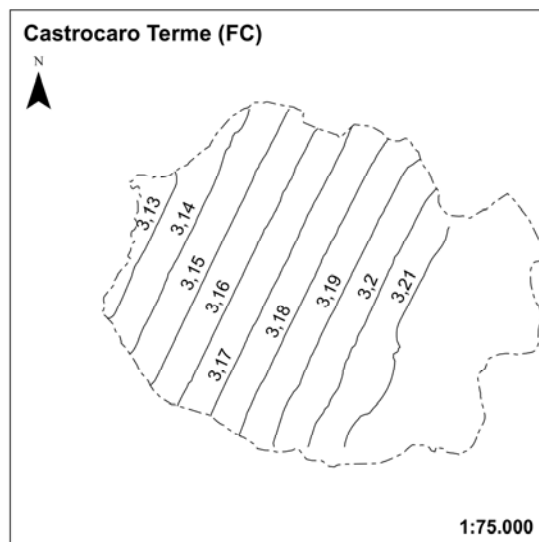
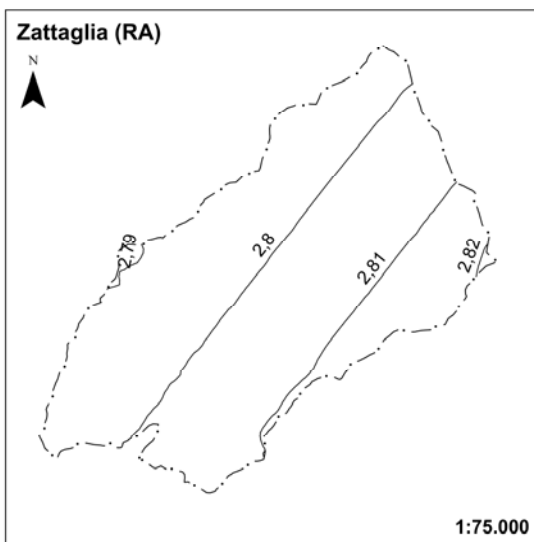
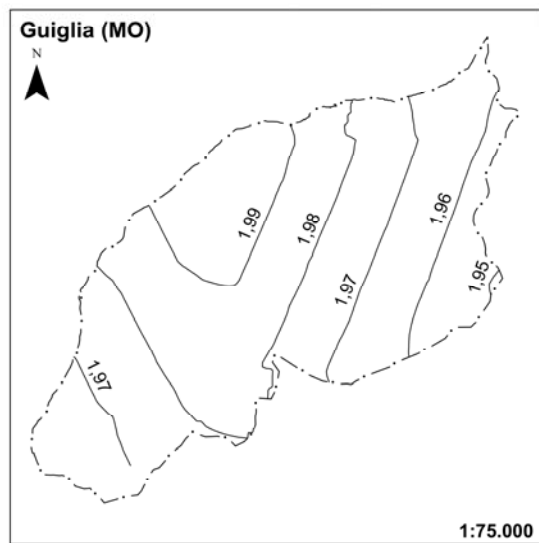
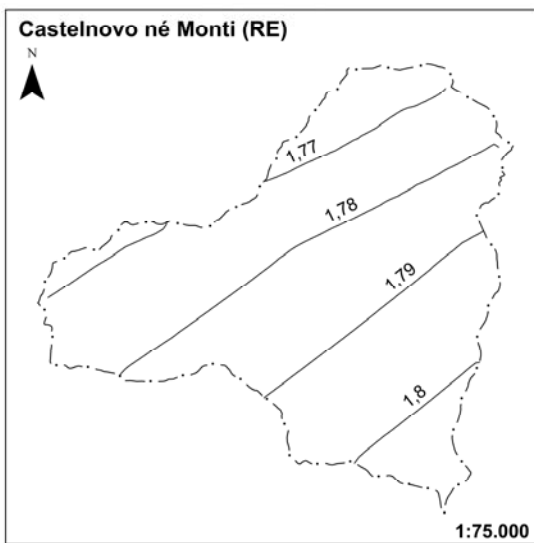
This Appendix contains the spatial representation of the offsets of the *datum* transformations from UTM RER/UTMA to WGS84 performed with the three different software: ConVER3-GPS7, Global Mapper 13 EN and Global Mapper 14 IT.

- a) UTM RER to WGS84 with ConVER3-GPS7
- b) UTM RER to WGS84 with Global Mapper 13 EN
- c) UTM RER to WGS84 with Global Mapper 14 IT
- d) UTMA to WGS84 with ConVER3-GPS7
- e) UTMA to WGS84 with Global Mapper 13 EN
- f) UTMA to WGS84 with Global Mapper 14 IT

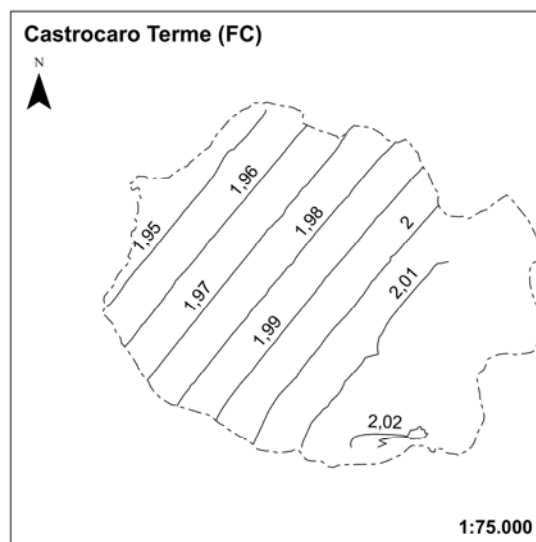
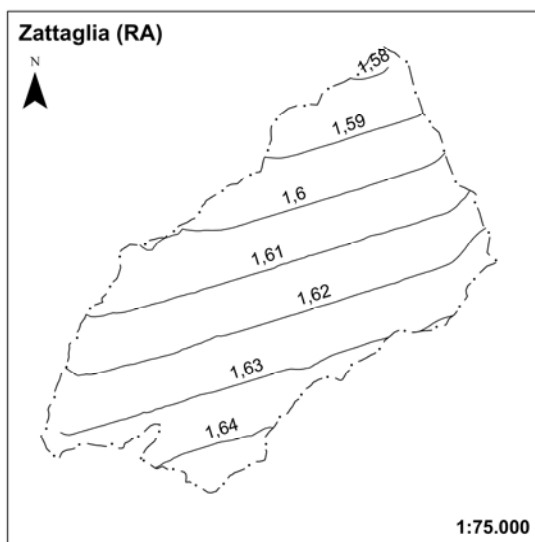
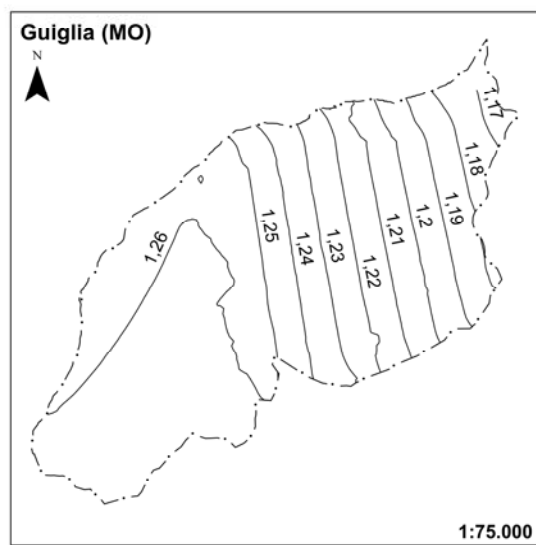
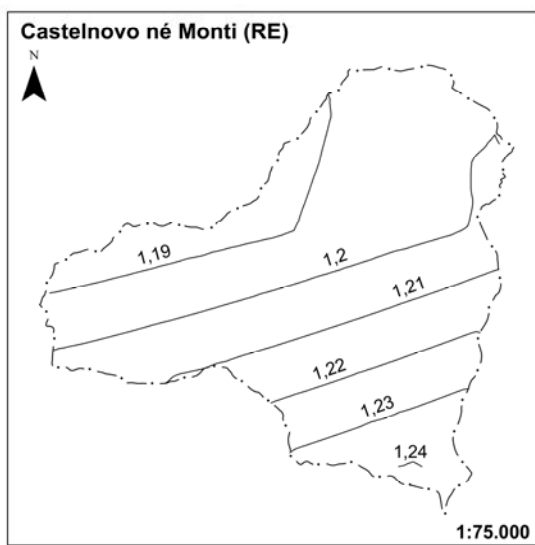
a)



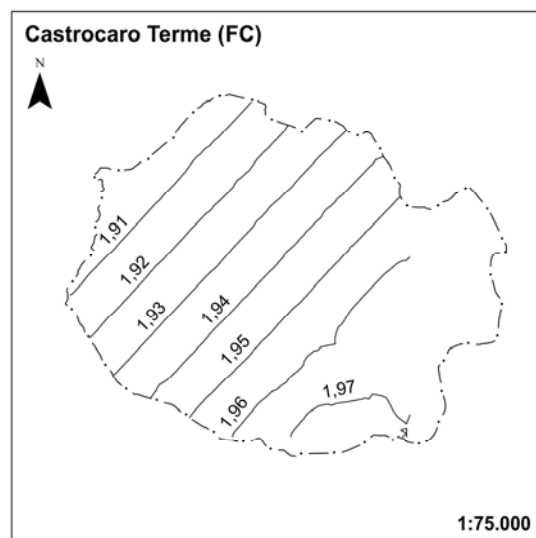
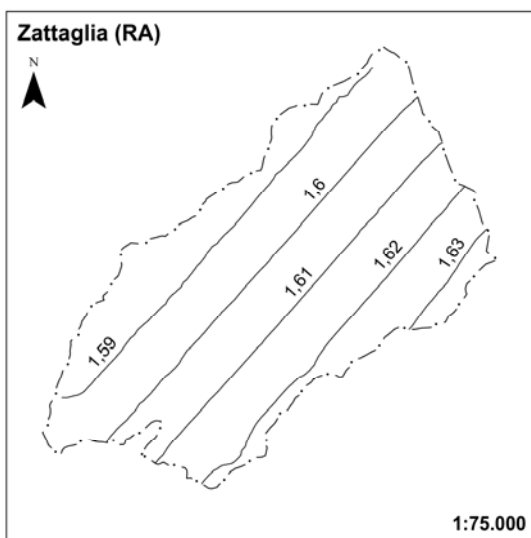
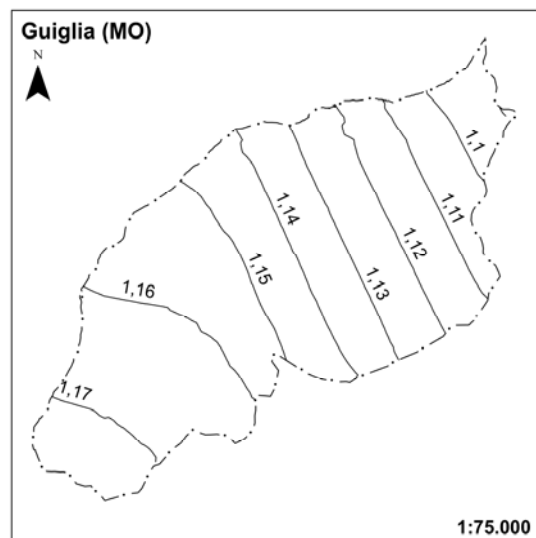
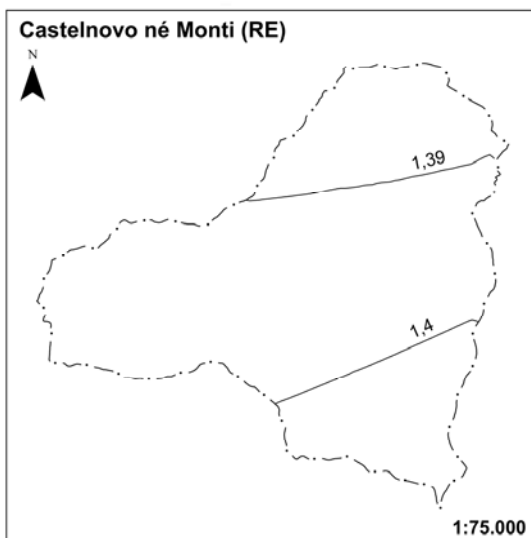
b)



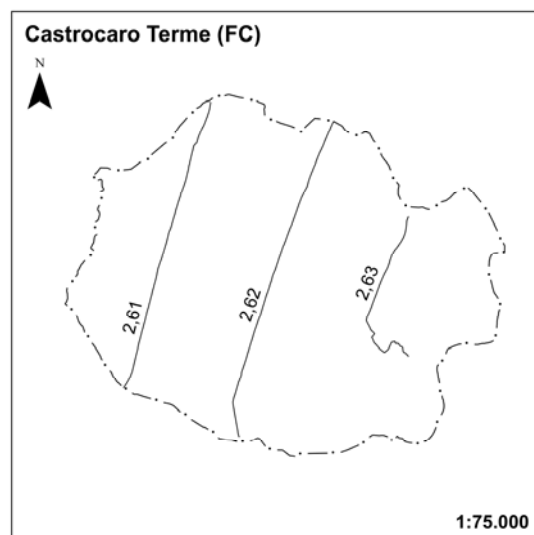
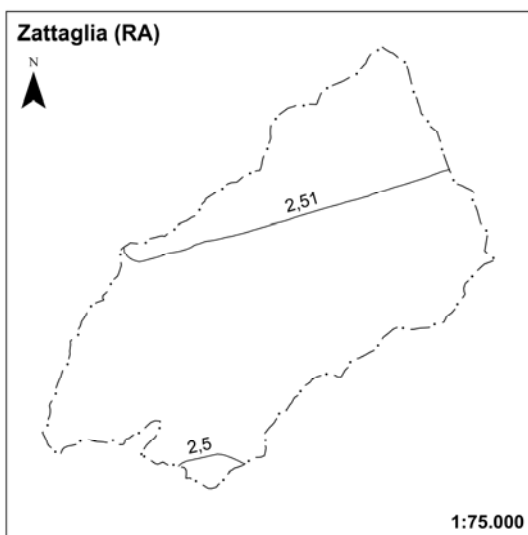
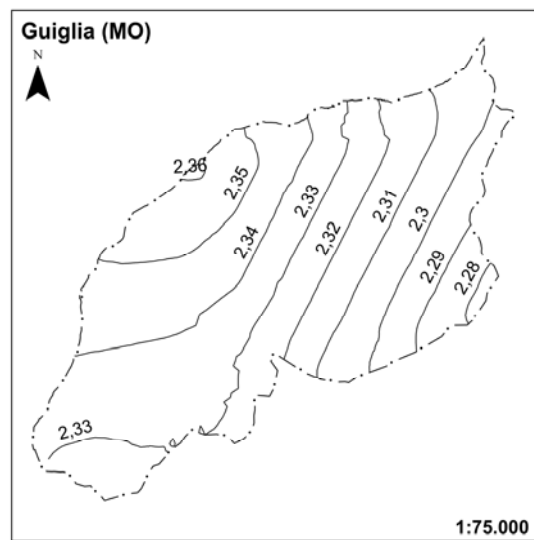
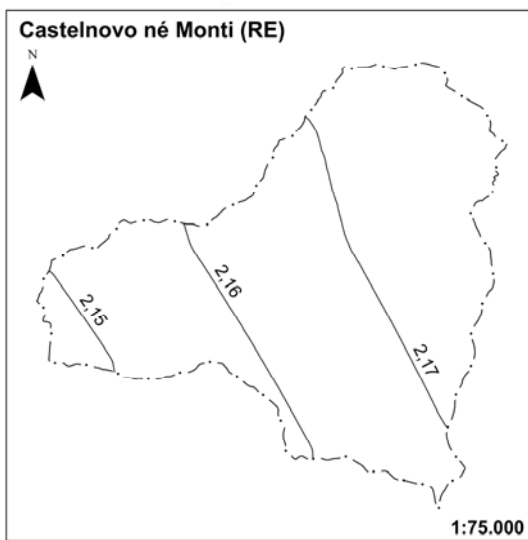
c)



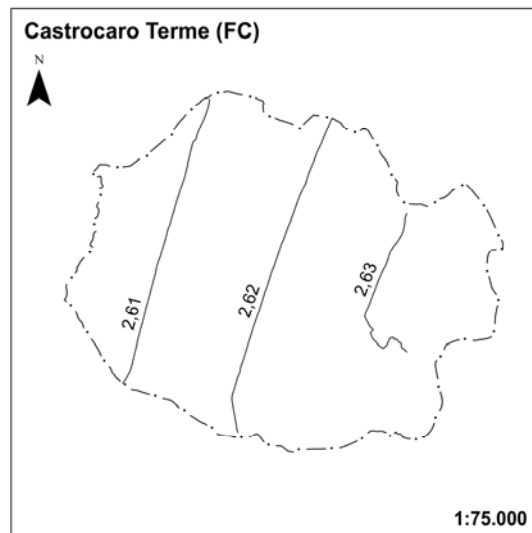
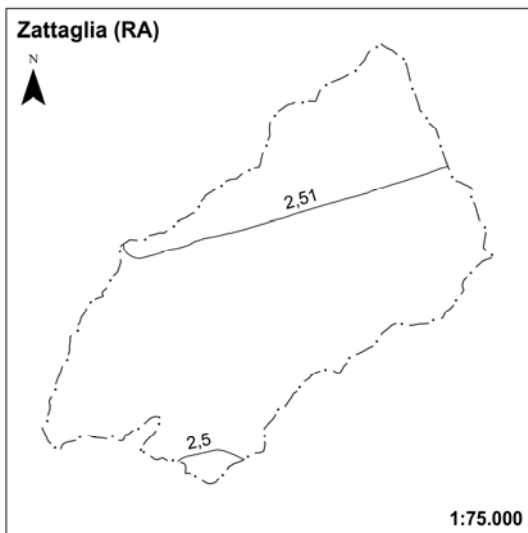
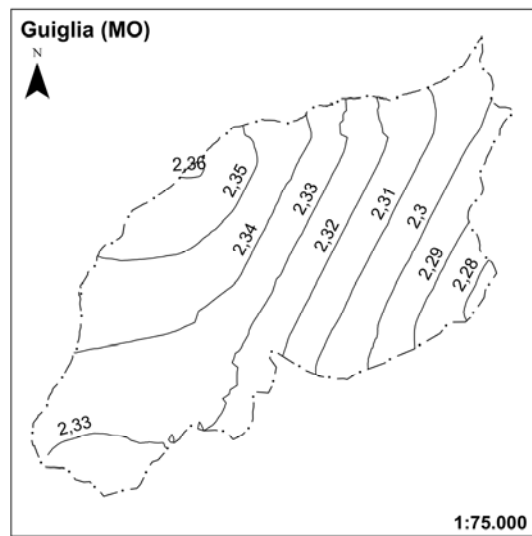
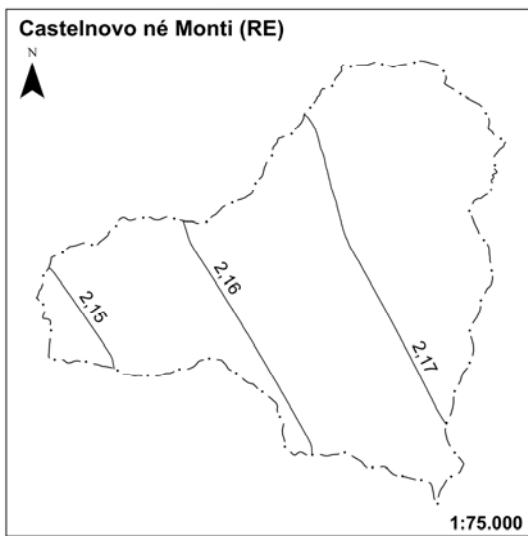
d)



e)



f)

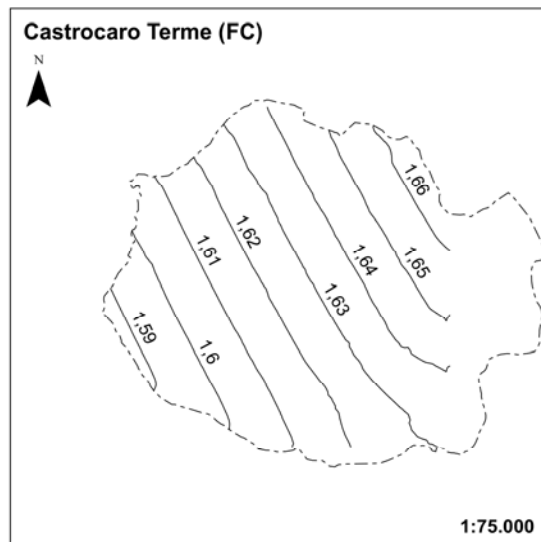
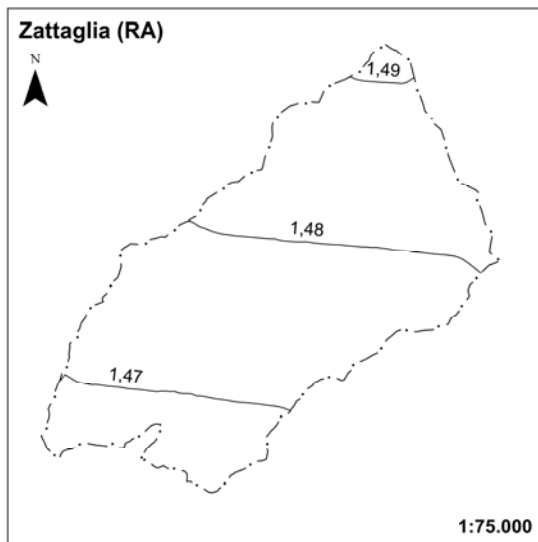
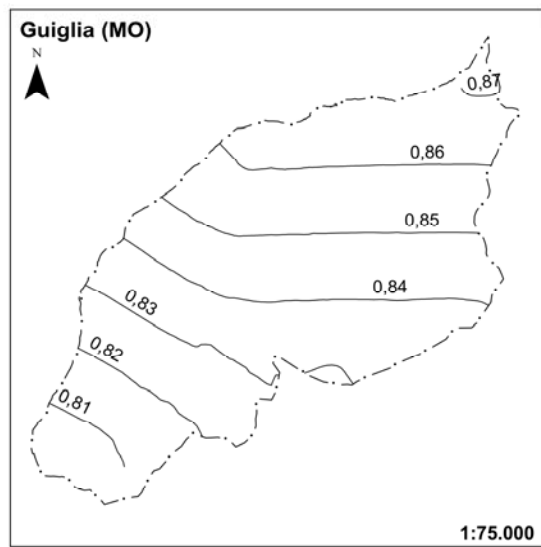
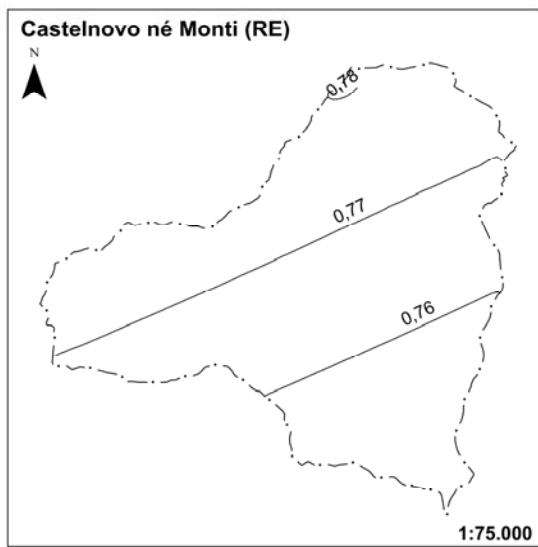


## APPENDIX B

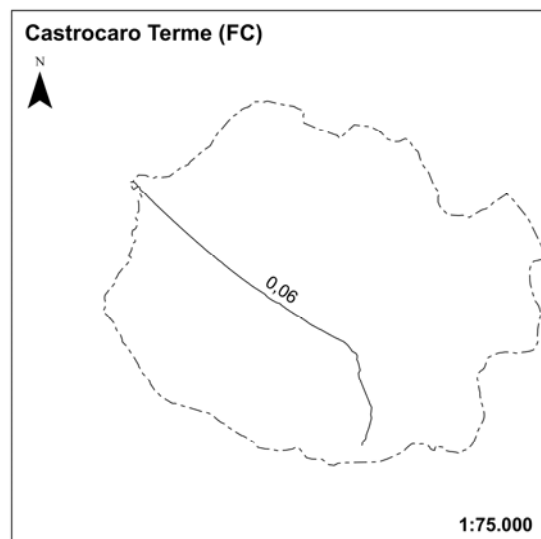
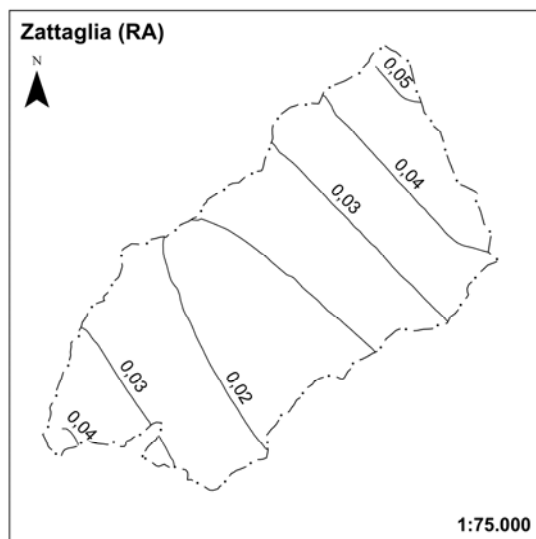
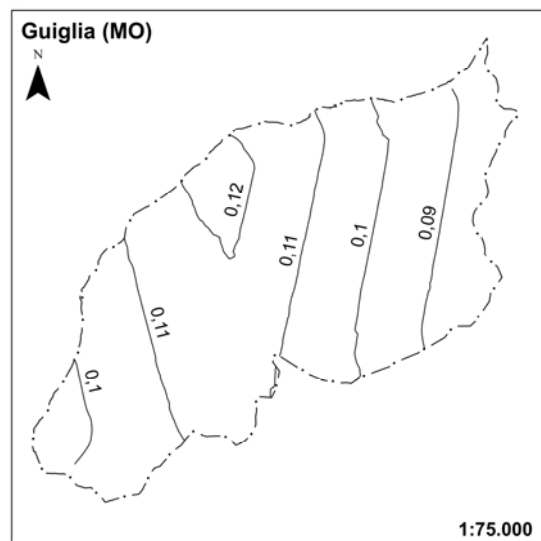
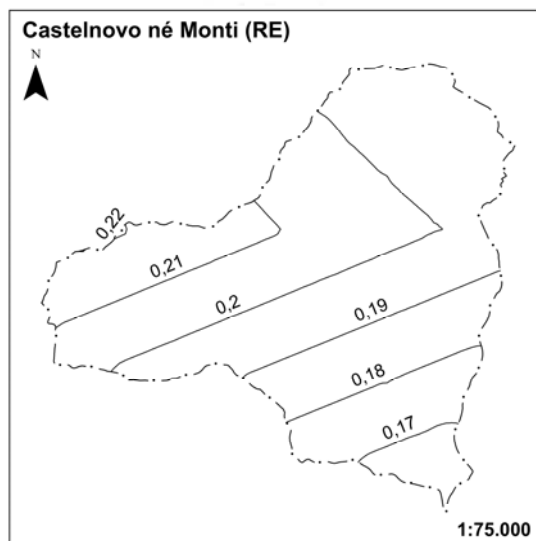
This Appendix contains the spatial representation of the offsets between the same *datum* transformation performed with two different software.

- a) UTM RER to WGS84 transformation: ConvER3-GPS7 vs Global Mapper 13 EN
- b) UTM RER to WGS84 transformation: ConvER3-GPS7 vs Global Mapper 14 IT
- c) UTM RER to WGS84 transformation: Global Mapper 13 EN vs Global Mapper 14 IT
- d) UTMA to WGS84 transformation: ConvER3-GPS7 vs Global Mapper 13 EN
- e) UTMA to WGS84 transformation: ConvER3-GPS7 vs Global Mapper 14 IT

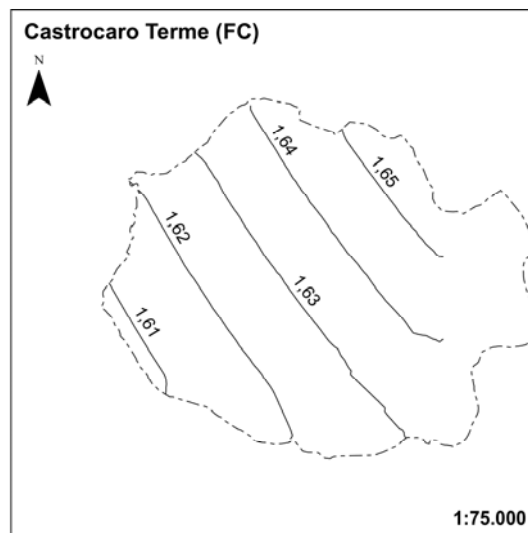
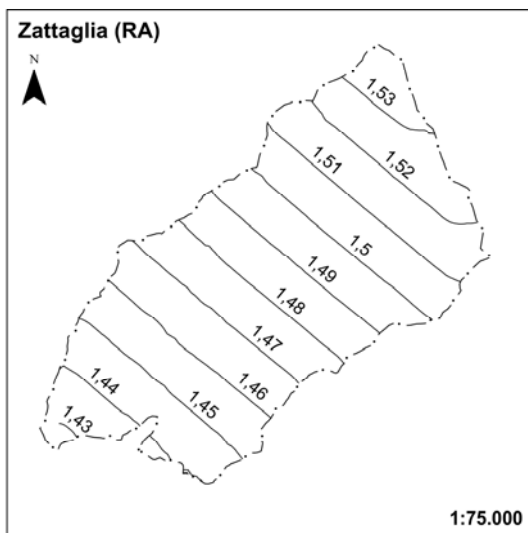
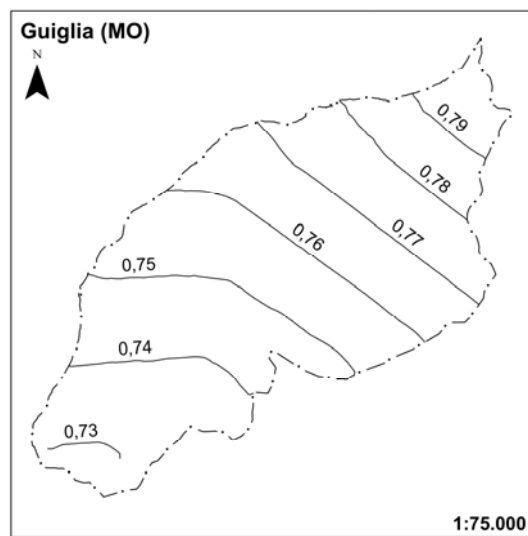
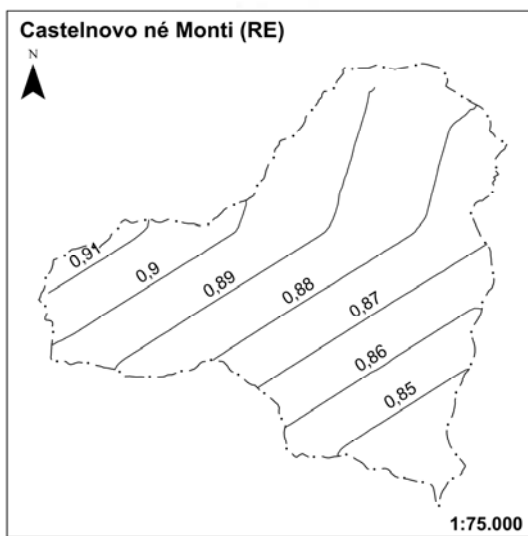
a)



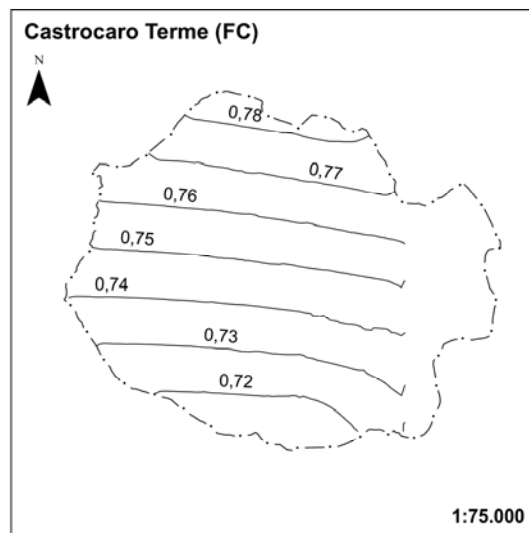
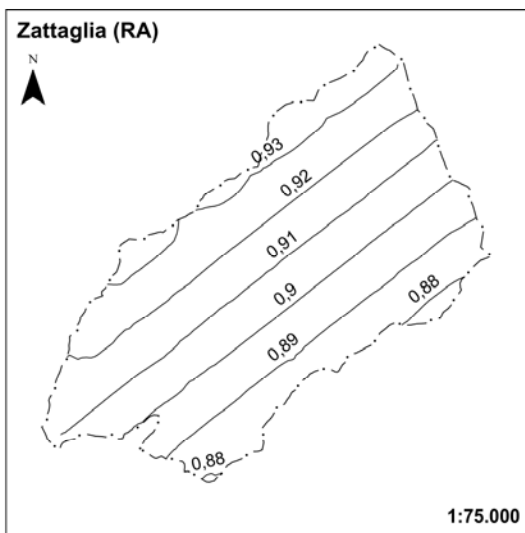
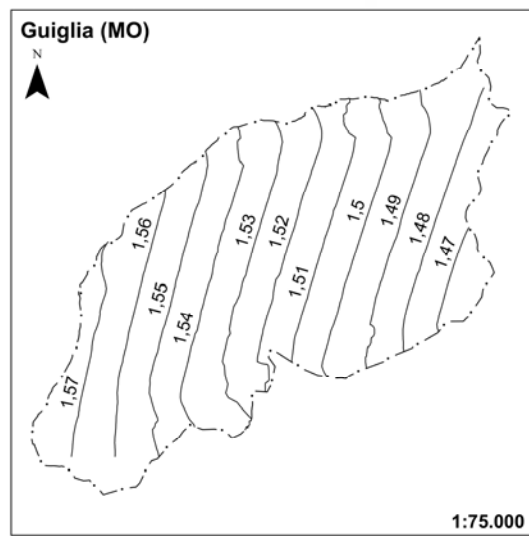
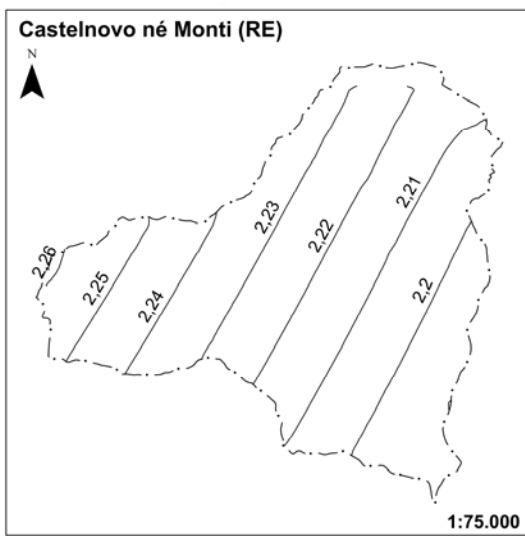
b)



c)



d)



e)

